

Project No. 5211.02073

Empa - Final Report

Assignment

Client:

Number of pages:

Summary of the project

BAFU/BAV, Switzerland

3

Project title: "FRP bogies for freight wagons: A feasibility study"

Project leader and contractor: Empa -Structural Engineering Research Laboratory

Project partners:

- PROSE (railway and certification knowledge),
- Ensinger (manufacturer, FRP knowledge),
- SBB cargo (consulting end user),
- WASCOSA (consulting end user),
- Empa 509 (noise control knowledge)

Dübendorf, 26.01.2023

Ali Saeedi / Moslem Shahverdi / Masoud Motavalli

1- Summary of the whole project

The present document is the final report of the project "FRP bogies for freight wagons" Phase I: feasibility study. The focus of the project in Phase I was to develop a conceptual design for replacing metallic bogies with a FRP one and examine its structural integrity, running dynamic characteristics, and noise emission regulations. To this end, eight different tasks were considered for the project. Meetings with all partners as well as bilateral meetings, were also held, as presented below, for technical and economic discussions. A summary of the tasks is given below.

No.	Meeting title	Date
1	Kick-off meeting	20 th January 2022
2	First workshop meeting	4 th March 2022
3	Second workshop meeting	7 th April 2022
4	First interim meeting	12 th April 2022
5	Visit from SBB workshop	10 th May 2022
6	Second interim meeting	15 th August 2022
7	Bilateral meeting with Empa 509	20 th July 2022
8	Bilateral meeting with Prose	19 th September 2022
9	Technical meeting with partners	18 th October 2022
10	Bilateral meeting with Empa 509	30 th November 2022
11	Bilateral meeting with Ensinger	7 th December 2022
12	Final meeting	15 th December 2022

Task 1: Definition of the requirements from standards, operation, and maintenance

Determining the required technical specifications, standards, load calculations, and validation procedures were performed in Task 1 and reported in the **first interim report**.

Task 2: Design concept(s)

Basic layout parameters were assessed during two workshops with the partners, and the configurations with the highest priorities were chosen. The best FRP concepts for the bogie frame were compared, taking into account technical, economic, and fabrication factors. The **first interim report** details the concepts and evaluation procedure.

Task 3: Material selection and drawing the first conceptual design and the interfaces

In task 3, the material selection and laminate design for the FRP parts were taken into consideration to complete the conceptual design of the bogie. A hybrid FRP/metal model was suggested to reduce costs. The developed concept can offer the necessary vertical and longitudinal stiffness and variable stiffness to guarantee the bogie's stability. The **second interim report** presents the conceptual design and its attributes.

Task 4: Finite element modeling and design of the FRP bogie

For the proposed hybrid GFRP/metal bogie, the finite element method was used to perform stress and stiffness analysis. From the outcomes of this task, the required stiffness in various directions for the running dynamic analysis was also extracted. The bogie's proper structural performance against the applied exceptional loads was revealed by the finite element analysis results. The bogie exhibits the proper vertical stiffness (which is comparable to the stiffness of the spring suspension systems in metallic bogies), and the longitudinal stiffness is also designed to be high enough to improve the bogie's stability at high speeds. In the **second interim report**, the obtained finite element results are presented.

Task 5: Rough running dynamic analyses

Running dynamic analysis of the bogie is presented as a separate report by PROSE. PROSE also proposed an adapted model for the bogie and reported the results for both models. According to the running dynamic report, the initial and the adapted bogie designs show promising results for safety against derailment, stability at 130 km/h, and radial steering. However, further optimization of the parameters is needed to reach all the dynamic limit values.

Task 6: Rough estimations of noise generation and comparisons with conventional steel bogies

A rough estimation of the noise generation of the hybrid GFRPT bogie compared to the metallic bogie was performed and presented in a separate report (**Report of Task 6**). According to the report, the GFRP bogie has several parameters that aid in noise reduction, and no appreciable noise increase can be found as described in this report. In addition, the use of disc brakes in the design reduces noise in the bogie. However, more information is needed to make an exact prediction of noise reduction.

Task 7: Cost estimation for manufacturing and maintenance of an FRP bogie configuration

The total life cycle costs for the hybrid GFRP bogie compared with the metallic Y25 bogie are calculated and presented in a separate report (**report of task 7**). Manufacturing costs, maintenance costs, and possible bonuses are taken into consideration for the calculation of total costs. The cost calculations lead to the conclusion that, there isn't a significant cost increase over the Y25 bogie for the GFRP hybrid bogie in the current Phase.

Task 8: Planning of the prototype bogie, proof-of-concept (follow-up phase), material test, extreme and fatigue load cases, real track test including running behavior, and homologation

The possible follow-up phase will be discussed and decided among the project partners.

Project No. 5211.02073

Empa report

Assignment

Task 7

Client:

BAFU/BAV, Switzerland

Number of pages:

18

Project title: "FRP bogies for freight wagons: A feasibility study"

Task 7: Cost estimation for manufacturing and maintenance of an FRP bogie configuration

Project leader and contractor: Empa -Structural Engineering Research Laboratory

Project partners:

- PROSE (railway and certification knowledge),
- Ensinger (manufacturer, FRP knowledge),
- SBB cargo (consulting end user),
- WASCOSA (consulting end user),
- Empa 509 (noise control knowledge)

Dübendorf, 07.12.2022

Ali Saeedi / Moslem Shahverdi / Masoud Motavalli

Contents

1- Overview of Task 7	5
2- Manufacturing costs.....	5
2-1- Manufacturing cost for FRP parts (By Ensinger).....	5
2-2- Manufacturing cost of the bogie.....	8
3- Maintenance costs	8
4- Total life cycle costs.....	10
5- Health monitoring of FRP parts	15
6- Conclusion.....	17
7- References.....	18

List of figures

Figure 1- The dimensions of the GFRP side beams for the GFRP hybrid bogie.....	6
Figure 2- Maintenance criteria based on EN 15857 standard	9
Figure 3- Total life cycle cost calculation for GFRP hybrid bogie.....	11
Figure 4- Possible damages in FRP composite structures in manufacturing and in service period.....	16

List of Tables

Table 1- The cost split for the down-beam.....	7
Table 2- The cost split for the up-beam.....	7
Table 3- Calculation of manufacturing costs for Y25 and GFRP hybrid bogies.....	8
Table 4- Comparison on maintenance steps for Y25 and GFRP hybrid bogie.....	9
Table 5- Cost estimation for manufacturing and maintenance of an FRP bogie configuration.....	12
Table 6- Estimation of maintenance costs for the bogie considering 10% reduction due to enhanced bogie steering behavior [3]	13
Table 7- Estimation of maintenance costs for IS2 wheelset check	13
Table 8- Estimation of maintenance costs for workshop runs	13
Table 9- Estimation of cost reduction due to reduced mass of the bogie.....	14
Table 10- Estimation of cost reduction due to reduced mass of the bogie	14
Table 11- Estimation of cost reduction due to enhanced steering of the bogie	15
Table 12- Estimation of cost reduction due to noise bonus	15
Table 13- Some utilized inspection methods for FRP composite structures in the literature	17
Table 14- Selected SHM method for GFRP hybrid bogie in the first workshop with partners.....	17

1- Overview of Task 7

The present report corresponds to Task 7: "Cost estimation for manufacturing and maintenance of an FRP bogie configuration" of the FRP bogie for freight bogie project. This section provides cost estimations for the manufacturing and maintenance of GFRP hybrid bogie configurations. After characterization of the FRP bogie concepts in structural, running dynamics, and noise emission points of view, an estimation of the costs should be provided for better investigation of the bogie's performance considering both technical and economic aspects. The cost estimation for the bogie consists of two major parts:

- Manufacturing costs
- Maintenance costs

Although FRP composites are less susceptible to deterioration than metals and have higher strength and stiffness to weight ratios, the initial cost of the components built of FRP can be relatively high, depending on the employed materials and fabrication methods. The total cost of the FRP structure can be calculated based on the manufacturing and life cycle costs. There are also some bonuses that can be considered for cost savings if the bogie has specified qualifications.

In the following sections, a comparison of costs between the newly introduced GFRP and conventional Y25 is performed. Cost reduction sources are also considered and introduced for better economic justification of the new bogie.

2- Manufacturing costs

In general, high manufacturing costs are one of the main parameters that limit the employment of composite materials and structures in the industry. As previously mentioned, compared to metals, the fabrication of composite replacements is usually more expensive. Such a price increase should then be compensated by the maintenance and lifecycle costs. However, for the developed hybrid GFRP/Metal bogie, the manufacturing costs are minimized by using composite materials only where they are really required, instead of fabricating the fully FRP frame. The main effective parameters for manufacturing costs are as follows:

- Raw materials
- Labor costs
- Cost saving for series production

The abovementioned parameters are used in the following section for manufacturing cost calculations of the FRP side beams and the whole bogie frame.

2-1- Manufacturing cost for FRP parts (By Ensinger)

For the GFRP hybrid bogie, the manufacturing cost consists of the costs for FRP parts and metallic components. The dimensions of the FRP parts are shown in Figure 1.

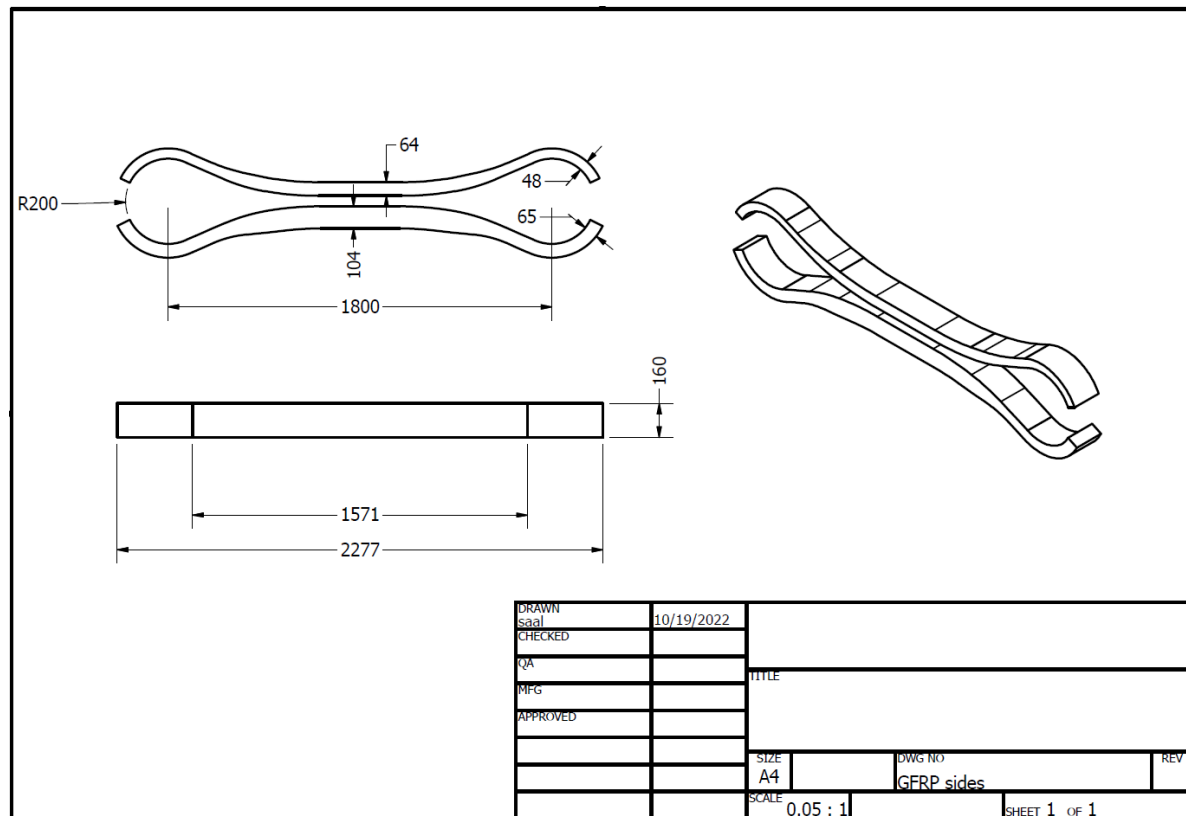


Figure 1- The dimensions of the GFRP side beams for the GFRP hybrid bogie

The manufacturing costs for the FRP parts was estimated by Ensinger, with the following assumption.

- Material price 5 EUR/kg (lower assumptions)
- Energy costs Switzerland (Otelfingen)
- Personal costs Switzerland
- OH costs based on our German rates for high-volume production facility
- No profit margin included – the costs are just the manufacturing costs + overheads
- Yearly volume 100 to 10'000 pcs.
- Amortisation period for moulds and investment 10 years
- investment in moulds: 130'000 EUR per beam, total 260'000 EUR
- Mould costs amortised in the part costs
- Depending on the possible required machining work, machining costs can be added to the calculations.

Based on the mentioned assumption, the manufacturing cost estimation for the GFRP side beams are calculated and presented in Tables 1 and 2 .

Table 1- The cost split for the down-beam

	100	500	1'000	2'500	5'000	10'000
material costs	334.88 €	334.88 €	334.88 €	334.88 €	334.88 €	334.88 €
machinery costs	267.56 €	266.87 €	266.78 €	266.73 €	266.71 €	266.70 €
personal costs	395.75 €	395.75 €	395.75 €	395.75 €	395.75 €	395.75 €
scrap costs	9.98 €	9.97 €	9.97 €	9.97 €	9.97 €	9.97 €
quality costs	10.83 €	10.83 €	10.83 €	10.83 €	10.83 €	10.83 €
deburring costs	0.00 €	0.00 €	0.00 €	0.00 €	0.00 €	0.00 €
machining costs	0.00 €	0.00 €	0.00 €	0.00 €	0.00 €	0.00 €
overhead and financial costs	534.33 €	529.29 €	528.66 €	528.28 €	528.15 €	528.09 €
margins	0.00 €	0.00 €	0.00 €	0.00 €	0.00 €	0.00 €
molds amortization	170.88 €	34.18 €	17.09 €	6.84 €	3.42 €	1.71 €
TOTAL	1'724.21 €	1'581.77 €	1'563.96 €	1'553.28 €	1'549.72 €	1'547.94 €

Table 2- The cost split for the up-beam

	100	500	1'000	2'500	5'000	10'000
material costs	227.24 €	227.24 €	227.24 €	227.24 €	227.24 €	227.24 €
machinery costs	177.24 €	176.55 €	176.46 €	176.41 €	176.39 €	176.38 €
personal costs	247.00 €	247.00 €	247.00 €	247.00 €	247.00 €	247.00 €
scrap costs	6.51 €	6.51 €	6.51 €	6.51 €	6.51 €	6.51 €
quality costs	10.83 €	10.83 €	10.83 €	10.83 €	10.83 €	10.83 €
deburring costs	0.00 €	0.00 €	0.00 €	0.00 €	0.00 €	0.00 €
machining costs	0.00 €	0.00 €	0.00 €	0.00 €	0.00 €	0.00 €
overhead and financial costs	344.29 €	339.25 €	338.62 €	338.24 €	338.11 €	338.05 €
margins	0.00 €	0.00 €	0.00 €	0.00 €	0.00 €	0.00 €
molds amortization	170.88 €	34.18 €	17.09 €	6.84 €	3.42 €	1.71 €
TOTAL	1'183.99 €	1'041.55 €	1'023.75 €	1'013.06 €	1'009.50 €	1'007.72 €

A sensitivity analysis on the up-beam shows:

- Mould costs: According to the "moulds amortisation" line – do not have a very big impact
- Cycle time: by reducing the cycle time by 50% the costs would go down by 250 EUR but this is not very realistic,
- By assuming a 10 EUR/kg instead of 5 EUR/kg the manufacturing cost would be +227 EUR per part

In an absolute best case scenario, the price can go down to approximately 750 EUR per part for the up-beam, without profit margin, which is usually 25-40%. Considering 2x up and 2x down beams per bogie, so accounting for approximately $2 \times 750 + 2 \times 1000 \text{ EUR} = 3500 \text{ EUR}$ per bogie costs, without profit.

2-2- Manufacturing cost of the bogie

The total manufacturing cost of the hybrid GFRP bogie can be estimated by taking into account the manufacturing costs of the FRP parts and other metallic components. A comparison of the manufacturing costs for Y25 and FRP bogie is presented in Table 3. For GFRP bogie, two different cases are considered for taking into consideration the effect of disc brakes.

Table 3- Calculation of manufacturing costs for Y25 and GFRP hybrid bogies

Components	Y25 Bogie			FRP Bogie with Disc brakes			FRP Bogie without Disc brakes (one-side push brake)		
	Weight (kg)	Material	Cost (Euro)	Weight (kg)	Material	Cost (Euro)	Weight (kg)	Material	Cost (Euro)
Bogie frame	1450	steel	7000	670* (200+370+100)	Hybrid	6400** (4400+1600+400)	670* (200+370+100)	Hybrid	6400** (4400+1600+400)
Wheelset	2000		4200	2000	steel	4200	2000	steel	4200
Brake components	130		2000	150	steel	2000	120	steel	1700
Axle box	900		1800	650	steel	1500	650	steel	1500
Disc brakes	---			650	steel	2000	---		
Cross links	---			100	steel	600	100	steel	600
Total (Euro)	17000-22000			16500-18000			14500-16000		

*The bogie frame consists of GFRP parts + metal bolster+ cross links

**For the GFRP parts, based on the best case scenario, the manufacturing cost is 4400 Euro (=3500 Euro +25% profit margin)

3- Maintenance costs

For the end user, the cost of maintenance of the bogie during its service life is an important parameter in addition to the initial cost of production. All bogies contain components that are vulnerable to wear and damage over their service life. Therefore, it is essential to adhere to a maintenance schedule in order to ensure functionality and safety, according to standard EN 15827 [1]. A schematic of the maintenance criteria is shown

in Figure 2. The maintenance plan consists of short-term initial plan and a longer term plan for additional maintenance and overhaul instructions.

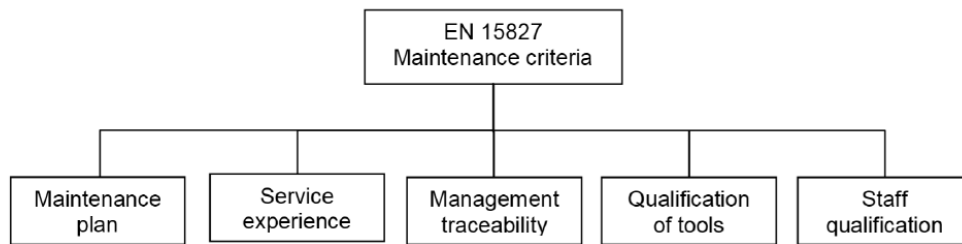


Figure 2- Maintenance criteria based on EN 15857 standard [1]

Currently, maintenance on the bogie and each of its parts is done in a preventative manner. Typically, a wagon enters the workshop for maintenance every six years, and everything is examined using visual inspection [2]. The maintenance costs can be calculated based on the maintenance plan, including the duration or mileage for inspections, workshop activities, types of inspections, etc. Different maintenance steps for Y25 and hybrid GFRP bogie are presented in Table 4.

Table 4- Comparison on maintenance steps for Y25 and GFRP hybrid bogie

Maintenance step	Maintenance parameter	Y25 Bogie	GFRP hybrid bogie
General bogie maintenance [2]	Wheelset holder webs and their security elements / Remove lift-offs and check	✓	✓
	Wheelsets remove and check	✓	✓
	Springs removal and exchange criteria	✓	✗
	Substitution of spring caps, pressure piece, and spring sliders	✓	✗
	Cleaning the bogie frame and components	✓	✓
	Bogie frame including the fixed points of spring suspension check for cracks, deformations, corrosion spots and abrasions	✓	✓
	Measure bogie frame	✓	✓
	Check Surface protection	✓	✓
	reassemble and check all removed parts	✓	✓
Health assessment of critical components [2]	Wheels Thermal cracks, Rolling contact fatigue, sub surface fatigue, Fatigue cracks, Spalling or shelled tread, Skidded wheels, Scaled wheels, Arises, Tread / flange wear	✓	✓

	Axles	✓	✓
	Frame The Bogie frames shall be visually inspected for cracks. If any cracks are found the vehicle shall be "red carded" and the bogie replaced. On the other hand, if the bogie frame is obviously bent the vehicle shall be red carded and the bogie replaced.	✓	✓
	Bearings	✓	✓
	Helical springs Broken springs, Seating, Solid height	✓	X
	Bolster	✓	✓
	Damping devices	✓	
	Rubber Element	X	✓
	Primary suspension system	✓	X

A comparative study between the maintenance costs for Y25 bogie and GFRP hybrid bogie is conducted in the present report. In the following section, a summary of the calculated maintenance and life cycle costs is presented.

4- Total life cycle costs

The total life cycle costs (LCC) for the FRP bogie can be estimated by considering the manufacturing costs, the required maintenance costs for the bogies (according to standard), and possible additional costs for the maintenance of FRP components. The total costs, therefore, will be the sum of manufacturing and maintenance costs after considering the possible cost increase and reduction factors. There are cost-increasing and cost saving factors for the hybrid GFRP bogie that affect the LCC. The effective parameters on the life cycle costs for the GFRP bogie are presented in Figure 3.

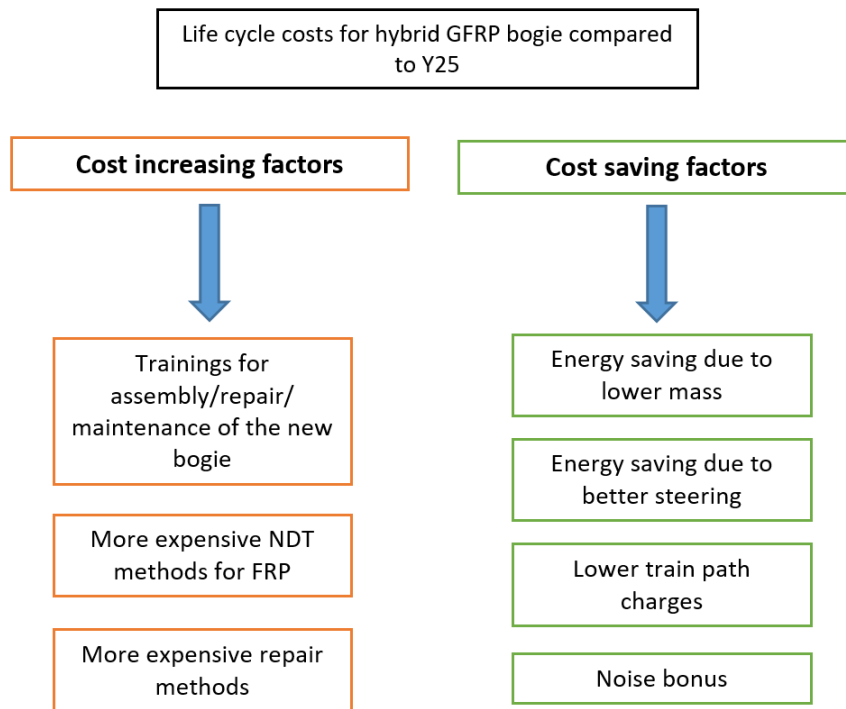


Figure 3- Total life cycle cost calculation for GFRP hybrid bogie

Taking into account the abovementioned parameters, the total costs can be compared for the Y25 and hybrid GFRP bogie as presented in Table 5. The cost calculations are mainly based on previously published cost estimation data in references [3-5]. For each parameter, the detailed calculations and assumptions are presented in separate tables (Tables 6 to 12). It is worth mentioning that the calculated costs are based on using disc brake system for the GFRP hybrid bogie. The required training for the inspections and assembly can be considered one-time costs. Moreover, in the case of the impact of small objects, reinforcement costs will be added to the estimation. This should be done in the detailed design step of the bogie structure.

Table 5- Cost estimation for manufacturing and maintenance of an FRP bogie configuration

Cost effective parameters		Unit	Y25 bogie (with push brake)	GFRP hybrid bogie (With disk brake)	Cost dif- ference for GFRP bogie	Refer- ence	Details
Estimated manufacturing costs		CHF	17,000- 22,000	14,500- 18,000		---	Table 3
Maintenance costs	Maintenance cost reduction due to better radial steering	CHF/bogie/year	---	---	-396	[3]	Table 6
	IS2 wheelset check	CHF/bogie/year	300	120	-180	[4]	Table 7
	Costs for workshop runs	CHF/bogie/year	280	200	-80	[4]	Table 8
Potential for cost reduction	due to energy saving- mass reduction	CHF/bogie/year	---	---	-232 (-2160)	[5] [4]	Table 9 Table 10
	due to energy saving- enhanced steering	CHF/bogie/year	---	---	-400	[3]	Table 11
	due to noise bonus	CHF/bogie/year	---	---	-2100	[6]	Table 12
Cost increase factors	Extra training for assembling the new bogie	CHF/bogie/year			+(...)		
	More expensive SHM/NDT methods for FRP	CHF/bogie/year			+(...)		

Table 6- Estimation of maintenance costs for the bogie considering 10% reduction due to enhanced bogie steering behavior [3]

Maintenance cost	Y25 with push brake	New bogie with 10% maintenance cost reduction	Difference
50,000 km per year	28.158 euro	27.772 euro	150 euro
100,000 km per year	43.558 euro	42.558 euro	400 euro
150,000 km per year	56.442 euro	54.971 euro	750 euro

Table 7- Estimation of maintenance costs for IS2 wheelset check

Cost parameters	Unit	Y25 (with push brake)	Hybrid GFRP bogie (with disc brake)
Cost of IS2 inspection	CHF/bogie	1800	1800
Execution IS2 after	km	600,000	1500,000
Mileage	Km/year	100,000	100,000

Table 8- Estimation of maintenance costs for workshop runs

Cost parameters	Unit	Y25 bogie (with push brake)	GFRP hybrid bogie (With disk brake)
Number of scheduled workshop run	Number/year	0.7	0.5
Costs per workshop run (freight costs, rent, shunting, administration, lost profit) at a flat rate	CHF	800	800
Cost per year	CHF/bogie/year	280	200

Table 9- Estimation of cost reduction due to reduced mass of the bogie

Cost parameters	Unit	value
Energy price for diesel	Euro/liter	1.15 (2013) [6]
Corresponding electric price	cents/kWh	11.533 [6]
Cost reduction ratio for the bogie	Euro/kg	13 [6]
Total mass reduction	Kg/bogie	540
Cost saving due to mass reduction	Euro/bogie/lifetime	7020
Yearly cost reduction	CHF/bogie/year	232

Table 10- Estimation of cost reduction due to reduced mass of the bogie

Cost parameters	Unit	value
Transport cost- loaded (min)	CHF/km/t	0.03 [4]
Transport cost- loaded (max)	CHF/km/t	0.08 [4]
Transport cost- empty	CHF/km/t	.015 [4]
Average transport cost	CHF/km/t	0.04
Total mass reduction	Kg/bogie	540
Cost saving due to mass reduction	CHF/bogie/year	2160

Table 11- Estimation of cost reduction due to enhanced steering of the bogie for millage of 50,000 km/year

	Unit	Y25 (with push brake)	Difference for a bogie with 4% reduction in energy	Difference for a bogie with 8% reduction in energy
Energy consumption (block train)	kWh/km	47.44	-1.897	-3.795
Energy cost (block train) per km	Euro/km	5.38	-0.215	-0.431
Energy Cost (block train per year)	Euro/year/train	269,205.26	-10,768.21	-21,536.42
Energy Cost (Bogie per year)	Euro/year/bogie	5,384.11	-215.36	-430.73

Table 12- Estimation of cost reduction due to noise bonus

Noise bonus	Unit	value
Noise bonus per km	CHF/axle/km	0.03
Mileage	Km/year	100,000
Estimated transport performance in CH	%	35
Noise bonus per year	CHF/bogie/year	2100

In addition to the cost-saving bonuses shown in Table 5, the employed structural health monitoring system and potential training requirements may raise the life-cycle costs for the GFRP hybrid bogie. The removal of numerous components, such as springs and dampers, made the GFRP hybrid bogie's assembly simpler, so it is estimated that the trainings will not have a significant impact on the price increase. However, the cost of maintenance could go up depending on the method used to monitor structural health. The following section provides an explanation of the health monitoring system.

5- Health monitoring of FRP parts

There are several structural health monitoring (SHM) and non-destructive inspection methods that have been used for composite materials and structures in various fields of applications. Defects and damages within an

FRP composite component can be generated both in manufacturing process and in-service working. Figure 4, depicts potential damage to the composite structure at various scales.

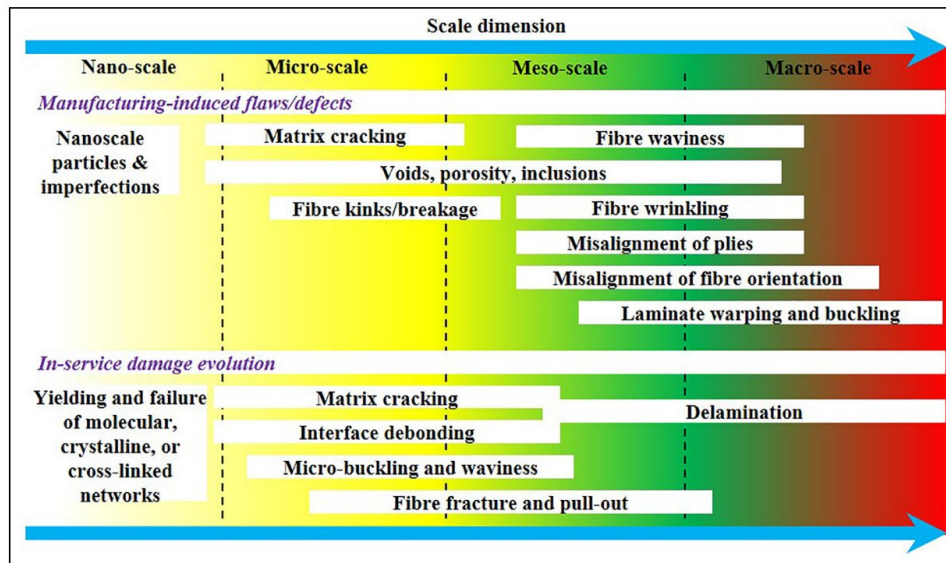


Figure 4- Possible damages in FRP composite structures in manufacturing and in service period

In general, SHM methods can be divided in to two categories (online and offline inspections) with their sub-categories:

- Online inspection
 - Fiber bragg sensors
 - Piezo-electric sensors
 - Acoustic emission
- Offline inspection
 - Visual inspections
 - Thermographic methods (impulse thermography)
 - Ultrasonic testing
 - X-ray radiography
 - X-ray Computed tomography

There are comprehensive reviews on the SHM of composite structures [7-9]. Table 13, gives a summary of some employed NDT methods for composite structures for different applications. Depending on the type of the structure, possible defects and damages, and the economic aspects, the proper SHM method can be selected for the FRP composite parts. For the FRP bogie, in the first workshop meeting with partners (on March 4th 2022), offline inspection and in particular regular NDT methods are selected to be the first priority for the bogie frame, considering both technical and economic aspects (Table 14).

Table 13- Some utilized inspection methods for FRP composite structures in the literature [7]

Inspection Type	NDT Method
Damage identification in aircraft composite structures (Andrzej Katunin et al. 2015; Polimeno & Meo, 2009) Aircraft composites assessment (Růžek et al. 2006) Health monitoring of aerospace composite structures (Loutas et al. 2012)	Ultrasonic Testing (Andrzej Katunin et al. 2015) Thermographic Testing (Maierhofer et al. 2014; Usamentiaga et al. 2013) Vibration Methods (Loutas et al. 2012; Rizos et al. 2008) Infrared Thermography (Meola & Carlomagno, 2014) Shearography (Růžek et al. 2006) XCT (Bull et al. 2013)
Health monitoring of a composite wing-box structure (Grondel et al. 2004)	Ultrasonic Testing (Grondel et al. 2004; Andrzej Katunin et al. 2015)
Structural Health Monitoring (SHM) (Staszewski et al. 2009)	Ultrasonic Testing (Andrzej Katunin et al. 2015; Staszewski et al. 2009)
Damage in GFRP (Meola & Carlomagno, 2010; Rique et al. 2015)	Thermographic Testing (Maierhofer et al. 2014; Usamentiaga et al. 2013) Radiography (Ataş & Soutis, 2013; Rique et al. 2015)
Auto-detection of impact damage in carbon fiber composites (Usamentiaga et al. 2013) Characterizing damage in CFRP structures (Ataş & Soutis, 2013; Maierhofer et al. 2014)	Thermographic Testing (Maierhofer et al. 2014; Usamentiaga et al. 2013) Radiography (Ataş & Soutis, 2013; Rique et al. 2015)
Impact damage in glass/epoxy with manufacturing defects (Meola & Carlomagno, 2014)	Infrared Thermography (Meola & Carlomagno, 2014)
damage assessment in sandwich structures (Meo et al. 2005) parameters influencing the damping of a structure (Adams et al. 1978) the structures behavior (Cawley; & Adams, 1979) dynamic characteristics for damage detection of structures (Cawley & Adams, 1978) skin damage statistical detection and restoration assessment (Rizos et al. 2008)	Vibration Methods (Loutas et al. 2012; Rizos et al. 2008; Trendafilova et al. 2008)
Multiple Cracks Detection (Zhang et al. 2010)	Neutron Radiography (Zhang et al. 2010)

Table 14- Selected SHM method for GFRP hybrid bogie in the first workshop with partners

Subject	Suggested concepts	Priority
7. Structural health Monitoring	7.1. Regular NDT	P1
	7.2. Fiber Bragg sensors	
	7.3. Piezoelectric sensors	

6- Conclusion

According to the cost calculations provided, the GFRP hybrid bogie's initial costs (manufacturing costs) are close to those of the Y25 bogie. Using low-cost composites (GFRP) and optimizing the use of FRP materials in the bogie frame structure helped to lower the initial cost of the bogie despite the high material and manufacturing costs for FRP composite components. The impact of cost-saving and cost-increasing factors was examined for the hybrid GFRP bogie's maintenance and total life cycle costs. The GFRP bogie's savings from lighter weight and better steering indicate a potential annual cost saving of up to 1200 CHF per bogie. A potential more additional annual reduction of 2100 CHF can be calculated if the low noise bonus is also taken into account. However, because the structural health monitoring systems for FRP structures are more expensive, inspection costs are higher. The cost calculations lead to the conclusion that at least in theory, there isn't significant cost increase over the Y25 bogie for the GFRP hybrid bogie in the current phase. Additional cost savings in the bogie service life may result from the bonuses for weight reduction and noise reduction.

7- References

- [1] DIN EN 15827: Railway applications - Requirements for bogies and running gears, 2011
- [2] FR8HUB, Definition of scenarios for CBM on wagon bogies and definition of subsystem architecture, FR8HUB (shift2rail.org), 2020
- [3] hwh Gesellschaft für Transport-und Unternehmensberatung mbH, Vergleich Drehgestell DRRS25 mit einem Standard-Drehgestell Y25, 2015 (presentation)
- [4] Peose, Drehgestellentwicklung Formica HP, Technical report, 2020
- [5] Scheier, B., Schumann, T., Meyer zu Hörste, M., Dittus, H., & Winter, J. (2013). Wissenschaftliche Ansätze für einen energieoptimierten Eisenbahnbetrieb. Eisenbahn Ingenieur Kalender 2014, 265-278.
- [6] BAFU, BAV, Der besonders lärmarme Güterwagen PFLICHTENHEFT, 2021
- [7] Gholizadeh, S. (2016). A review of non-destructive testing methods of composite materials. Procedia structural integrity, 1, 50-57.
- [8] Wang, B., Zhong, S., Lee, T. L., Fancey, K. S., & Mi, J. (2020). Non-destructive testing and evaluation of composite materials/structures: A state-of-the-art review. Advances in mechanical engineering, 12(4), 1687814020913761.
- [9] Jolly, M. R., Prabhakar, A., Sturzu, B., Hollstein, K., Singh, R., Thomas, S., ... & Shaw, A. (2015). Review of non-destructive testing (NDT) techniques and their applicability to thick walled composites. Procedia CIRP, 38, 129-136.

Differences from the time plan according to the application

All expected tasks in the proposal have been carried out. The tasks are conducting according to the project time table.

Diverse

There is no diverse compare to the plan.

Project No. 5211.02073

Empa report

Assignment

Task 6

Client:

BAFU/BAV, Switzerland

Number of pages:

23

Project title: "FRP bogies for freight wagons: A feasibility study"

Task 6: Rough estimations of noise generation and comparisons with conventional steel bogies

Project leader and contractor: Empa -Structural Engineering Research Laboratory

Project partners:

- PROSE (railway and certification knowledge),
- Ensinger (manufacturer, FRP knowledge),
- SBB cargo (consulting end user),
- WASCOSA (consulting end user),
- Empa 509 (noise control knowledge)

Dübendorf, 07.12.2022

Ali Saeedi / Moslem Shahverdi / Masoud Motavalli

Contents

1- Overview.....	5
2- Noise emission in railway vehicles	5
3- Modeling procedure	7
3.1. Assumptions.....	10
3.2. Static structural analysis	10
3.3. Modal and harmonic analysis.....	12
3.4. Harmonic acoustic analysis	15
4- Estimated noise reduction	21
4.1. Potential noise reduction due to GFRP design.....	21
4.2. Potential noise reduction due to disk brake system	21
5- Conclusion.....	22
6. References	23

List of figures

Figure 1- An overview of the tasks of the project and current step	5
Figure 2- Schematic of rolling noise generation [3]	6
Figure 3- Calculation of total rolling noise considering the effect of wheel, rail and sleepers [3]	6
Figure 4- Geometrical model of the GFRP bogie with the surrounding environment	8
Figure 5- Workflow of harmonic acoustic analysis in Ansys software.....	8
Figure 6- Geometrical model of GFRP bogie	9
Figure 7-Geometrical model of Y25 bogie.....	9
Figure 8- Simplified models of side-beams for GFRP and Y25 bogies	9
Figure 9- The geometrical and finite element models for GFRP bogie frame	10
Figure 10- The geometrical and finite element models for Y25 bogie frame.....	11
Figure 11- Static deformation of bogie frames subjected to applied vertical load	11
Figure 12- Extracted natural frequencies for GFRP bogie (up) and Y25 bogie frame (down)	12
Figure 13- Vibrational mode shapes for the first six natural frequencies for GFRP bogie frame.....	13
Figure 14- Vibrational mode shapes for the first six natural frequencies for Y25 bogie frame	14
Figure 15- Vertical vibration velocity and phase angle for GFRP hybrid bogie.....	15
Figure 16-Vertical vibration velocity and phase angle for Y25 bogie	15
Figure 17- Meshed domain for harmonic acoustic analysis of GFRP bogie	16
Figure 18- Meshed domain for harmonic acoustic analysis of Y25 bogie.....	17
Figure 19- Imported nodal velocities on the GFRP and Y25 bogie frames	17
Figure 20- Frequency dependent nodal velocities for GFRP and Y25 frames.....	18
Figure 21- SPL results for GFRP frame at 200 Hz (left) and 3000 Hz (right)	19
Figure 22-SPL results for Y25 frame at 200 Hz (left) and 3000 Hz (right).....	19
Figure 23- Normalized SPL results for GFRP and Y25 bogie frames at 3.5 m from the center of the bogie.....	20
Figure 24- Damping factors for the wheel with and without disk brakes [7].....	22
Figure 25- Utilizing wheel absorbers (left) and innovative wheel coating (right) for noise reduction [7]	22

List of Tables

Table 1- Reference properties of the surrounding air	16
Table 2- Effective parameters on the estimation of noise reduction in GFRP bogie	21
Table 3- predicted noise emission for the wheels with and without disk brakes [7]	22

1- Overview of Task 6

With the rapid expansion of railway vehicles, the issue of vibration and noise has become more prominent. In addition to proper static strength and good running dynamic behavior, the noise emission of the bogie should be considered an important parameter in the design and development stages. The current report corresponds to Task 6, "Rough estimations of noise generation and comparisons with conventional steel bogies" of the FRP bogie for freight wagons project (phase I). The developed conceptual design in Task 3, and finite element analysis results in Task 4, are used to conduct a comparative evaluation of noise emission for the bogie, as illustrated in Figure 1. Following the definition of noise analysis parameters, different sources of noise emission are introduced in the following sections. Among those, structure-born noise of the bogie frame is investigated using the finite element approach, and noise emissions of the newly introduced GFRP bogie and the standard Y25 bogie are compared. This type of analysis allows for an estimation of the noise-reduction capabilities of GFRP bogie design.

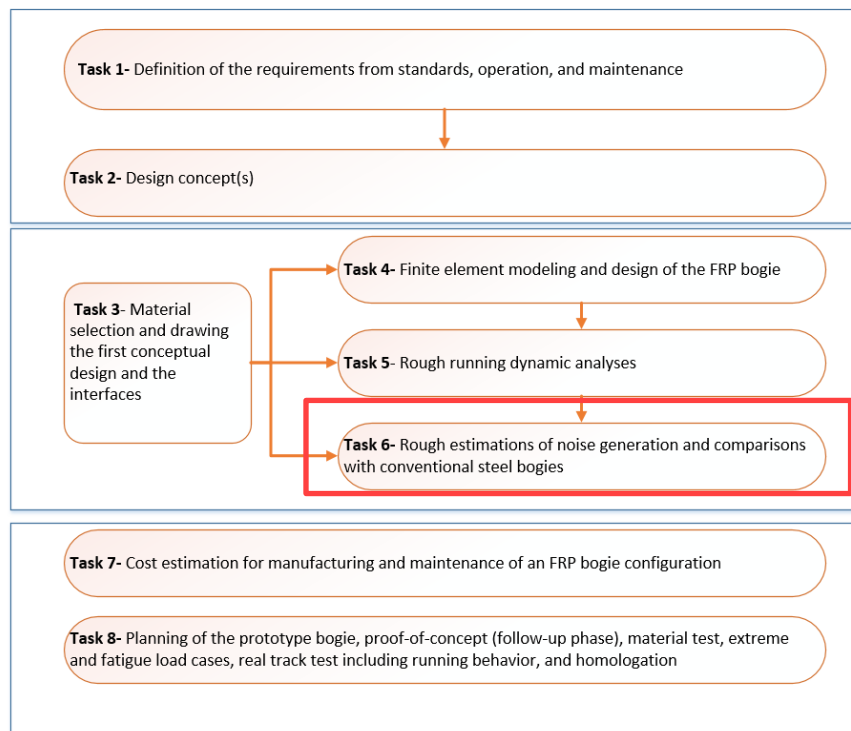


Figure 1- An overview of the tasks of the project and current step

2- Noise emission in railway vehicles

The sound pressure level (SPL) is the tool used to measure acoustic wave intensity most frequently. The SPL can represent loudness and can be measured with inexpensive tools. The reference SPL is calibrated to a young person's hearing threshold. The resultant level is 0 dB when the sound pressure is equal to the reference pressure. The sound pressure level is defined as [1]:

$$L_p = 10 \log \frac{P^2}{P_{ref}^2}$$

Where P is the sound pressure and p_{ref} is the reference sound pressure that is $2 \times 10^{-5} Pa$. Weighted sound pressure level is the frequency and time weighted sound pressure in decibels and is also known as the sound level. Standard frequency weightings A, B and C, and standard exponential time weightings fast (F), slow (S) and impulse (I) are given in IEC 651 sound level meters [2].

There are several sources of noise emission in the railway vehicles. The most important sources that produce audible noises (20 to 20000 Hz) can be categorized as follows [3]:

- **Rolling noise**

The main and most significant source of rail vehicle noise emission can be regarded as rolling noise. As schematically shown in Figure 2, the rolling noise is produced at the point where the wheel and rail make contact and is greatly influenced by the degree of roughness on the wheel and rail sides. Thus, the bogie is not the only component of the noise emission; rails and sleepers also play a significant role. The total noise can be calculated by taking into account the noise emissions from wheels, rails, and sleepers, as shown in Figure 3.

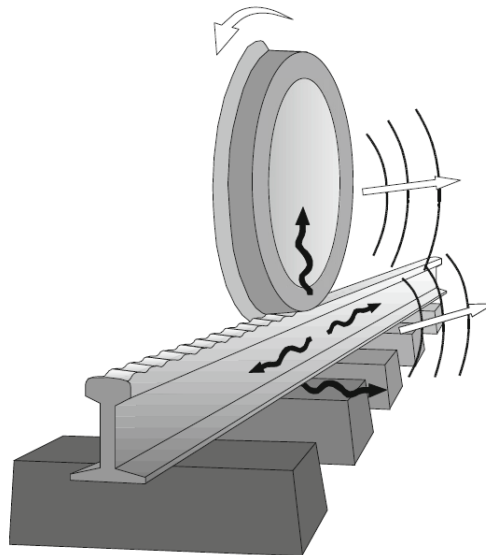


Figure 2- Schematic of rolling noise generation [3]

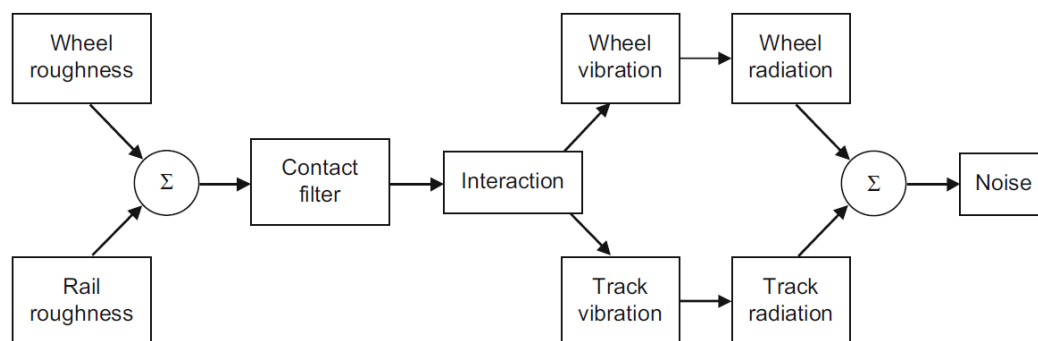


Figure 3- Calculation of total rolling noise considering the effect of wheel, rail and sleepers [3]

- **Curve squeal noise**

Curve squeal is a sound produced by contact between the wheels and rails. The wheel is excited by the applied transverse forces, and as a result of the resonance phenomenon, audible noise is produced at the wheel/rail contact region.

- **Aerodynamic noise**

The fluid/solid interaction in high speeds is the source of excitation for this type of noise, and the rail vehicle's running speed has a significant impact on the noise level. However, aerodynamic noise dominates when it comes to car bodies and high-speed trains, but other noise sources are essentially dominant when it comes to freight bogies.

- **Component's structure born noise**

The structure-borne noise is generated as a result of structural vibration of the railway vehicle's components. The entire bogie frame and attached parts, such as the suspension and damping systems, brake parts, etc., contribute to the overall noise emission. The design of railway components heavily relies on predictions of structure-borne noise and sound propagation.

3- Modeling procedure

In this section, the numerical analysis takes into account bogie frame structure-born noise, one of the previously mentioned sources for noise emission. In order to simulate the noise emission characteristics of the developed GFRP bogie and compare it to the Y25 bogie, finite element analysis (FEM) was used. The steady-state response of a particular structure, like a bogie frame, and the surrounding air medium to loads and excitations that vary harmonically over time can be investigated using harmonic acoustic analysis. Harmonic acoustic analysis on 3D geometries is possible with the aid of Ansys software.

The air surrounding the physical geometry needs to be modeled as a component of the overall geometry for the harmonic acoustic analysis. GFRP bogie frame geometry is shown in Figure 4, along with air that has been prepared for the harmonic acoustic analysis.

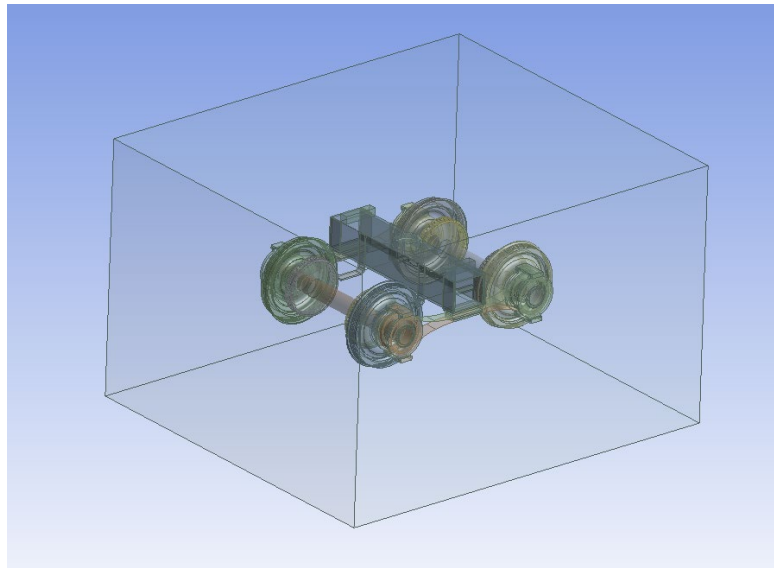


Figure 4- Geometrical model of the GFRP bogie with the surrounding environment

Figure 5, depicts the acoustic simulation's workflow. In order to apply the pre-stress effect caused by the structural load on the vibrational characteristics of the bogie frame, a structural analysis is first performed. To obtain the structural vibrational velocities required as inputs for the acoustic calculation, FEM structural dynamics analysis (modal and harmonic) is then performed. Finally, harmonic acoustic analysis is used to determine the radiated sound field in the 200 to 5000Hz frequency range.

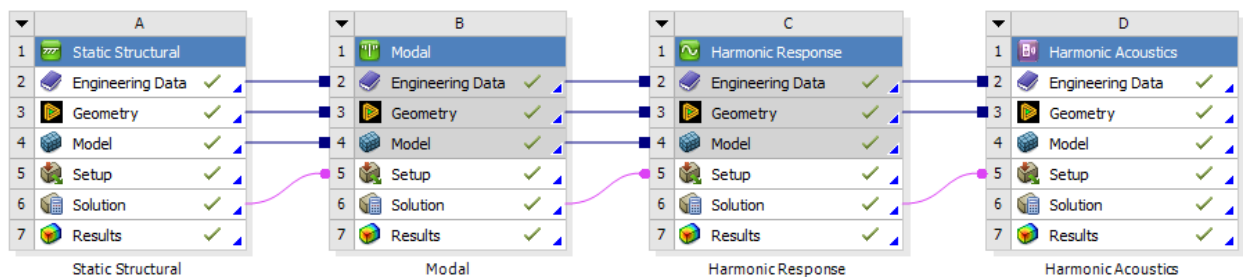


Figure 5- Workflow of harmonic acoustic analysis in Ansys software

Two geometrical models are first prepared for the analysis, as seen in Figures 6 and 7, for the new hybrid GFRP bogie and the conventional Y25 bogie, respectively. It was determined following a meeting with noise specialists (Empa 509) on July 20 that too much detail is lacking for quantitative work. Therefore, rather than obtaining quantitative results for the noise amount, we chose to use simplified models and focus on the comparative study of the Y25 and new FRP bogies. The main distinction between the two aforementioned bogie models can be seen in the side beams of the bogie frames, which make up the simplified models. Figure 8, provides an illustration of the simplified models' geometries.

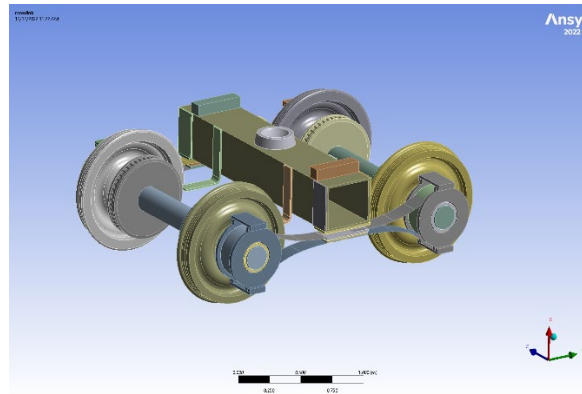


Figure 6- Geometrical model of GFRP bogie

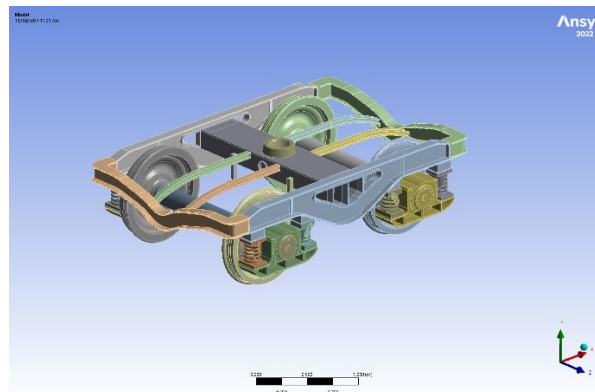


Figure 7-Geometrical model of Y25 bogie

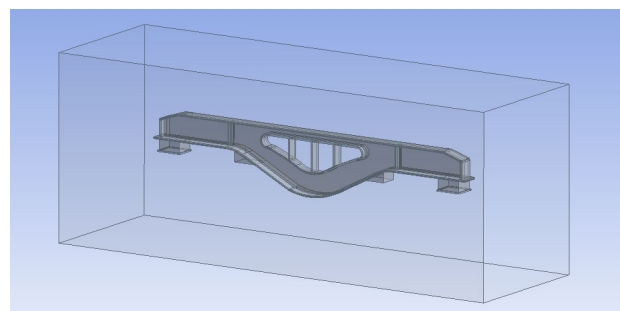
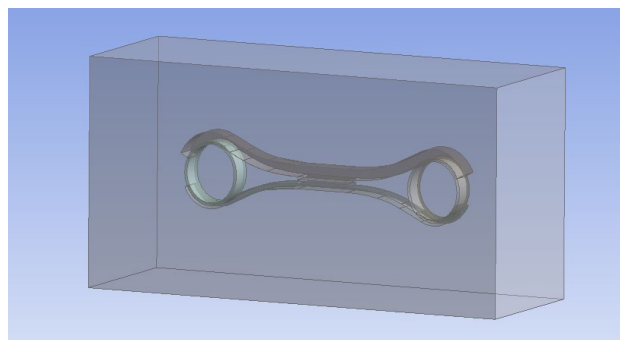


Figure 8- Simplified models of side-beams for GFRP and Y25 bogies

To perform a harmonic acoustic analysis, the element size must meet certain criteria. The element size should be small enough to capture the pressure mode shapes and is frequency dependent. For linear element formulation, at least 12 elements per wavelength (i.e. $\lambda = c/f$) are needed while six elements per wavelength are needed for quadratic element formulation [4, 5]. On the other hand, the acoustic enclosure of the FEM model requires to include at least one quarter wave length distance to the closest source point. This implies that the truncation of the far field domain (i.e. distance of the acoustic enclosure) is driven by the lowest frequency of interest (i.e. f_{min}) [5].

Symmetry condition was used to reduce the analysis time by taking into account the analysis's required element count in accordance with the frequency range (200 Hz - 5000 Hz). In this case, only one-fourth of the geometry was modeled, and symmetric boundary conditions were used in both the structural and acoustic simulations on the symmetry planes.

3.1. Assumptions

The assumptions that are taken into consideration are as follows:

- The frequency range between 200 Hz and 5000 Hz is considered for the analysis.
- One symmetry plane is used for the analysis.
- The results for SPL are extracted at a distance of 3.5 m from the center of the component.
- For static analysis, vertical exceptional loading is taken into account.
- For harmonic loading, a unique load was applied for both bogie models.
- Radiation boundary condition is applied to the boundaries of the model.

3.2. Static structural analysis

Static analysis of the frames is carried out as the first step of the harmonic-acoustic prediction by applying an exceptional vertical load. Figures 9 and 10, show the frame geometries (for two different types of bogie frames) and the mesh part.

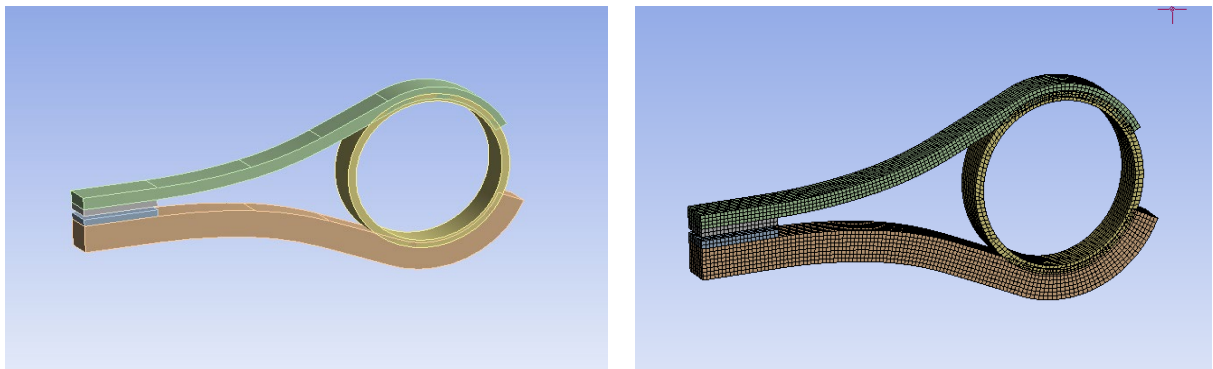


Figure 9- The geometrical and finite element models for GFRP bogie frame

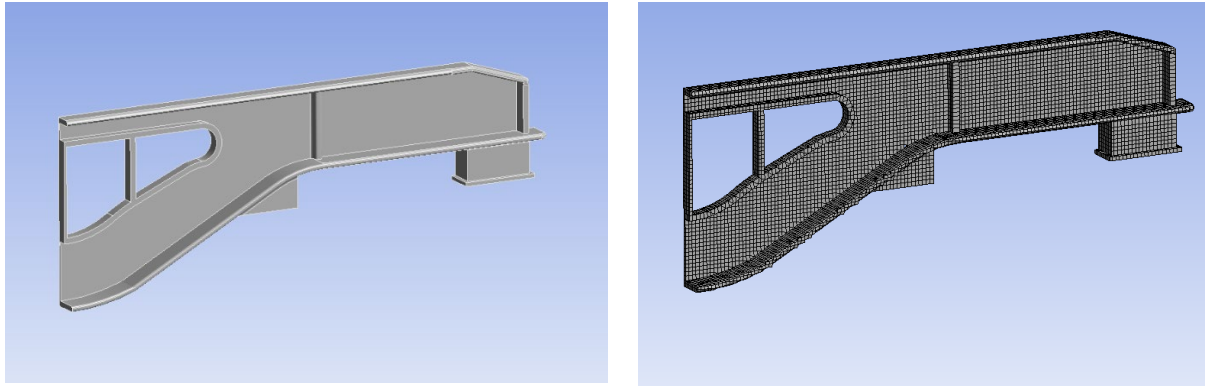


Figure 10- The geometrical and finite element models for Y25 bogie frame

Figure 11, shows the results of the frames' total deformation. Elastic supports were designed for the Y25 bogie frame to simulate the effect of a suspension system. The deformation results are used to adjust the stiffness of the elastic support foundation.

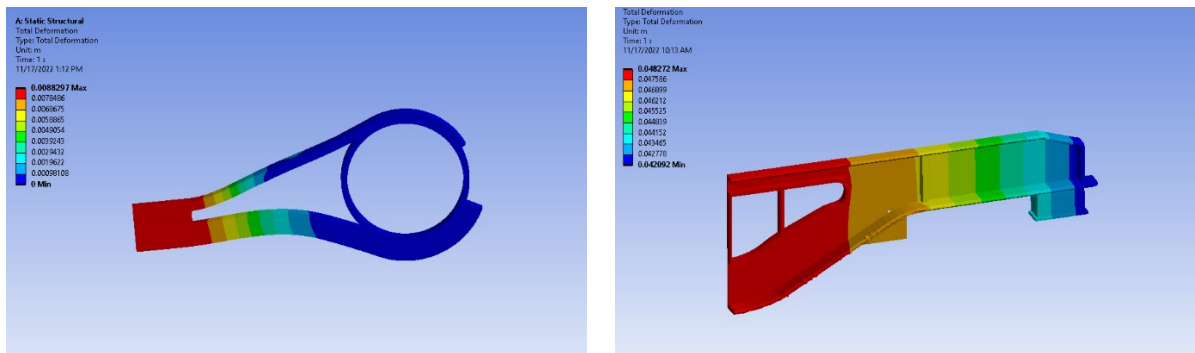


Figure 11- Static deformation of bogie frames subjected to applied vertical load

3.3. Modal and harmonic analysis

The second and third steps of the harmonic acoustic analysis are the modal and harmonic analyses. The bogie frames were first subjected to a modal analysis using pre-stress input information from an earlier static structural analysis. The natural frequencies were extracted using a selected frequency range of 200 Hz to 5000 Hz. In the current project, the modal analysis is used to determine the resonance frequencies of the bogie frames. In order to properly choose the frequencies for the harmonic analysis and shorten the simulation time, the obtained eigen-frequencies are used. Figure 12, displays the obtained natural frequencies for two bogie frames.

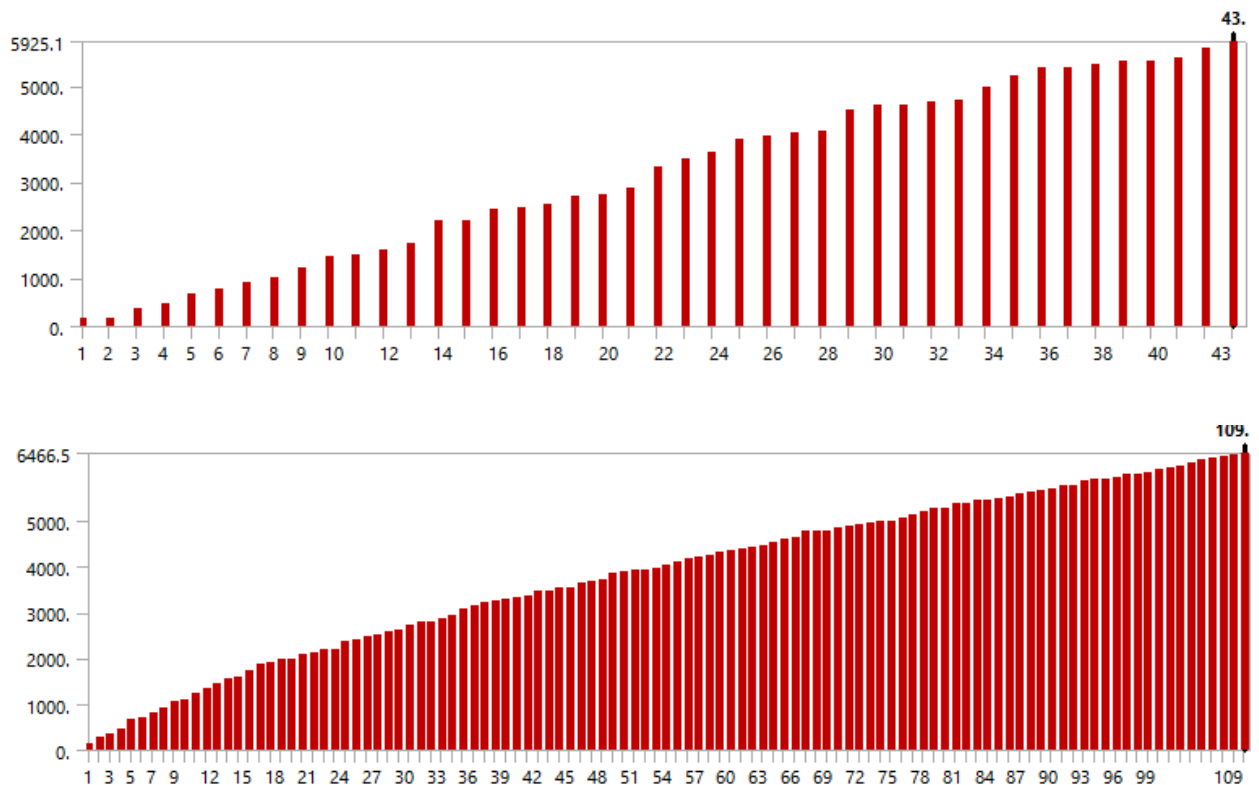


Figure 12- Extracted natural frequencies for GFRP bogie (up) and Y25 bogie frame (down)

Within the required analytical range, the vibration mode shapes can also be extracted for the obtained natural frequencies. Figure 13, illustrates the mode shapes for the GFRP frame's first six natural frequencies. Figure 14, shows the same requested mode shapes for the Y25 bogie frame.

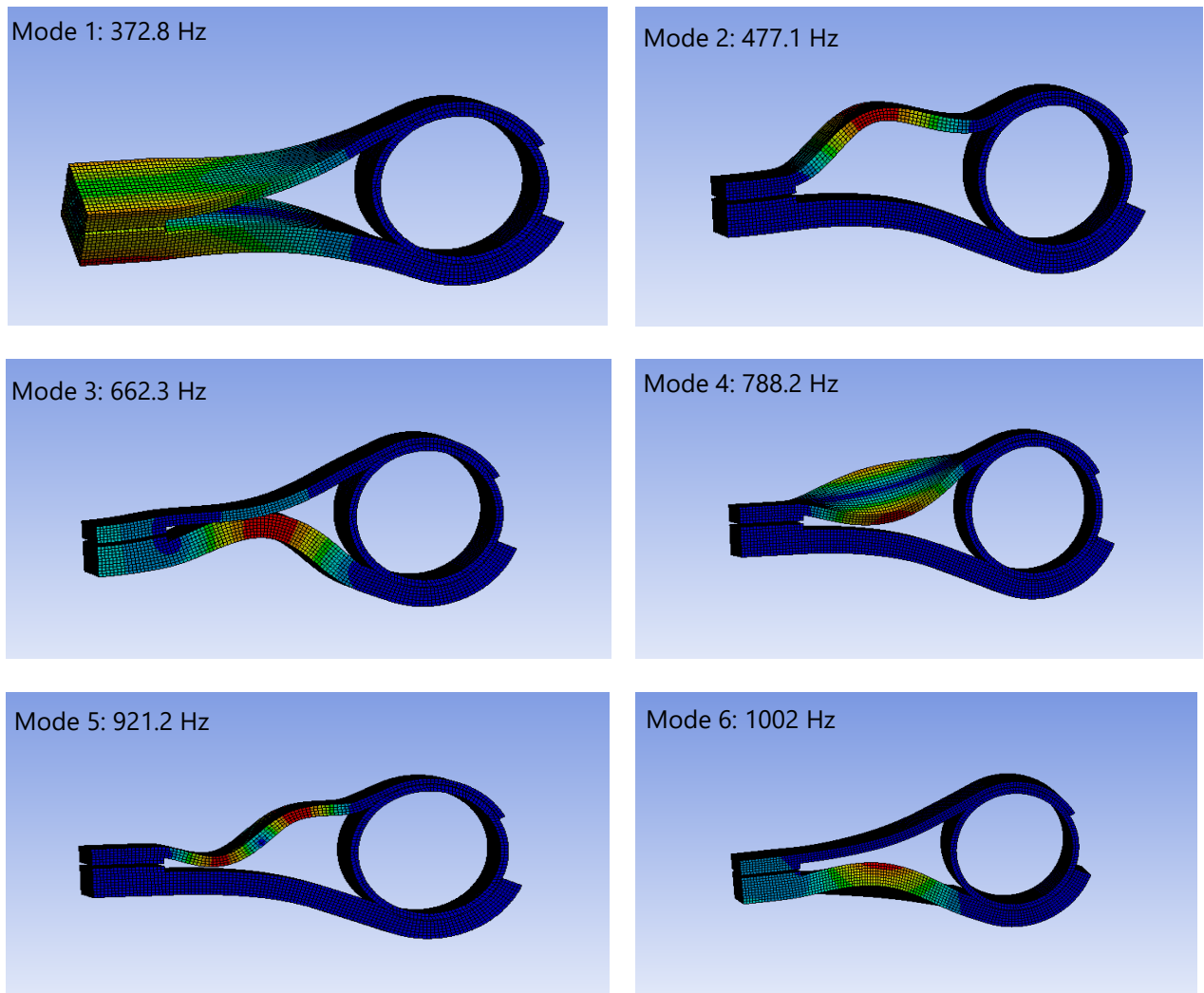


Figure 13- Vibrational mode shapes for the first six natural frequencies for GFRP bogie frame

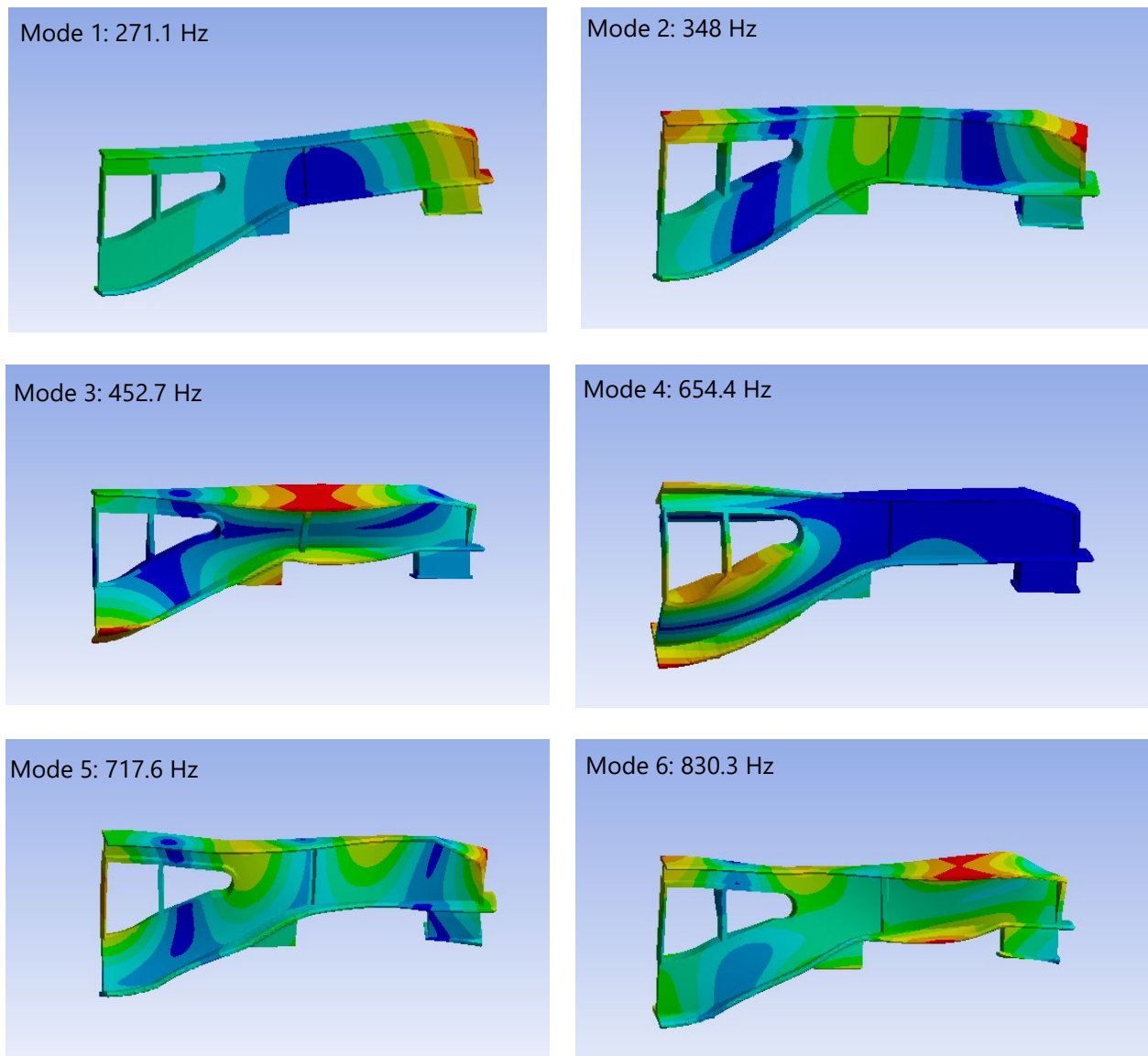


Figure 14- Vibrational mode shapes for the first six natural frequencies for Y25 bogie frame

The bogie frame structure is subjected to harmonic analysis in the following stage. A unit vertical force was applied to the bogie as the excitation and for comparison purposes. The results can be used to extract the frequency-dependent directional velocities in the vertical direction. The GFRP bogie's amplitudes and phase angles, as well as the Y25 bogie frame's, are shown in Figures 15 and 16, respectively, for the directional velocities.

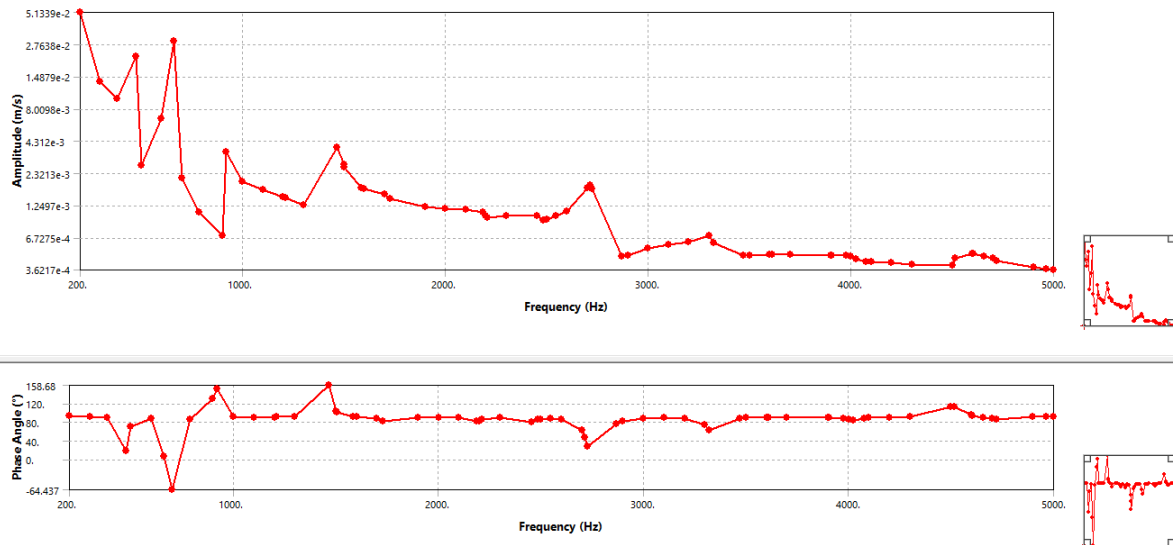


Figure 15- Vertical vibration velocity and phase angle for GFRP hybrid bogie

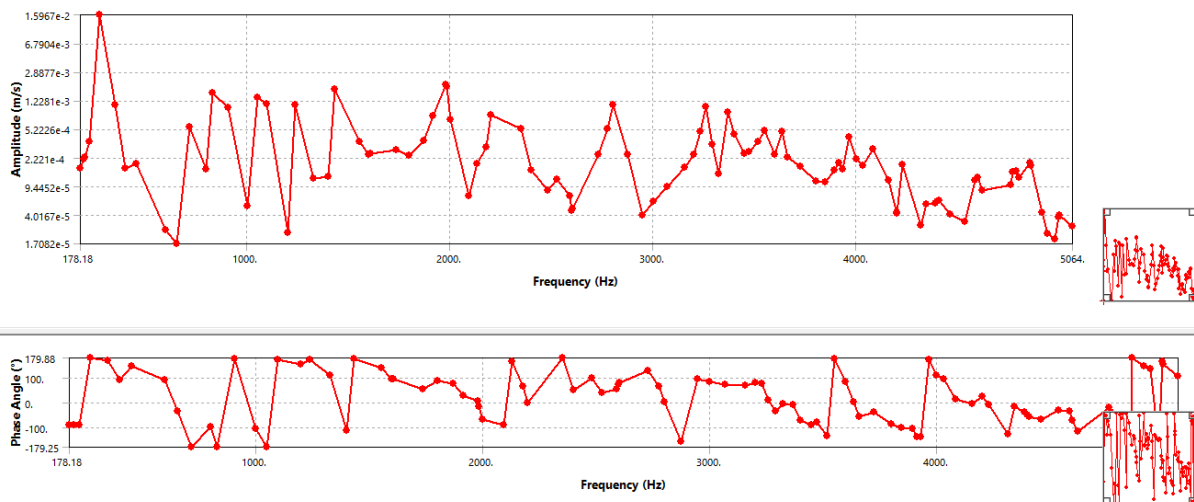


Figure 16-Vertical vibration velocity and phase angle for Y25 bogie

3.4. Harmonic acoustic analysis

To estimate the structure-borne noise emission, harmonic acoustic analysis is applied to the bogie frames using the obtained nodal velocities from the previous analysis (harmonic analysis) as the inputs. The surrounding air environment around the frames is meshed and analyzed in the harmonic acoustic analysis. Table 1, lists the reference attributes of the surrounding environment.

Table 1- Reference properties of the surrounding air

Air	
Density	1.225 kg/m ³
Thermal	
Isotropic Thermal Conductivity	0.0242 W/m·°C
Specific Heat Constant Pressure	1006.4 J/kg·°C
Magnetic	
Isotropic Relative Permeability	1
Fluid	
Speed of Sound	346.25 m/s
Viscosity	1.7894e-05 Pa·s
Other	
Molecular Weight	28.966 kg/kmol
Lennard Jones Length	3.711 m
Lennard Jones Energy	78.6 J
Thermal Accom Coefficient	0.9137
Velocity Accom Coefficient	0.9137 m/s
Formation Entropy	1.9434e+05 J/°C
Reference Temperature	25 °C
Critical Pressure	3.758e+06 J/m ³
Critical Temperature	-140.85 °C
Acentric Factor	0.033
Critical Volume	0.002857 m ³
Absorption Coefficient	0 1/m

Based on the presumptions in Section 3, the model was meshed. The meshed models of the GRFP and Y25 bogies are displayed in Figures 17 and 18, respectively.

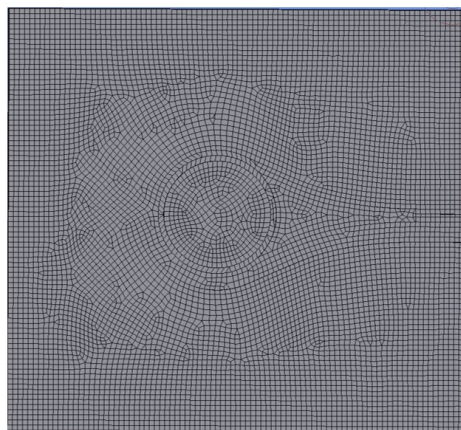


Figure 17- Meshed domain for harmonic acoustic analysis of GFRP bogie

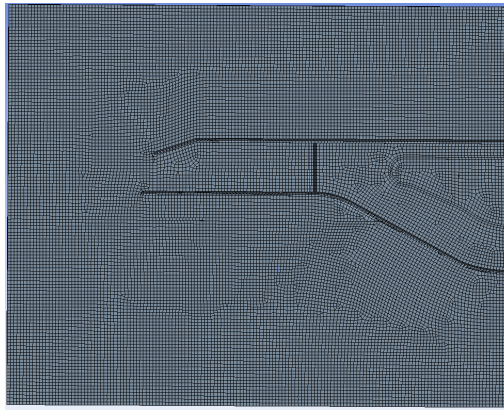


Figure 18- Meshed domain for harmonic acoustic analysis of Y25 bogie

The harmonic acoustic model's nodes are then mapped with the nodal velocities that were imported from harmonic analysis. In Figure 19, the imported velocities are depicted. In Figure 20, a comparison chart for the velocity results on the GFRP and Y25 frames is shown. Lower values are shown for the majority of frequencies within the applied frequency range in the GFRP frame results.

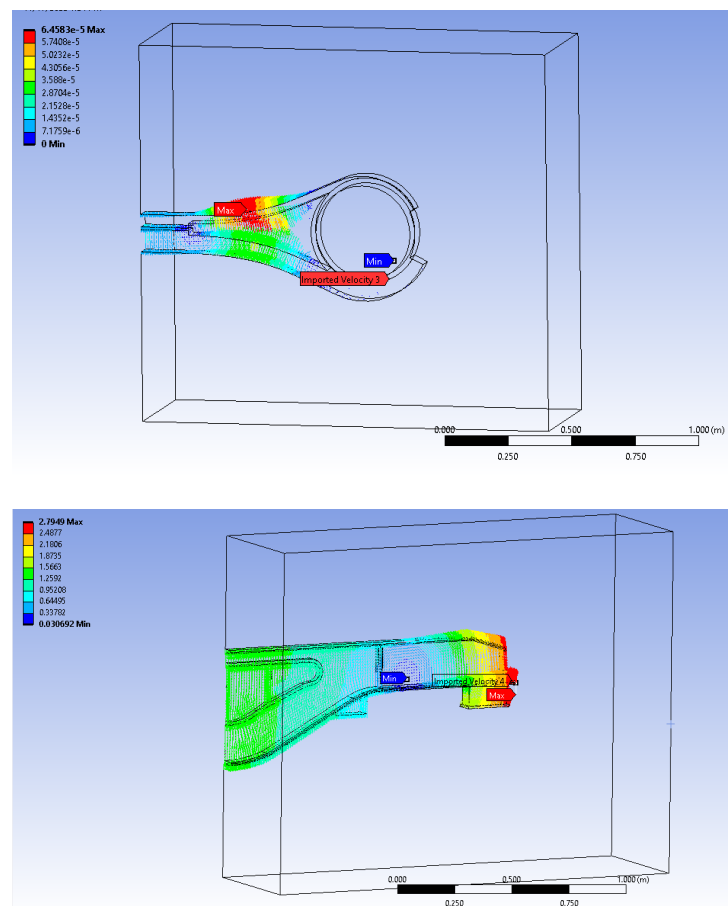


Figure 19- Imported nodal velocities on the GFRP and Y25 bogie frames

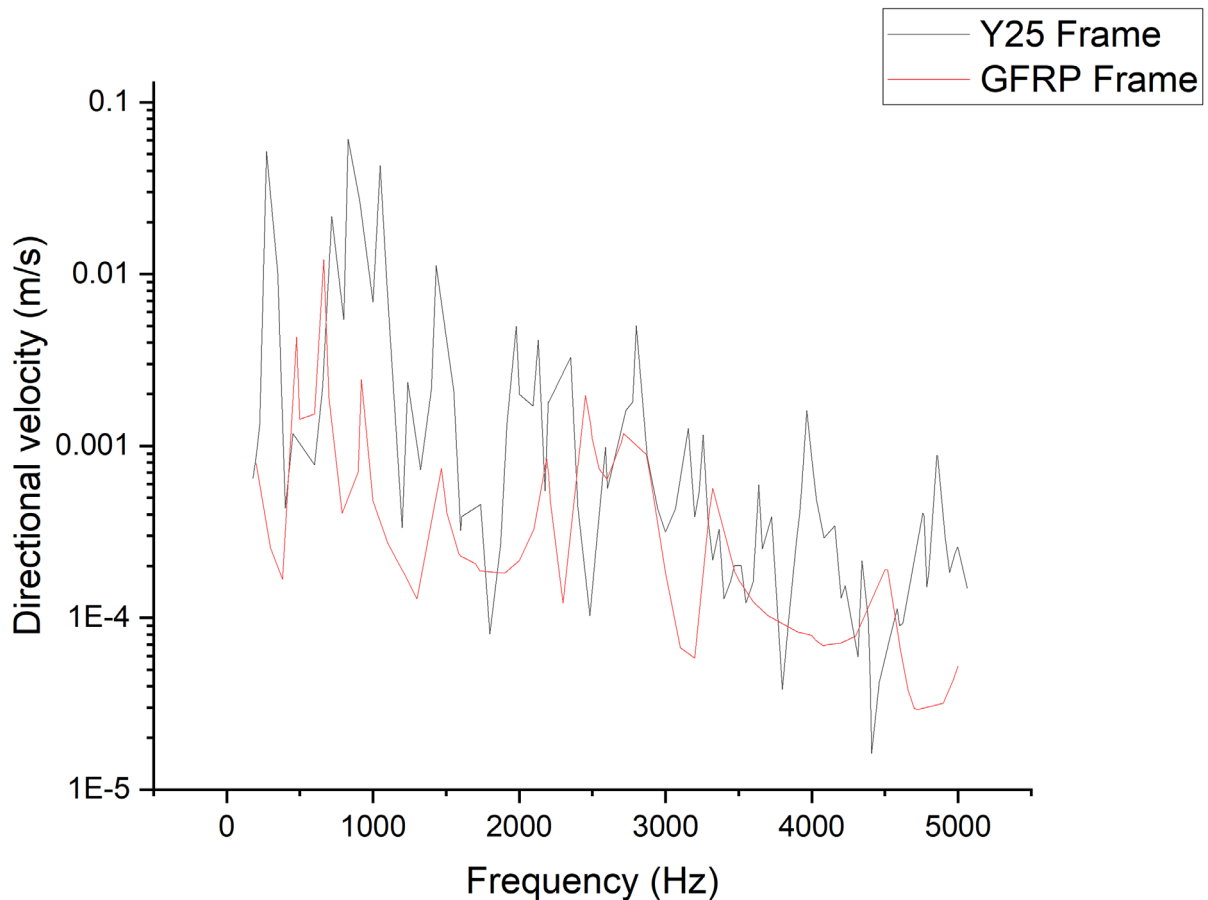


Figure 20- Frequency dependent nodal velocities for GFRP and Y25 frames

Pressure, impedance boundary, absorption surface, absorbing element, radiation surface, rigid wall, free surface, port, far field radiation surface, symmetry plane, and thermo-viscous boundary are the acoustic boundary conditions that are available in ANSYS acoustic simulations. Radiation boundaries were applied to the enclosure's exterior faces in the current project. The Radiation Boundary condition enables the analysis to approximate infinity and to dampen the effect of sound pressure on the impedance boundary.

The weighted sound pressure level can be obtained from the simulation as a result of acoustic analysis. As a sample, the distribution of the weighted sound pressure level for the frequencies 200 and 3000 Hz is shown in Figures 21 and 22, for the acoustic domain of GFRP and Y25 frames, respectively.

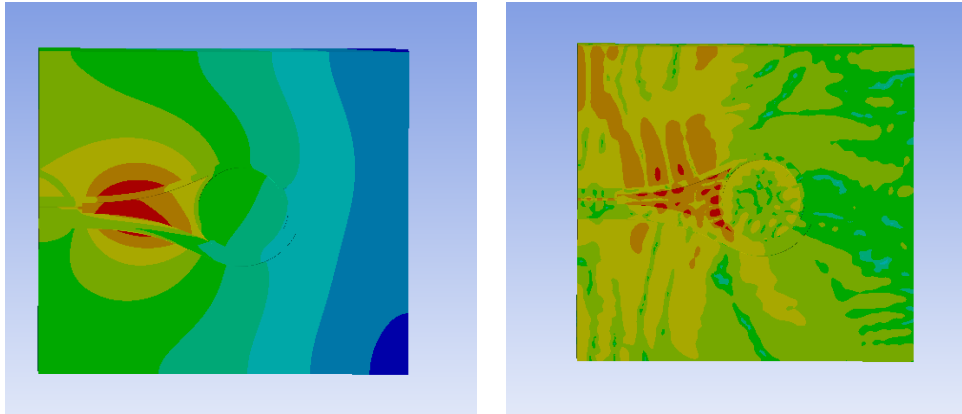


Figure 21- SPL results for GFRP frame at 200 Hz (left) and 3000 Hz (right)

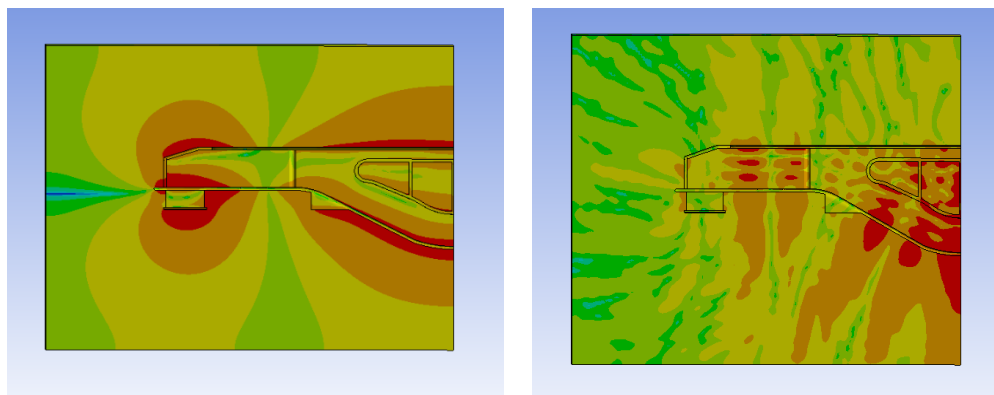


Figure 22-SPL results for Y25 frame at 200 Hz (left) and 3000 Hz (right)

Sound pressure level (SPL) results were extracted in the required frequency range to compare the noise emission between GFRP and Y25 frames (200 – 5000 Hz). The results are only used for comparison between two cases, as was previously mentioned in section 3, due to a lack of necessary inputs. The SPL results are normalized in this regard (divided by the highest SPL amount for Y25 frame). Figure 23, reveals the frequency dependent normalized SPL results for GFRP and Y25 frames. The maximum SPL for the GFRP bogie, as shown in the results, is 0.9 of that of the Y25 frame, which equates to a 5% reduction in SPL for the GFRP frame in comparison to the Y25 bogie frame.

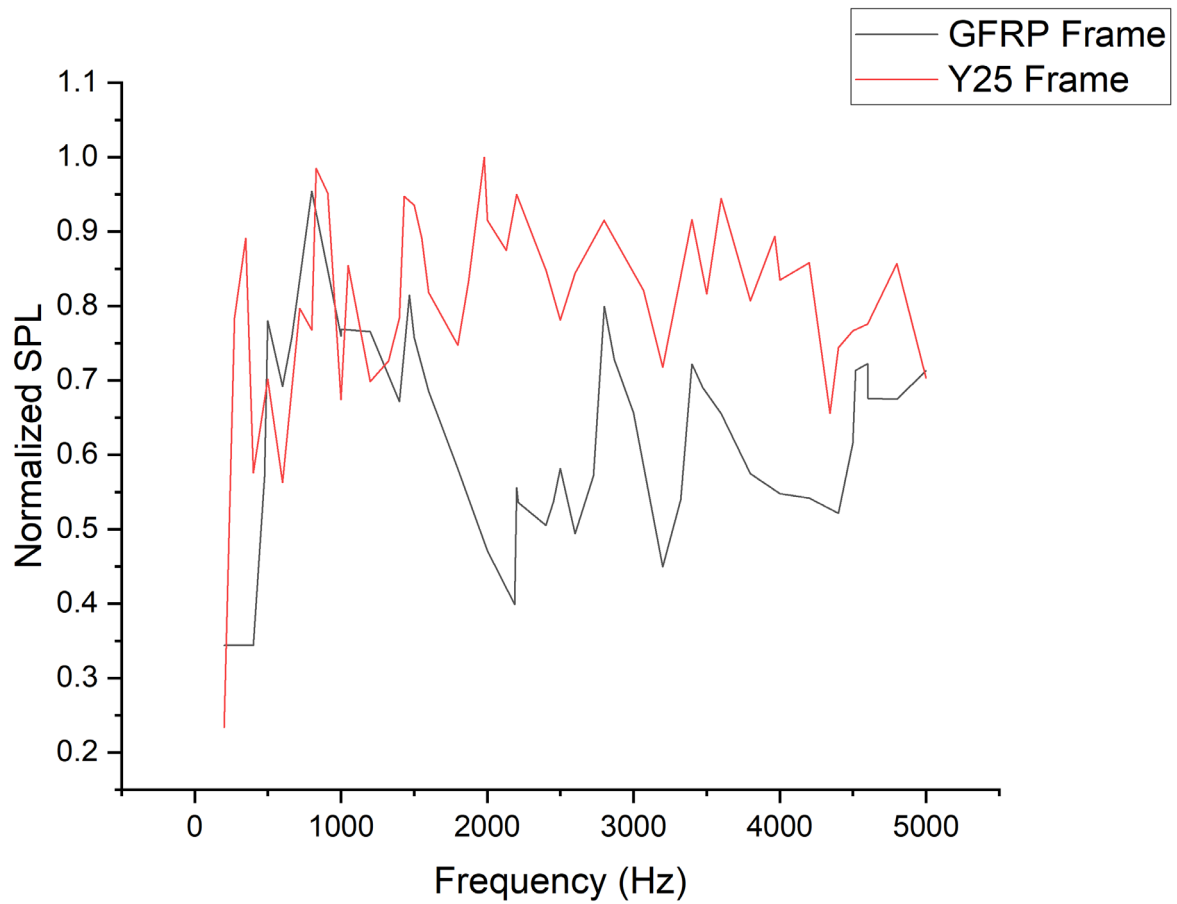


Figure 23- Normalized SPL results for GFRP and Y25 bogie frames at 3.5 m from the center of the bogie

4- Estimated noise reduction

There are two categories of noise reduction potential for the newly introduced GFRP bogie. The first group of parameters relates to the bogie's design specifications, and the second group is concerned with the use of the disk brake system in the bogie. The following subsections provide a summary of the expected noise reduction factors, which are shown in Table 2, and discussed there.

Table 2- Effective parameters on the estimation of noise reduction in GFRP bogie

No.	Effective parameters on noise reduction	Noise reduction potential	Noise reduction group
1	Structural born noise of the bogie frame	Reduction (5%)	GFRP design
2	Removing frictional damper	...	GFRP design
3	Removing suspension springs	...	GFRP design
4	Decoupling structural born noise by rubber elements	...	GFRP design
5	better running dynamic (Curve Squeal Noise)	...	GFRP design
6	Noise reduction of using disk brakes	~1 dB [7]	Disc brake
7	Noise reduction of using wheel absorbers	~2.5 dB [6]	Disc brake
8	Noise reduction of wheel-axle- cover	~2 dB [6]	Disc brake
9	Using wheel with straight bridge	...	Disc brake

4.1. Potential noise reduction due to GFRP design

The total noise emission of the bogie structure is dependent on a number of factors, including the working speed, the joints and connections between parts, attached components to the bogie, brake system, etc., as was mentioned in section 3. Structure-born noise from the bogie frame was taken into account and compared for two different types of bogies in section 3.3. For the GFRP bogie, a 5% reduction in maximum SPL was calculated from FEM. The contribution of the structure-borne noise emission of the frame to the overall audible noise from the bogie must be measured experimentally or predicted by a more in-depth numerical study and verified by experiment, depending on the working conditions and other mentioned parameters.

There are additional design requirements for GFRP bogies that, in addition to the frame structure-born noise, may result in noise reduction. Bogie noise can be significantly reduced by removing the frictional damper (Lenoir damper) and primary suspension system (springs). Additionally, using rubber components in the contact areas aids in decoupling noise generated by the structure in the bogie structure. Curve squeal noise can also be reduced by enhancing the running dynamic behavior by using cross-beams and flexible FRP components.

4.2. Potential noise reduction due to disk brake system

In addition to GFRP design, employing a disk brake system rather than a push brake has the advantage of being less noisy. According to [7] and as shown in Figure 24, the use of disk brake systems increases the frequency dependent damping ratio. As a result, a significant noise reduction is possible. According to Table 3, from a study on freight locomotive, using disk brake system is expected to result in a noise reduction of 1 dB overall and 2 dB for the wheels.

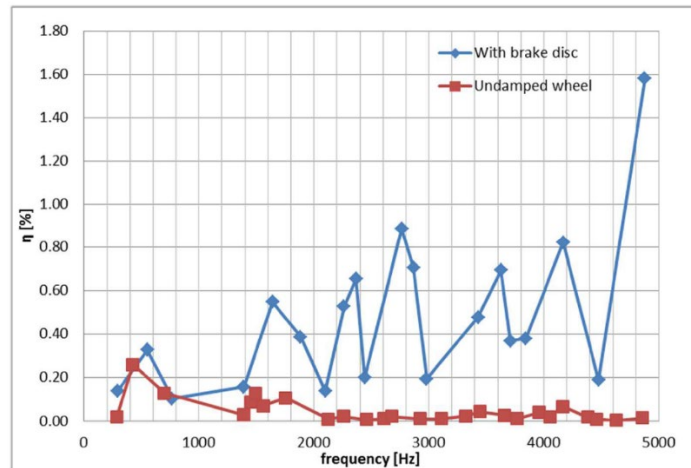


Figure 24- Damping factors for the wheel with and without disk brakes [7]

Table 3- predicted noise emission for the wheels with and without disk brakes [7]

Lp [dB (A) ref.2x10 ⁻⁵ Pa]	Total	Wheel	Track
Wheel without brake disk	77	72	74
Wheel with brake disk	76	70	74

Additionally, using a disk brake system enables the inner side of the wheels and the axle to be coated with innovative coating materials. Such coatings reportedly have a 2 dB noise reduction potential. In typical working conditions, using wheel absorbers can also result in a 2.5 dB noise reduction [6, 7]. Figure 25, shows a sample of the inner coating and wheel absorbers.



Figure 25- Utilizing wheel absorbers (left) and innovative wheel coating (right) for noise reduction [7]

5- Conclusion

The two different types of bogie frames—the newly developed GFRP and the Y25 bogie frame—were subjected to a comparative harmonic acoustic analysis. The preliminary results indicated that GFRP frames can reduce noise by about 5% (for frame structure born noise); however, it is necessary to investigate the impact of bogie frames on overall audible noise using experimental data. The potential to further reduce noise exists in the

removal of dampers and suspension systems, as well as in the presence of rubber components for decoupling structure-born noise. Disk brakes, in addition to the frame design, can also reduce the bogie's noise because they improve the wheel/rail contact, which in turn reduces rolling noise. Moreover, employing a disk brake system makes it possible to use additional innovating coating and absorbers to reduce the noise emission.

The GFRP bogie has several parameters that aid in noise reduction, and no appreciable noise increase can be found as described in this report. However, more information is needed to make an exact prediction of noise reduction.

6. References

- [1] Hansen, C. H. (2001). Fundamentals of acoustics. *Occupational Exposure to Noise: Evaluation, Prevention and Control. World Health Organization*, 1(3), 23-52.
- [2] IEC651, M. E. E. T., STANDARD, T. C., ABSORBER, U. B. N., HOLD, M., MAX, R., FAST, M., ... & MOUNTABLE, T. (1979). Sound Level Meter.
- [3] Thompson, D. (2008). *Railway noise and vibration: mechanisms, modelling and means of control*. Elsevier.
- [4] Marburg, S. (2002). Six boundary elements per wavelength: Is that enough?. *Journal of computational acoustics*, 10(01), 25-51.
- [5] Towards noise and weight reduction by application of FRP wheelset for freight wagons - Acoustic Modelling, Empa report, 2018
- [6] Mitusch, K., & Hecht, M. (2017). Strategien zur effektiven Minderung des Schienengüterverkehrslärms.
- [7] Dyna Freight, Noise reduction on freight locomotive bogies, Ares(2019)217263 - 15/01/2019

Differences from the time plan according to the application

All expected tasks in the proposal have been carried out. The tasks are conducting according to the project time table.

Diverse

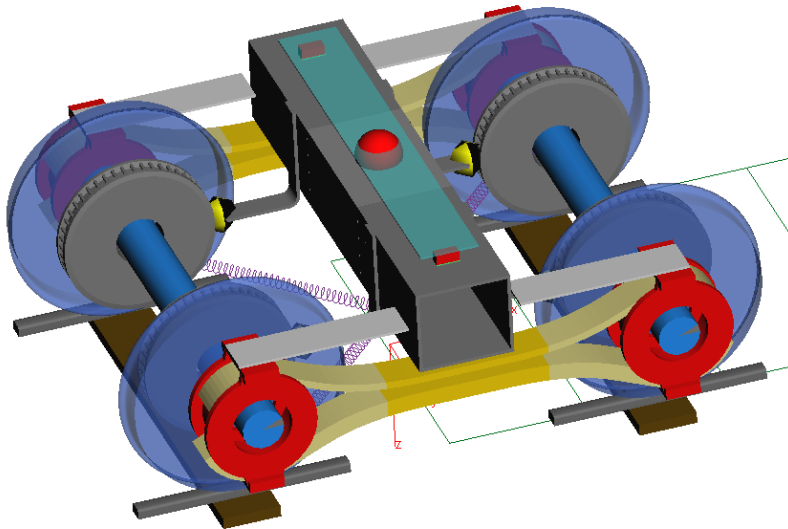
There is no diverse compare to the plan.

Previously submitted reports

Running dynamics analyses

Concept calculation

Report



Project PROSE: CH01-03137-01
EMPA FRP Bogie Laufdynamik Analyse

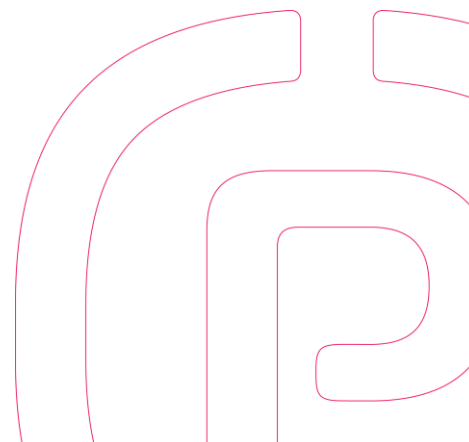
EMPA

Prepared	Checked	Released	
Demian Meuter	Florine Frank	Demian Meuter	
Document Number	Version	Status	Release Date
PO000001876	1.0	Released	03.08.2022

PROSE AG
Zürcherstrasse 41
8400 Winterthur
Switzerland

www.prose.one

+41 52 262 74 00
info@prose.one



Distribution

Company/Department/Name	Remarks

Version	Prepared	Checked	Released	Date
Ver 1.0	Demian Meuter	Florine Frank	Demian Meuter	03.08.2022

Modifications

Version	Description

This document discloses subject matter in which the PROSE Ltd., Winterthur (Switzerland) or one of its subsidiary companies, has proprietary rights. Neither receipt nor possession thereof confers any right to reproduce or disclose the document, any part thereof, any information contained therein, or any physical article or device, or to practise any methods or process, except by written permission from or written agreement with, PROSE Ltd., Winterthur (Switzerland).

This document is computer-generated and valid without signature.

1	Introduction	4
2	Analysis specification.....	4
3	Summary of simulation results.....	4
3.1	Safety against derailment	4
3.2	Radial steering and wear analysis	4
3.3	Non-linear running stability	4
3.4	Dynamic analysis	4
4	Conclusion	5
5	Bibliography.....	6

Annex

A	Initial model description	7
B	Adjustment of bogie characteristics	10
B.1	Vertical load on central pivot	10
B.2	Transverse force on central pivot	14
B.3	Longitudinal force on central pivot.....	15
B.4	Lifting of wheel	16
B.5	Lateral force on wheel	18
B.6	Natural frequencies for side-down component.....	19
B.7	Summary of testbench results.....	19
C	Adapted bogie concept	20
D	Safety against derailment	22
D.1	Analysis method.....	22
D.2	Results initial bogie	24
D.3	Results adapted bogie	25
E	Radial steering and wear analysis	27
E.1	Analysis method.....	27
E.2	Results initial bogie	27
E.3	Results adapted bogie	28
F	Non-linear running stability	30
F.1	Analysis method.....	30
F.2	Results initial bogie	30
F.3	Results adapted bogie	32
G	Dynamic analysis	34
G.1	Analysis method.....	34
G.2	Results adapted bogie	35

1 Introduction

EMPA has been commissioned by the Bundesamt für Umwelt (BAFU) to conduct a feasibility study for a FRP (fiber-reinforced plastic) bogie for freight rail transport. PROSE is to support EMPA with railroad expertise in the form of an accompanying consultancy and the performance of the running dynamics analysis.

The basis for the running dynamics analysis is a bogie concept which was setup during joint meetings. The concept was modelled by EMPA and a FE-Analysis was done to get an initial parameter set for the running dynamics simulations. Based on insights gained through first simulations, this initial bogie design was optimized and an adapted bogie design was proposed.

2 Analysis specification

Following simulations are performed:

- Safety against derailment
- Radial steering and wear analysis
- Non-linear running stability
- Dynamic analysis

3 Summary of simulation results

3.1 Safety against derailment

The initial and the adapted bogie design show promising results for the safety against derailment with Y/Q values both for empty and fully loaded vehicle below the limit value. For the adapted design concept, the vertical stiffness must be recalculated to match the maximal deflections of a Y25 bogie.

3.2 Radial steering and wear analysis

After adding a low stiffness rubber / connection between the FRP parts and the axleboxes, both designs show a slightly better curving behavior than the simplified Y25 bogie. Further optimization of the drawbar / crosslinks could decrease the wheel/rail wear and angle of attack even more.

3.3 Non-linear running stability

Both concepts show a good running stability up to 130 km/h on a track with an equivalent conicity of around 0.2. Further investigations for the full range of possible conicities must be done in the next design loops for the more detailed bogie concept to get a more complete picture.

3.4 Dynamic analysis

The adapted bogie design shows values that exceed the limit values of EN 14363 for running safety by a slight margin with the empty vehicle and by a bigger margin with a fully loaded vehicle. Mainly the SumY, Y/Q and lateral carbody accelerations are exceeded. First detailed investigations show high accelerations around 3 Hz in the carbody which could indicate low body motion. Further investigation of the damping of the FRP parts as well as optimizations of the parameters should enable lowering these values.

4 Conclusion

The initial bogie design shows high parasitic influence of secondary elements (T-Link) on the vertical and lateral stiffness of the bogie suspension. This results for the T-Links in very high loads which make the design unfeasible or only possible with a lot of effort in designing the interfaces and load paths.

Based on this insight, an adapted design is proposed, where the FRP suspension is decoupled from the axis and the T-Links are replaced by a longitudinal bar connecting the axle boxes. This design should enable better load paths and easier optimization due to less parasitic effects. The chosen parameters must be reevaluated as soon as the concept is further developed.

The safety against derailment, radial steering and wear and non-linear running stability show generally good results for both the initial and the adapted bogie. The additional dynamic simulations done with the adapted design exceed a few limit values. To reach these limit values further optimization of the parameters is needed.

5 Bibliography

- [1] *Prepared data for running dynamic analysis of FRP bogie*
R1, EMPA, 03.06.2022
- [2] *Graphs.xlsx*
-, EMPA, 23.06.2022
- [3] *MBS Parameter - List*
PO000001845, PROSE AG, Rev. 1, D. Meuter
- [4] *EN 14363+A1:2019 en*
Railway applications – Testing for acceptance of running characteristics of railway vehicles

A Initial model description

The MBS model of the FRP bogie was created with the multi-body simulation software SIMPACK, version 2019x and is based on the bogie CAD model, provided FE analysis [2] and initial parameter list by EMPA [1].

Bogie components like the wheelset, wheel and brake disc or bolster and brake brackets are modelled combined in a single body and connected via force elements and constraints. The constraints are chosen to match the possible movements of the bodies.

To recreate the flexibility of the FRP structures, the suspension components and the bolster are subdivided in 5 parts and connected with force elements. The initial stiffness of the forces elements is chosen to match the FE analysis provided.

Undefined parameters were defined based on experience of previous projects.

During the project, these stiffnesses were adapted to reach the different criteria for stability and safety against derailment (see adapted bogie concept).

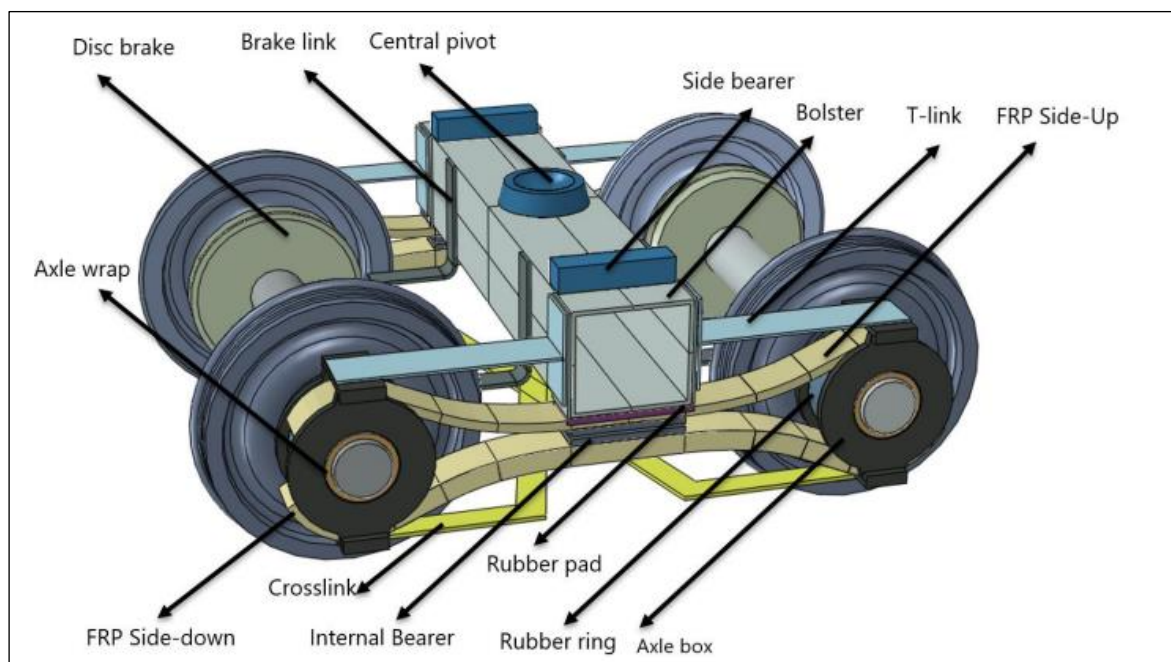


Figure 1: CAD Model of FRP Bogie Concept [1]

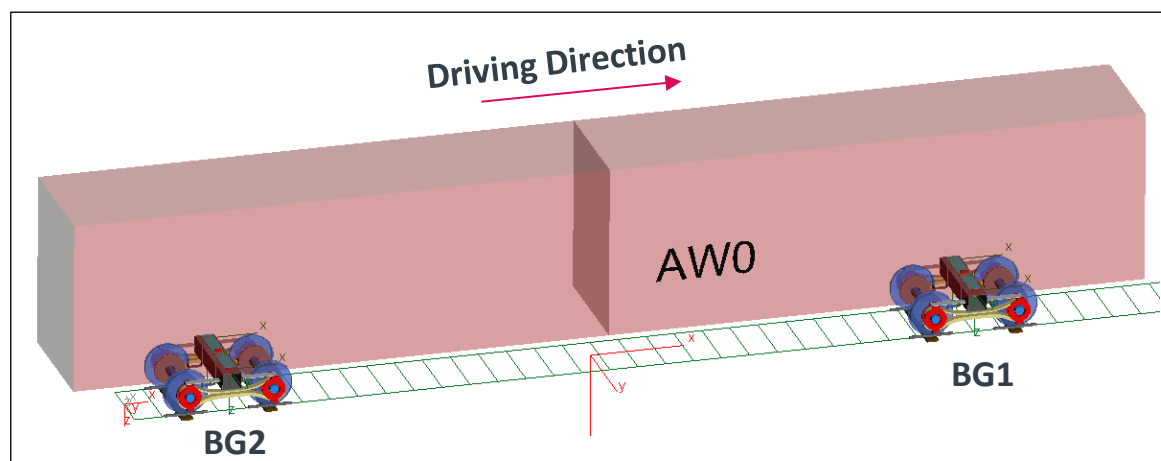


Figure 2: Simpack MBS Model of Vehicle with FRP Bogies

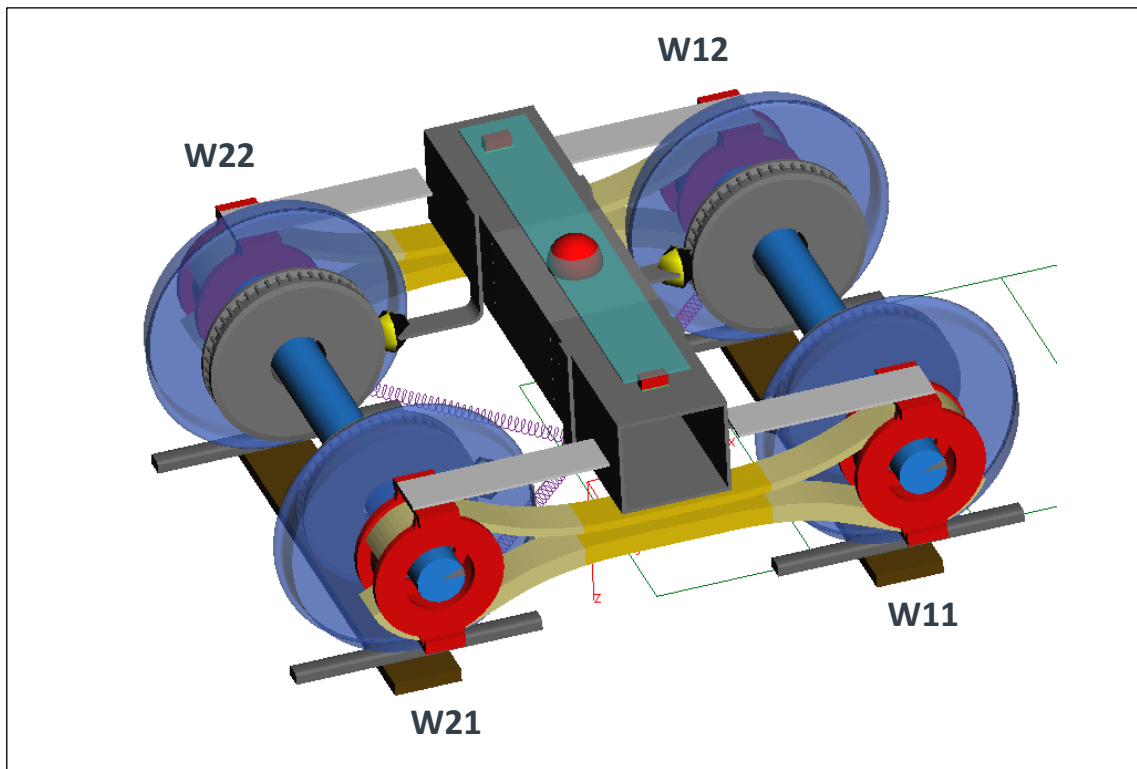


Figure 3: Simpack MBS Model of FRP Bogie Concept

Description	Symbol	Value	Unit
Track Gauge		1.435	m
Wheel Profile		S1002	-
Rail Profile		UIC60	-
Rail Cant		1:40	
Bogie Wheelbase	$2a^+$	1.8	m
Pivot Distance	$2a$	16	m
Minimum Axle Load		4	t
Maximum Axle Load		22.5	t

Table 1: Excerpt of Model Parameters FRP Bogie from Parameter List [3]

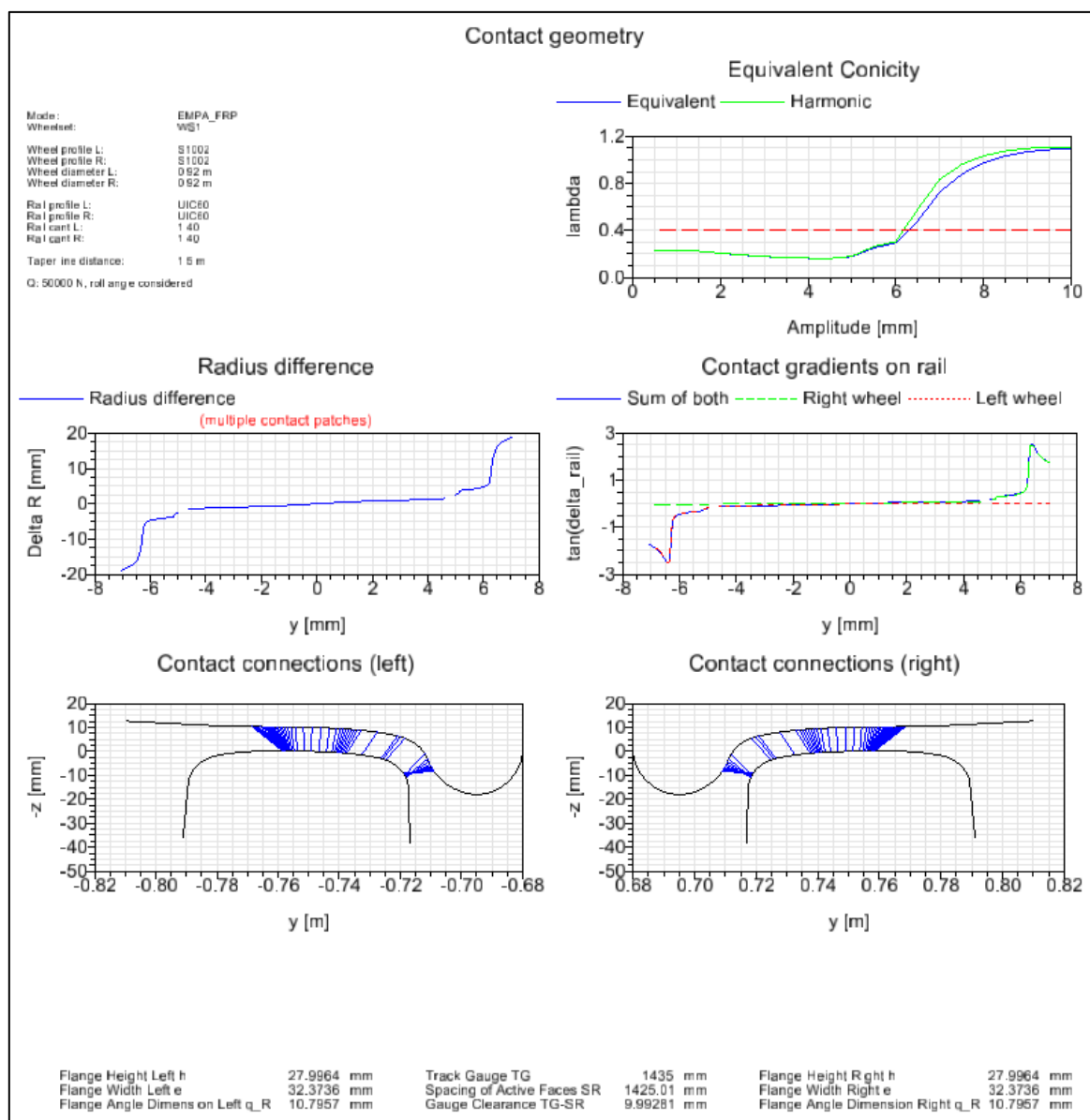


Figure 4: Wheel-Rail Contact

B Adjustment of bogie characteristics

To obtain the bogie characteristics for the multi body simulations, a testbench was built in Simpack to replicate the provided FE calculation. The test rig in Simpack is a singular FRP bogie where the wheel contact points on the wheelsets are held with constraints and a force is applied.

The obtained characteristics are documented in the parameter list [3].

The pivot and side bearer force are applied through a mounting body (MT) to replicate a section of the carbody.

The standard running dynamics model has a rotation joint (around y axis) connecting the axles to the axle box. It seems that the FE-analysis sometimes uses a spherical joint, allowing rotation around X and Z axis of the bearing. The reality is due to manufacturing tolerances in the bushings somewhere in between.

The crosslinks are not included in the FE-analysis as well as in the test bench simulations.

B.1 Vertical load on central pivot

The full proof load is applied either:

- 1) Completely through the central pivot
- 2) Split between the central pivot and one side bearer

The load displacement curves for load case 1), shown in Figure 6 and Figure 7 show a good match of the results of the FE and MBS testbench. The axle box displacement is further off but shows a similar movement and magnitude to the FE calculation.

The displacement curve of the axle box could only be matched by adding a non-linear stiffness in x-direction to the simplified T-Links of the MBS model. This is plausible as the stiffness in x-direction would change in the FE analysis due to the bending and general deformation of the T-Links during the application of the load.

The MBS simulation also shows a big influence of the stiffness of the T-Links on the overall vertical stiffness of the initial concept and very high loads of > 200 kN in x-direction of the T-Links due to the rotation around the y-axis of the axle box. This gives an initial indication that the setup of the initial concept leads to not ideal load paths.

Load case 2), shown in Figure 9 and Figure 10, shows a higher stiffness of the MBS model compared to the FE model but matches good enough for a concept.

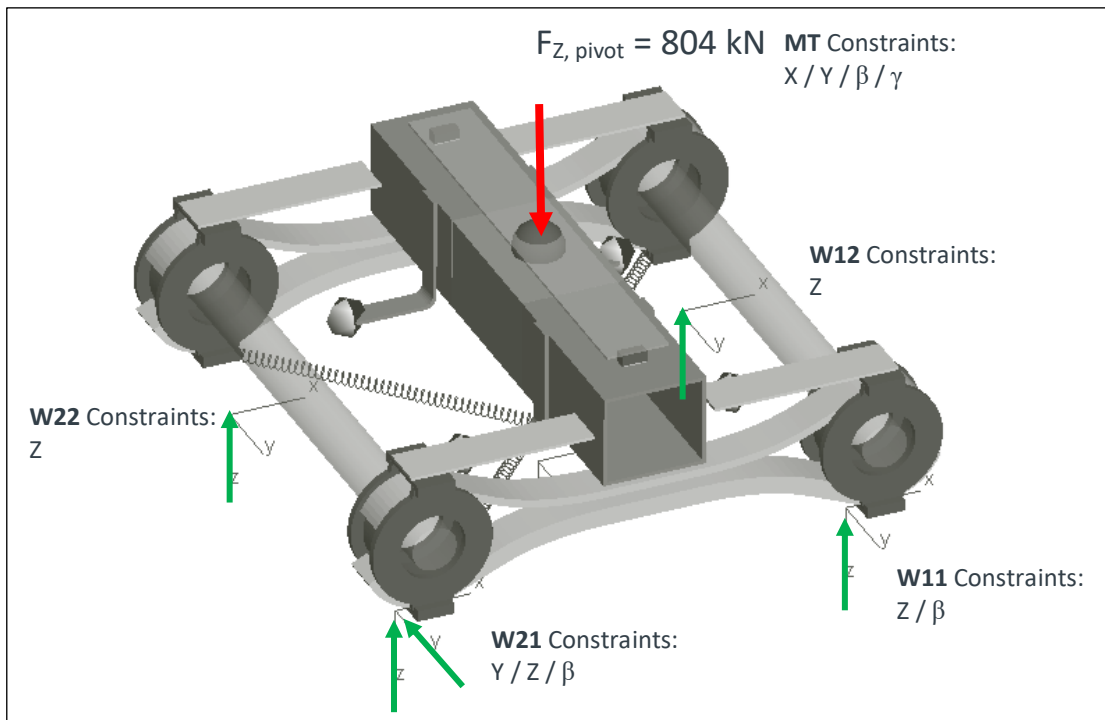


Figure 5: Load case 1) Total vertical proof load on central pivot

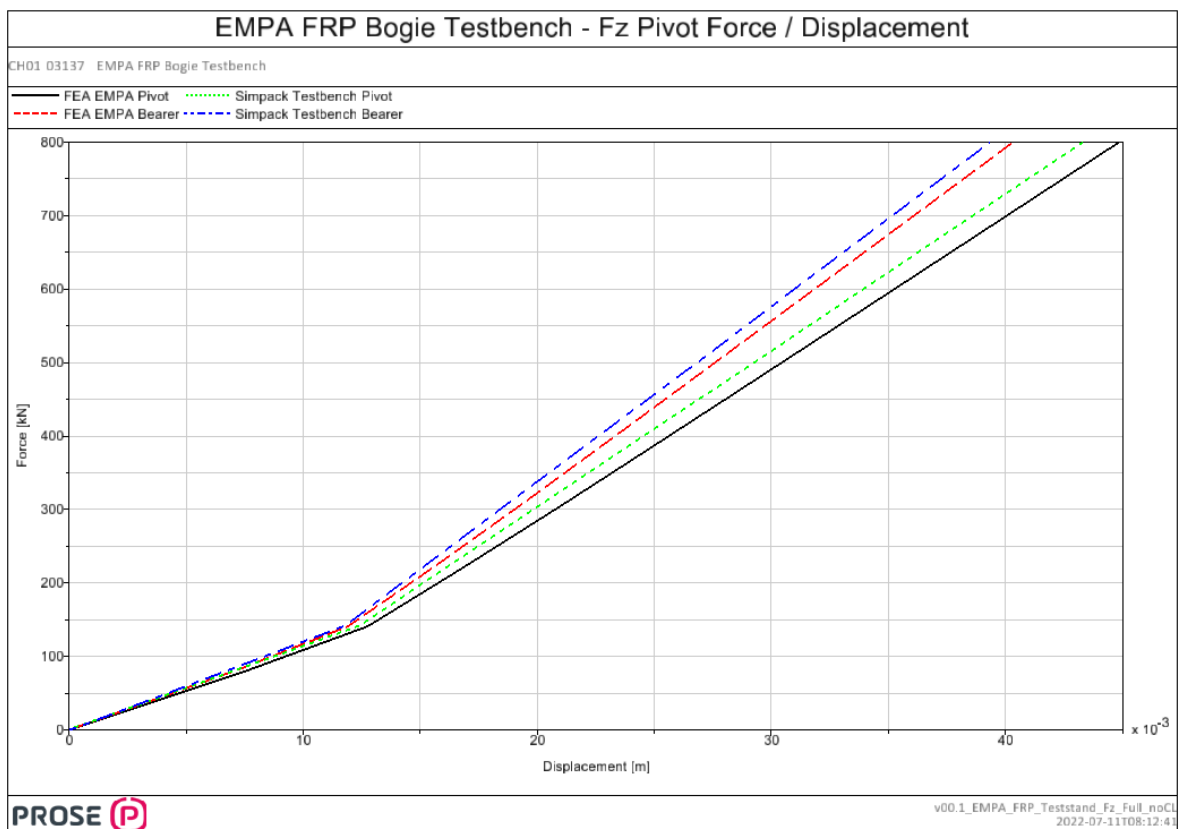


Figure 6: Load case 1) Pivot force Fz – pivot Z-displacement curve

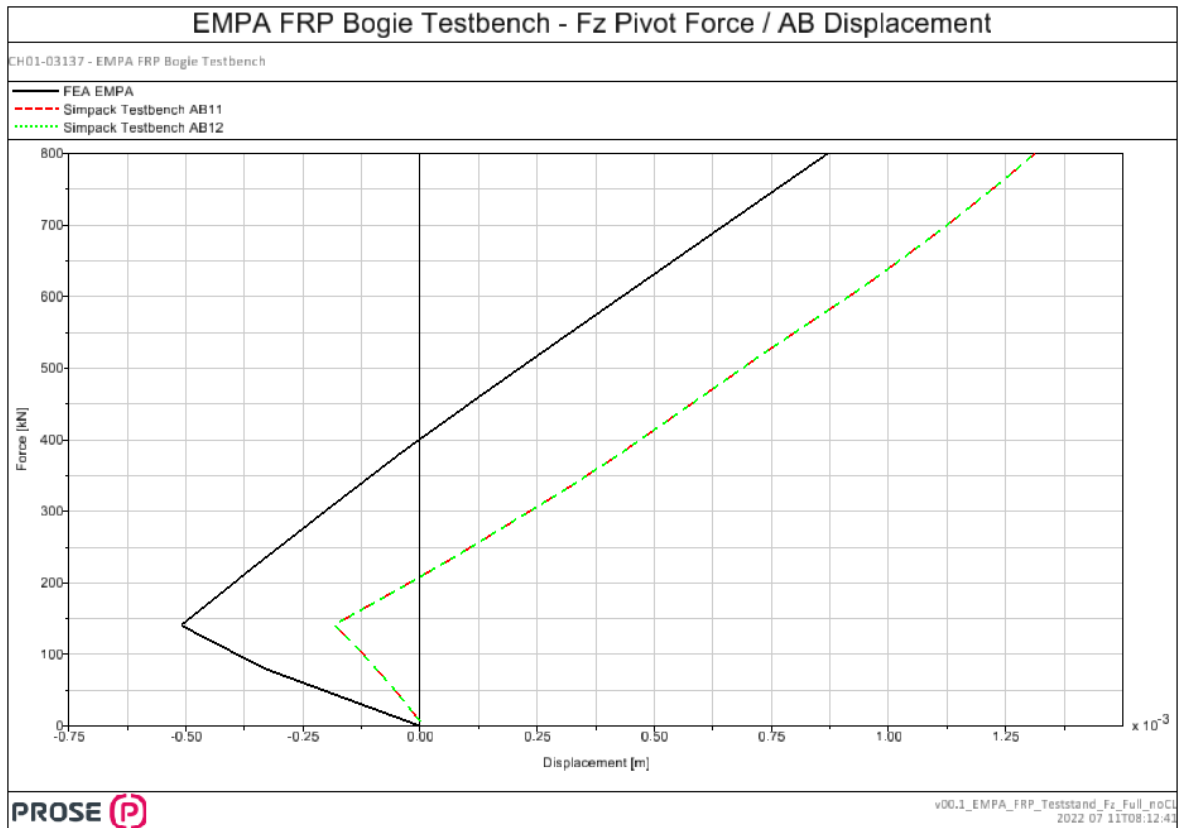


Figure 7: Load case 1) Pivot force F_z – axlebox x-displacement curve

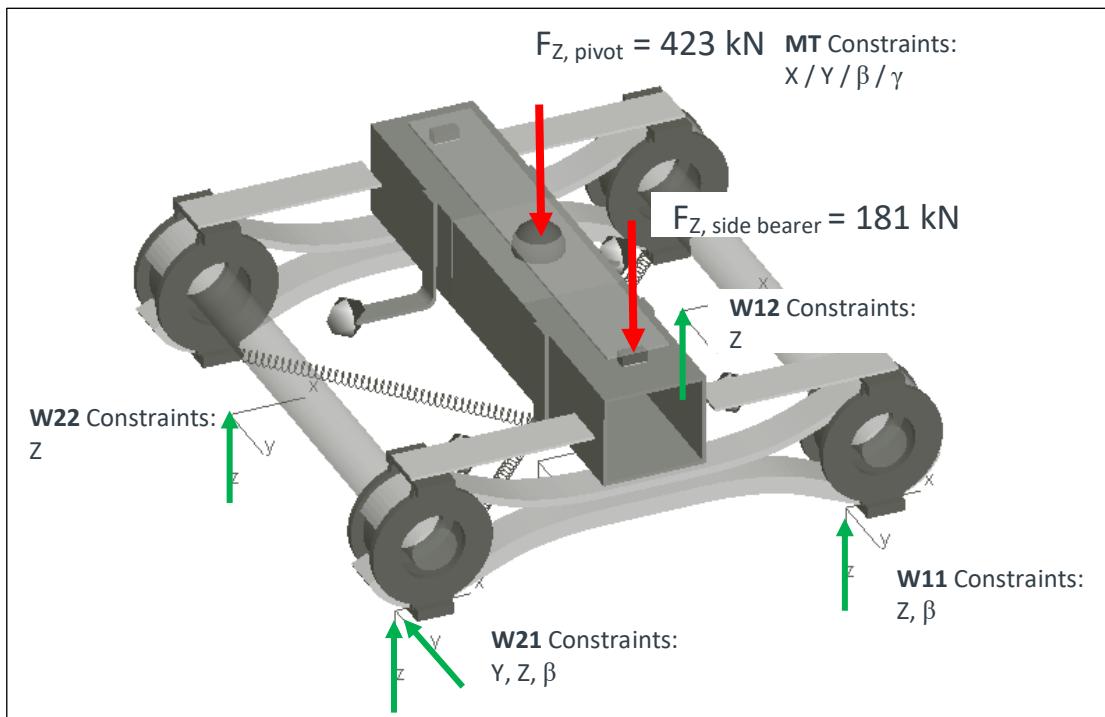


Figure 8: Load Case 2) Divided vertical proof load on central pivot and side bearer

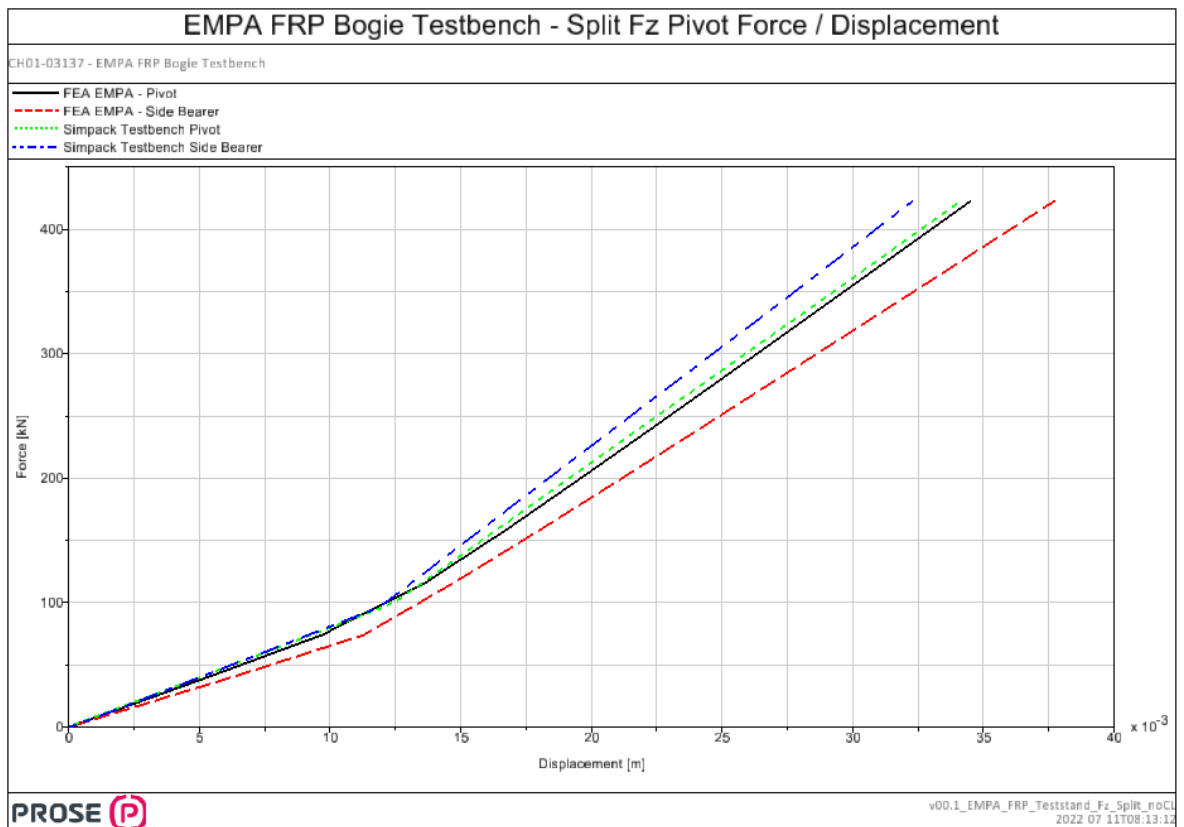


Figure 9: Load case 2) Pivot force Fz – pivot Z-displacement curve

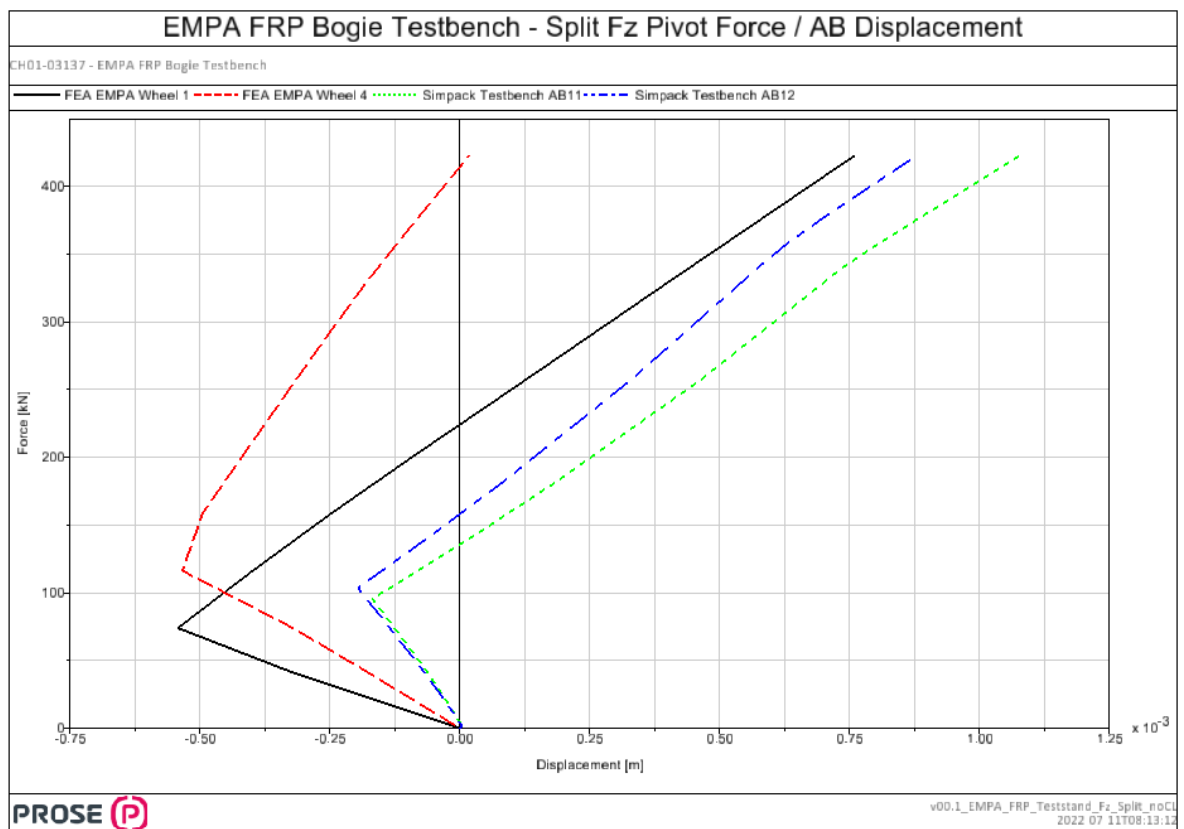


Figure 10: Load case 2) Pivot force Fz – axlebox X-displacement curve

B.2 Transverse force on central pivot

In a first step, the full vertical load is applied to the pivot. In a second step the lateral force is applied on the central pivot.

The results shown in Figure 12 show the big impact of the two different axle box joint types (spherical joint / rotation joint beta) on the lateral stiffness of the system. The parameters for the MBS model were chosen to reach a compromise between this load case and load case B.5 lateral force on wheel.

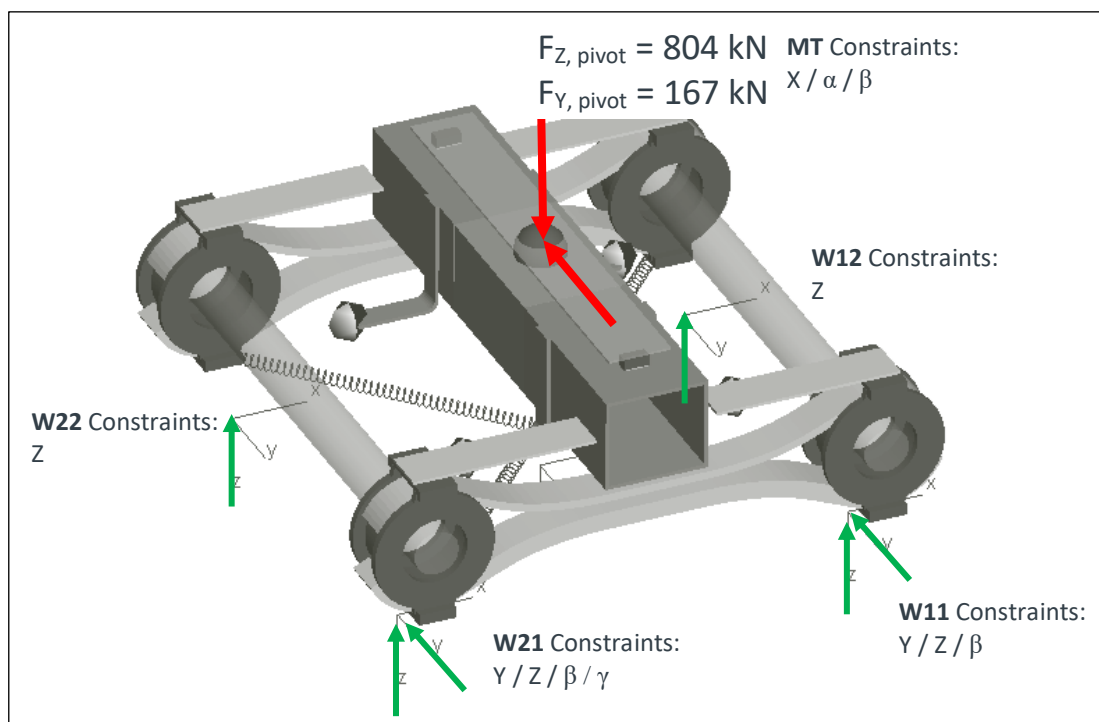


Figure 11: Load case total vertical and lateral proof load on central pivot

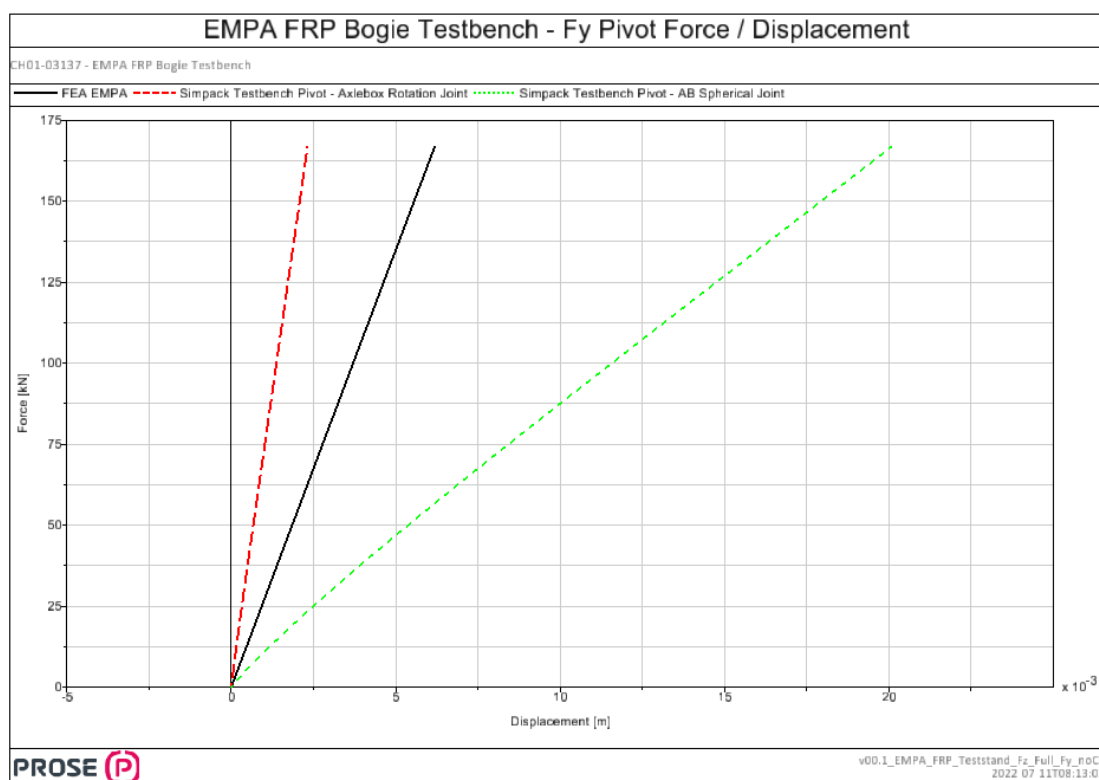


Figure 12: Pivot force F_y – pivot Y-displacement curve

B.3 Longitudinal force on central pivot

In a first step, the full vertical load is applied to the pivot. In a second step the longitudinal force is applied on the central pivot.

The MBS testbench shows an initial displacement of the pivot due to the vertical pivot force. The stiffness due to the force in x-direction shows a close match to the FEA.

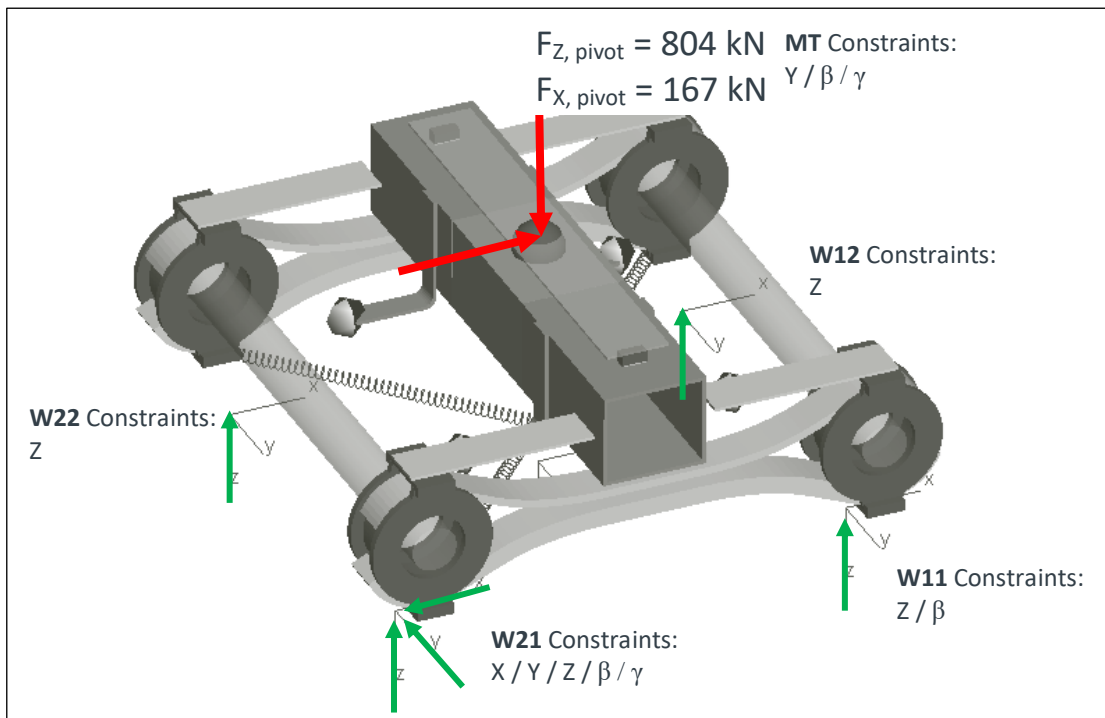


Figure 13: Load Case total vertical and lateral proof load on central pivot

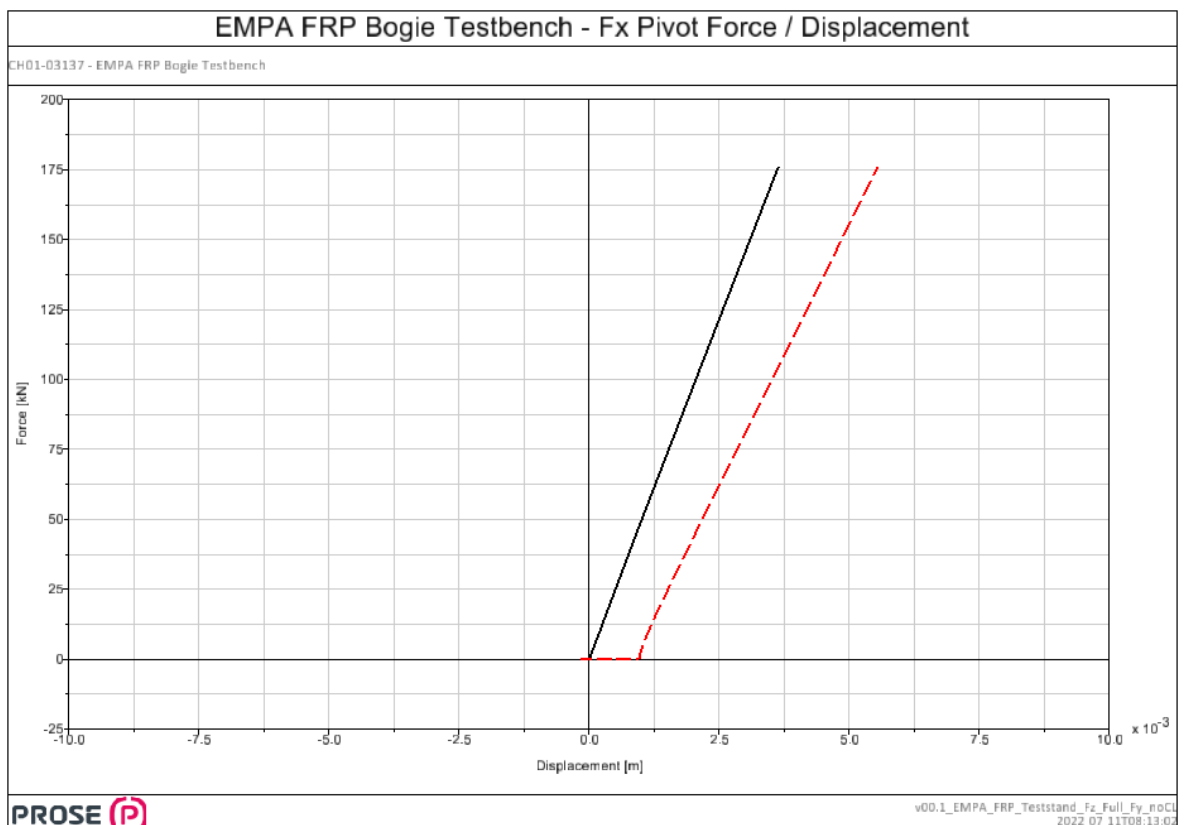


Figure 14: Pivot force F_x – pivot X-displacement curve

B.4 Lifting of wheel

The vertical displacement on the wheel is applied without a vertical force or constraint on the pivot.

The results shown in Figure 16 show again a big difference between the two different types of joints between axle and axle box and the curve could not be matched with the current level of detail of the model.

A parameter variation showed a high influence on the vertical stiffness during lifting of the wheel not only from the vertical stiffness of the FRP parts but also from the axle box joint type, the x-stiffness of the T-Links as well as the torsional stiffness (around x-axis) of the FRP parts.

It is very difficult to define and match vertical stiffnesses when there are many parasitic influences due to other elements.

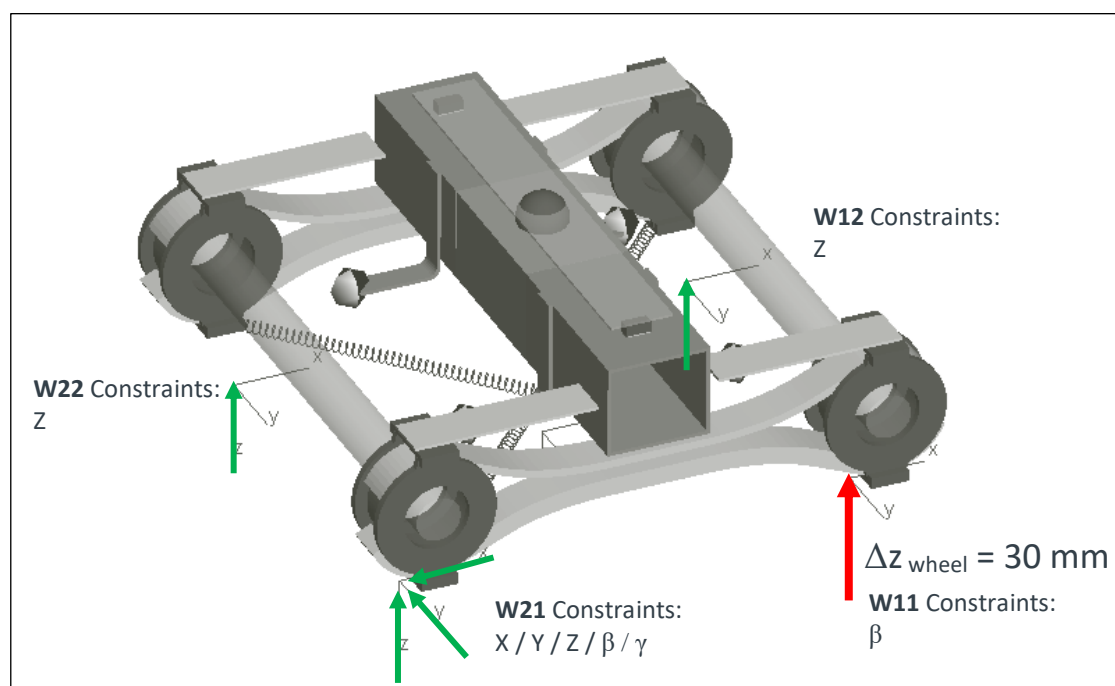


Figure 15: Load case vertical lifting of wheel

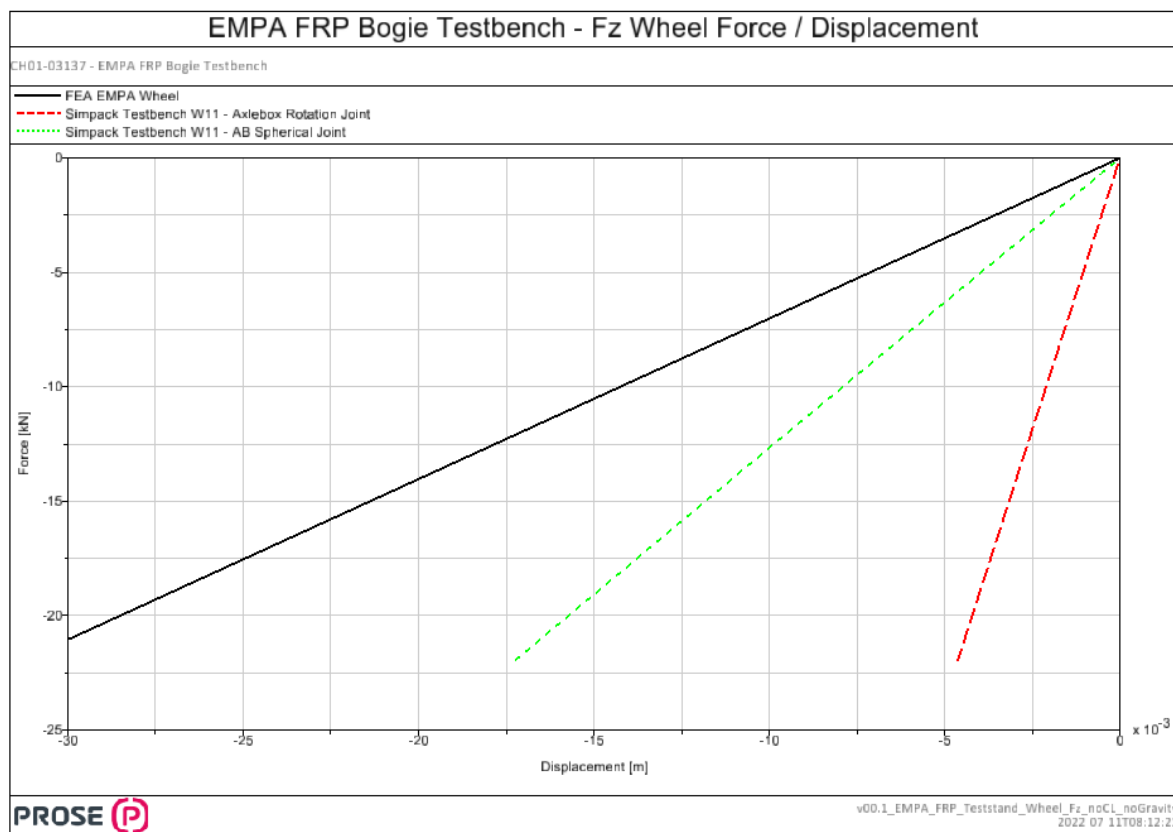


Figure 16: Wheel force Fz – wheel Z-displacement curve

B.5 Lateral force on wheel

The full force on the wheelset is applied without a vertical force or constraint on the pivot.

The results shown in Figure 18 show again a big difference between the two possible axlebox joints. The MBS parameters were chosen to match the results of a spherical joint as good as possible.

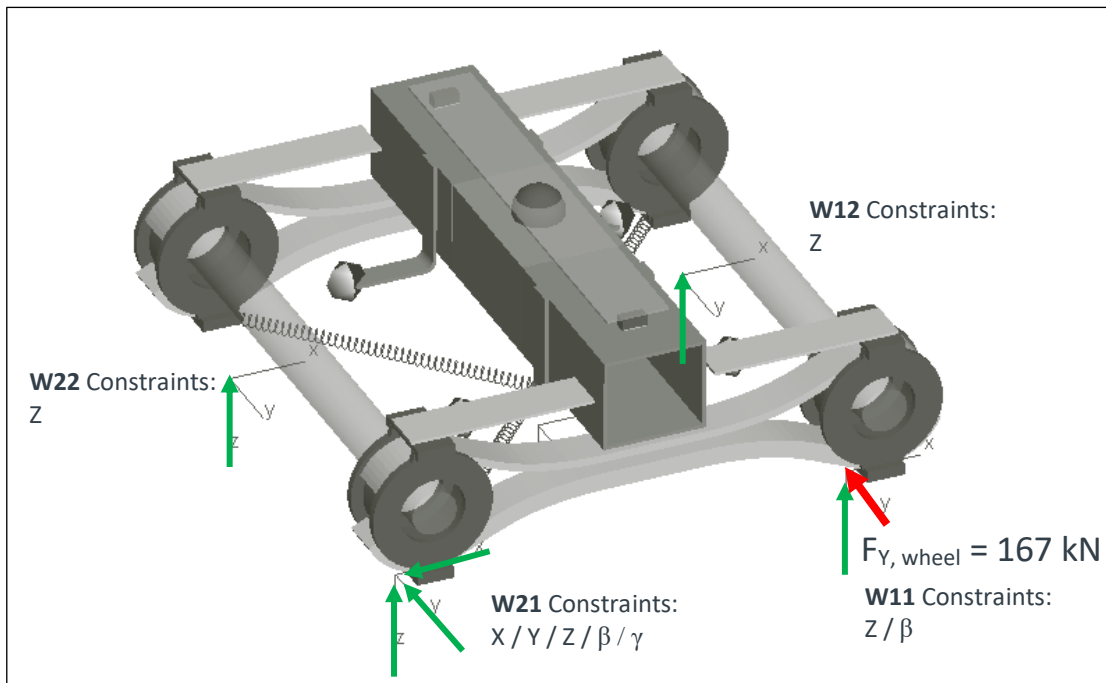


Figure 17: Load case lateral load on wheel

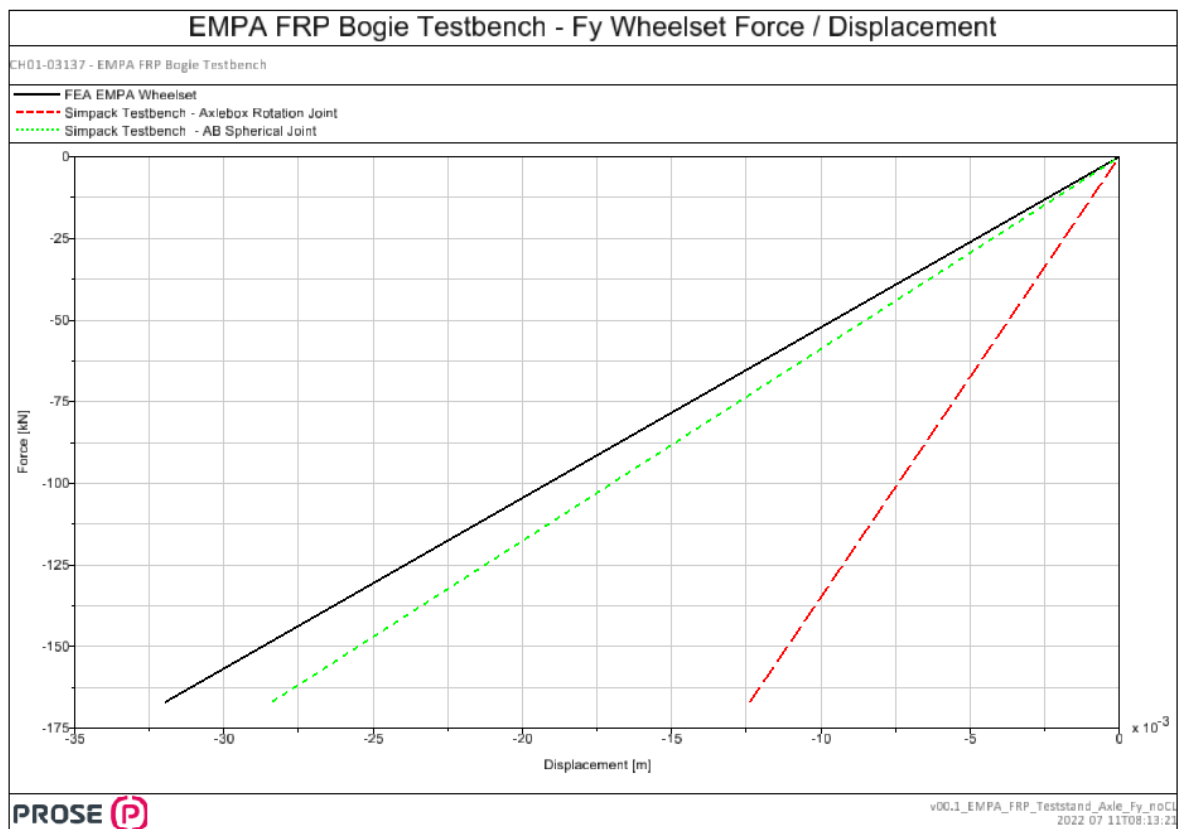


Figure 18: Wheelset force F_y – wheelset Y-displacement curve

B.6 Natural frequencies for side-down component

The chosen fraction of pure z-stiffness and bending stiffness around the y-axis led to a good matching of the first bending mode of the FRP side-down component.

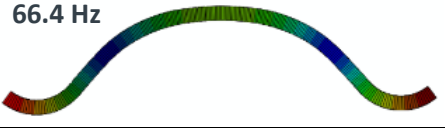
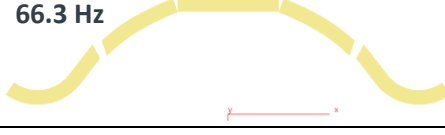


FEA	Simpack
<p>66.4 Hz</p> 	<p>66.3 Hz</p> 
<p>179 Hz</p> 	<p>177.5 Hz</p> 

Table 2: Comparison bending modes of FRP side-down component

B.7 Summary of testbench results

In general, the chosen parameters of the MBS simulation model match the characteristics of the FE-analysis well apart from the single wheel lifting case. The transverse loadcases (B.2 and B.5) show different values depending on the chosen type of joints used in the axlebox connection to the wheelsets. For these cases, a compromise for the parameters was chosen.

The results show many parasitic influences on the stiffness over multiple elements which make optimization difficult.

The T-Link sees very high bending- and x-forces which will be hard to manage on the design and strength calculation side.

For the running dynamics simulations, an additional rubber element was added between the FRP / T-Link and the axle box / cross link part with low longitudinal stiffness to enable good radial steering and stability. This rubber element was not part of the testbench model.

C Adapted bogie concept

Based on the initial calculations, an adaption of the bogie concept was made. The visualized placement of the new elements is just as reference and can be moved and changed to fit the needs of the overall design. Important is mainly the function that they serve.

The adaption focuses on reducing the parasitic effects on the stiffness and removing the need for the T-Links and thus improving the force flow. By removing the T-Links, the vertical system stiffness is reduced and must be increased again to match the displacements of a Y25 bogie.. The current displacement of the axle box relative to the bolster with empty and fully loaded vehicle is shown in Figure 21.

Instead of the T-Links, the longitudinal connection between bolster and axles is done via a longitudinal bar which has two rotation joints at each end, connecting two end pieces (dark gray) to a center part (light gray).

The center part (light gray) of the longitudinal bar is fixated to the bolster and the center part (dark yellow) of the upper FRP spring.

This longitudinal bar decouples the FRP springs from influencing any other then the z-stiffness of the system.

A rubber bushing / layer spring connects the endpieces (dark gray) of the longitudinal bar with the axle box (red). This spring should have a high vertical (C_z) stiffness and low lateral and longitudinal stiffness ($C_{x,y}$) to enable good steering mechanism.

The crosslink steering mechanism is switched to a drawbar system (Deichselanlenkung) which should be easier to fit in the design space.

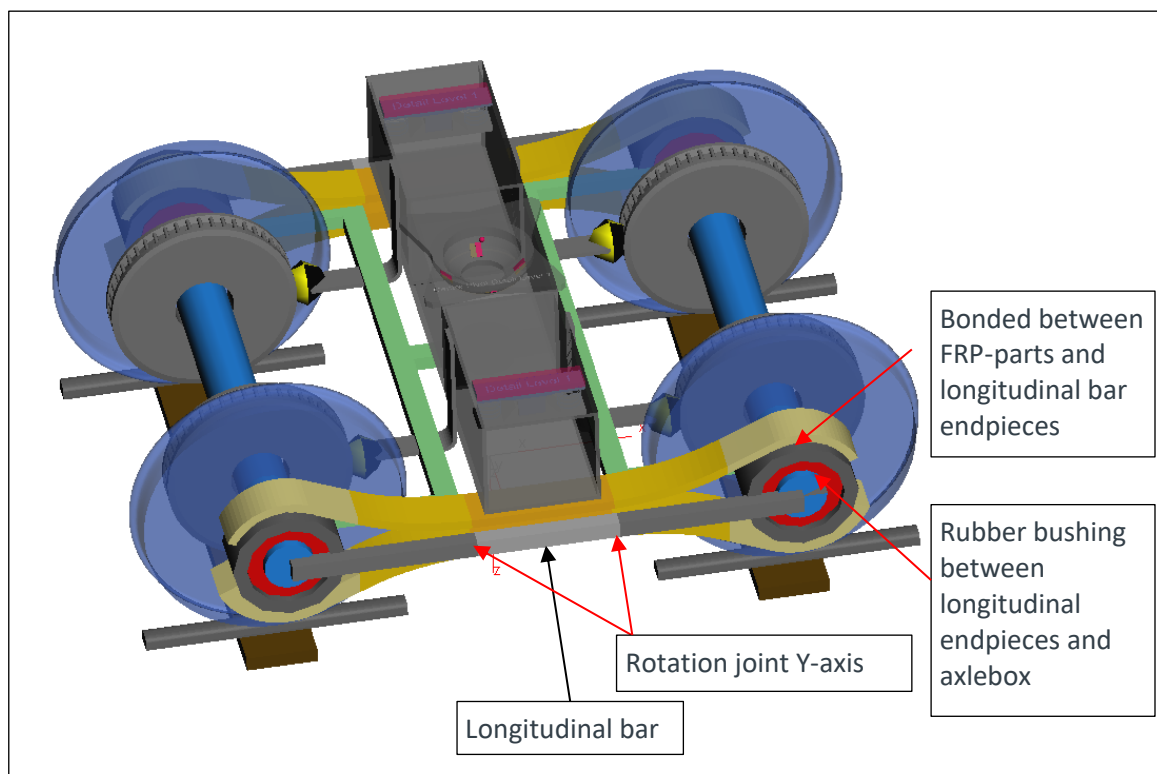


Figure 19: 3D view of the adapted bogie design

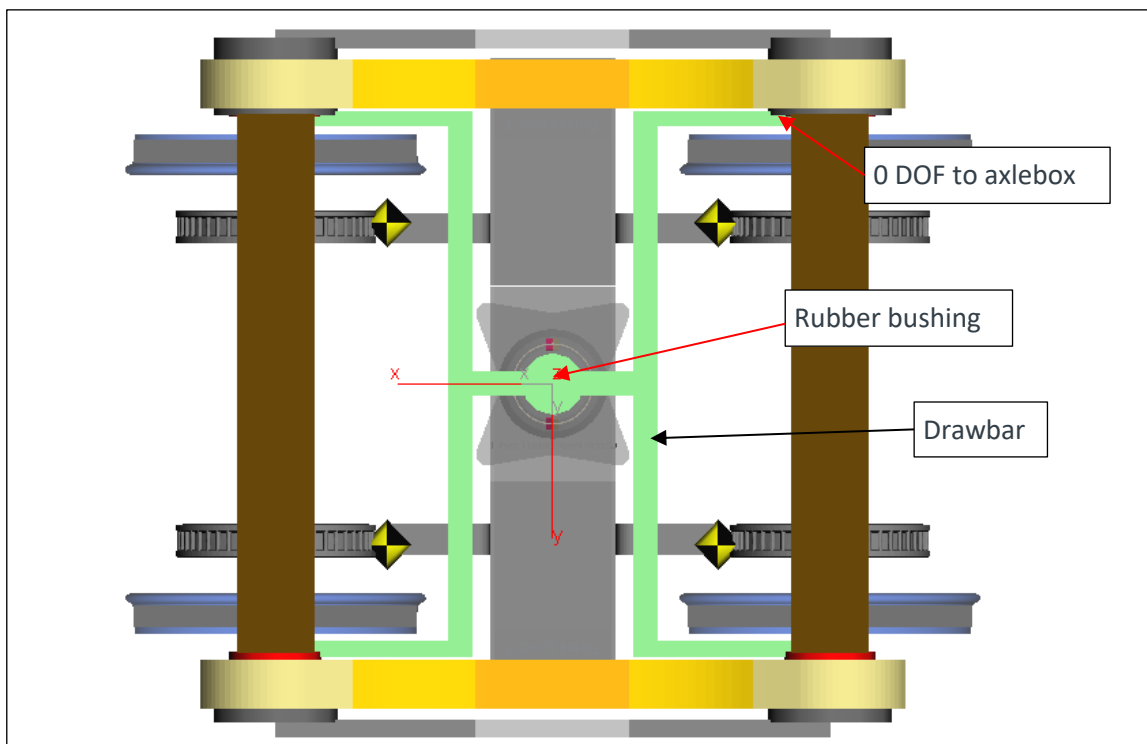


Figure 20: Bottom view of the adapted bogie design

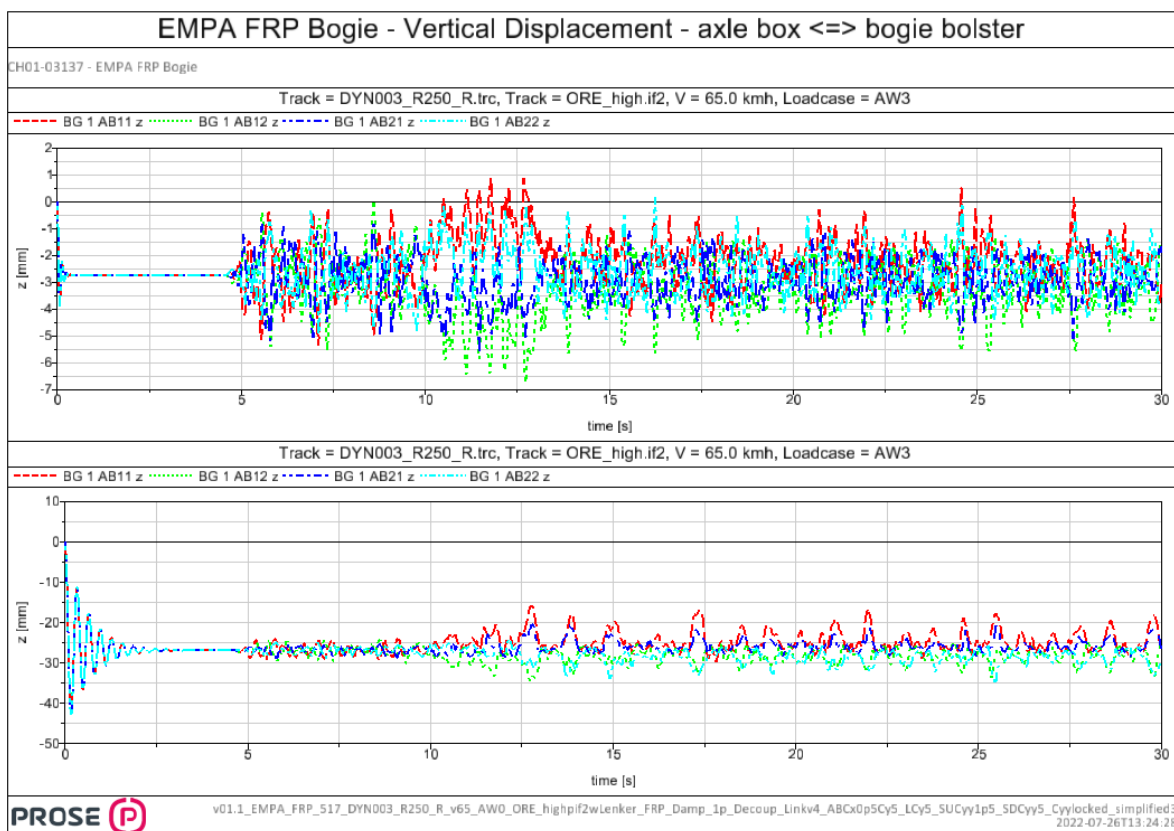


Figure 21: Vertical displacement at v_{\max} in AW0 and AW3 for the increased stiffness of the suspension

D Safety against derailment

The safety against derailment on twisted tracks was calculated acc. to method 2 of EN 14363 [4] and compared to the allowable limit Y/Q as defined by Nadal's formula for the flange angle of the S1002 wheel profile.

D.1 Analysis method

The derailment safety on twisted tracks was assessed according to method 2 of the EN 14363 [4].

The wheel unloading is obtained by simulating the twisted track on a test rig.

Following nominal values are used on the twist test rig:

	Formula acc. to EN 14363	Twist
Bogie	$g_{lim}^+ = 7 - \frac{5}{2a^+}$	4.2 ‰
Vehicle body	$g_{lim}^* = \frac{5}{2a} + 2$	2.9 ‰

Table 3: Twist for wheel unloading test following method 2 of the EN 14363

During the simulation, the bogie twist is increased an additional 15%. The values for the results are taken during nominal twist.

$2a^+$ is the bogie wheelbase in m, $2a$ is the distance between center pivots of the vehicle in m.

The twist is applied in stages and over the cross to minimize the effect of rolling of the carbody.

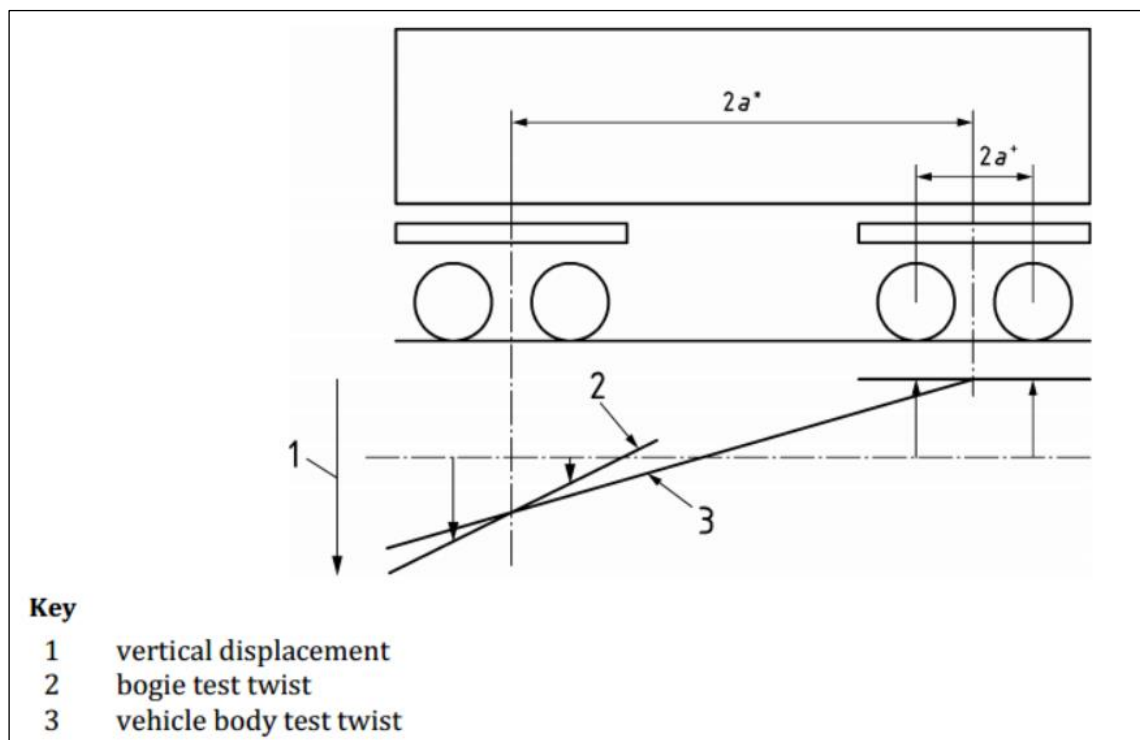


Figure 22: Combination of bogie and vehicle body test twist, Figure 1 from EN 14363 [4]

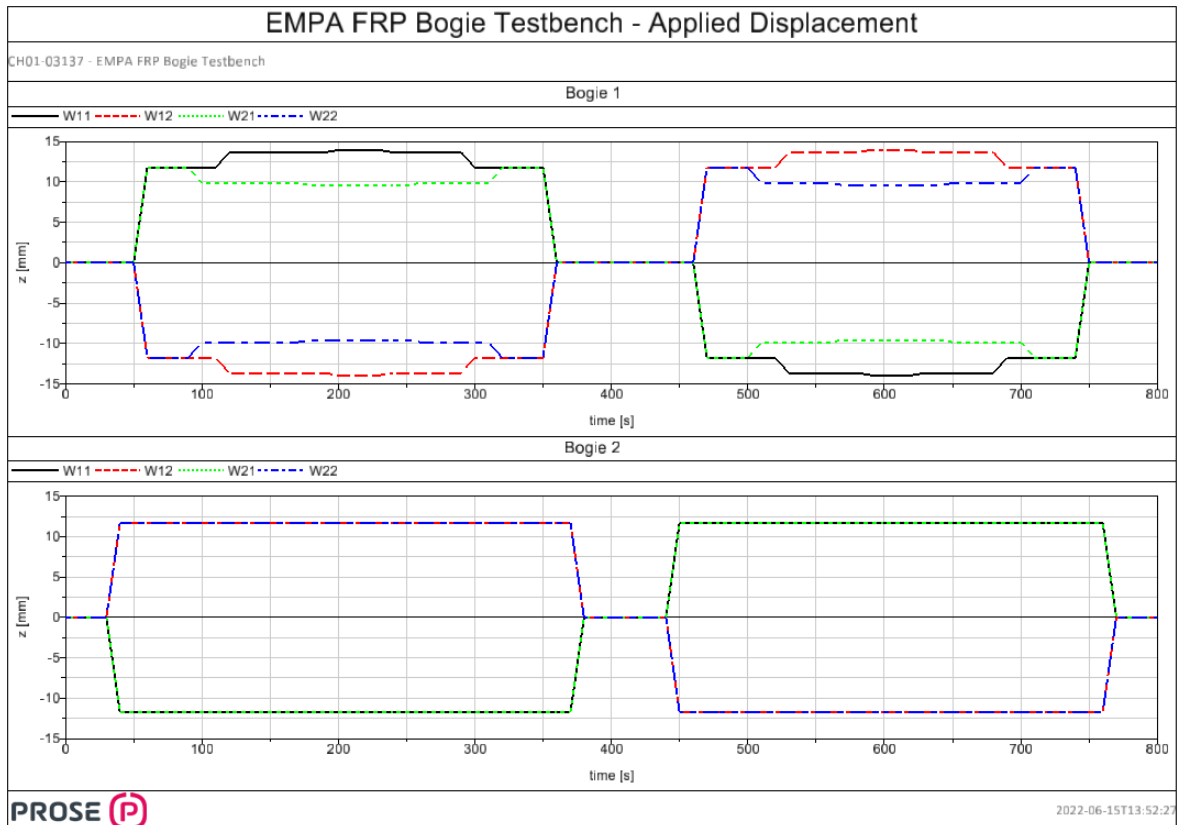


Figure 23: Applied displacements for wheel unloading on test rig

The lateral load is obtained from driving through a constant curve of 150 m. The curve is without transition curve and a gauge widening of 5 mm is applied. The friction coefficient applied is 0.51 on the running surface and 0.36 on the flange.

According to EN 14363 [4], the lateral forces must be evaluated:

- when the tested bogie has entered the curve by at least 3 m and before the next bogie has entered the curve
- when the complete vehicle is stably running in the curve

For each location, 3 measurements shall be taken and averaged. The assessment is done with the higher of the two averages. For the simulation, three values at a distance of 1 m are used.

Track	Speed [km/h]	Curve radius [m]	Gauge widening [mm]
DRT001	3.6	150	+5 mm

Table 4: Track definition for derailment method following method 2 of the EN 14363

The following formula shall be evaluated:

$$\left(\frac{Y}{Q}\right)_{j,a} = \frac{Y_{j,a,mean}}{Q_{jk,min} + \Delta Q_{j,H}}$$

Where $Y_{j,a,mean}$ is the higher of the two mean values of the lateral guiding force, $Q_{jk,min}$ is the smallest vertical force evaluated by the twist test and $\Delta Q_{j,H}$ is the change of the vertical wheel force due to the moment of the sum of lateral wheel forces: $\Delta Q_{j,H} = \sum Y \cdot h / 2bA$. h is the effective height of the primary lateral suspension and $2bA$ is the lateral distance of the wheel contact points ($2bA = 1.5$ m und $h = 0.46$ m)

The limit value is calculated by:

$$\left(\frac{Y}{Q}\right)_{a,lim} = \frac{\tan \beta - \mu}{1 + \mu \cdot \tan \beta} = \frac{\tan 70^\circ - 0.36}{1 + 0.36 \cdot \tan 70^\circ} = 1.2$$

Where β is the angle of the wheel flange and μ is the friction coefficient between the rail and the wheel at the flange.

D.2 Results initial bogie

The initial design shows a low Y/Q coefficient for both the empty and full vehicle and is safe against derailment.

	Yj,a,mean	Qjk,min	SumY	Y/Q
	[N]	[N]	[N]	[-]
AW0	8'385	9'505	8'978	0.68
AW3	29'492	90'500	32'247	0.29

Table 5: Safety against derailment assessment for initial bogie design

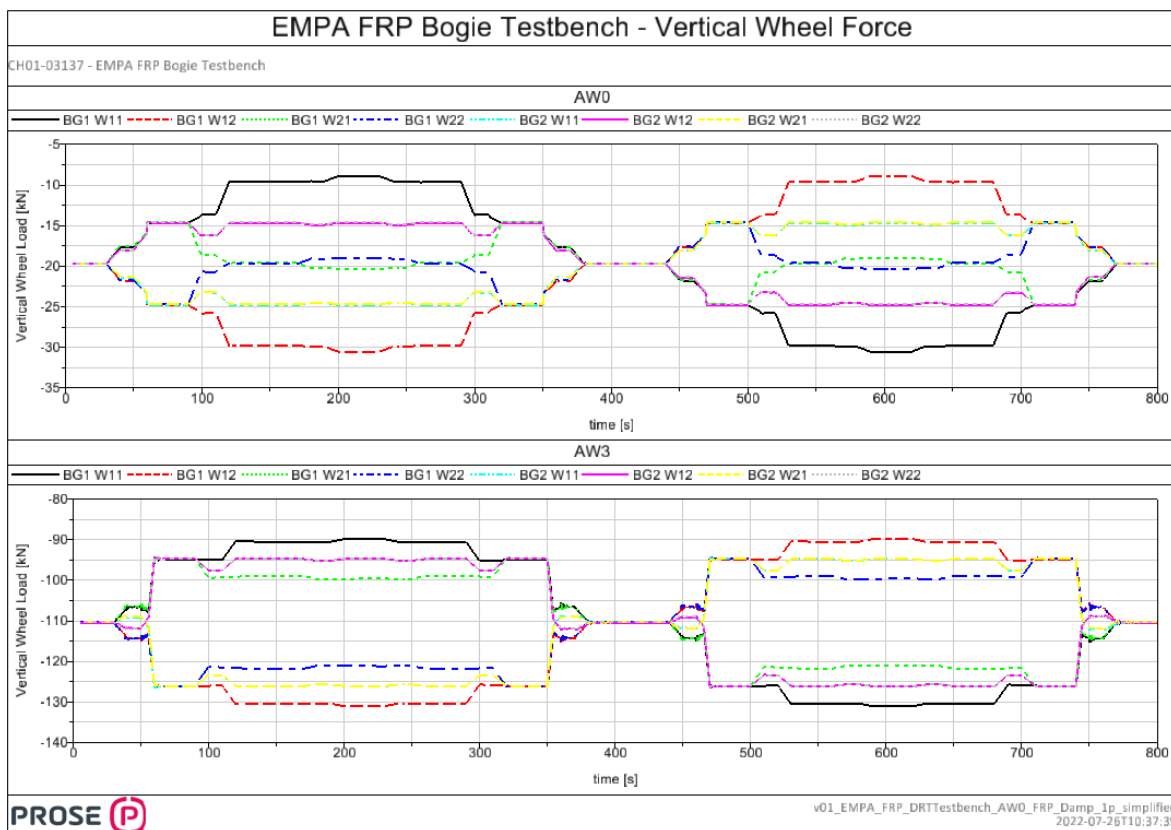


Table 6: Vertical wheel force of initial bogie design

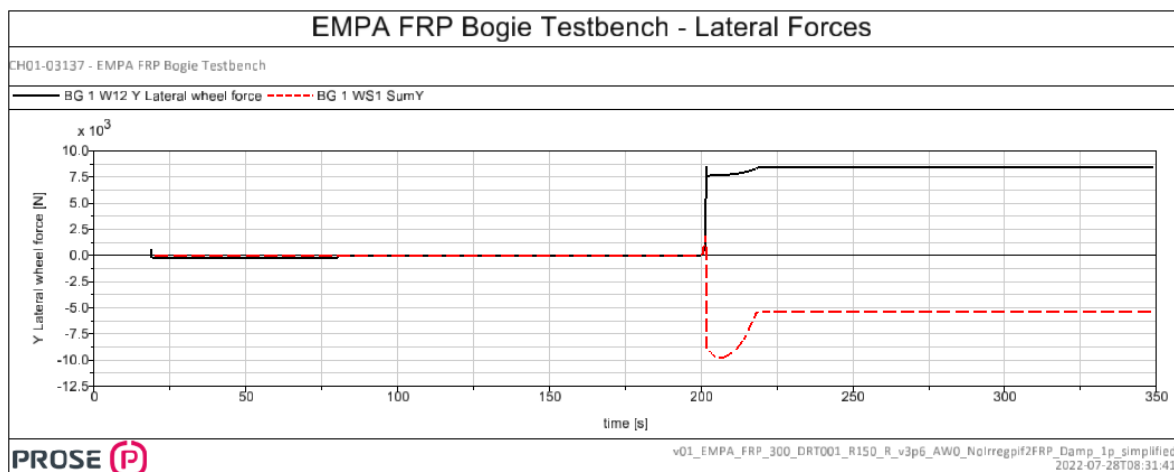


Table 7: Lateral wheel force of initial bogie design with AW0 loading

D.3 Results adapted bogie

The results for the adapted bogie design shows, with the preliminary chosen values for the suspension, sufficient safety against derailment. On the test rig for the vertical wheel forces, the influence of the non-linear behaviour of the side bearer friction plates can be seen.

The suspension stiffness must be updated and calculated correctly in a new FEA analysis to match the maximal suspension movement.

	Yj,a,mean	Qjk,min	SumY	Y/Q
	[N]	[N]	[N]	[-]
AW0	8'589	11'620	8'988	0.60
AW3	39'802	92'960	32'617	0.39

Table 8: Safety against derailment assessment for adapted bogie design

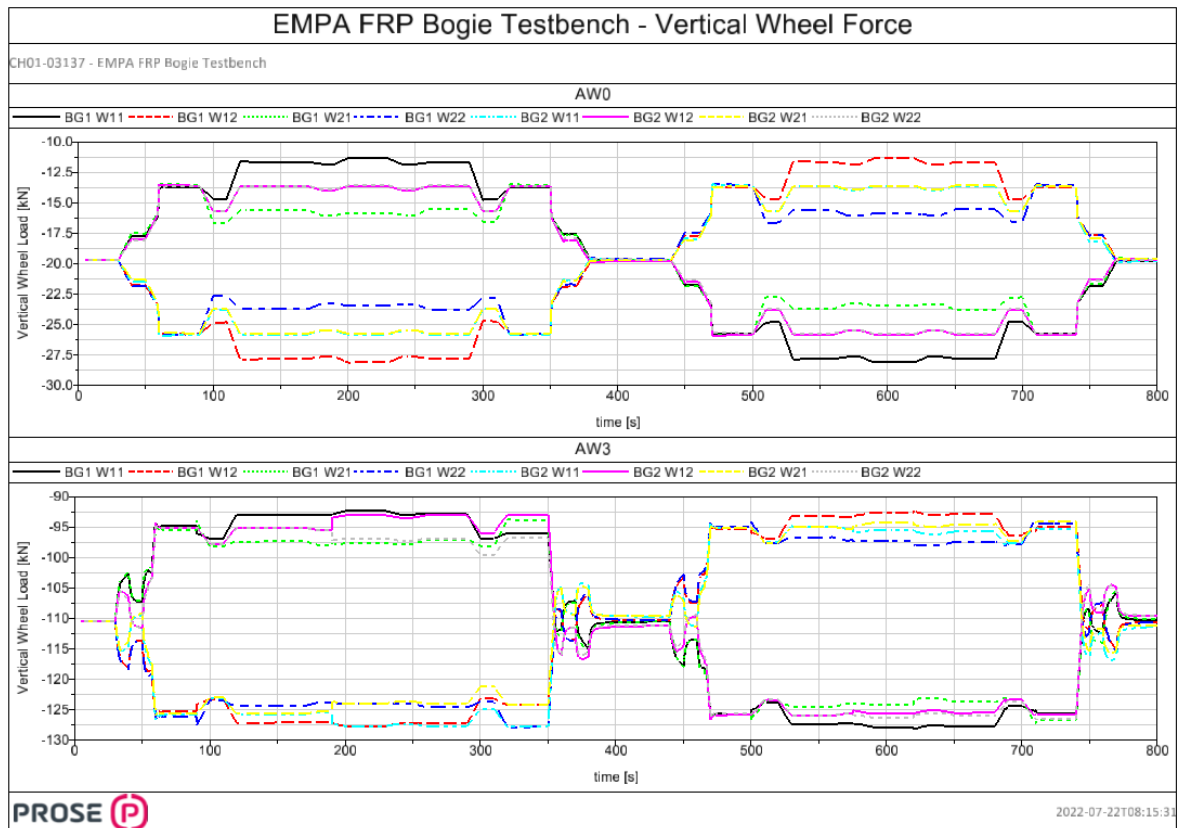


Table 9: Vertical wheel force of adapted bogie design

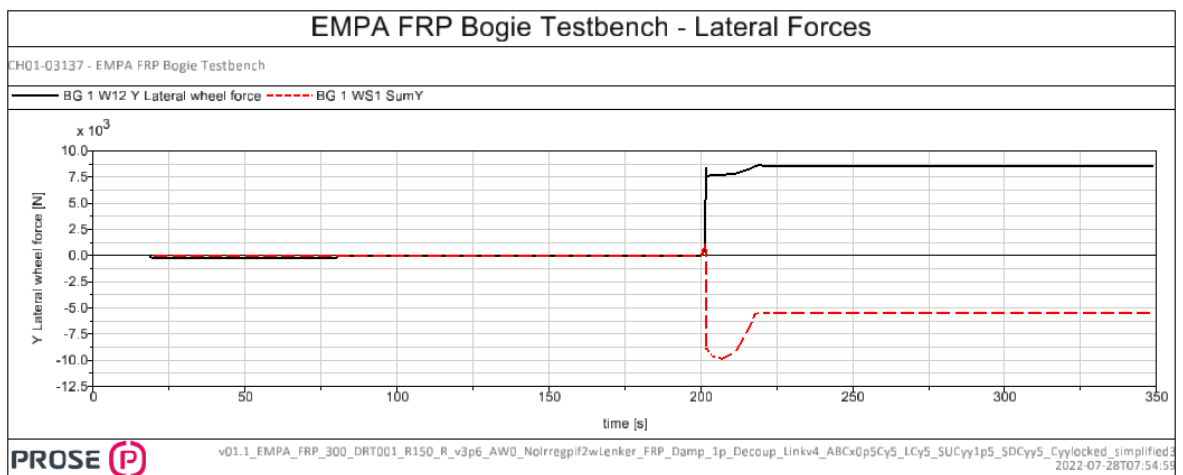


Table 10: Lateral wheel force of adapted bogie design with AW0 loading

E Radial steering and wear analysis

E.1 Analysis method

To compare the radial steering and wear index to other bogies, the same simulations with the simplified Y25 bogie as in the previous ECO bogie project were performed.

The mean values during a righthand curve excluding the transition curve were compared for a fully loaded vehicle (AW3).

The values are for information only and are an initial estimate regarding the wear behaviour.

Type	Speed	aq	Radius	Transition Curve	Super-elevation
	[km/h]	[m/s ²]	[m]	[m]	[mm]
Cant deficiency	65	+0.58	250	55	110
Equilibrium speed	48.3	0	250	55	110
Cant excess	21.3	-0.58	250	55	110

Table 11: Tracks for radial steering and wear assessment

E.2 Results initial bogie

The result for the initial bogie design show good curving capabilities. The mean values are compared to the simplified Y25 bogie good but show a high bandwidth which might indicate a lack of damping.

aq	Maximal mean Wear Index T_{γ}		Mean angle of attack leading wheeset BG1	
[m/s ²]	[J/m]		[mrad]	
	FRP	Y25	FRP	Y25
+0.58	108	197	-1.32	-2.26

Table 12: Radial steering and wear results for initial bogie design

E.3 Results adapted bogie

Like the results of the initial design, the adapted design shows good steering capabilities under full load and with different uncompensated lateral accelerations.

Even though the mean value for the wear index is comparably low, results shown in Figure 24 show a big bandwidth for the wear number, which could indicate inadequate damping of the bogie.

aq	Maximal mean Wear Index T_γ		Mean angle of attack leading wheaset BG1	
[m/s ²]	[J/m]		[mrad]	
	FRP	Y25	FRP	Y25
+0.58	130	197	-1.6	-2.26
0	116	205	-1.5	-2.69
-0.58	117	226	-1.9	-3.92

Table 13: Radial steering and wear results for adapted bogie design

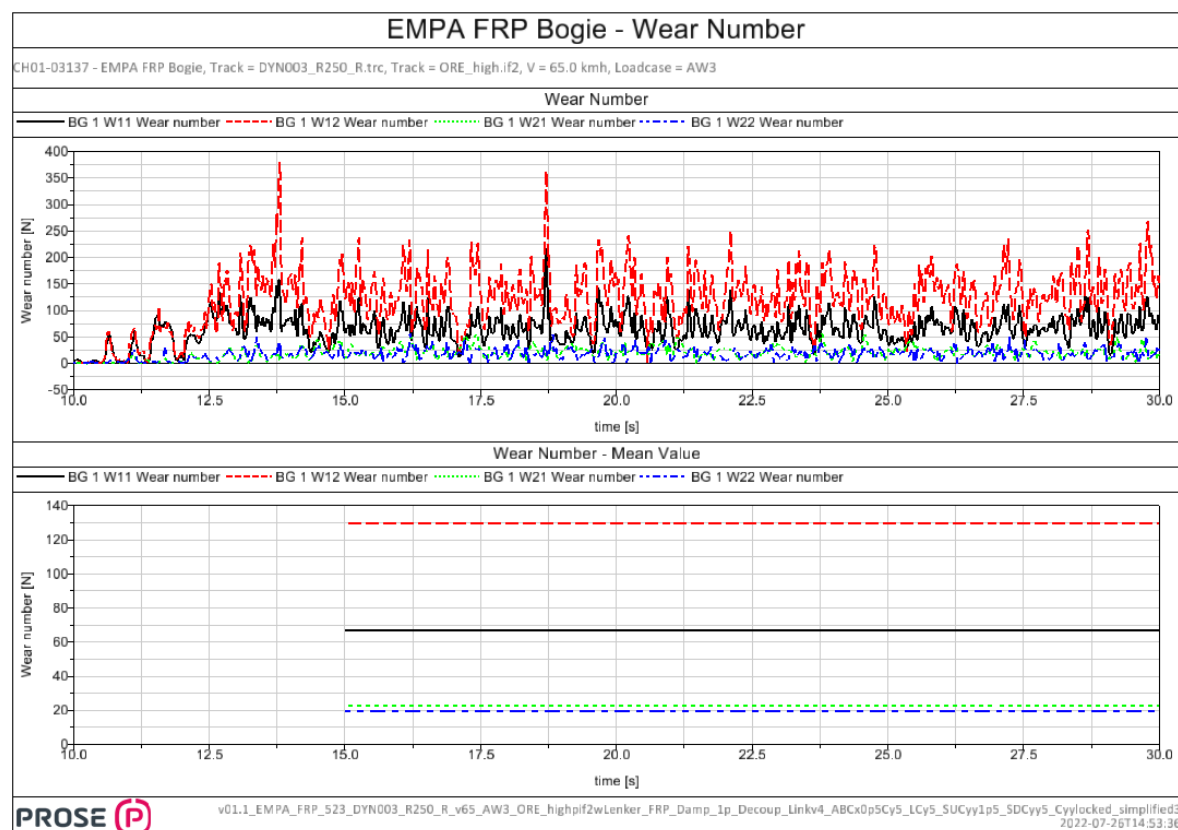


Figure 24: Wear number of adapted bogie design under full load and +0.58 aq

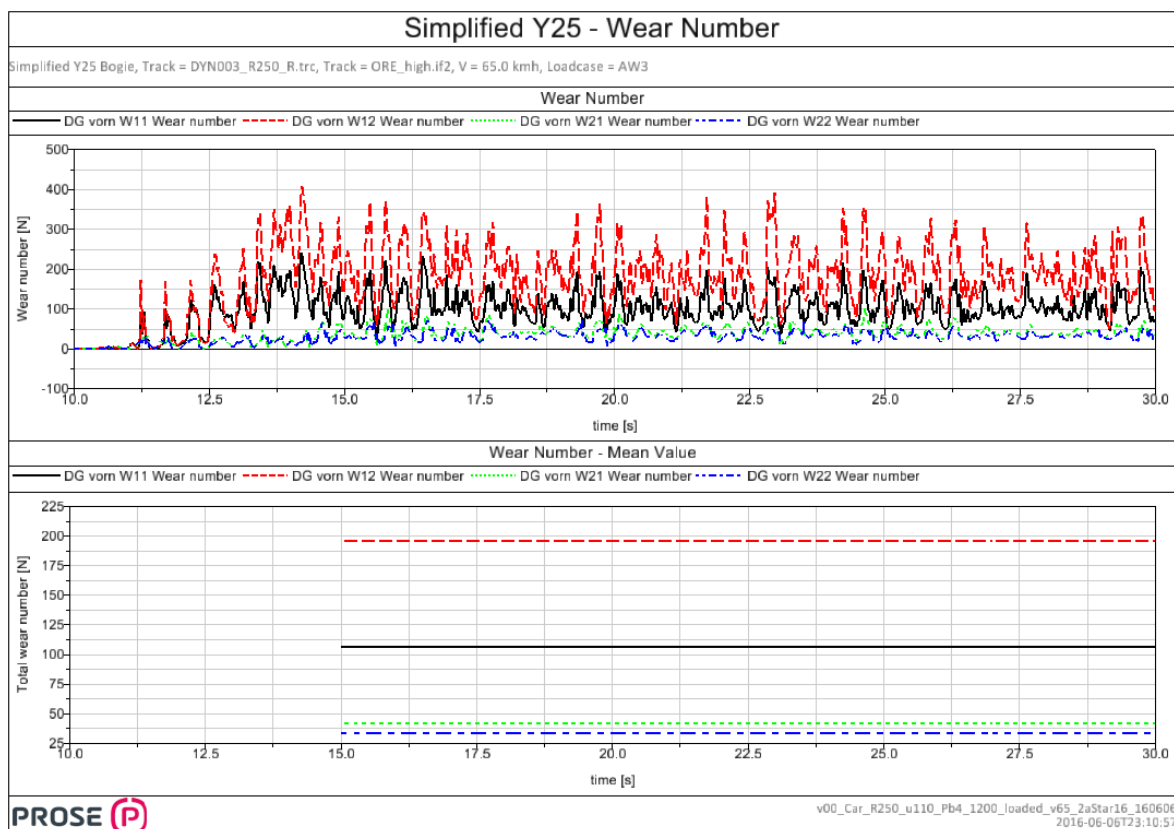


Figure 25: Wear number of simplified Y25 bogie under full load and +0.58 aq

F Non-linear running stability

F.1 Analysis method

The running stability of the FRP bogie was assessed by a nonlinear simulation with SIMPACK. The nonlinear model of the vehicle is riding through a straight track (no excitation) with an initial constant velocity. Directly after the start a short lateral force impulse is applied on each wheelset to create an excitation on the vehicle components. In the case of instability, the damping of the unstable eigenmodes is lower than zero and the affected oscillation amplitudes increase.

The analysis was performed for both load conditions up to 130 km/h.

As assessment values, the lateral wheelset displacement after the impulse is analysed as well as an instability criteria ΣY_{rms} for main line railways defined in EN 14363 [4].

Signal	Abbreviation	Filtering	Limit Value EN 14363
Wheelset Lateral Force	ΣY_{rms}	Bandpass, frequency: 0.4-12 Hz Sliding RMS window length 100 m, Step length 10m	$(10\text{kN} + P_{F0}/3) \cdot 0.85/2$ *) AW0: 9.8 kN AW3: 35.5 kN

Table 14: Signal filtering of the assessment values

*) P_{F0} nominal static vertical wheelset force in kN

The analysis is performed with nominal wheel / rail profiles and rail cant of 1:40 as shown in Figure 4. This results in an equivalent conicity of around 0.2. In further project phases, a complete range of possible equivalent conicities must be checked.

F.2 Results initial bogie

The results for the initial design shows for empty load a certain rest oscillation amplitude. This amplitude is steady and does not seem to increase over time.

The ΣY_{rms} criteria is fulfilled for both loading conditions with the equivalent conicity of around 0.2.

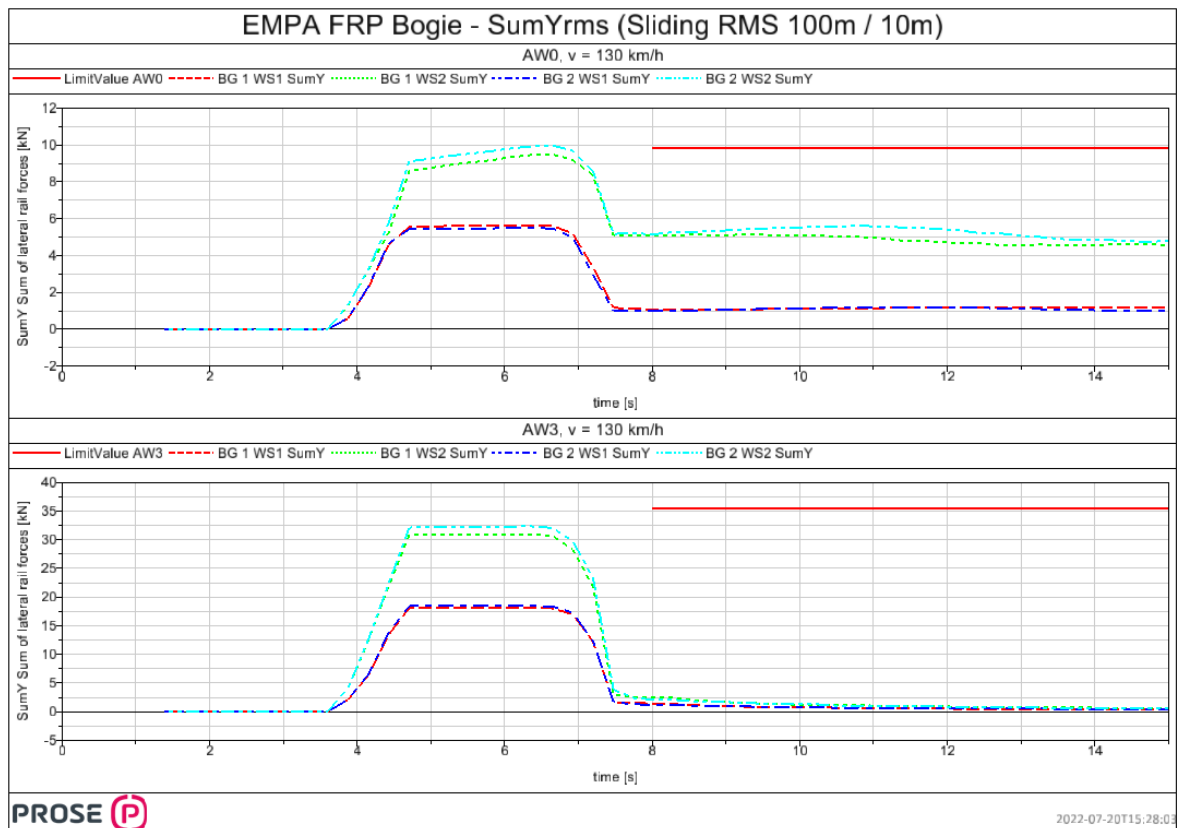


Figure 26: SumYrms for initial bogie design

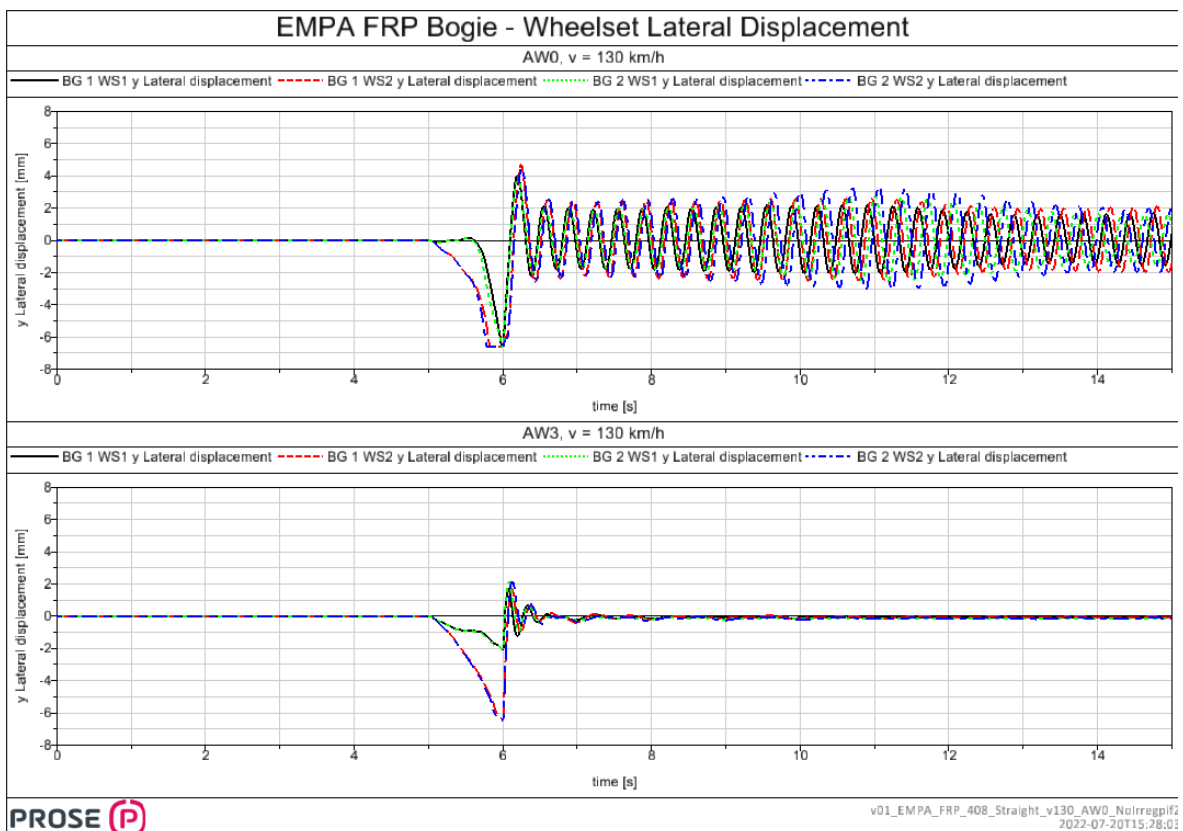


Figure 27: Lateral wheelset displacement for initial bogie design

F.3 Results adapted bogie

The result for the adapted design shows similar behaviour than the initial design. For empty load a certain steady rest oscillation can be seen.

The SumYrms criteria is fulfilled for both loading conditions with the equivalent conicity of around 0.2.

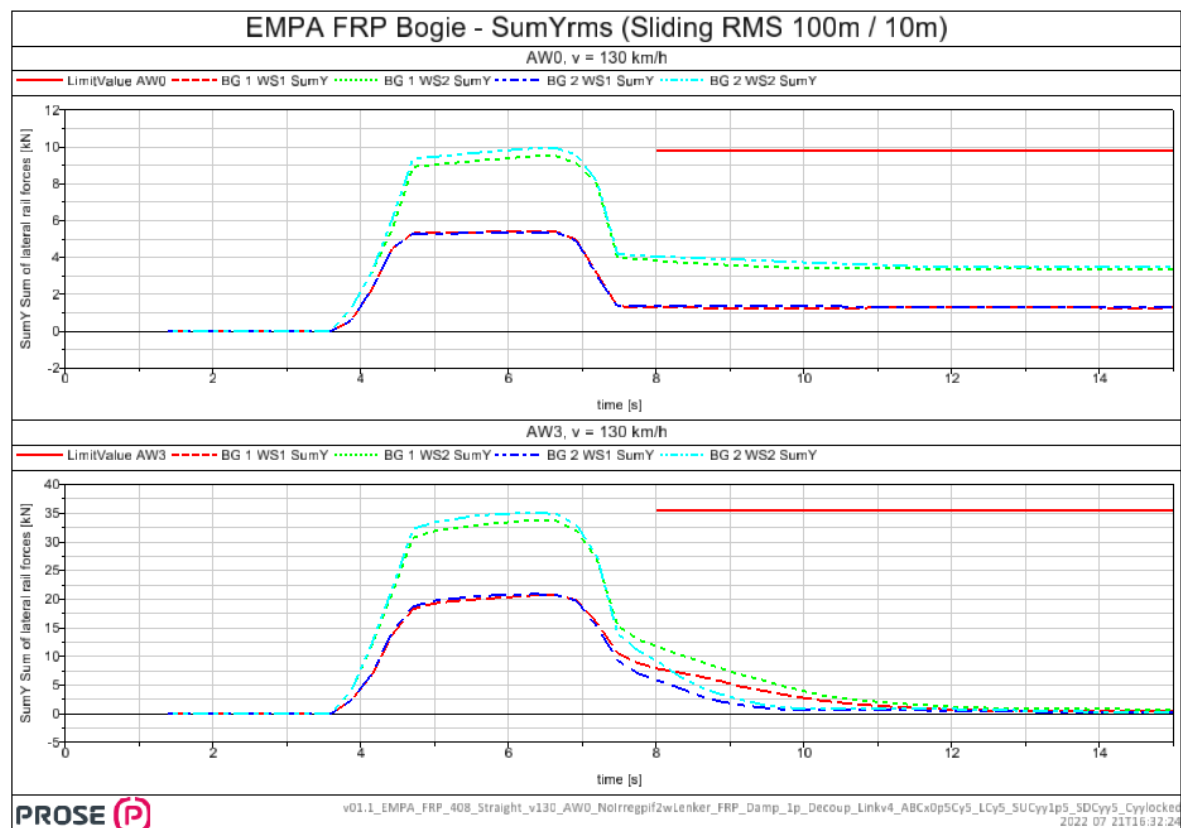


Figure 28: SumYrms for adapted bogie design

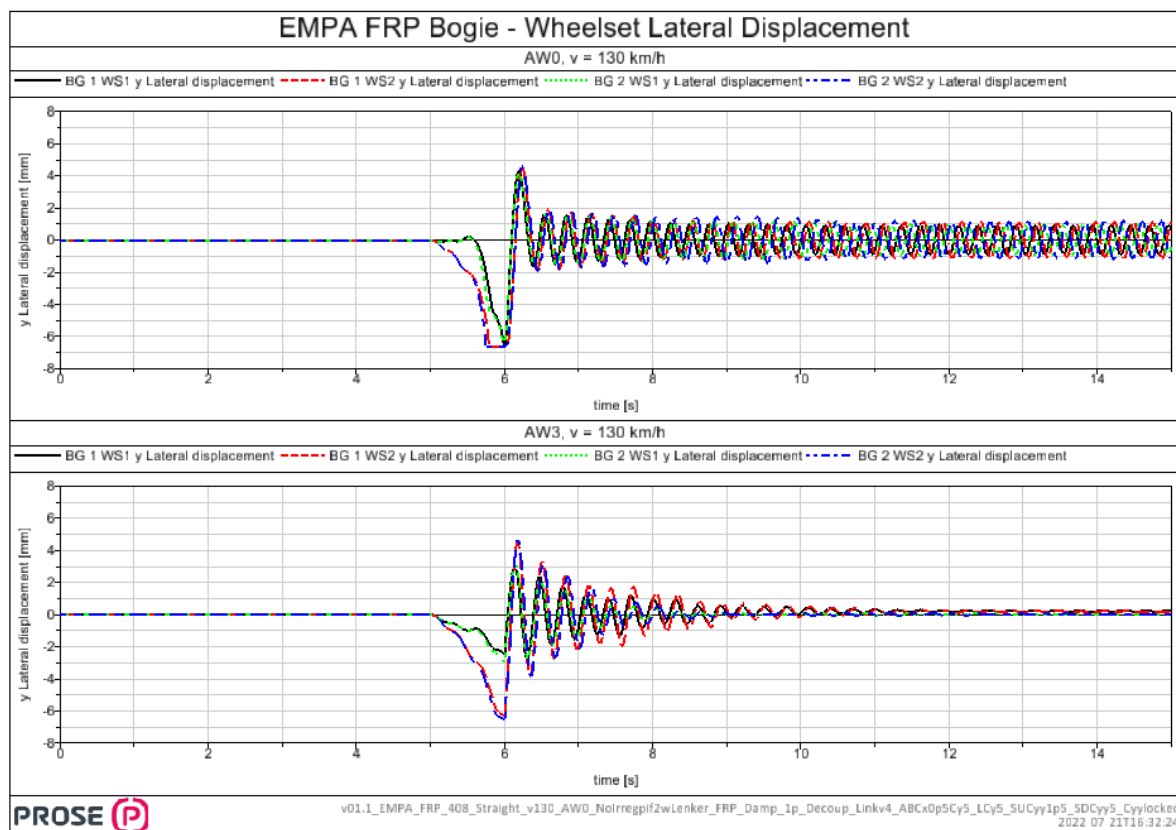


Figure 29: Lateral wheelset displacement for adapted bogie design

G Dynamic analysis

G.1 Analysis method

To analyse the dynamic behaviour of the FRP bogie, some assessment values according to EN 14363 [4] are taken.

The assessment values are to analyse the running safety, track loading and general ride characteristics.

Signal	Abbreviation	Filtering	Limit Value EN 14363
Running Safety			
Lateral force	$\Sigma Y_{j,max}$	Lowpass, corner frequency: 20 Hz Sliding mean value 2 m 0.15 % / 99.85 % Percentile	$(10kN + P_{F0}/3) \cdot 0.85$ *) AW0: 19.6 kN AW3: 71.0 kN
Ratio of guiding force and vertical wheel force leading wheelset	$(Y/Q)_{j,a,max}$	Lowpass, corner frequency: 20 Hz Sliding mean value 2 m 0.15 % / 99.85 % Percentile	0.8 (during curving)
Acceleration on bogie frame	$\ddot{y}_{j,max}^+$	Lowpass, corner frequency: 10 Hz 0.15 % / 99.85 % Percentile	$12 \text{ m/s}^2 - (m+ / 5t) \cdot$ $\text{m/s}^2 = 11.1 \text{ m/s}^2$ $m+ = \text{bogie weight}$
Acceleration in vehicle body	$\ddot{y}_{j,max}^*$	Lowpass, corner frequency: 6 Hz 0.15 % / 99.85 % Percentile	3 m/s^2
	$\ddot{z}_{j,max}^*$	Bandpass, corner frequency: 0.4 Hz to 4 Hz 0.15 % / 99.85 % Percentile	5 m/s^2
Running Safety - Stability			
Lateral Force	$\Sigma Y_{j,rms}$	Bandpass, frequency: 0.4-12 Hz Sliding RMS window length 100 m, Step length 10m Max Value	$(10kN + P_{F0}/3) \cdot 0.85/2$ *) AW0: 9.8 kN AW3: 35.5 kN
Track Loading			
Guiding force	$Y_{j,a,qst}$	Lowpass, corner frequency: 20 Hz 50 % Percentile	60 kN
Vertical wheel force	$Q_{j,a,qst}$	Lowpass, corner frequency: 20 Hz 50 % Percentile	145 kN
	$Q_{j,a,max}$	Lowpass, corner frequency: 20 Hz 99.85 % Percentile	AW0: 109.6 kN AW3: 200 kN

Table 15: Signal filtering of the assessment values

*) P_{F0} nominal static vertical wheelset force in kN

The assessment is carried out on different test zones.

Zone	Type	Nominal		Overspeed		Radius [m]	Transition Curve [m]	Super- elevation [mm]
		Speed [km/h]	aq [m/s ²]	Speed [km/h]	aq [m/s ²]			
1	Straight Track	120	-	132	-	-	-	-
2	Large radius	120	0.61	132	0.94	700	70	150
4	Small radius	80	0.65	86.6	0.95	300	45	150

Table 16: Tracks for dynamic performance assessment

G.2 Results adapted bogie

The results for the empty vehicle from the initial dynamic analysis show a few values that slightly exceed the limit values given by the EN 14363 [4].

The values that exceed the limit values are for AW0 mainly the SumY max values as well as the lateral acceleration and Y/Q values during the R700 curve. The stability and track loading results are all ok.

For the AW3 the results show high lateral acceleration in the vehicle as well as high lateral wheelsets loads. These values are significantly higher than the allowed limit value and must be further investigated in a next phase.

Looking at the frequency spectrum of the carbody accelerations, the highest amplitudes are grouped around 3 Hz for rolling, yawing as well as lateral accelerations over the bogies in the carbody. This indicates instabilities due to carbody low body motion, see Figure 36.

Before doing a more in detail investigation of the dynamic forces, the damping of the FRP parts of the bogie must be determined.

Overspeed		Running Safety				
		SumY max [kN]	(Y/Q) max [-]	y+ max [m/s ²]	y* max [m/s ²]	z* max [m/s ²]
AW0	Straight	19.8	0.70	4.82	3.22	1.59
	R700	22.9	0.82	6.23	4.03	1.59
	R300	18.8	0.63	3.00	2.32	0.74
AW3	Straight	141.1	0.76	8.6	6.8	3.3
	R700	147.7	0.78	9.3	7.4	3.0
	R300	74.1	0.40	3.6	3.5	2.4

Figure 30: Running safety results for adapted bogie design

Overspeed		Stability and Trackloading			
		SumY rms [kN]	Yqst [kN]	Q qst [kN]	Q max [kN]
AW0	Straight	9.1	0.4	20	34
	R700	9.7	6.0	24	37
	R300	6.4	5.5	22	43
AW3	Straight	70.3	0.3	110.3	206.6
	R700	70.9	25.4	142.8	216.4
	R300	24.5	18.3	133.8	211.8

Figure 31: Stability and track loading results for adapted bogie design

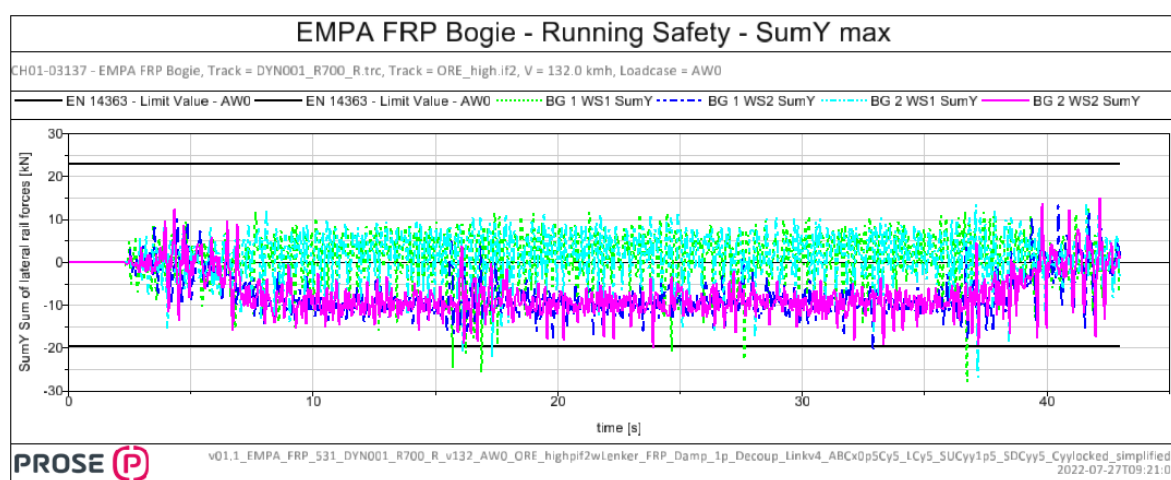


Figure 32: SumY results for the adapted design, empty vehicle on R 700 m track

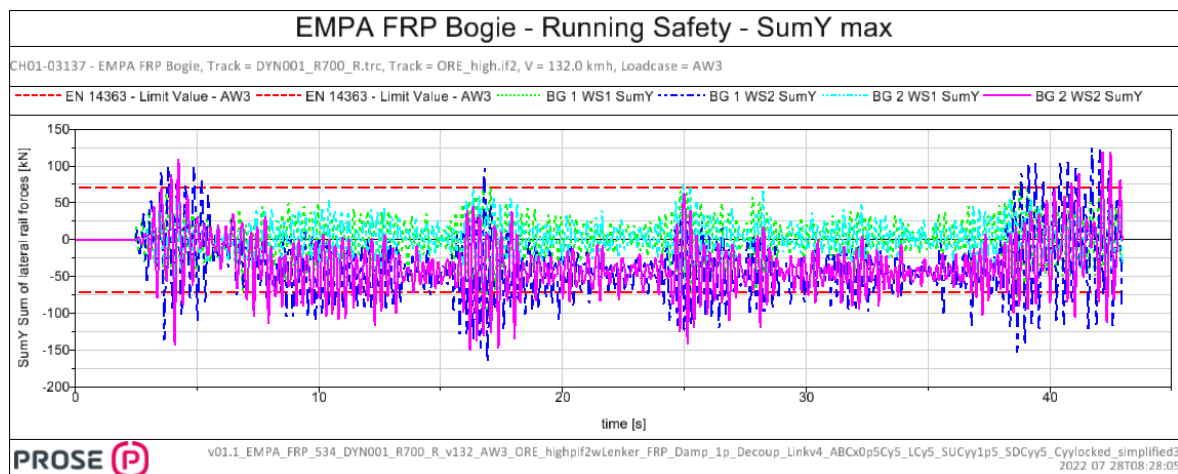


Figure 33: SumY results for the adapted design, fully loaded vehicle on R 700 m track

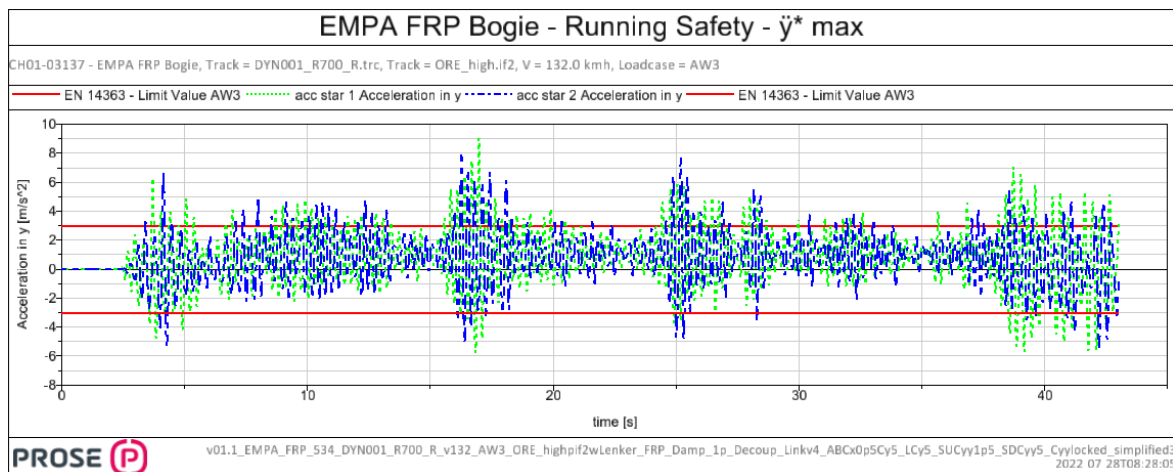


Figure 34: y^* results for the adapted design, fully loaded vehicle on R 700 m track

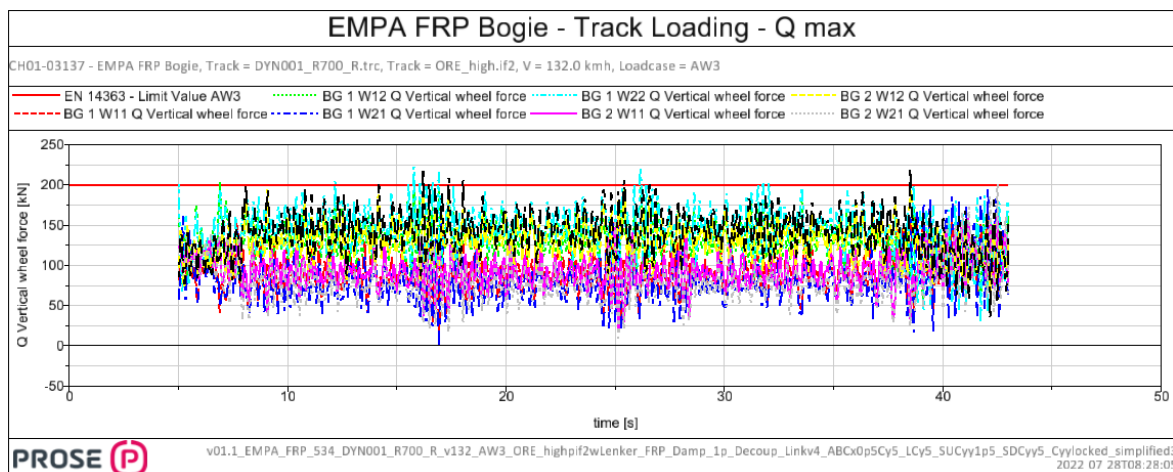


Figure 35: Qmax results for the adapted design, fully loaded vehicle on R 700 m track

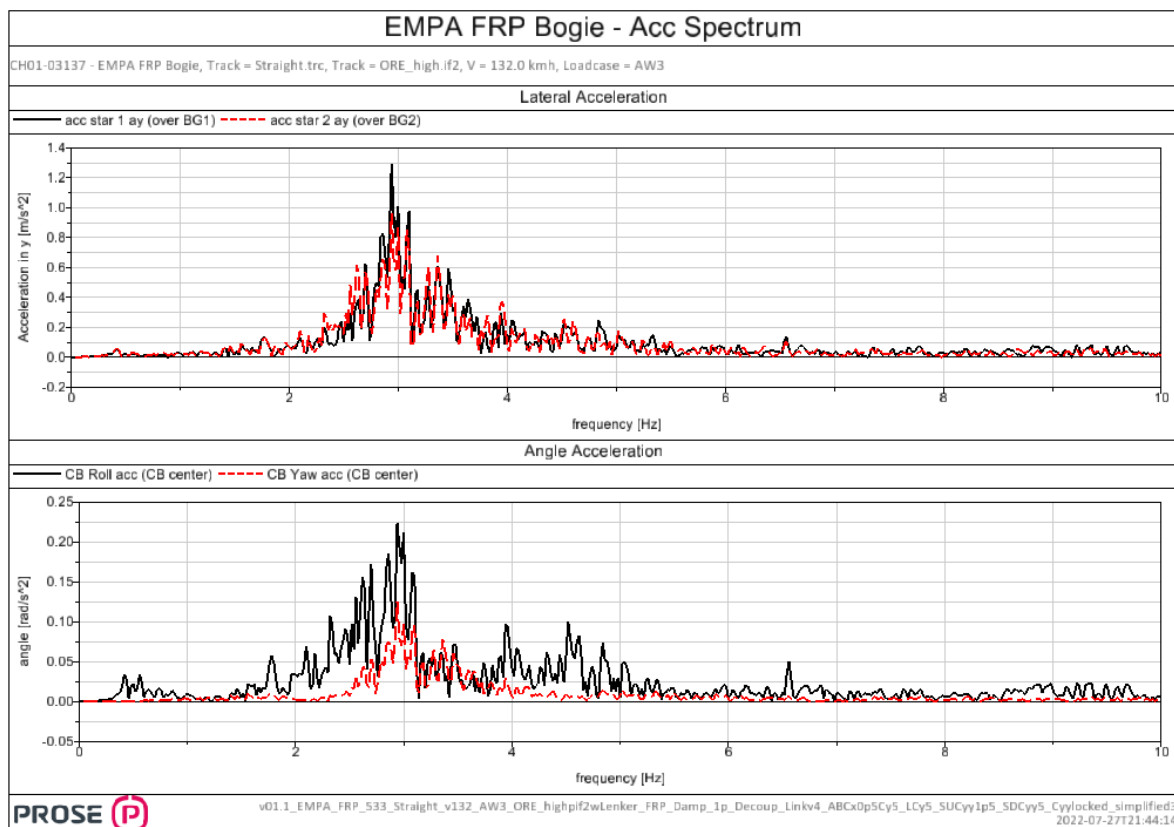


Figure 36: Frequency spectrum for the adapted design, fully loaded vehicle on straight track

Parameterlist FRP Bogie - Initial Concept

Technical specification

Collection of parameters for multi-body simulation (MBS)



Project PROSE: CH01-03137-01
EMPA FRP Bogie Laufdynamik Analyse

EMPA

Prepared	Checked	Released	
D. Meuter	F. Frank	D. Meuter	
Document Number	Version	Status	Release Date
PO000001845	1.0	Released	29.07.2022

PROSE Ltd

Zuercherstrasse 41
8400 Winterthur
Switzerland

www.prose.one
Phone +41 52 262 74 00
info@prose.one

Version Index

Version	Prepared	Checked	Released	Release Date
First issue	D. Meuter	F. Frank	D. Meuter	29.07.2022

Modifications

Version	Description

This document discloses subject matter in which the PROSE Ltd., Winterthur (Switzerland), has proprietary rights. Neither receipt nor possession thereof confers any right to reproduce or disclose the document, any part thereof, any information contained therein, or any physical article or device, or to practise any methods or process, except by written permission from or written agreement with, PROSE Ltd., Winterthur (Switzerland).

This document is computer-generated and valid without signature.

Content

1. Introduction	4
2. Reference documents	4
2.1 Customer's specification	4
2.2 PROSE specifications and drawings	4
2.3 Standards	4
3. General remarks	4
4. Acronyms	5
5. Parameters	6
5.1 Vehicle principal data	6
5.1.1 Geometry	6
5.1.2 Environmental conditions	6
5.1.3 Maximum speed / acceleration	6
5.2 Wheel / rail / track principal data	6
5.2.1 Geometry	6
5.2.2 Contact conditions	7
5.3 Bogie principal data	7
5.3.1 Geometry / mass properties	7
5.3.2 Maximum movements	7
5.4 Rigid bodies	8
5.4.1 Car body	8
5.4.2 Bogie	8
5.4.2.1 Bolster	8
5.4.2.2 Wheelset	9
5.4.2.3 FRP Side-up	9
5.4.2.4 FRP Side-down	9
5.4.2.5 Side bearer	9
5.4.2.6 T-Link	10
5.4.2.7 Crosslink	10
5.4.2.8 Axlewrap	10
5.4.2.9 Centralpivot	10
5.4.2.10 Axlebox	11
5.4.2.11 Brakelink	11
5.4.2.12 Brake	11
5.5 Linking elements	12
5.5.1 T-Link	12
5.5.2 Bolster (bending)	13
5.5.3 FRP Side-up	13
5.5.4 FRP Side-down	14
5.5.5 Axle box bushing	15
5.5.6 Crosslink	15
5.5.7 Drawbar Bushing	15
5.5.8 Side bearer	16
5.5.9 Pivot	16
6. Coordinate systems	17

1. Introduction

This document is a compilation of all parameters necessary to perform the running dynamics simulation.

2. Reference documents

2.1 Customer's specification

Item	Title	Document No.
[A01]	Prepared data for running dynamic analysis of FRP bogie R1, EMPA, 03.06.2022	
[A02]	CAD Model: FRPBogieAssembly.stp, EMPA, 03.06.2022	
[A03]	comments.pdf, EMPA, 03.06.2022	
[A04]		
[A05]		
[A06]		
[A07]		
[A08]		
[A09]		

2.2 PROSE specifications and drawings

Item	Title	Document No.
[R01]		
[R02]		

2.3 Standards

Item	Title	Document No.
[S01]		
[S02]		

3. General remarks

- All geometrical data is provided with regard to unworn wheels and at tare load condition (or according to the load state of any provided bogie drawings).
- Definition of coordinate system (COS) is illustrated in chapter 6.
- All parameters (as mass moments of inertia, stiffness, damping, etc.) are always given in the orientation of the global coordinate system. Exceptions are mentioned in the according tables.
- Translatory quantities are named with x, y, z, while the corresponding rotational quantities are indexed with xx, yy and zz in accordance to the coordinate directions from chapter 6.
- Initials load of specific elements are zero in case they are not further specified.
- All specifications refer to room temperature.

4. Acronyms

TOR	Top of rail
COS	Coordinate system
COG	Center of gravity
MBS	Multi-body simulation
Cx	Translational stiffness cx
Cy	Translational stiffness cy
Cz	Translational stiffness cz
Dx	Translational damping dx
Dy	Translational damping dy
Dz	Translational damping dz
Cxx	Rotational stiffness cxx
Cyy	Rotational stiffness cyy
Czz	Rotational stiffness czz
Dxx	Rotational damping dxx
Dyy	Rotational damping dyy
Dzz	Rotational damping dzz

5. Parameters

5.1 Vehicle principal data

5.1.1 Geometry

Description	Symbol	Value	Unit	Reference	Additional information
Total length		-	m		Single car model without coupling
Total length car body		23	m		only for graphical representation
Total height (above rail level)		4.715	m		only for graphical representation
Total width		2.73	m		only for graphical representation
Pivot distance (between bogies)		16	m	[A03]	
Minimal axle load		4	t	[A03]	
Maximum axle load		22.5	t	[A03]	

5.1.2 Environmental conditions

Description	Symbol	Value	Unit	Reference	Additional information
Minimum outside temperature					
Maximum outside temperature					

5.1.3 Maximum speed / acceleration

Description	Symbol	Value	Unit	Reference	Additional information
Maximum design speed		132	km/h		Max. operating speed +10%
Maximum operating speed		120	km/h		
Maximum uncompensated lateral acceleration		0.65	m/s ²		assumption, 0.65m/s ² nominal and 0.95m/s ² extremal

5.2 Wheel / rail / track principal data

5.2.1 Geometry

Description	Symbol	Value	Unit	Reference	Additional information
Track gauge		1.435	m		
Track gauge vertical measurement distance (relative to TOR)		0.014	m		
Wheel profile		S1002	-	[A03]	
Wheel flange height		0.028	m		
Wheel flange thickness		0.0324	m		
Wheel diameter new		0.92	m		
Wheel diameter worn		-	m		
Tape circle distance		1.5	m		
Wheel back to back distance		1.36	m		1.353m in CAD model
Rail profile		UIC60	-	[A03]	
Rail cant		1:40	-	[A03]	
Track irregularities		ORE high (ERRI B 176)	-		assumption

5.2.2 Contact conditions

Description	Symbol	Value	Unit	Reference	Additional information
Friction coefficient wheel/rail tread					
Nominal	μ_T	0.4	-		values for dry rail
Derailment		0.51			
Friction coefficient wheel/rail flange					
Nominal	μ_F	0.4	-		values for dry rail
Derailment		0.36			
Kalker factor		1	-		common value

5.3 Bogie principal data

5.3.1 Geometry / mass properties

Description	Symbol	Value	Unit	Reference	Additional information
Distance of wheel-sets in bogie		1.8	m		
Total weight bogie		4220	kg	[A01]	

5.3.2 Maximum movements

Description	Symbol	Value	Unit	Reference	Additional information
Primary suspension					
Longitudinal			m		
Lateral			m		
Vertical up (lift stop)			m		
Vertical down (bump stop)			m		
Secondary suspension					
Longitudinal			m		
Lateral			m		
Vertical up (lift stop)			m		
Vertical down (bump stop)			m		

5.4 Rigid bodies

5.4.1 Car body

1 per car

Description	Symbol	Value	Unit	Reference	Additional information
General information					
Carbody torsional flexibility					
Specific torsional stiffness around x-axis		fixed			
Specific torsional damping around x-axis		fixed			
z-coordinate of neutral axis		fixed			

5.4.1.1 Car body tare load condition (AW0)

Description	Symbol	Value	Unit	Reference	Additional information
Mass	m	7'560	kg	[A03]	16t-2x BG
x-coordinate centre of gravity (cog)	xG	0.000	m		COS 2
y-coordinate centre of gravity (cog)	yG	0.000	m		COS 2
z-coordinate centre of gravity (cog)	zG	-1.500	m	[A03]	COS 2
Mass moment of inertia xx relative to cog	Jxx	14'400	kgm ²		estimate
Mass moment of inertia yy relative to cog	Jyy	340'000	kgm ²		estimate
Mass moment of inertia zz relative to cog	Jzz	336'000	kgm ²		estimate

5.4.1.2 Car body gross load condition (AW3)

Description	Symbol	Value	Unit	Reference	Additional information
Mass	m	81'560	kg	[A03]	90t -2x BG
x-coordinate centre of gravity (cog)	xG	0.000	m		COS 2
y-coordinate centre of gravity (cog)	yG	0.000	m		COS 2
z-coordinate centre of gravity (cog)	zG	-1.800	m		COS 2
Mass moment of inertia xx relative to cog	Jxx	145'000	kgm ²		estimate
Mass moment of inertia yy relative to cog	Jyy	3'410'000	kgm ²		estimate
Mass moment of inertia zz relative to cog	Jzz	3'370'000	kgm ²		estimate

5.4.2 Bogie

5.4.2.1 Bolster

1 per bogie

Description	Symbol	Value	Unit	Reference	Additional information
Mass	m	369	kg	[A01]	Steel
x-coordinate centre of gravity (cog)	xG	0.000	m		COS 1
y-coordinate centre of gravity (cog)	yG	0.000	m		COS 1
z-coordinate centre of gravity (cog)	zG	-0.727	m		COS 1
Mass moment of inertia xx relative to cog	Jxx	145.39	kgm ²		
Mass moment of inertia yy relative to cog	Jyy	17.39	kgm ²		
Mass moment of inertia zz relative to cog	Jzz	146.77	kgm ²		

5.4.2.2 Wheelset

2 per bogie

Description	Symbol	Value	Unit	Reference	Additional information
Mass	m	1'380	kg	[A01]	1/2 of wheels 1200 kg, axles 800kg, disc brakes 760 kg
x-coordinate centre of gravity (cog)	xG	0.000	m		Center wheelset
y-coordinate centre of gravity (cog)	yG	0.000	m		Center wheelset
z-coordinate centre of gravity (cog)	zG	0.000	m		Center wheelset
Mass moment of inertia xx relative to cog	Jxx	688	kgm ²		estimate
Mass moment of inertia yy relative to cog	Jyy	97	kgm ²		estimate
Mass moment of inertia zz relative to cog	Jzz	688	kgm ²		estimate

5.4.2.3 FRP Side-up

2 per bogie

Description	Symbol	Value	Unit	Reference	Additional information
Mass	m	24	kg	[A01]	GFRP
x-coordinate centre of gravity (cog)	xG	0.000	m		COS 1
y-coordinate centre of gravity (cog)	yG	± 0.972	m		COS 1
z-coordinate centre of gravity (cog)	zG	-0.567	m		COS 1
Mass moment of inertia xx relative to cog	Jxx	0.151	kgm ²		
Mass moment of inertia yy relative to cog	Jyy	10.37	kgm ²		
Mass moment of inertia zz relative to cog	Jzz	10.32	kgm ²		

5.4.2.4 FRP Side-down

2 per bogie

Description	Symbol	Value	Unit	Reference	Additional information
Mass	m	54	kg	[A01]	GFRP
x-coordinate centre of gravity (cog)	xG	0.000	m		COS 1
y-coordinate centre of gravity (cog)	yG	± 0.972	m		COS 1
z-coordinate centre of gravity (cog)	zG	-0.331	m		COS 1
Mass moment of inertia xx relative to cog	Jxx	0.367	kgm ²		
Mass moment of inertia yy relative to cog	Jyy	24.67	kgm ²		
Mass moment of inertia zz relative to cog	Jzz	24.54	kgm ²		

5.4.2.5 Side bearer

2 per bogie

Description	Symbol	Value	Unit	Reference	Additional information
Mass	m	5	kg	[A01]	Rubber
x-coordinate centre of gravity (cog)	xG	0.000	m		COS 1
y-coordinate centre of gravity (cog)	yG	± 0.85	m		COS 1
z-coordinate centre of gravity (cog)	zG	-0.951	m		COS 1
Mass moment of inertia xx relative to cog	Jxx	0.0081	kgm ²		
Mass moment of inertia yy relative to cog	Jyy	0.0756	kgm ²		
Mass moment of inertia zz relative to cog	Jzz	0.0765	kgm ²		

5.4.2.6 T-Link

4 per bogie

Description	Symbol	Value	Unit	Reference	Additional information
Mass	m	4	kg	[A01]	GFRP
x-coordinate centre of gravity (cog)	xG	± 0.485	m		COS 1
y-coordinate centre of gravity (cog)	yG	± 0.964	m		COS 1
z-coordinate centre of gravity (cog)	zG	-0.745	m		COS 1
Mass moment of inertia xx relative to cog	Jxx	0.0231	kgm ²		
Mass moment of inertia yy relative to cog	Jyy	0.295	kgm ²		
Mass moment of inertia zz relative to cog	Jzz	0.297	kgm ²		

5.4.2.7 Crosslink

2 per bogie

Description	Symbol	Value	Unit	Reference	Additional information
Mass	m	40	kg	[A01]	Steel, added to bolster weight in MBS
x-coordinate centre of gravity (cog)	xG	-0.010	m		COS 1
y-coordinate centre of gravity (cog)	yG	-/+ 0.01	m		COS 1
z-coordinate centre of gravity (cog)	zG	-0.175	m		COS 1
Mass moment of inertia xx relative to cog	Jxx	22.86	kgm ²		
Mass moment of inertia yy relative to cog	Jyy	7.74	kgm ²		
Mass moment of inertia zz relative to cog	Jzz	30.59	kgm ²		

5.4.2.8 Axlewrap

4 per bogie

Description	Symbol	Value	Unit	Reference	Additional information
Mass	m	3.5	kg	[A01]	Rubber, added to axlebox weight in MBS model
x-coordinate centre of gravity (cog)	xG	± 0.9	m		COS 1
y-coordinate centre of gravity (cog)	yG	± 1	m		COS 1
z-coordinate centre of gravity (cog)	zG	-0.466	m		COS 1
Mass moment of inertia xx relative to cog	Jxx	0.03	kgm ²		
Mass moment of inertia yy relative to cog	Jyy	0.043	kgm ²		
Mass moment of inertia zz relative to cog	Jzz	0.03	kgm ²		

5.4.2.9 Centralpivot

1 per bogie

Description	Symbol	Value	Unit	Reference	Additional information
Mass	m	39	kg	[A01]	Steel, added to bolster weight in MBS model
x-coordinate centre of gravity (cog)	xG	0.000	m		COS 1
y-coordinate centre of gravity (cog)	yG	0.000	m		COS 1
z-coordinate centre of gravity (cog)	zG	-0.945	m		COS 1
Mass moment of inertia xx relative to cog	Jxx	0.287	kgm ²		
Mass moment of inertia yy relative to cog	Jyy	0.287	kgm ²		
Mass moment of inertia zz relative to cog	Jzz	0.537	kgm ²		

5.4.2.10 Axlebox

4 per bogie

Description	Symbol	Value	Unit	Reference	Additional information
Mass	m	104	kg	[A01]	Steel
x-coordinate centre of gravity (cog)	xG	0.900	m		COS 1
y-coordinate centre of gravity (cog)	yG	0.970	m		COS 1
z-coordinate centre of gravity (cog)	zG	-0.466	m		COS 1
Mass moment of inertia xx relative to cog	Jxx	3.81	kgm ²		
Mass moment of inertia yy relative to cog	Jyy	4.45	kgm ²		
Mass moment of inertia zz relative to cog	Jzz	2.33	kgm ²		

5.4.2.11 Brakelink

4 per bogie

Description	Symbol	Value	Unit	Reference	Additional information
Mass	m	23	kg	[A01]	Steel, added to bolster weight in MBS model
x-coordinate centre of gravity (cog)	xG	0.390	m		COS 1
y-coordinate centre of gravity (cog)	yG	0.520	m		COS 1
z-coordinate centre of gravity (cog)	zG	-0.547	m		COS 1
Mass moment of inertia xx relative to cog	Jxx	3	kgm ²		
Mass moment of inertia yy relative to cog	Jyy	3.35	kgm ²		
Mass moment of inertia zz relative to cog	Jzz	2.67	kgm ²		

5.4.2.12 Brake

4 per bogie

Description	Symbol	Value	Unit	Reference	Additional information
Mass	m	176	kg	[A01]	Mass for all 4 breaks, value separated in MBS model
x-coordinate centre of gravity (cog)	xG	0.537	m		COS 1
y-coordinate centre of gravity (cog)	yG	0.522	m		COS 1
z-coordinate centre of gravity (cog)	zG	-0.457	m		COS 1
Mass moment of inertia xx relative to cog	Jxx	1	kgm ²		point mass
Mass moment of inertia yy relative to cog	Jyy	1	kgm ²		point mass
Mass moment of inertia zz relative to cog	Jzz	1	kgm ²		point mass

5.5 Linking elements

5.5.1 T-Link

4 per bogie

Description	Symbol	Value	Unit	Reference	Additional information
Connection point on axle box	AB	Initial	Adapted	[A02]	
x-coordinate	x	± 0.900	- m		COS 1
y-coordinate	y	± 0.965	- m		COS 1
z-coordinate	z	-0.751	- m		COS 1
Connection point on bolster	BB			[A02]	
x-coordinate	x	± 0.241	- m		COS 1
y-coordinate	y	± 0.965	- m		COS 1
z-coordinate	z	-0.751	- m		COS 1
Parameter - Center	AB				Axlebox connection
Translational stiffness cx	cx	4.00E+09	- N/m		fixed
Translational stiffness cy	cy	6.50E+06	- N/m		
Translational stiffness cz	cz	5.00E+07	- N/m		
Translational damping dx	dx	4.00E+06	- Ns/m		1% of Stiffness
Translational damping dy	dy	6'500.0	- Ns/m		1% of Stiffness
Translational damping dz	dz	50'000.0	- Ns/m		1% of Stiffness
Rotational stiffness cxx	cxx	500.0	- Nm/rad		free
Rotational stiffness cyy	cyy	-	- Nm/rad		free
Rotational stiffness czz	czz	100'000.0	- Nm/rad		fixed
Rotational damping dxx	dxx	0.5	- Nms/rad		1% of Stiffness
Rotational damping dyy	dyy	-	- Nms/rad		1% of Stiffness
Rotational damping dzz	dzz	100.0	- Nms/rad		1% of Stiffness
Parameter - Center	CT				
Translational stiffness cx	cx	1.12E+08	- N/m		initial stiffness, non-linear
Translational stiffness cy	cy	1.12E+08	- N/m		
Translational stiffness cz	cz	5.00E+07	- N/m		
Translational damping dx	dx	1.12E+06	- Ns/m		1% of Stiffness
Translational damping dy	dy	1.12E+06	- Ns/m		1% of Stiffness
Translational damping dz	dz	5.00E+05	- Ns/m		1% of Stiffness
Rotational stiffness cxx	cxx	500	- Nm/rad		free
Rotational stiffness cyy	cyy	250'000	- Nm/rad		
Rotational stiffness czz	czz	100'000	- Nm/rad		
Rotational damping dxx	dxx	1	- Nms/rad		1% of Stiffness
Rotational damping dyy	dyy	250	- Nms/rad		1% of Stiffness
Rotational damping dzz	dzz	100	- Nms/rad		1% of Stiffness
Parameter - BB	BB				Rot. joint YY
Rotational stiffness cyy	cyy	60'000	- Nm/rad		
Rotational damping dyy	dyy	60	- Nms/rad		1% of Stiffness

5.5.2 Bolster (bending)

2 per bogie

Description	Symbol	Value		Unit	Reference	Additional information
Connection point torsion	Tors	Initial	Adapted			
x-coordinate	x	0.000	0.000	m		COS 1
y-coordinate	y	± 0.31725	0.317	m		COS 1, estimated
z-coordinate	z	-0.720	-0.720	m		COS 1, estimated
Parameter - BB	Tors					Rot. joint YY
Rotational stiffness cxx	cxx	3.36E+07	3.36E+07	Nm/rad		
Rotational damping dxx	dxx	33'600	33'600	Nms/rad		0.1% of Stiffness

5.5.3 FRP Side-up

2 per bogie

Description	Symbol	Value		Unit	Reference	Additional information
Contact point vertical hardstop to side-down	SD	Initial	Adapted		[A02]	
x-coordinate	x	0.000	0.000	m		COS 1
y-coordinate	y	± 0.975	± 0.975	m		COS 1
z-coordinate	z	-0.465	-0.465	m		COS 1
Center piece <=> transition	CP				[A02]	
x-coordinate	x	± 0.25	± 0.25	m		COS 1
y-coordinate	y	± 0.975	± 0.975	m		COS 1
z-coordinate	z	-0.500	-0.500	m		COS 1
Center piece <=> bolster	BB				[A02]	
x-coordinate	x	0.000	0.000	m		COS 1
y-coordinate	y	± 0.975	± 0.975	m		COS 1
z-coordinate	z	-0.525	-0.525	m		COS 1
Transition <=> end piece	EP				[A02]	
x-coordinate	x	± 0.650	± 0.650	m		COS 1
y-coordinate	y	± 0.975	± 0.975	m		COS 1
z-coordinate	z	-0.582	-0.582	m		COS 1
Parameter - BB	BB					Rubber Pad
Translational stiffness cx	cx	5.00E+09	5.00E+09	N/m		fixed
Translational stiffness cy	cy	1.00E+09	1.00E+09	N/m		fixed
Translational stiffness cz	cz	1.24E+09	1.24E+09	N/m		fixed
Translational damping dx	dx	5.00E+06	5.00E+06	Ns/m		0.1% of Stiffness
Translational damping dy	dy	1.00E+06	1.00E+06	Ns/m		0.1% of Stiffness
Translational damping dz	dz	1.24E+06	1.24E+06	Ns/m		0.1% of Stiffness
Rotational stiffness cxx	cxx	5'000	5'000	Nm/rad		
Rotational stiffness cyy	cyy	40'000	40'000	Nm/rad		
Rotational stiffness czz	czz	1.00E+08	1.00E+08	Nm/rad		fixed
Rotational damping dxx	dxx	5	5	Nms/rad		0.1% of Stiffness
Rotational damping dyy	dyy	40	40	Nms/rad		0.1% of Stiffness
Rotational damping dzz	dzz	100'000	100'000	Nms/rad		0.1% of Stiffness
Parameter - CP	CP					
Translational stiffness cx	cx	9.00E+07	9.00E+07	N/m		
Translational stiffness cy	cy	8.00E+07	8.00E+07	N/m		
Translational stiffness cz	cz	7.50E+07	7.50E+07	N/m		
Translational damping dx	dx	9.00E+05	9.00E+05	Ns/m		1% of Stiffness
Translational damping dy	dy	8.00E+05	8.00E+05	Ns/m		1% of Stiffness
Translational damping dz	dz	7.50E+05	7.50E+05	Ns/m		1% of Stiffness
Rotational stiffness cxx	cxx	75'000	75'000	Nm/rad		
Rotational stiffness cyy	cyy	115'000	172'500	Nm/rad		

Rotational stiffness czz	czz	780'000	780'000	Nm/rad	
Rotational damping dxx	dxx	750	750	Nms/rad	1% of Stiffness
Rotational damping dyy	dyy	1'150	1'725	Nms/rad	1% of Stiffness
Rotational damping dzz	dzz	7'800	7'800	Nms/rad	1% of Stiffness
Parameter - EP		EP			
Translational stiffness cx	cx	9.00E+07	9.00E+07	N/m	
Translational stiffness cy	cy	8.00E+07	8.00E+07	N/m	
Translational stiffness cz	cz	7.50E+07	7.50E+07	N/m	
Translational damping dx	dx	9.00E+05	9.00E+05	Ns/m	1% of Stiffness
Translational damping dy	dy	8.00E+05	8.00E+05	Ns/m	1% of Stiffness
Translational damping dz	dz	7.50E+05	7.50E+05	Ns/m	1% of Stiffness
Rotational stiffness cxx	cxx	75'000	75'000	Nm/rad	
Rotational stiffness cyy	cyy	207'000	310'500	Nm/rad	
Rotational stiffness czz	czz	780'000	780'000	Nm/rad	
Rotational damping dxx	dxx	750	750	Nms/rad	1% of Stiffness
Rotational damping dyy	dyy	2'070	3'105	Nms/rad	1% of Stiffness
Rotational damping dzz	dzz	7'800	7'800	Nms/rad	1% of Stiffness
Parameter - Vertical hard stop between FRP side-up and -down		HS			
Gap	dZ	0.010	0.010	m	

5.5.4 FRP Side-down

2 per bogie

Description	Symbol	Value		Unit	Reference	Additional information
Contact point vertical hardstop to side-up	SU	Initial	Adapted		[A02]	
x-coordinate	x	0.000	0.000	m		COS 1
y-coordinate	y	± 0.975	± 0.975	m		COS 1
z-coordinate	z	-0.455	-0.455	m		COS 1
Center piece <=> transition	CP				[A02]	
x-coordinate	x	± 0.25	± 0.25	m		COS 1
y-coordinate	y	± 0.975	± 0.975	m		COS 1
z-coordinate	z	-0.400	-0.400	m		COS 1
Transition <=> end piece	EP				[A02]	
x-coordinate	x	± 0.650	± 0.650	m		COS 1
y-coordinate	y	± 0.975	± 0.975	m		COS 1
z-coordinate	z	-0.316	-0.316	m		COS 1
Parameter - CP	CP					
Translational stiffness cx	cx	5.00E+07	5.00E+07	N/m		
Translational stiffness cy	cy	1.40E+07	1.40E+07	N/m		
Translational stiffness cz	cz	2.00E+07	2.00E+07	N/m		
Translational damping dx	dx	5.00E+05	5.00E+05	Ns/m		1% of Stiffness
Translational damping dy	dy	1.40E+05	1.40E+05	Ns/m		1% of Stiffness
Translational damping dz	dz	2.00E+05	2.00E+05	Ns/m		1% of Stiffness
Rotational stiffness cxx	cxx	82'500	82'500	Nm/rad		
Rotational stiffness cyy	cyy	520'150	2'600'750	Nm/rad		
Rotational stiffness czz	czz	1'040'000	1'040'000	Nm/rad		
Rotational damping dxx	dxx	825	825	Nms/rad		1% of Stiffness
Rotational damping dyy	dyy	5'202	26'008	Nms/rad		1% of Stiffness
Rotational damping dzz	dzz	10'400	10'400	Nms/rad		1% of Stiffness
Parameter - EP	EP					
Translational stiffness cx	cx	5.00E+07	5.00E+07	N/m		
Translational stiffness cy	cy	1.40E+07	1.40E+07	N/m		

Translational stiffness cz	cz	2.00E+07	2.00E+07	N/m	
Translational damping dx	dx	5.00E+05	5.00E+05	Ns/m	1% of Stiffness
Translational damping dy	dy	1.40E+05	1.40E+05	Ns/m	1% of Stiffness
Translational damping dz	dz	2.00E+05	2.00E+05	Ns/m	1% of Stiffness
Rotational stiffness cxx	cxx	82'500	82'500	Nm/rad	
Rotational stiffness cyy	cyy	740'000	740'000	Nm/rad	
Rotational stiffness czz	czz	1'040'000	1'040'000	Nm/rad	
Rotational damping dxx	dxx	825	825	Nms/rad	1% of Stiffness
Rotational damping dyy	dyy	7'400	7'400	Nms/rad	1% of Stiffness
Rotational damping dzz	dzz	10'400	10'400	Nms/rad	1% of Stiffness

5.5.5 Axle box bushing

2 per bogie

Description	Symbol	Value		Unit	Reference	Additional information
Connection point		Initial	Adapted		[A02]	Initial: FRP <=> axlebox
x-coordinate	x	± 0.900	± 0.900	m		Adapted: bar <=> axlebox
y-coordinate	y	± 0.969	0.975	m		COS 1
z-coordinate	z	-0.460	-0.455	m		COS 1
Parameter	BSH	Initial	Adapted			Initial: FRP <=> Axlebox
Translational stiffness cx	cx	5.00E+06	5.00E+06	N/m		Adapted: bar <=> axlebox
Translational stiffness cy	cy	2.00E+06	1.00E+07	N/m		
Translational stiffness cz	cz	1.00E+08	1.00E+08	N/m		
Translational damping dx	dx	5'000	5'000	Ns/m		0.1% of Stiffness
Translational damping dy	dy	2'000	10'000	Ns/m		0.1% of Stiffness
Translational damping dz	dz	100'000	100'000	Ns/m		0.1% of Stiffness
Rotational stiffness cxx	cxx	1'000	1'000	Nm/rad		
Rotational stiffness cyy	cyy	10'000	10'000	Nm/rad		
Rotational stiffness czz	czz	10'000	10'000	Nm/rad		
Rotational damping dxx	dxx	1	1	Nms/rad		0.1% of Stiffness
Rotational damping dyy	dyy	10	10	Nms/rad		0.1% of Stiffness
Rotational damping dzz	dzz	10	10	Nms/rad		0.1% of Stiffness

5.5.6 Crosslink

2 per bogie

Description	Symbol	Value		Unit	Reference	Additional information
Parameter	BSH	Initial	Adapted			Data Eco bogie, center bearing
Stiffness c	c	1.00E+09	-	N/m		very stiff
Damping d	d	80'000	-	Nms/rad		

5.5.7 Drawbar Bushing

1 per bogie

Description	Symbol	Value		Unit	Reference	Additional information
Bushing		Initial	Adapted			
x-coordinate	x	-	0.000	m		
y-coordinate	y	-	0.000	m		COS 1
z-coordinate	z	-	-0.460	m		COS 1
Parameter	BSH	Initial	Adapted			
Translational stiffness cx	cx	-	2.00E+06	N/m		
Translational stiffness cy	cy	-	3.75E+07	N/m		
Translational stiffness cz	cz	-	7.50E+06	N/m		
Translational damping dx	dx	-	10'000	Ns/m		0.5% of Stiffness
Translational damping dy	dy	-	187'500	Ns/m		0.5% of Stiffness

Translational damping dz	dz	-	37'500	Ns/m	0.5% of Stiffness
Rotational stiffness cxx	cxx	-	0	Nm/rad	
Rotational stiffness cyy	cyy	-	100'000	Nm/rad	
Rotational stiffness czz	czz	-	0	Nm/rad	
Rotational damping dxx	dxx	-	0	Nms/rad	0.5% of Stiffness
Rotational damping dyy	dyy	-	100	Nms/rad	0.5% of Stiffness
Rotational damping dzz	dzz	-	0	Nms/rad	0.5% of Stiffness

5.5.8 Side bearer

2 per bogie

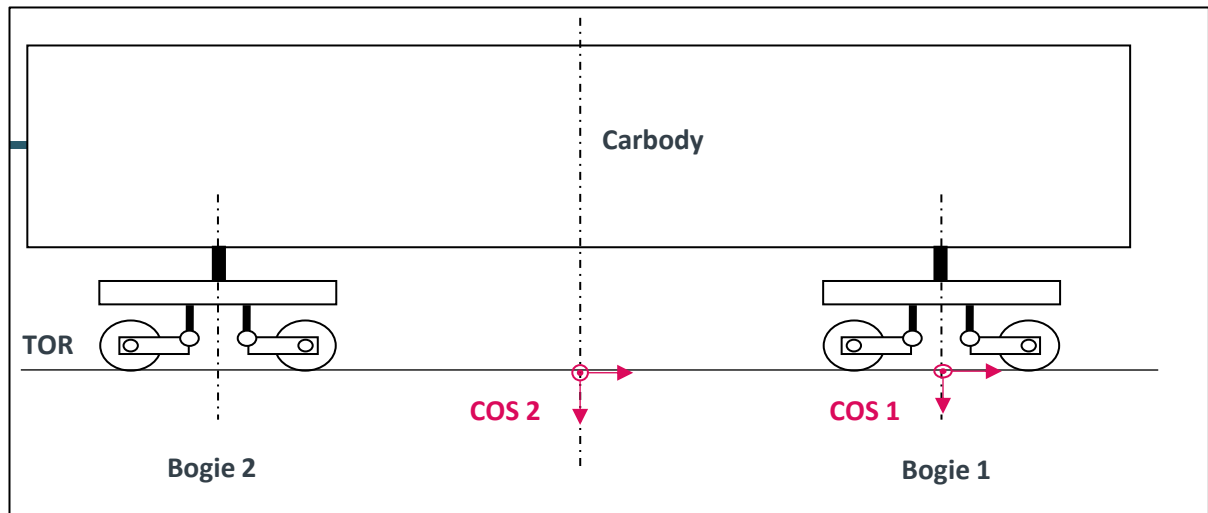
Description	Symbol	Value		Unit	Reference	Additional information
Connection point on bogie bolster		Initial	Adapted			
x-coordinate	x	0.000	0.000	m		COS 1
y-coordinate	y	± 0.85	± 0.805	m		COS 1
z-coordinate	z	-0.905	-0.905	m		COS 1
Parameter						
Gap X	dX	±0.001	0.001	m		Logitudinal movement friciton pad
Longitudinal stiffness	Cx	540'000	540'000	N/m		
Preload vertical	Fz0	16'000	16'000	N		
Vertical stiffness	Cz	570'000	570'000	N/m		
Vertical hard stop	dZ	0.010	0.010	m		Vertical movement friction pad
Friction coefficient		0.35	0.35	-		

5.5.9 Pivot

1 per bogie

Description	Symbol	Value		Unit	Reference	Additional information
Rotation center		Initial	Adapted			
x-coordinate	x	0.000	0.000	m		COS 1
y-coordinate	y	0.000	0.000	m		COS 1
z-coordinate	z	-0.925	-0.925	m		COS 1
Parameter						
Friction coefficient stick		0.2178	0.2178	-		
Friction coefficient slip		0.22	0.22	-		
Friction radius	rzz	0.130	0.130	m		

6. Coordinate systems



The y-origin of the coordinate systems COS 1 and COS 2 is located in the middle of the track. The z-origin of COS 1 and COS 2 is located at the top of the rail.

Project No. 5211.02073

Empa report

Assignment

Client:

Number of pages:

Second interim report

BAFU/BAV, Switzerland

41

Project title: "FRP bogies for freight wagons: A feasibility study"

Project leader and contractor: Empa 303-Structural engineering research lab

Project partners:

- PROSE (railway and certification knowledge),
- Ensinger (manufacturer, FRP knowledge),
- SBB cargo (consulting end user),
- WASCOSA (consulting end user),
- Empa 509 (noise control knowledge)

Dübendorf, 09.08.2022

Ali Saeedi / Moslem Shahverdi / Masoud Motavalli

Contents

1- Overview.....	6
2- Visit of SBB workshop	7
3- Conceptual design of the proposed FRP bogie.....	8
3-1- Design criteria	8
3-2- The proposed concept	11
3-3- Material Selection	16
4- Finite element analysis.....	18
5- Finite element results	20
4-1- Deformations.....	20
4-2- Stress results in the components	23
4-3- Stiffness results in different directions	26
4-4- Modal results.....	29
6- Running dynamic simulations.....	32
7- Summary and conclusion.....	32
8- References.....	32
9- Appendix.....	33

List of figures

Figure 1- An overview of the tasks of the project and current step	6
Figure 2- The time-table of the project and current stage.....	7
Figure 3- Different types of metallic bogies (from visit of a SBB workshop).....	8
Figure 4- Primary suspension system of Y25 bogie with its outer and inner coil springs	9
Figure 5- Force displacement diagram of the primary suspension of Y25 bogie as received from SBB.....	9
Figure 7- Force displacement diagram for the primary suspension system of the Formica bogie as received from Prose	10
Figure 8- Lenoir damping system in Y25 primary suspension	11
Figure 9- Hydraulic dampers in Formica bogie	11
Figure 10- The proposed concept for the newly designed FRP bogie and its components	12
Figure 11- side view of FRP bogie with reference coordinate system	12
Figure 12- Employing two-piece FRP side beams with an initial gap for generating variable stiffness in the vertical direction	14
Figure 13- Employing two-piece FRP side beams with opposite curvature to minimize the wheelset separation due to the applied vertical loads.....	14
Figure 14- Utilizing metallic bolster with FRP side beams in the proposed bogie	15
Figure 15- Weight reduction vs costs for the proposed multi-material system	16
Figure 16- Simplified 3D models of the FRP bogie.....	18
Figure 17- The created full assembly of the FRP bogie in Abaqus for FE analysis.....	18
Figure 18- Finite element model (Mesh view) of the FRP bogie	19
Figure 19- Definition of stacking sequence for FRP side beams in FEM	19
Figure 20- Fiber, matrix and thickness direction in the FRP side beam for creating the proper stacking sequence	20
Figure 21- The calculated load cases for FE analysis.....	20
Figure 22- Deformation of the FRP bogie before and after applying external vertical force on the central pivot	21
Figure 23- the deformation of FRP side beams and filling the initial gap by increasing the applied vertical load on the central pivot	22
Figure 24- Stress in fiber direction in FRP side beams in inner, middle and outer layers	24
Figure 25- Calculated stress in T-shaped links in fiber direction	25
Figure 26- Calculated von-Mises stress in the metallic bolster	25
Figure 27- Vertical force vs vertical displacement at central pivot.....	27

Figure 28- Vertical force at central pivot vs longitudinal displacement of wheels, left) total force on central pivot and right) force on central pivot and side bearer (the result presented for two wheels on the same axle)	28
Figure 29- Transverse force vs transverse displacement at central pivot	28
Figure 30- Longitudinal force vs longitudinal displacement at central pivot	29
Figure 31- Free boundary conditions for modal analysis of FRP component	29

List of Tables

Table 1- General properties of combined FRP-Metallic bogie.....	13
Table 2- Engineering constant of different FRPs [received from Ensinger]	17
Table 3- Stress results for FRP side beams in different directions	26
Table 4- Natural frequencies and mode shapes for FRP component	30
Table 5- Natural frequencies and mode shapes for whole assembly.....	31
Table 6- Geometry and mass properties of FRP bogie components.....	33

1- Overview

In the first interim reports [1], the definition of requirements, evaluation parameters, and proposed design solutions for the FRP frame were presented. Moreover, the initial conceptual model of the selected design based on the pre-determined design criteria was introduced. Tasks 1, 2, and the first portions of Task 3 were the main parts of the first interim report as presented in Figure 1. The finalization of task 3 is first presented in the current report (the second interim report), by introducing the geometrical model and components of the selected design and assigning the proper materials. Considering task 4 of the project, the finite element analysis on the selected conceptual model subjected to different loading cases is then presented. The load-deflection curves for different loading directions and the stress results in the FRP components are discussed. The running dynamics simulation of the bogie (task 5) is currently under investigation and has been partially reported. As illustrated in the project timeline (Figure 2), the project is currently in running dynamic simulation step and the acoustic simulation (task 6) has also begun.

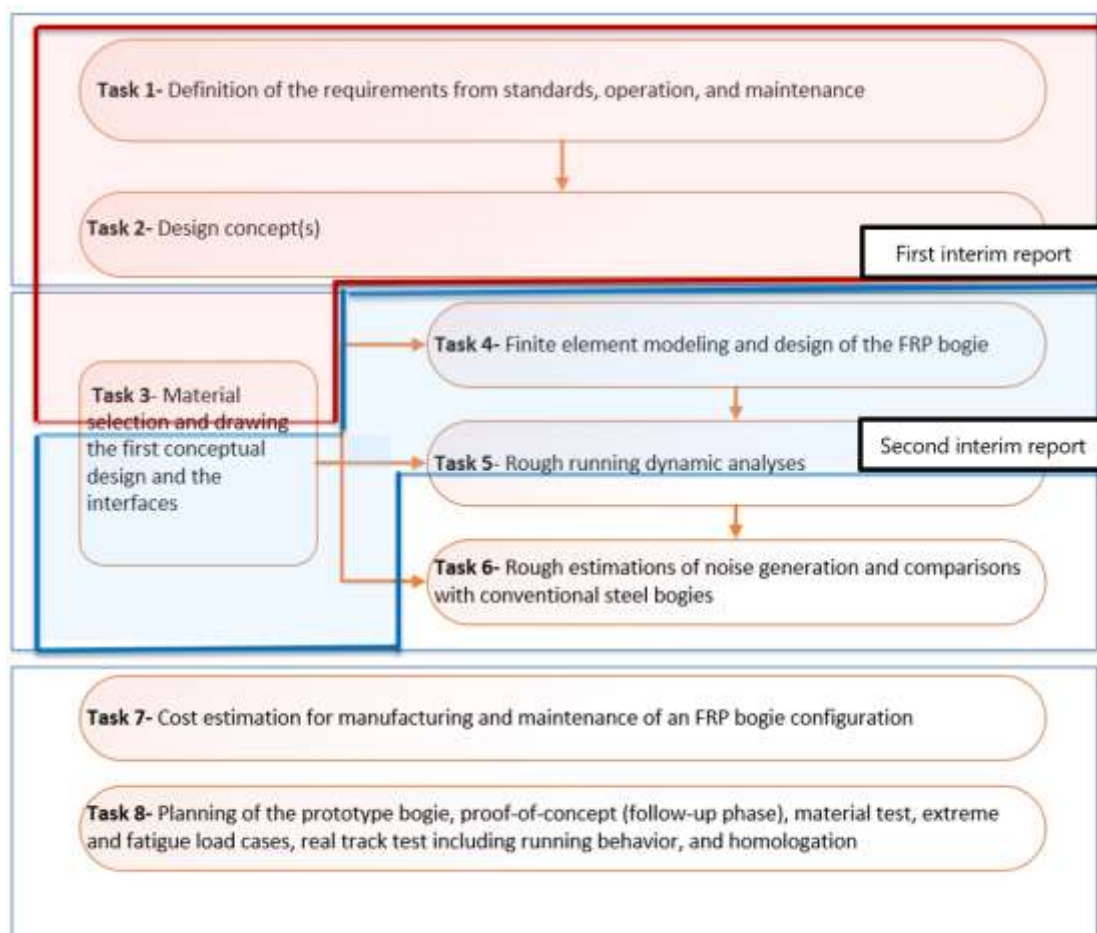


Figure 1- An overview of the tasks of the project and current step

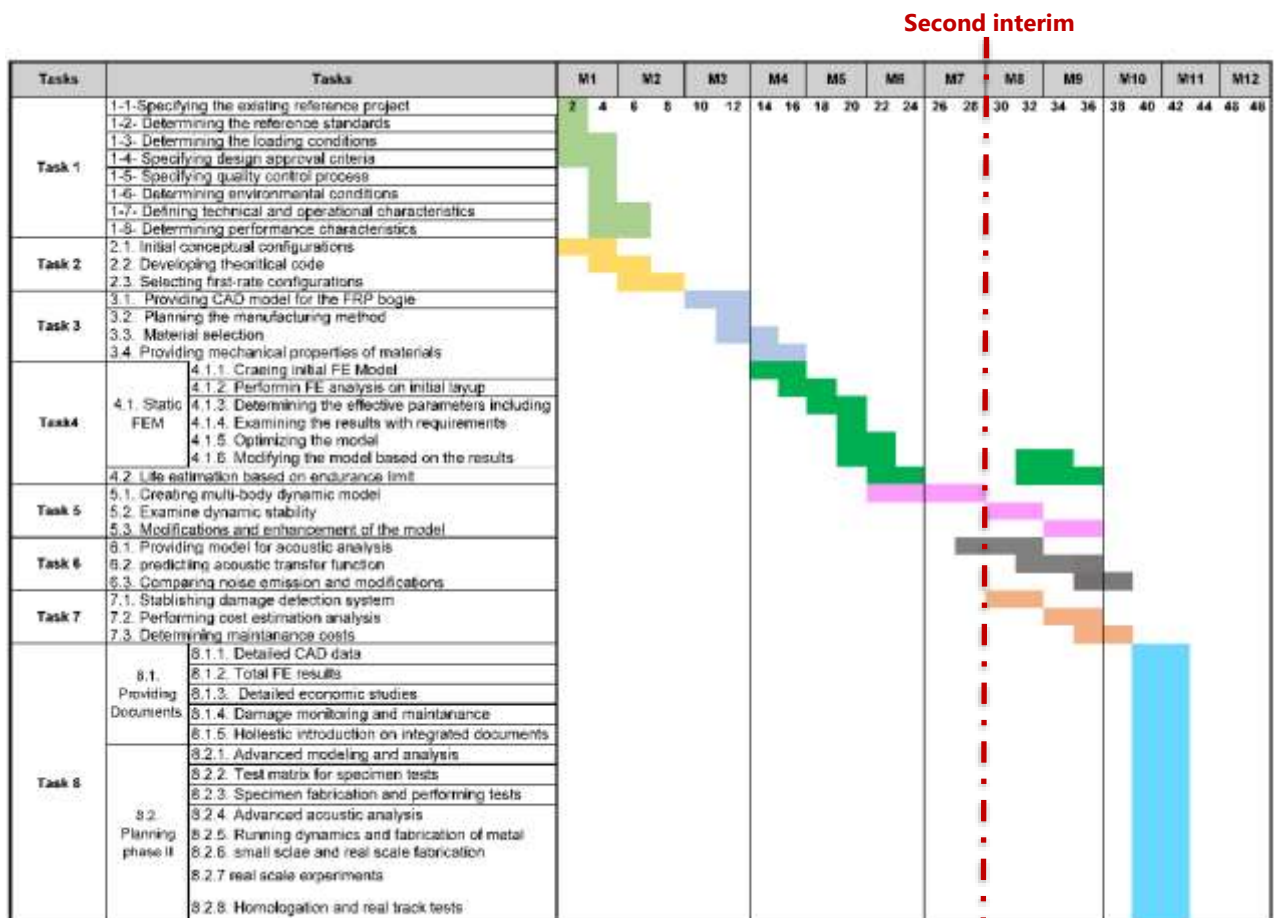


Figure 2- The time-table of the project and current stage

2- Visit of SBB workshop

A visit was made to the SBB workshop in Basel on 10th May 2022, to obtain a more thorough overview of various previously designed and manufactured bogie types. Different types of metallic bogies were visited, including traditional Y25, ELH RC25, TVP Y25D, and DDRs25 bogies, as presented in Figure 3. The interfaces and connections to the car body, brake mechanisms (disk brake and wheel push brakes), damping elements (e.g., single Lenoir damper, double Lenoir damper), and suspension elements were the main parameters that were investigated in different bogie types. Moreover, a load-displacement diagram for the primary suspension system of the traditional Y25 bogie was also received from SBB and will be presented in Sec. 3.

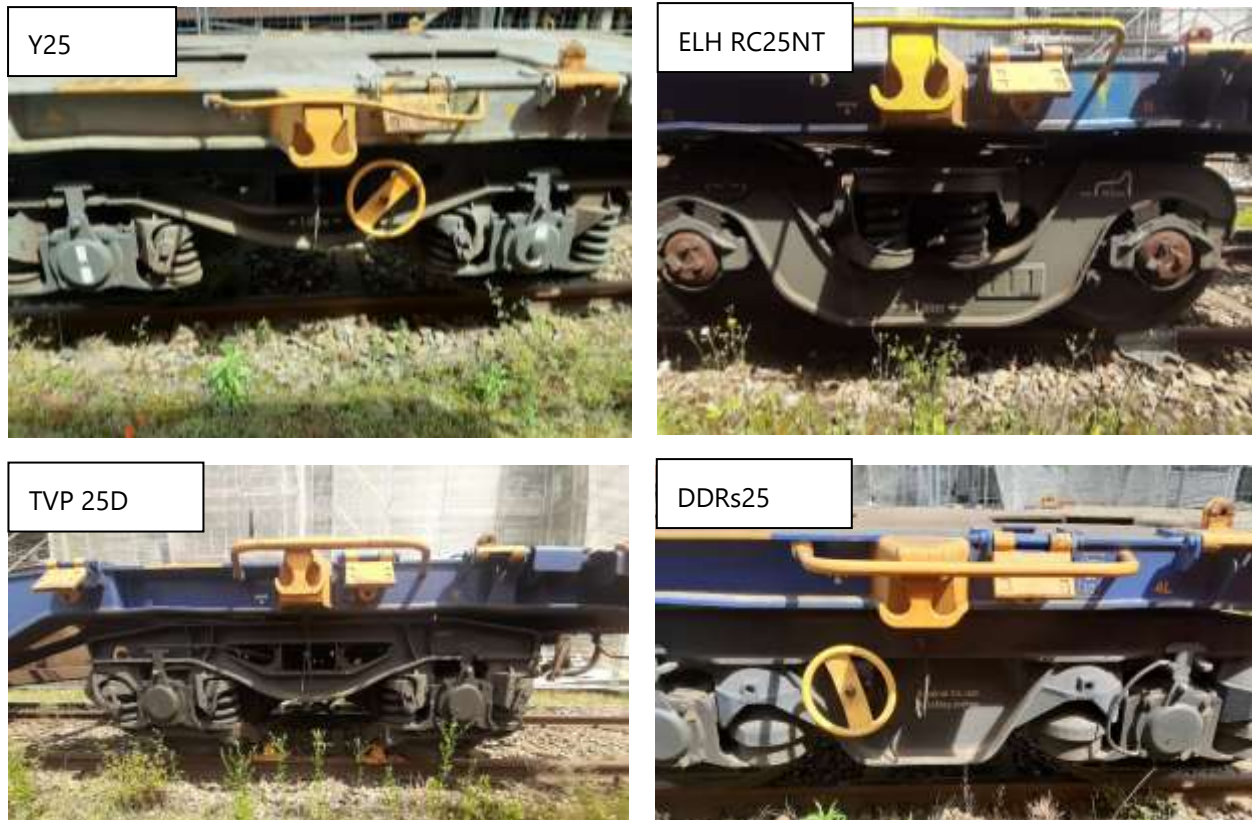


Figure 3- Different types of metallic bogies (visit to the SBB workshop in Basel)

3- Conceptual design of the proposed FRP bogie

As presented in the first interim report, the conceptual design of the FRP bogie was conducted based on the evaluation of design parameters in the workshops with project partners. In the following sections, the required mechanical characteristics for the bogie are first introduced. Afterward, the offered solutions by the proposed FRP bogie will be reviewed.

3-1- Design criteria

- Variable stiffness

The bogies should withstand variable loads due to the variable mass of the train. According to the load calculations for the freight bogies, the range of vertical load variations is between the weights of the empty wagon and the fully loaded one. The variation in the weight makes it necessary to design variable stiffness behavior for the suspension system. Traditional metallic bogies provide variable stiffness characteristics, usually by employing two sets of springs in the suspension systems. As an example, the primary suspension system of the Y25 bogie is schematically illustrated in Figure 4. Two sets of coil springs (inner and outer springs)

work together to provide load-proportional stiffness for the bogie. For the empty wagon condition, only the inner springs work, whereas, for the fully loaded wagon, both springs work as parallel suspension elements. Provided by SBB, the resulting load-displacement curve for the Y25 bogie is presented in Figure 5.

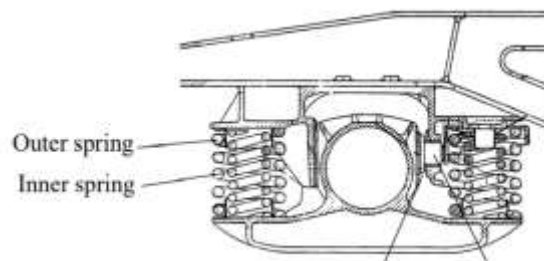


Figure 4- Primary suspension system of Y25 bogie with its outer and inner coil springs

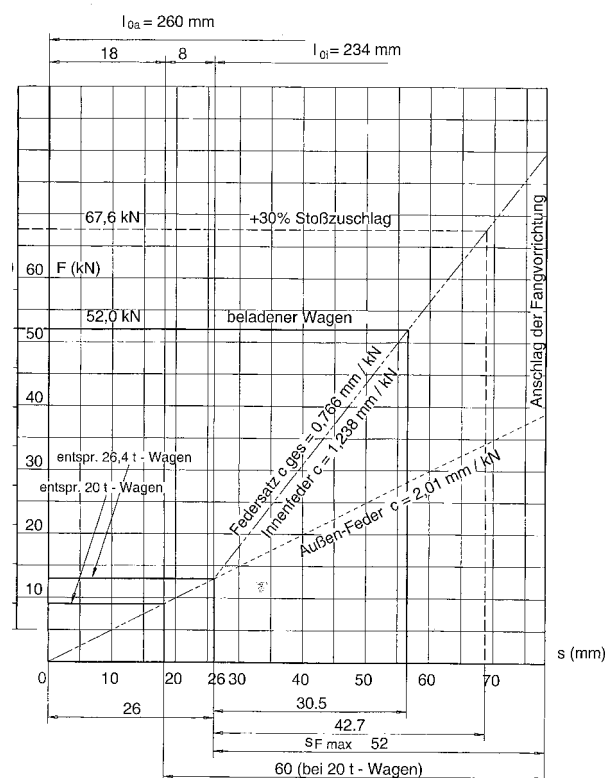


Figure 5- Force displacement diagram of the primary suspension of Y25 bogie [received from SBB]

Another example of load-proportional stiffness is the suspension system of the Formica bogie, the new bogie design introduced by Prose. The load-displacement diagram for the Formica bogie is presented in Figure 6.

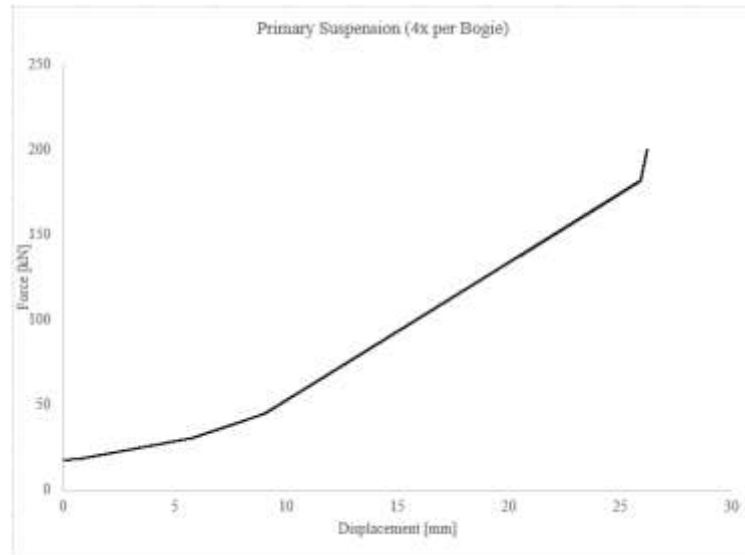


Figure 6- Force displacement diagram for the primary suspension system of the Formica bogie [received from Prose]

For a proper running dynamic behavior, variable stiffness should be provided in the newly designed FRP bogie. The challenging issue is that, based on previously established criteria, the springs in the primary suspension system will be eliminated in the FRP bogie. The bogie frame itself should therefore generate the variable stiffness.

- Stability and steering

In addition to providing the required strength, bogie design should be done in a way that provides the required stability at high speeds during service work. On the other hand, the steering properties of the bogie, which control the navigation of the carbody in the curves, should also be considered as design criteria. Generally, stability at high velocities and steering properties show opposite behavior; i.e., increasing the stability of the bogie may lead to decreasing its self-steering behavior. In this regard, the vertical and longitudinal stiffness of the FRP bogie frame should be designed in such a way that provides both steering and stability characteristics for the bogie. Modifications and optimizations will be performed to enhance the stability and steering behavior of the final model of the FRP bogie, based on the running dynamic simulations.

Damping behavior

The damper components should provide energy dissipation in the bogie structure. In the conventional Y25 bogie, an innovative damping element (the Lenoir damper) was employed to enhance the energy dissipation in the bogie. A schematic of the Lenoir damper and its tension element is illustrated in Figure 7. Alternatively, as shown in Figure 8 for the Formica bogie (introduced by Prose), hydraulic dampers can also be utilized. However, such dampers increase the complexity of the bogie and consequently increase maintenance costs. Moreover, the car body should have unique connections to attach the damping elements.

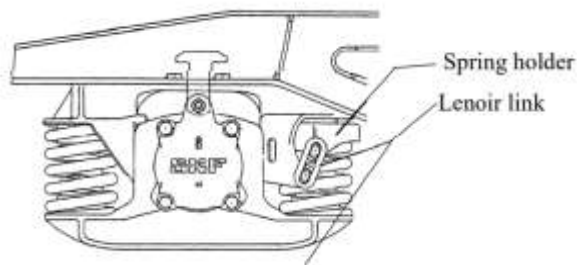


Figure 7- Lenoir damping system in Y25 primary suspension

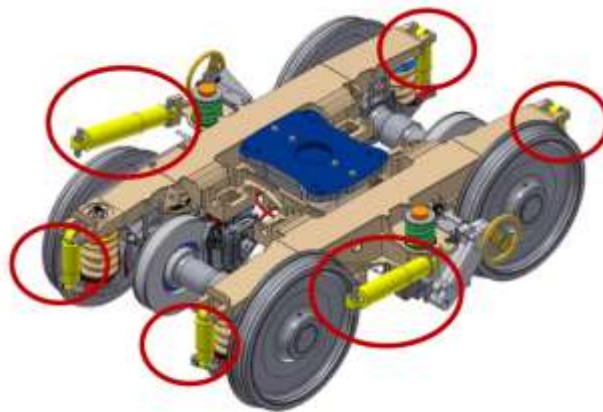


Figure 8- Hydraulic dampers in Formica bogie (Formica project-PROSE)

3-2- The proposed concept

Considering the mentioned design criteria, an FRP bogie design is introduced and presented, as illustrated in Figure 9. The proposed bogie is a three-piece structure consisting of FRP side beams and a steel bolster as the bogie cross link. FRP T-shaped links are also employed to increase the longitudinal stiffness of the bogie. The general properties regarding the mass

distribution of the bogie and rail profile are presented in Table 1. More detailed data regarding the mass, center of gravity, and moment of inertia for each component is provided in the appendix. The reference coordinate system for calculating the center of gravity and mass moment of inertia for the components is specified in Figure 10. In the following, it will be discussed how the proposed FRP bogie addresses the design criteria.

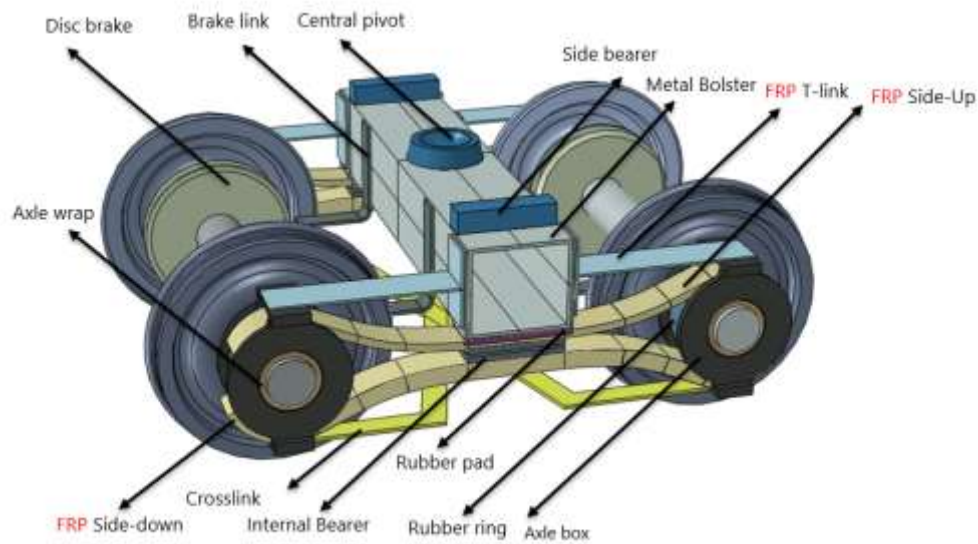


Figure 9- The proposed concept for the newly designed combined FRP-Metallic bogie and its components

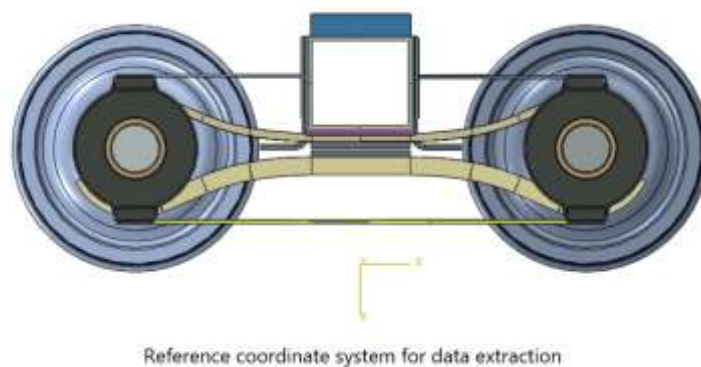


Figure 10- side view of FRP bogie with reference coordinate system (yellow parts are made of FRP)

Table 1- General properties of combined FRP-Metallic bogie

Parameter	Value	Remarks
Gauge	1.435 m	
Wheel profile	S1002	
Rail profile	UIC60	
Mass of bogie frame	620 kg	FRP side beams/ steel bolster /T-links/cross links
Mass of brake calipers	176 kg	
Mass of Wheels	1200 kg	
Mass of axles	800 kg	
Mass of disc brakes	760 kg	
Mass of axle boxes	640 kg	
Total bogie mass	4220 kg	

- Variable stiffness

The variable stiffness in the suspension system was presented as the first design criteria of the bogie. Two FRP side beams with an initial gap are considered for generating such a load-proportional stiffness. As shown in Figure 11, different vertical stiffness can be obtained by increasing the load and filling the gap between the FRP components. The stiffnesses of the bogie in vertical, longitudinal, and transverse directions are presented in Section 4.

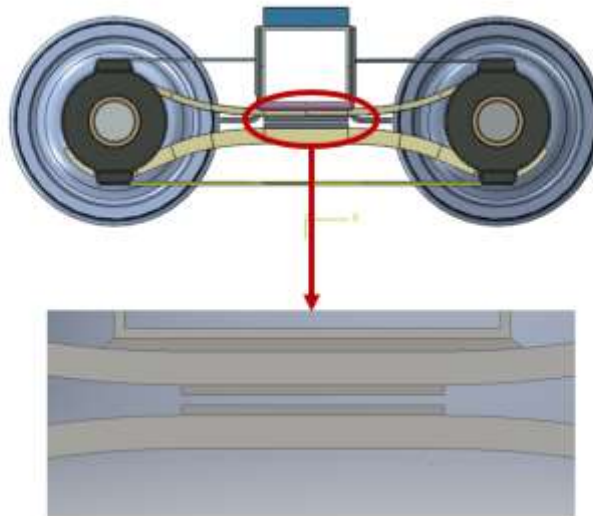


Figure 11- Employing two-piece FRP side beams with an initial gap for generating variable stiffness in the vertical direction

- Stability and steering

In order to enhance the stability of the bogie, the effect of vertical applied load on the horizontal deformation is reduced by using FRP side beams with opposite curvatures, as shown in Figure 12. With this design, the wheel separation due to the applied vertical load is minimized, which leads to increased stability and proper steering performance.

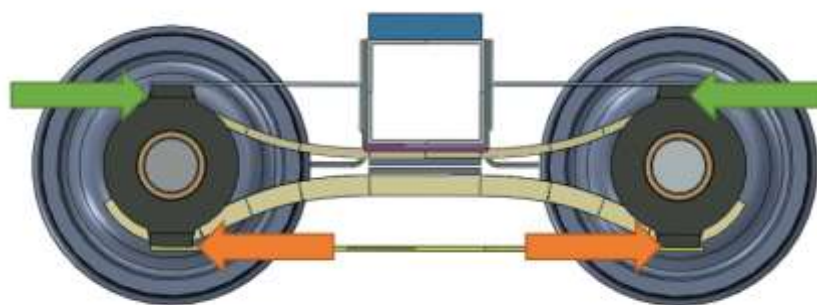


Figure 12- Employing two-piece FRP side beams with opposite curvature to minimize the wheelset separation due to the applied vertical loads

- Damping

In addition to the design concept of FRP side beams, additional elements were also employed to enhance the longitudinal stiffness of the bogie. In this regard, the T-shaped links were utilized to attach the bolster to the axle boxes. Moreover, crosslinks were also employed to connect the wheelsets, to enhance both stability and steering in the curves for the bogie.

For providing the required damping properties for the bogie, the following parameters are taken into consideration:

- Intrinsic damping of FRP laminates
- Frictional damping between FRP/FRP and FRP/metal
- Employing extra elements to improve damping behavior such as friction pads

- Costs

The cost estimation of the proposed bogie and economic comparison of the FRP bogie with metallic ones will be conducted intensively in task 7. However, because the final cost of the bogie is one of the high-importance parameters that significantly affects using the FRP bogie in the railway transport system, special consideration is given in the design step to keeping the cost of the FRP bogie as low as possible.

The proposed design makes it possible to employ a multi-material system. For example, metallic and FRP parts can work together to improve both the functionality and economic aspects of the bogie. In this regard, as an optimum design, the initial analyses were performed on the bogies with FRP side beams and metallic bolster (Figure 13). By considering the possibility of employment of the expensive CFRP and hybrid CFRP/GFRP composites, different designs with different weights and costs can be offered, as illustrated in Figure 14.

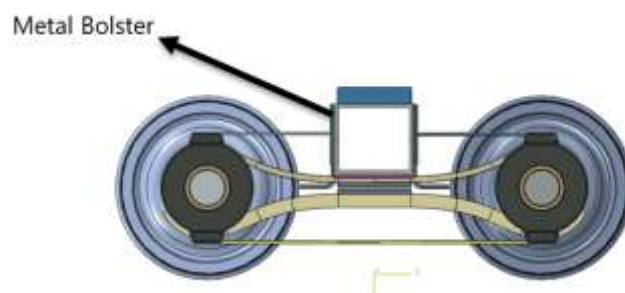


Figure 13- Utilizing metallic bolster with FRP side beams in the proposed bogie

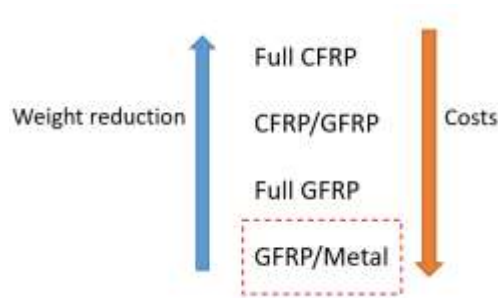


Figure 14- Weight reduction vs costs for the proposed multi-material system

In addition to providing a multi-material system, the proposed bogie consists of simple separated FRP components that make it easy to fabricate, replace, and assemble the parts. This also helps to reduce the final price of the newly designed FRP bogie.

3-3- Material Selection

Considering the multi-material system of the proposed bogie, different materials can be considered for different parts. In this regard, as the initial inputs, the following materials are selected for the design and analysis of the FRP bogie:

- Carbon fiber reinforced polymer composites (CFRPs) in unidirectional (UD) and Woven fabrics.
- Glass fiber reinforced polymer composites (GFRPs) in unidirectional (UD) and Woven fabrics.
- Steel (for metallic parts)

The mechanical and physical properties of the FRP plies, as provided by Ensinger, are demonstrated in Table 2. The presented material properties are employed in finite element analysis to obtain the stiffness and strength of the bogie and its components. However, to reduce the costs, efforts have been made to present the final design based on GFRPs instead of using expensive CFRP composites.

Table 2- Engineering constant of different FRPs [received from Ensinger]

FRP Material	Engineering constants
UD-GFRP	E11 = 45000.0 E22 = 13000.0 E33 = 13000.0 (MPa) G23 = 5040.0 G31 = 4400.0 G12 = 4400.0 (MPa) N23 = 0.290 N31 = 0.290 N12 = 0.290 (1) ALF1 = 0.600E-05 ALF2 = 0.260E-04 ALF3 = 0.260E-04 (1/K) LAM1 = 0.100E-03 LAM2 = 0.100E-03 LAM3 = 0.100E-03 (W/(mK)) D1 = 0.100E-03 D2 = 0.100E-03 D3 = 0.100E-03 RHO = 2.000 (G/CCM) VF = 60.0 (%) XT = 1200.0 YT = 65.0 ZT = 65.0 (MPa) XC = 700.0 YC = 150.0 ZC = 150.0 (MPa) SYZ = 62.0 SZX = 62.0 SXY = 62.0 (MPa) Ply thickness ca. 0.125 mm
Woven - GFRP	E11 = 22000.0 E22 = 22000.0 E33 = 13000.0 (MPa) G23 = 4500.0 G31 = 4500.0 G12 = 4400.0 (MPa) N23 = 0.290 N31 = 0.290 N12 = 0.290 (1) ALF1 = 0.80E-05 ALF2 = 0.80E-05 ALF3 = 0.260E-04 (1/K) LAM1 = 0.100E-03 LAM2 = 0.100E-03 LAM3 = 0.100E-03 (W/(mK)) D1 = 0.100E-03 D2 = 0.100E-03 D3 = 0.100E-03 RHO = 2.000 (G/CCM) VF = 60.0 (%) XT = 600.0 YT = 600.0 ZT = 65.0 (MPa) XC = 350.0 YC = 350.0 ZC = 150.0 (MPa) SYZ = 62.0 SZX = 62.0 SXY = 62.0 (MPa) ply thickness ca. 0.25 mm
UD - CFRP	E11 = 135000.0 E22 = 10000.0 E33 = 10000.0 (MPa) G23 = 3846.0 G31 = 5000.0 G12 = 5000.0 (MPa) N23 = 0.300 N31 = 0.270 N12 = 0.270 (1) ALF1 = -0.600E-06 ALF2 = 0.400E-04 ALF3 = 0.400E-04 (1/K) LAM1 = 0.100E-03 LAM2 = 0.100E-03 LAM3 = 0.100E-03 (W/(mK)) D1 = 0.100E-03 D2 = 0.100E-03 D3 = 0.100E-03 (???) RHO = 1.580 (G/CCM) VF = 60.0 (%) XT = 1450.0 YT = 55.0 ZT = 55.0 (MPa) XC = 1400.0 YC = 170.0 ZC = 170.0 (MPa) SYZ = 90.0 SZX = 90.0 SXY = 90.0 (MPa) Ply thickness ca. 0.125 mm
Woven - CFRP	E11 = 55000.0 E22 = 55000.0 E33 = 10000.0 (MPa) G23 = 3500.0 G31 = 3500.0 G12 = 5000.0 (MPa) N23 = 0.280 N31 = 0.280 N12 = 0.270 (1) ALF1 = 3E-06 ALF2 = 3E-06 ALF3 = 0.400E-04 (1/K) LAM1 = 0.100E-03 LAM2 = 0.100E-03 LAM3 = 0.100E-03 (W/(mK)) D1 = 0.100E-03 D2 = 0.100E-03 D3 = 0.100E-03 (???) RHO = 1.580 (G/CCM) VF = 60.0 (%) XT = 650.0 YT = 650.0 ZT = 55.0 (MPa) XC = 600.0 YC = 600.0 ZC = 170.0 (MPa) SYZ = 90.0 SZX = 90.0 SXY = 90.0 (MPa) Ply thickness ca. 0.125 mm

4- Finite element analysis

The finite element analysis of the bogie was conducted using Abaqus software. Simplified models (considering only FRP side beams) were initially used to obtain the initial FRP parameters, including laminate stacking sequence and overall thickness of the main FRP components. Figure 15, presents the simplified models for the side FRP side beams. In the mentioned models, other bogie components are replaced by boundary conditions on the side beams.



Figure 15- Simplified 3D models of the FRP bogie

After initial design of the FRPs using simplified models, the full 3D model of the bogie was imported to Abaqus to perform FE analysis. It is noteworthy to mention that although the geometrical model of the bogie is symmetric (in longitudinal and transverse directions), some of the loading cases are not symmetric. Therefore, the FE analysis was performed on the full 3D model. The assembled model in Abaqus and the finite element model are shown in Figure 16 Figure 17, respectively.

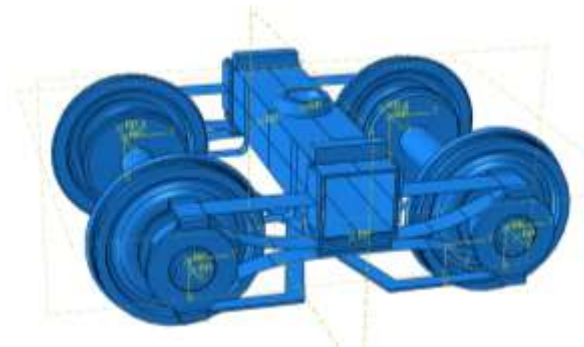


Figure 16- The created full assembly of the FRP bogie in Abaqus for FE analysis



Figure 17- Finite element model (Mesh view) of the FRP bogie

Conventional shell formulation for the shell sections was selected for modeling FRP components. In this regard, the composite parts were modeled as shell structures, and the thickness of the composites was then defined using the composite stacking sequence. As an example, Figure 18 shows the assignment of the composite layup properties, including material, thickness, and orientation of each layer for the FRP composite side beam. The defined orientation of the layers is shown in Figure 19. Directions 1, and 2 represent the fiber and matrix (perpendicular to the fibers) directions, respectively. Unit vector 3 presents the thickness direction of the FRP composite component.

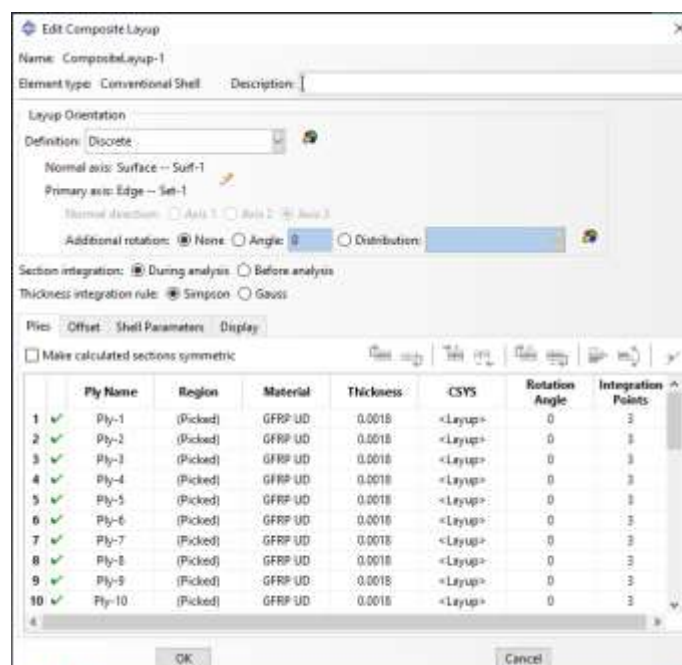


Figure 18- Definition of stacking sequence for FRP side beams in FEM

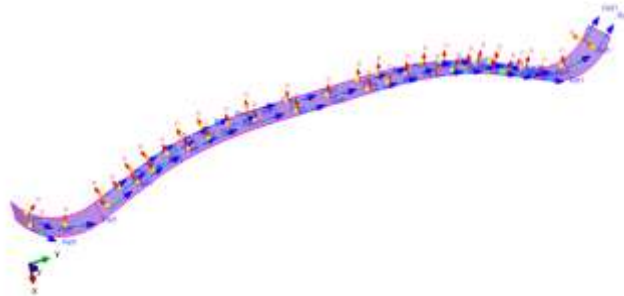


Figure 19- Fiber, matrix and thickness direction in the FRP side beam for creating the proper stacking sequence

As was presented in the first interim report, the applied loads were calculated based on EN 13749 [2] standard for the FRP bogie (by considering the weight of the new bogie components). Based on the calculated loads, different loading cases were also generated, as presented in Figure 20. The loading cases were applied to the model, and FE analysis was performed by using the static structural solver. The finite element results are presented in the next section (Sec. 4).

Case Number	Load combinations	Exceptional loads (N)				
		Fz (on pivot)	or Fz2 (on side frame)	Fy	Fx	Twist (e.g. delta Z)
1	Vertical (Case1)	804143.2	0	0	0	0
2	Vertical (Case2)	422174.33	180931.77	0	0	0
3	Vertical (Case1)+ Transverse	804143.2	0	82549.5	0	1% twist
4	Vertical (Case2)+ Transverse	422174.33	180931.77	82549.5	0	1% twist
5	Vertical (case 1)+longitudinal (Loosening)	804143.2	0	0	44129.3	0
6	Vertical (case 2)+longitudinal (Loosening)	422174.33	180931.77	0	44129.3	0
7	Vertical (Case 1)+ Transverse+Twist (Case 1)	804143.2	0	82549.5	0	1% twist
8	Vertical (Case 2)+ Transverse+Twist (Case 1)	422174.33	180931.77	82549.5	0	1% twist
9	Vertical (Case 1)+ twist case 2 (unloading of a wheel)	TARE Weight (0000)	0	0	0	mm at wheel contact point
10	Vertical (Case 2)+ twist case 2 (unloading of a wheel)	422174.33	180931.77	82549.5	0	mm at wheel contact point
11	Vertical (case 1)+ Shunt	804143.2	0	0	196132	0
12	Vertical (Case 2)+ Shunt	422174.33	180931.77	0	196132	0

Figure 20- The calculated load cases for FE analysis

5- Finite element results

4-1- Deformations

Finite element analysis was performed on the proposed bogie to ensure proper mechanical performance of the bogie subjected to the expected loading cases. Deformations, stresses, and stiffness are the main results to be extracted and be compared for different types of parameters. The deformation of the bogie subjected to the applied exceptional vertical load

to the central pivot is shown in Figure 21. For better presentation, the deformation in the figure is shown by the scale factor of 2.

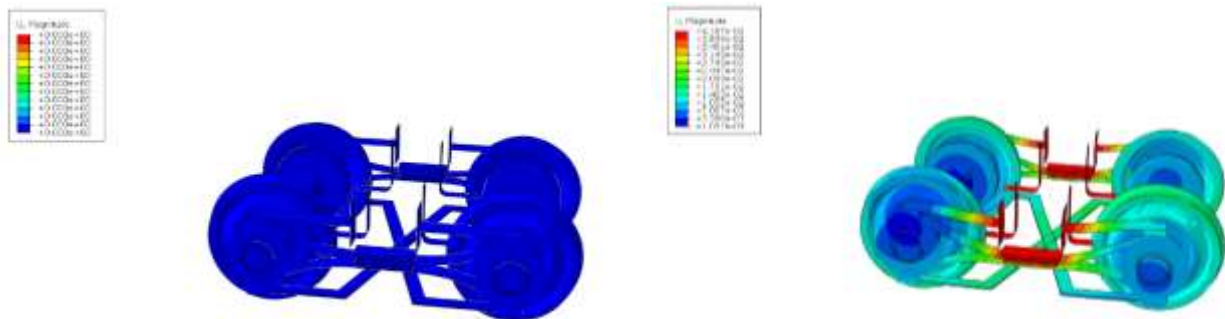


Figure 21- Deformation of the FRP bogie before and after applying external vertical force on the central pivot

Figure 22, depicts the change in deformation of the FRP parts caused by the applied vertical force in the central pivot. As was previously mentioned in the conceptual design section, there is an initial gap between two FRP composite side beams, which is filled by increasing the applied load and generating the contact force between the parts. The vertical stiffness of the bogie is different before and after the contact between the FRP side beams.

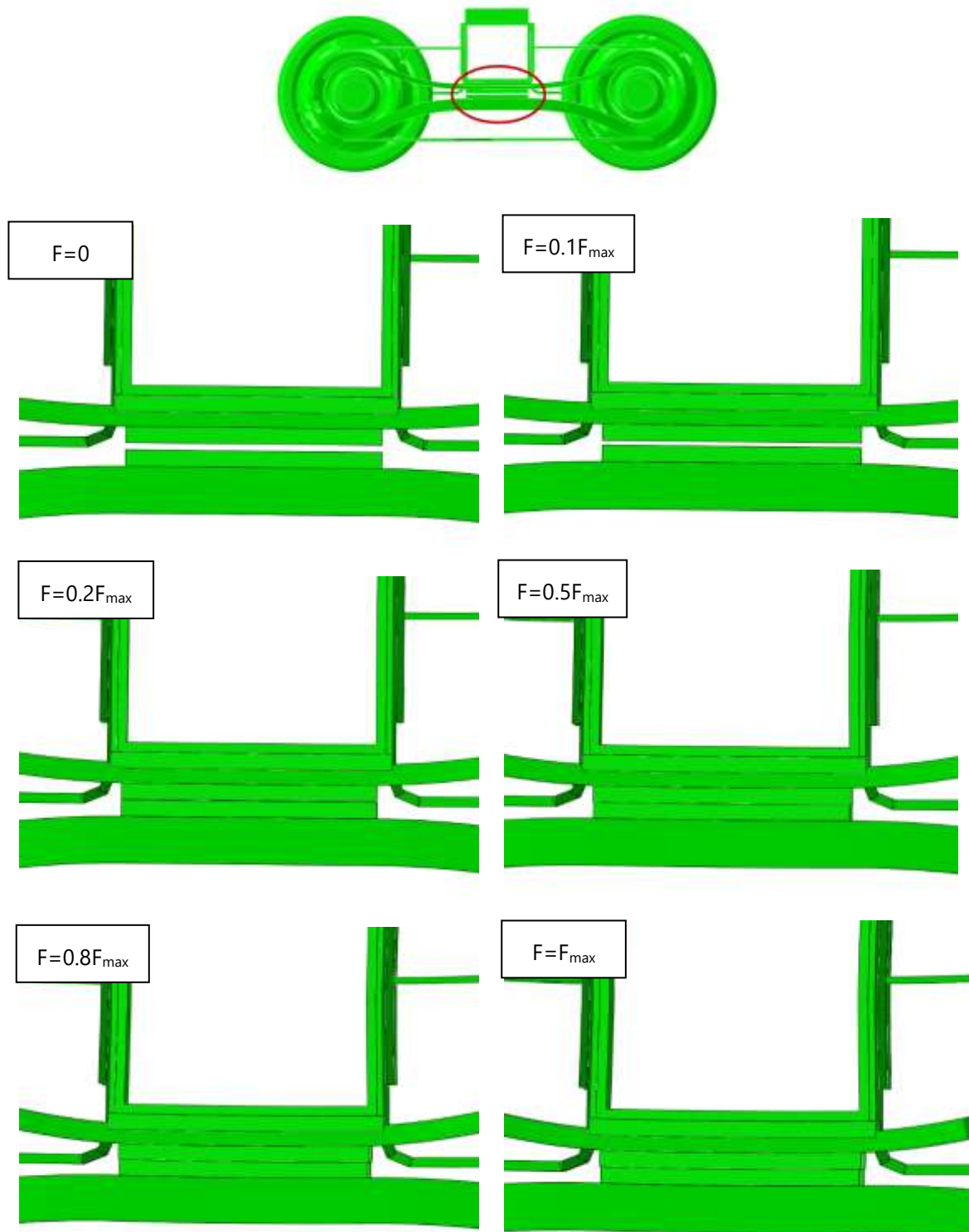


Figure 22- the deformation of FRP side beams and filling the initial gap by increasing the applied vertical load on the central pivot

4-2- Stress results in the components

The stresses in the FRP composite parts are calculated to ensure the proper mechanical strength of the proposed FRP bogie. Unlike the stress analysis in the metallic parts, there is no properly defined equivalent stress in the composite laminates (e.g., von-Mises stress for the isotropic materials). The stresses, therefore, must be calculated separately for each direction, along fiber direction, matrix direction (perpendicular to the fibers) and shear direction. It is noteworthy to mention that, as is presented in material properties, the strengths of composites are also different in compression and tension cases. Therefore, the sign of the stresses in fiber and matrix direction is important to be considered. In addition to the direction dependency of the stresses and strengths, considering the laminated composite, the calculations must be conducted for each separate layer to indicate the critical layer and critical stresses.

The calculated stresses in fiber direction for three representative layers at the top, middle, and bottom of the laminate for the FRP side beams are presented in Figure 23. As previously mentioned, the critical layer will be obtained by examining the results for each separate layer. However, considering the bending as the main loading behavior on the FRP side beams, the critical layers are expected to be the outer plies of the FRP composites.

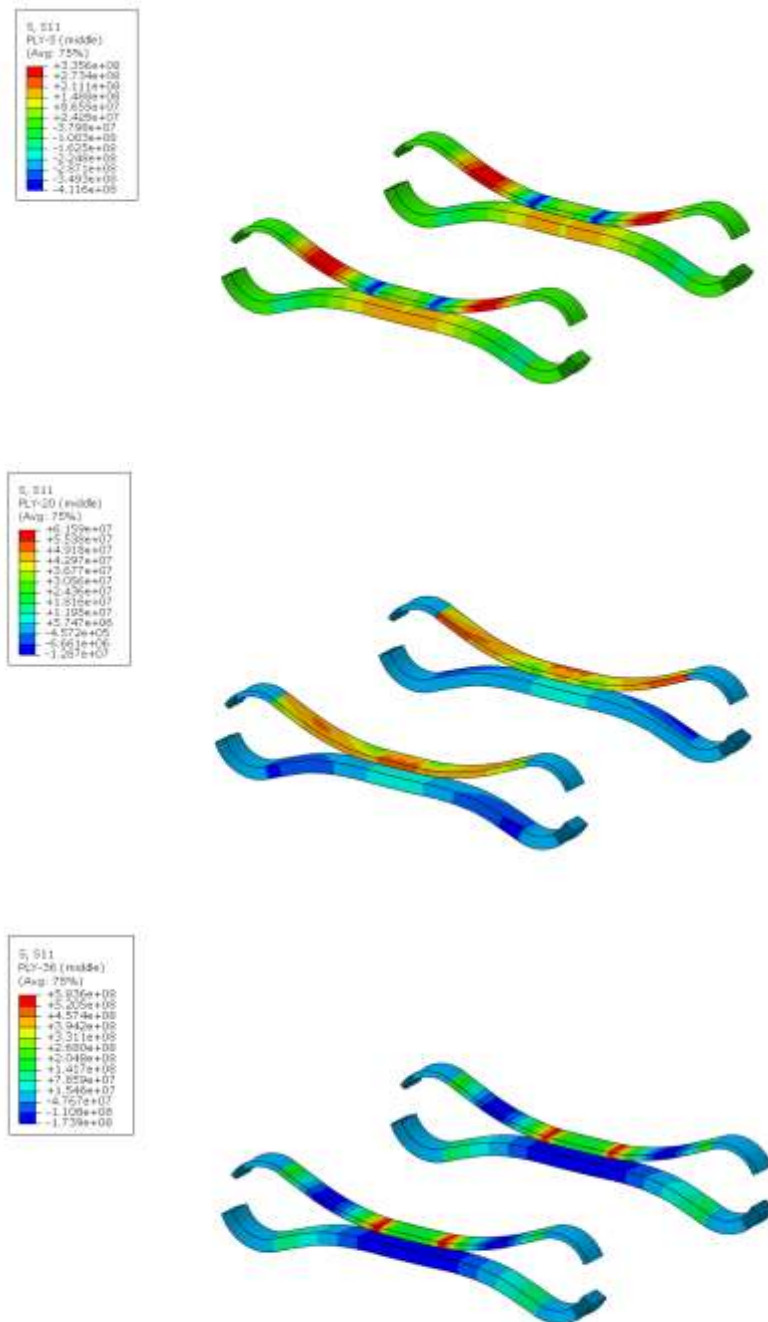


Figure 23- Stress in fiber direction in FRP side beams in inner, middle and outer layers

The longitudinal stress distribution for the T-shaped links is presented in Figure 24. It is noteworthy to mention that after finalizing the running dynamic simulations, the FRP parts, in particular the T-links will be possibly modified to obtain the optimized results.

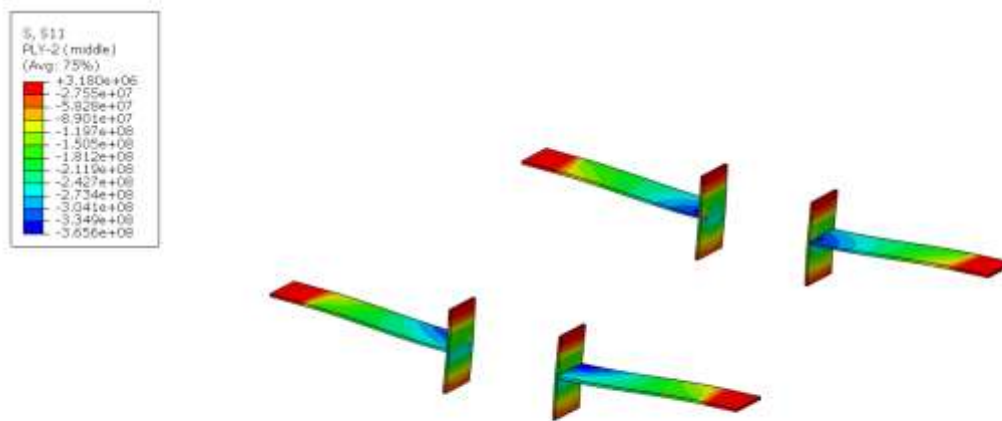


Figure 24- Calculated stress in T-shaped links in fiber direction under vertical loading

In addition to FRP composite parts, metallic components are also considered for examining stress distribution. The calculated von-Mises equivalent stress on the steel bolster is shown in Figure 25. Similar to the FRP parts, the metallic parts will also be subjected to modifications and optimizations after obtaining the initial running dynamic results.

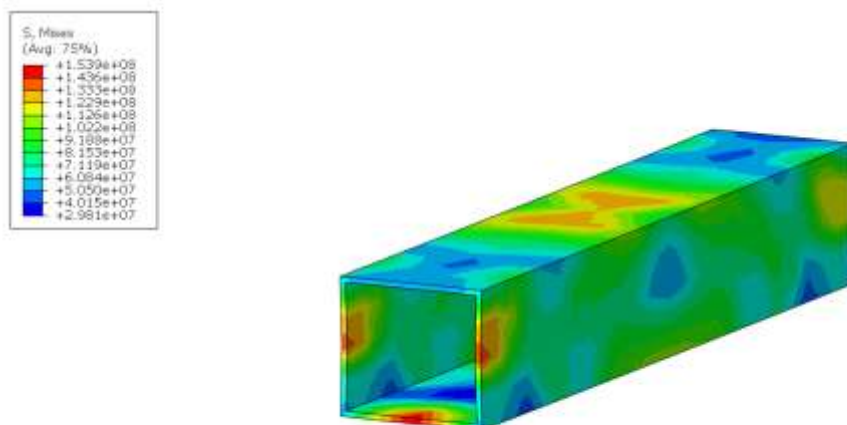


Figure 25- Calculated von-Mises stress in the metallic bolster under vertical loading

As a summary of the stress results in the components, the critical stresses for critical layers are obtained for the FRP composite side beams and are presented in Table 3.

Table 3- Stress results for FRP side beams in different directions

Loading type	S11 (MPa)	S11 (MPa)	S22 (MPa)	S22 (MPa)	S12 (MPa)
	Tensile	Compressive	Tensile	Compressive	(Shear)
Vertical proof (case 1)	568	-427	37	-36	9
Vertical proof (case 2)	552	-396	35	-34	8
Vertical (case 1) + Transverse	686	-466	42	-39	16
Vertical (case 2) + Transverse	656	-433	38	-36	17
Vertical (case 1) + Longitudinal	589	-442	40	-49	9
Vertical (case 2) + Longitudinal	560	-412	37	-35	8
Vertical (case 1) + Twist	150	-125	9	-9	4
Vertical (case 2) + Twist	318	-202	14	-13	16

4-3- Stiffness results in different directions

Besides the stress distribution and structural integrity, the stiffness of the bogie is of high importance because of its significant influence on the mechanical behavior and running dynamic properties of the newly designed bogie. In order to investigate the stiffness of the bogie in the required directions, the load-displacement curves for different loading conditions were extracted from the results. As the first loading case, the vertical load-displacement behavior of the bogie was obtained and illustrated in Figure 26. Two different cases were considered for the vertical loading case based on the standard and according to the load calculations:

1. The total vertical proof load was applied on the central pivot (804kN)
2. Vertical load was divided between central pivot and one of the side bearers (423kN on central pivot + 181kN on side bearer)

As shown in Figure 26, the stiffness variation in the vertical direction is obtained as expected by employing the two-piece side beam. The obtained stiffness is close to the stiffness of the metallic bogie (Formica) with a spring suspension system.

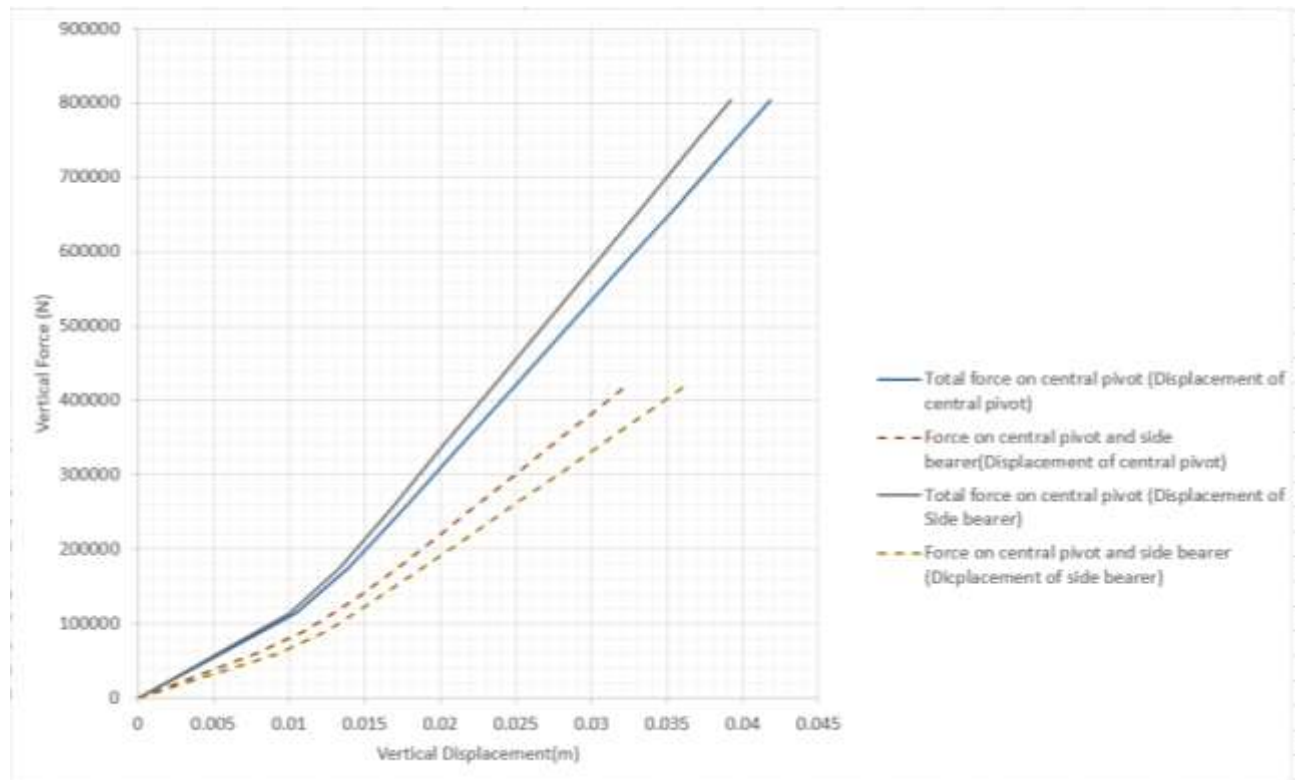


Figure 26- Vertical force vs vertical displacement at central pivot

The longitudinal displacement of the wheels by applying the vertical load (two cases) is also extracted from the results and is presented in Figure 27. As can be seen in the curves, there is a change in the direction of the movements of the axle box due to the increased vertical loads. This change is a result of two-piece side beams. However, the separation of wheels by applying the vertical load is very small in comparison to the other FRP bogies, and this helps the bogie to show stable behavior at higher velocities and reduces the tendency of the bogie to wrong steering behavior in the curves. Such mechanical characteristics are expected to reduce the wear on the wheels and on the rails. This enhancement is examined by running dynamic simulations.

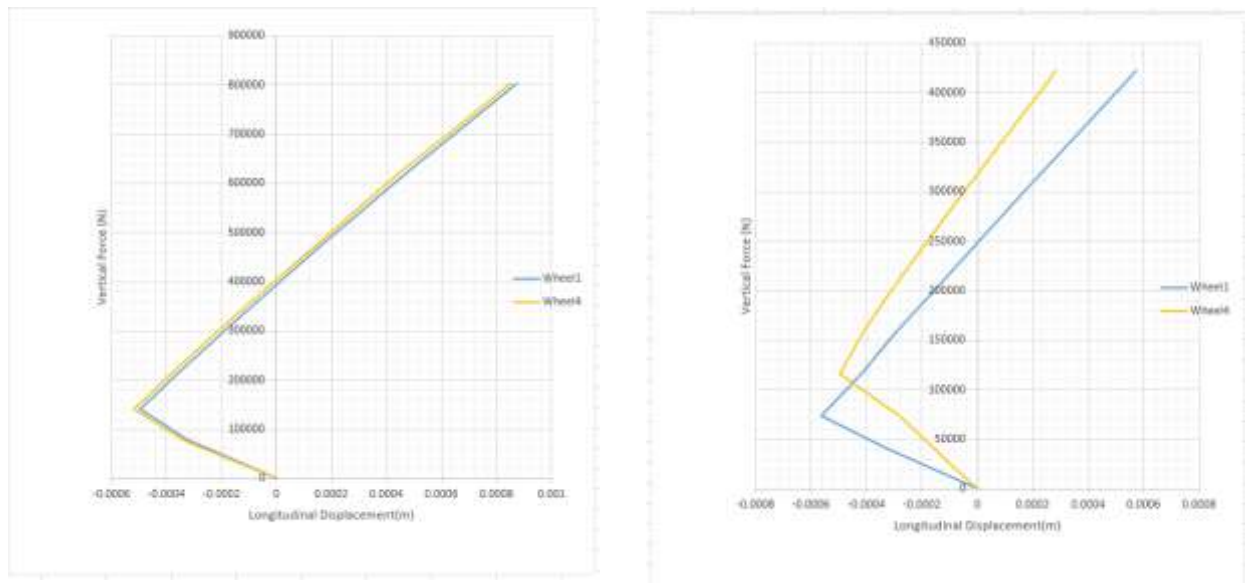


Figure 27- Vertical force at central pivot vs longitudinal displacement of wheels, left) total force on central pivot and right) force on central pivot and side bearer (the result presented for two wheels on the same axle)

Transverse stiffness should also be calculated for verifying the multibody simulations and consequently for examining the running dynamic behavior of the bogie. Figure 28, presents the transverse load-displacement diagram for the bogie. In this case, the vertical load (two cases) is applied before the transverse loads.

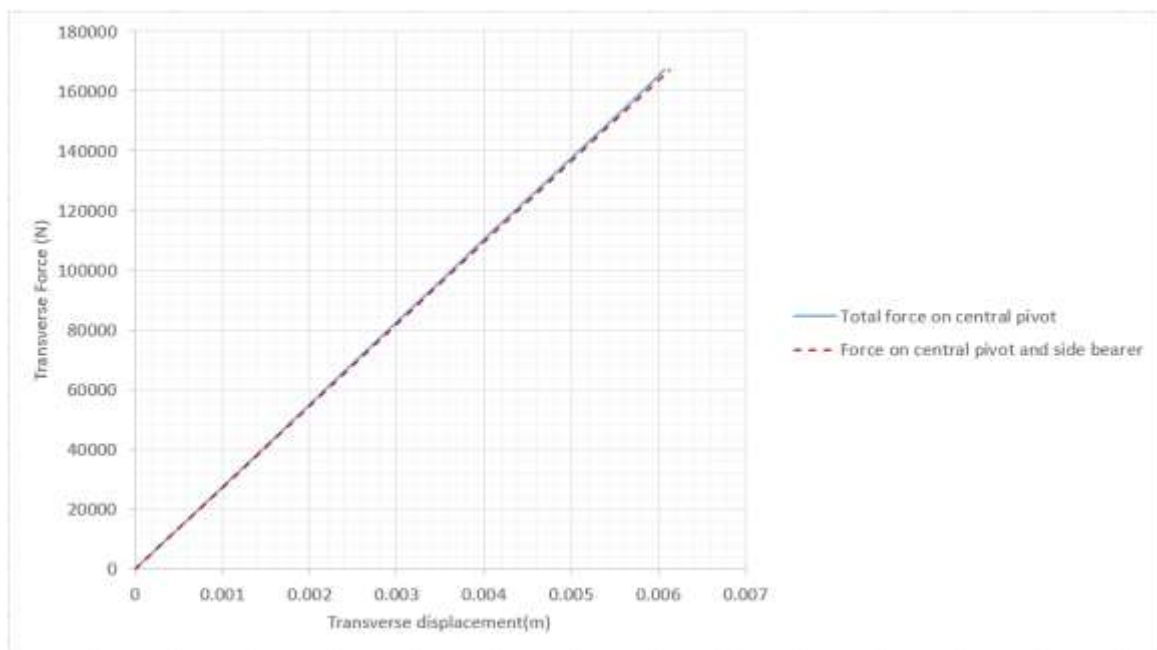


Figure 28- Transverse force vs transverse displacement at central pivot

Along with the vertical and transverse stiffness of the bogie, its longitudinal stiffness has a significant effect on the stability of the bogie at high velocities. Longitudinal stiffness, therefore, should be investigated for the newly designed FRP bogie by applying the longitudinal loading case on the bogie. Longitudinal force displacement diagram of the bogie is provided in Figure 29. Similar to previous results, two cases of vertical loads are considered.

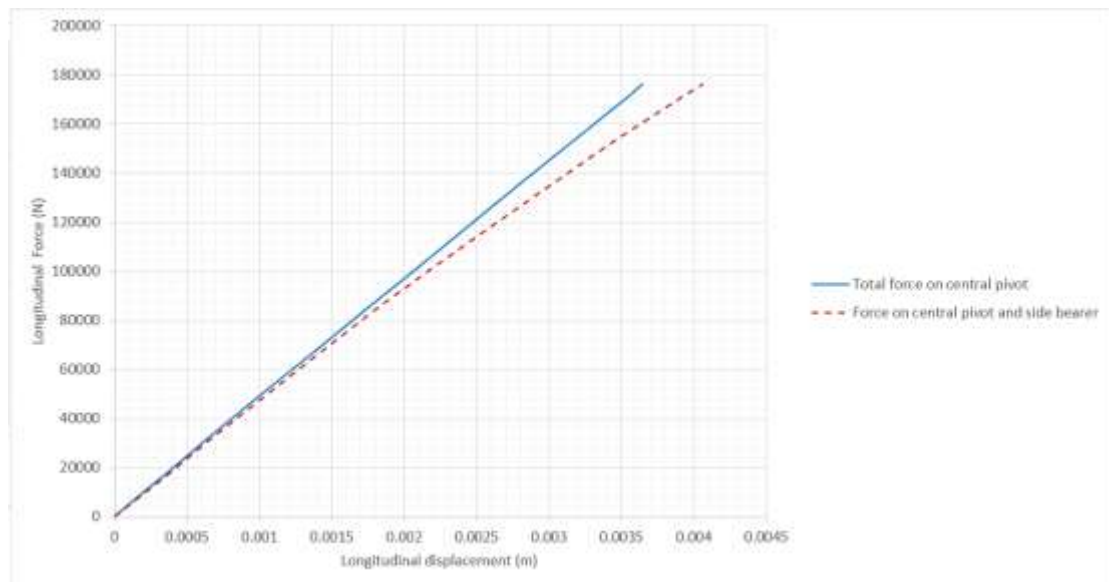


Figure 29- Longitudinal force vs longitudinal displacement at central pivot






4-4- Modal results

The natural frequencies of the bogie and its individual components are obtained by modal analysis of the bogie. The calculated results are employed for comparing with the multi body simulation for the running dynamic analysis to ensure the similarity of the models in both FEM and MBS. In addition, the modal results will be used as an input for acoustic analysis in the future task to specify the noise emission of the bogie. At first, the FRP side beams were considered separately. The first five natural frequencies of the side-down component are shown in Table 4. The boundary condition is free-free, as shown in Figure 30.




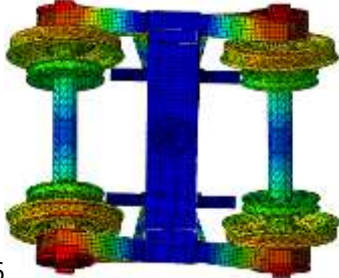

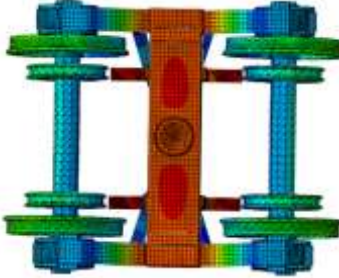
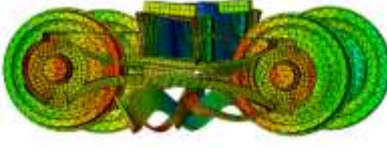
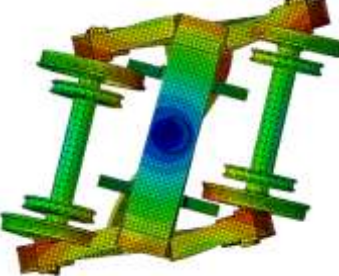
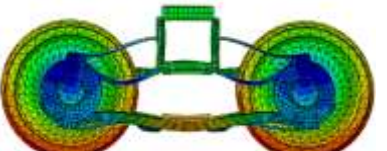
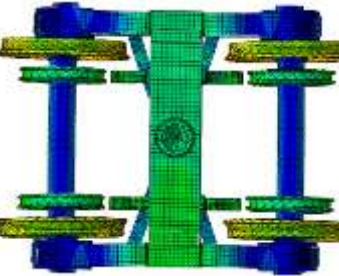

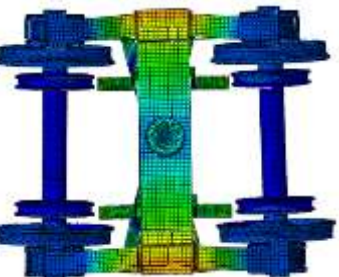
Figure 30- Free boundary conditions for modal analysis of FRP component

Table 4- Natural frequencies and mode shapes for FRP component

No.	Mode	Frequency (cycle/s)	Mode Shape
1	7	66.4	
2	8	136.8	
3	9	163.8	
4	10	179.0	
5	11	229.8	

Modal analysis was also conducted on the subassemblies and finally, the full assembly of the bogie. The natural frequencies and mode shapes for the whole assembly are provided in Table 5. The local mode shapes (e.g. for crosslinks) are not presented in the results. The assembly was analyzed without mechanical constraints (free).

Table 5- Natural frequencies and mode shapes for whole assembly

No.	Mode	Frequency (cycle/s)	Mode Shape	
1	17	15.1		 6
2	21	21.2		
3	24	22.8		
4	27	28.5		
5	31	35.3		

6- Running dynamic simulations

The initial running dynamic simulations were performed by Prose and the detailed results is provided with the running dynamic report [3]. Safety against derailment, radial steering and wear and nonlinear running stability were examined for the FRP design concept. An adopted model was also proposed by replacing the T-shaped links with a longitudinal beam connecting the axleboxes together. Based on the running dynamic report it was obtained that, "the safety against derailment, radial steering and wear and non-linear running stability show generally good results for both the initial and the adapted bogie. The additional dynamic simulations done with the adapted design exceed a few limit values. To reach these limit values further optimization of the parameters is needed" [3].

7- Summary and conclusion

In the present report, the conceptual design of the proposed FRP bogie was introduced and the designed properties to address the presented challenges were described. The results of finite element analysis revealed the proper structural performance of the bogie against the applied exceptional loads. The bogie shows proper vertical stiffness (close to the stiffness of the spring suspension systems in metallic bogies) and the longitudinal stiffness is also designed to be high enough to increase the stability of the bogie at high velocities. Initial running dynamic simulations show good performance of the bogie regarding derailment, stasteering and stability characteristics. The required modifications to the components and the concept will also be performed as planned in the project time plan. In the next steps, rough acoustic simulation will be performed to obtain the expected noise emission of the FRP bogie compared with the traditional metallic ones. A cost analysis will also be conducted to examine the efficiency of the bogie in terms of the economic aspects.

8- References

- [1] First interim report, Empa, FRP bogies for freight wagons: A feasibility study, 22. 04.2022
- [2] EN13749, Railway applications - Wheelsets and bogies - Method of specifying the structural requirements of bogie frames
- [3] EMPA FRP Bogie Laufdynamik Analyse, PROSE, 03.08.2022

9- Appendix

The detailed information of the different components of the proposed FRP bogie including the material and geometrical parameters, is given in Table 6:

Table 6- Geometry and mass properties of FRP bogie components

Component name: Bolster			
Parameter	Unit	Value	Remarks
Mass	kg	369	Steel bolster
Center of gravity in X	m	0	
Center of gravity in Y		0	
Center of gravity in Z		-0.727	
Mass Moment of inertia I _{xx}	Kgm ²	145.39	
Mass Moment of inertia I _{yy}		17.39	
Mass Moment of inertia I _{zz}		146.77	
Component name: FRP Side-up-1			
Parameter	Unit	Value	Remarks
Mass	kg	24	GFRP
Center of gravity in X	m	0	
Center of gravity in Y		0.972	
Center of gravity in Z		- 0.567	
Mass Moment of inertia I _{xx}	Kgm ²	0.151	
Mass Moment of inertia I _{yy}		10.37	
Mass Moment of inertia I _{zz}		10.32	
Component name: FRP Side-up-2			
Parameter	Unit	Value	Remarks
Mass	kg	24	GFRP
Center of gravity in X	m	0	
Center of gravity in Y		-0.972	

Center of gravity in Z		- 0.567	
Mass Moment of inertia I _{xx}	Kgm ²	0.151	
Mass Moment of inertia I _{yy}		10.37	
Mass Moment of inertia I _{zz}		10.32	
Component name: FRP Side-down-1			
Parameter	Unit	Value	Remarks
Mass	kg	54	GFRP
Center of gravity in X	m	0	
Center of gravity in Y		0.972	
Center of gravity in Z		-0.331	
Mass Moment of inertia I _{xx}	Kgm ²	0.367	
Mass Moment of inertia I _{yy}		24.67	
Mass Moment of inertia I _{zz}		24.54	
Component name: FRP Side-down-2			
Parameter	Unit	Value	Remarks
Mass	kg	54	GFRP
Center of gravity in X	m	0	
Center of gravity in Y		-0.972	
Center of gravity in Z		-0.331	
Mass Moment of inertia I _{xx}	Kgm ²	0.367	
Mass Moment of inertia I _{yy}		24.67	
Mass Moment of inertia I _{zz}		24.54	
Component name: Side bearer-1			
Parameter	Unit	Value	Remarks
Mass	kg	5	Rubber
Center of gravity in X	m	0	
Center of gravity in Y		0.850	
Center of gravity in Z		-0.951	
Mass Moment of inertia I _{xx}	Kgm ²	0.0081	

Mass Moment of inertia I_{yy}		0.0756	
Mass Moment of inertia I_{zz}		0.0765	
Component name: Side bearer-2			
Parameter	Unit	Value	Remarks
Mass	kg	5	Rubber
Center of gravity in X	m	0	
Center of gravity in Y		-0.850	
Center of gravity in Z		-0.951	
Mass Moment of inertia I_{xx}	Kgm ²	0.0081	
Mass Moment of inertia I_{yy}		0.0756	
Mass Moment of inertia I_{zz}		0.0765	
Component name: T-link-1			
Parameter	Unit	Value	Remarks
Mass	kg	4	GFRP
Center of gravity in X	m	-0.489	
Center of gravity in Y		0.964	
Center of gravity in Z		-0.754	
Mass Moment of inertia I_{xx}	Kgm ²	0.0231	
Mass Moment of inertia I_{yy}		0.295	
Mass Moment of inertia I_{zz}		0.297	
Component name: T-link-2			
Parameter	Unit	Value	Remarks
Mass	kg	4	GFRP
Center of gravity in X	m	0.489	
Center of gravity in Y		0.964	
Center of gravity in Z		-0.754	
Mass Moment of inertia I_{xx}	Kgm ²	0.0231	
Mass Moment of inertia I_{yy}		0.295	
Mass Moment of inertia I_{zz}		0.297	

Component name: T-link-3			
Parameter	Unit	Value	Remarks
Mass	kg	4	GFRP
Center of gravity in X	m	0.489	
Center of gravity in Y		-0.964	
Center of gravity in Z		-0.754	
Mass Moment of inertia I _{xx}	Kgm ²	0.0231	
Mass Moment of inertia I _{yy}		0.295	
Mass Moment of inertia I _{zz}		0.297	
Component name: T-link-4			
Parameter	Unit	Value	Remarks
Mass	kg	4	GFRP
Center of gravity in X	m	-0.489	
Center of gravity in Y		-0.964	
Center of gravity in Z		-0.754	
Mass Moment of inertia I _{xx}	Kgm ²	0.0231	
Mass Moment of inertia I _{yy}		0.295	
Mass Moment of inertia I _{zz}		0.297	
Component name: Crosslink-1			
Parameter	Unit	Value	Remarks
Mass	kg	40	steel
Center of gravity in X	m	-0.01	
Center of gravity in Y		-0.01	
Center of gravity in Z		-0.175	
Mass Moment of inertia I _{xx}	Kgm ²	22.86	
Mass Moment of inertia I _{yy}		7.74	
Mass Moment of inertia I _{zz}		30.59	
Component name: Crosslink-2			
Parameter	Unit	Value	Remarks

Mass	kg	40	steel
Center of gravity in X	m	-0.01	
Center of gravity in Y		0.01	
Center of gravity in Z		-0.175	
Mass Moment of inertia I _{xx}	Kgm ²	22.86	
Mass Moment of inertia I _{yy}		7.74	
Mass Moment of inertia I _{zz}		30.59	
Component name: Axlewrap-1			
Parameter	Unit	Value	Remarks
Mass	kg	3.5	Rubber
Center of gravity in X	m	-0.900	
Center of gravity in Y		1	
Center of gravity in Z		-0.466	
Mass Moment of inertia I _{xx}	Kgm ²	0.0300	
Mass Moment of inertia I _{yy}		0.0430	
Mass Moment of inertia I _{zz}		0.0300	
Component name: Axlewrap-2			
Parameter	Unit	Value	Remarks
Mass	kg	3.5	Rubber
Center of gravity in X	m	0.900	
Center of gravity in Y		1	
Center of gravity in Z		-0.466	
Mass Moment of inertia I _{xx}	Kgm ²	0.0300	
Mass Moment of inertia I _{yy}		0.0430	
Mass Moment of inertia I _{zz}		0.0300	
Component name: Axlewrap-3			
Parameter	Unit	Value	Remarks
Mass	kg	3.5	Rubber
Center of gravity in X	m	0.900	

Center of gravity in Y	Kgmm ²	-1	
Center of gravity in Z		-0.466	
Mass Moment of inertia I _{xx}		0.0300	
Mass Moment of inertia I _{yy}		0.0430	
Mass Moment of inertia I _{zz}		0.0300	
Component name: Axlewrap-4			
Parameter	Unit	Value	Remarks
Mass	kg	3.5	Rubber
Center of gravity in X	m	-0.900	
Center of gravity in Y		-1	
Center of gravity in Z		-0.466	
Mass Moment of inertia I _{xx}	Kgmm ²	0.0300	
Mass Moment of inertia I _{yy}		0.0430	
Mass Moment of inertia I _{zz}		0.0300	
Component name: Central pivot			
Parameter	Unit	Value	Remarks
Mass	kg	39	Steel
Center of gravity in X	m	0	
Center of gravity in Y		0	
Center of gravity in Z		-0.945	
Mass Moment of inertia I _{xx}	Kgmm ²	0.287	
Mass Moment of inertia I _{yy}		0.287	
Mass Moment of inertia I _{zz}		0.537	
Component name: Axlebox-1			
Parameter	Unit	Value	Remarks
Mass	kg	104	Steel
Center of gravity in X	m	-0.900	
Center of gravity in Y		0.970	
Center of gravity in Z		-0.466	

Mass Moment of inertia I _{xx}	Kgm ²	3.81	
Mass Moment of inertia I _{yy}		4.45	
Mass Moment of inertia I _{zz}		2.33	
Component name: Axlebox-2			
Parameter	Unit	Value	Remarks
Mass	kg	104	Steel
Center of gravity in X	m	0.900	
Center of gravity in Y		0.970	
Center of gravity in Z		-0.466	
Mass Moment of inertia I _{xx}	Kgm ²	3.81	
Mass Moment of inertia I _{yy}		4.45	
Mass Moment of inertia I _{zz}		2.33	
Component name: Axlebox-3			
Parameter	Unit	Value	Remarks
Mass	kg	104	Steel
Center of gravity in X	m	0.900	
Center of gravity in Y		-0.970	
Center of gravity in Z		-0.466	
Mass Moment of inertia I _{xx}	Kgm ²	3.81	
Mass Moment of inertia I _{yy}		4.45	
Mass Moment of inertia I _{zz}		2.33	
Component name: Axlebox-4			
Parameter	Unit	Value	Remarks
Mass	kg	104	Steel
Center of gravity in X	m	-0.900	
Center of gravity in Y		-0.970	
Center of gravity in Z		-0.466	
Mass Moment of inertia I _{xx}	Kgm ²	3.81	
Mass Moment of inertia I _{yy}		4.45	

Mass Moment of inertia I _{zz}		2.33	
Component name: Brakelink-1			
Parameter	Unit	Value	Remarks
Mass	kg	23	Steel
Center of gravity in X	m	-0.390	Point mass at the end of link: -0.537 0.522 -0.457 (The effect of point mass is already considered on the center of gravities)
Center of gravity in Y		0.502	
Center of gravity in Z		-0.547	
Mass Moment of inertia I _{xx}	Kgm ²	3.00	
Mass Moment of inertia I _{yy}		3.35	
Mass Moment of inertia I _{zz}		2.67	
Component name: Brakelink -2			
Parameter	Unit	Value	Remarks
Mass	kg	23	Steel
Center of gravity in X	m	0.390	Point mass at the end of link 0.537 0.522 -0.457 (The effect of point mass is already considered on the center of gravities)
Center of gravity in Y		0.502	
Center of gravity in Z		-0.547	
Mass Moment of inertia I _{xx}	Kgm ²	3.00	
Mass Moment of inertia I _{yy}		3.35	
Mass Moment of inertia I _{zz}		2.67	
Component name: Brakelink -3			
Parameter	Unit	Value	Remarks
Mass	kg	23	Steel
Center of gravity in X	m	0.390	Point mass at the end of link 0.537
Center of gravity in Y		-0.502	
Center of gravity in Z		-0.547	

Mass Moment of inertia I_{xx}	Kgm ²	3.00	-0.522
Mass Moment of inertia I_{yy}		3.35	-0.457
Mass Moment of inertia I_{zz}		2.67	(The effect of point mass is already considered on the center of gravities)
Component name: Brakelink -4			
Parameter	Unit	Value	Remarks
Mass	kg	23	Steel
Center of gravity in X	m	-0.390	Point mass at the end of link
Center of gravity in Y		-0.502	
Center of gravity in Z		-0.547	
Mass Moment of inertia I_{xx}	Kgm ²	3.00	-0.522
Mass Moment of inertia I_{yy}		3.35	-0.457
Mass Moment of inertia I_{zz}		2.67	(The effect of point mass is already considered on the center of gravities)

Differences from the time plan according to the application

All expected tasks in the proposal have been carried out. The tasks are conducting according to the project time table.

Outlook to the next working steps

1. In the next step, the modification of the FRP bogie design will be performed by considering the running dynamic results
2. Acoustic analysis for comparing the noise emission of the FRP bogie with traditional metal bogie will be conducted.
3. Cost analysis of the FRP bogie will be completed.
4. Based on the outcomes, planning of the follow-up project will be conducted.

Diverse

There is no diverse compare to the plan.

Project No. 5211.02073

Empa report

Assignment

Client:

Number of pages:

First interim report

BAFU/BAV, Switzerland

44

Project title: "FRP bogies for freight wagons: A feasibility study"

Project leader and contractor: Empa -Structural Engineering Research Laboratory

Project partners:

- PROSE (railway and certification knowledge),
- Ensinger (manufacturer, FRP knowledge),
- SBB cargo (consulting end user),
- WASCOSA (consulting end user),
- Empa 509 (noise control knowledge)

Dübendorf, 22.04.2022

Ali Saeedi / Moslem Shahverdi / Masoud Motavalli

Contents

1-	Introduction.....	6
2-	Overview of the project	8
3-	Design specifications.....	10
4-	Load calculations.....	13
5-	Evaluation parameters	16
6-	Developing a theoretical tool for weight estimation.....	26
7-	FRP frame concepts	29
7-1-	Skin-Stiffener-based structures.....	29
7-2-	Leaf spring-based structures.....	31
7-3-	Shell –based structures.....	34
7-4-	Pultruded/pull-winding profile based structures.....	35
8-	Workshop scores for concepts.....	38
9-	New Ideas in the 2nd workshop.....	39
10-	Conclusions	42
11-	References.....	43

List of figures

Figure 1- The previously presented FRP bogies.....	8
Figure 2- The defined tasks for the feasibility phase of the FRP bogie project.....	9
Figure 3- The time plan for the feasibility phase of the FRP bogie project (with some margins for possible delays)	10
Figure 4- Schematic of the standard Y25 bogie and attached components [12].....	12
Figure 5- Bogie type categories according to EN13749 [13]	12
Figure 6- Schematic of primary and secondary suspension systems in bogies [14]	13
Figure 7- Schematic of the force and deflection directions in the bogie [13]	14
Figure 8- Input parameters for load calculations	15
Figure 9- Calculated exceptional and normal service loads for bogie analysis	15
Figure 10- Load combinations for exceptional forces	16
Figure 11- Load combinations for normal service forces.....	16
Figure 12- The evaluation parameters for basic layout and FRP design concepts	18
Figure 13- Schematic of inboard and outboard axle configuration [15].....	21
Figure 14- Schematic of steering configuration. Self-steering, connected wheels, connecting to the car body [18].....	25
Figure 15- Material and geometrical input parameters for the theoretical tool.....	27
Figure 16- Calculated bending and shear strength for the FRP component.....	28
Figure 17- Calculated safety factors for the FRP components	29
Figure 18- Example 1 of using skin-stiffener concept for bogie frame	30
Figure 19- Example 2 of using skin-stiffener concept for bogie frame	30
Figure 20- Example 3 of using skin-stiffener concept for bogie frame	30
Figure 21- Example 4 of using skin-stiffener concept for bogie frame	31
Figure 22- Example 1 of using leaf-spring concept for bogie frame.....	32
Figure 23- Example 2 of using leaf-spring concept for bogie frame.....	32
Figure 24- Example 3 of using leaf-spring concept for bogie frame.....	33
Figure 25- Example 4 of using leaf-spring concept for bogie frame.....	33
Figure 26- Example 5 of using leaf-spring concept for bogie frame.....	33
Figure 27- Example 1 of using shell-based concept for bogie frame	34
Figure 28-Example 2 of using shell-based concept for bogie frame.....	35
Figure 29- Example 1 of using pre-fabricated profiles for bogie frame.....	36

Figure 30-Example 2 of using pre-fabricated profiles for bogie frame	36
Figure 31- Example 3 of using pre-fabricated profiles for bogie frame	36
Figure 32- Example 4 of using pre-fabricated profiles for bogie frame	37
Figure 33- Example 5 of using pre-fabricated profiles for bogie frame	37
Figure 34- Example 6 of using pre-fabricated profiles for bogie frame	37
Figure 35- Example 7 of using pre-fabricated profiles for bogie frame	38
Figure 36- Evaluation results for FRP frame concept for the new bogie.....	39
Figure 37- First presented three-piece model in the second workshop	39
Figure 38- Second presented three-piece model in the second workshop.....	40
Figure 39- Second presented three-piece model in the second workshop.....	41
Figure 40-Cross link components for enhancement of steering and stability	41
Figure 41- Initial model for performing finite element analysis	42

List of Tables

Table 1- Previously presented FRP bogies and their properties	7
Table 2- Characteristics of standard Y25 bogie.....	11
Table 3- Definition of force and displacement directions for bogie analysis [13].....	14
Table 4- Definition of mass parameters for bogie analysis [13]	14
Table 5- Evaluation form for basic layout of the new FRP bogie	19
Table 6- Evaluation form for FRP frame concept for the new FRP bogie	20
Table 7- Evaluation results for axle configuration.....	22
Table 8- Evaluation results for brake configuration	22
Table 9- Evaluation results for suspension systems	23
Table 10- Evaluation results for materials and structures	23
Table 11- Evaluation results for fabrication methods	24
Table 12- Evaluation results for basic frame configurations	25
Table 13- Evaluation results for steering behavior.....	26
Table 14- Evaluation results for structural health monitoring	26

1- Introduction

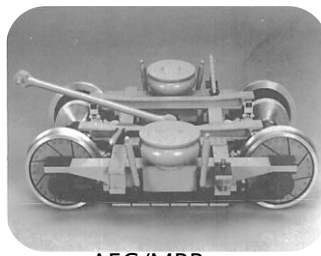
Over the past decade, fiber-reinforced composite structures have replaced metallic parts in various engineering applications and infrastructures. Their exceptional mechanical and physical properties have attracted the tremendous attention of scientists and engineers in various fields, especially in the transportation industries.

With FRP's high strength-to-weight ratio, high corrosion resistance, and good fatigue properties, composite structures can accelerate the evolution of ground transportation. Considering that the demand for a safe, rapid, and efficient transportation system is rising, the railway transportation system should be improved to meet the growing demands. Therefore, using composite structures can be considered a high-rate solution for the enhancement of the railway industry by the reduction in weight and costs of the system.

So far, unlike aerospace or marine applications, the full capacities of composite structures have not been significantly used in railway industries. Advanced composite materials and structures allow the designers to reduce the total weight of the bogie and take advantage of their high damping properties to reduce the system noises and enhance the comfort of passengers. From 1983 until now, scientific and industrial efforts have been made to provide more efficient, more functional, and cost-effective bogies for using composite materials and structures in railway industries. However, there are only a few real-world examples of FRP composites bogies. A summary of the previously presented FRP bogies with their obtained weight reduction is presented in Table 1. The fabricated bogies are demonstrated in Figure 1. Different concepts and manufacturing methods are employed to ensure the functionality of the presented FRP bogies.

Table 1- Previously presented FRP bogies and their properties

No.	Institution/ Company	Commercial name	Reported weight reduction	Country	Presented in	FRP type	Ref.
1	AEG Westinghouse MBB	---	25% (bogie weight)	Germany	1988	GFRP	[1, 2]
2	Alstom	TER Bogie frame	30% (bogie frame weight)	France	2002	GFRP	[3]
3	Korean railroad research institute (KRRI)	---	31% (bogie frame weight)	South Korea	2010	GFRP	[4, 5]
4	Department of Trade and Industry (DTI) /Eureka Project	EUROBOGIE	1 Ton (bogie frame weight)	EU	2012	GFRP	[6]
5	Japanese Railway Technical Research Institute	efWING	40% (bogie frame weight)	Japan	2016	CFRP	[7,8]
6	UK Rail Research and Innovation Network/ Institute of Railway Research (IRR)	CaFiBo	36% (with metallic fixtures) 60% (with composite fixtures)	UK	2020	CFRP (Re-cycled fibers)	[9]
7	CG rail			Germany	2020	CFRP	[10]

AEG/MBB
bogie (1988)

KRRi bogie (2010)



Eurobogie (2012)



efWING (2016)



CaFiBo (2020)

Figure 1- The previously presented FRP bogies

The current feasibility project aims to study the possible application of composite materials in the railway industry by developing a new FRP bogie. The project's primary target is to conceptually design an FRP bogie with acceptable functional and mechanical properties, particularly reducing the bogie's weight (compared to conventional bogies) with reasonable total life costs.

2- Overview of the project

As presented in the project proposal and kick-off meeting, the feasibility phase (phase I) of the project contains eight different tasks that will be completed within 12 months. The definition of the tasks and the project timetable are presented in Figure 2 and Figure 3, respectively. As the first interim report, the current report is concentrated on tasks 1 and 2 and the initial parts of task 3. Task 1 is about the definition of general specifications, including standards, load cases, and design validation for the new FRP design. The reference bogie type for the project was selected to be the traditional Y25 bogie as one of the most frequently used freight bogies in Europe. After choosing the reference bogie type, determining the required standards and extracting the load conditions are performed in task 1. Design approval criteria for new bogie design in case of static and dynamic functionality are also considered in Task 1.

Following the determination of the required specifications and parameters in Task 1, preparing the design concepts is carried out in Task 2. The first workshop with the partners was held to discuss the possible concepts and collect new ideas for the design of the FRP bogie. The basic layout design for the bogie, including the wheelset configuration, brake system, suspension system, fabrication methods, and health monitoring systems, were discussed and evaluated in the workshop. Moreover, design concepts for FRP load-carrying elements were also discussed to evaluate the presented designs and collect new ideas for the FRP bogie frame. For a rough estimation of the required dimensions (especially for the pre-fabricated FRP elements) and comparing the total mass of the presented concepts, a theoretical tool was developed based on the flexural and shear strength of the FRP elements of the bogie frame. Evaluations of the design parameters and concepts were performed after full discussions on the concepts, considering the technical, economic, manufacturing, and maintenance aspects. The evaluation process will be discussed in more detail in section 5 of the report.

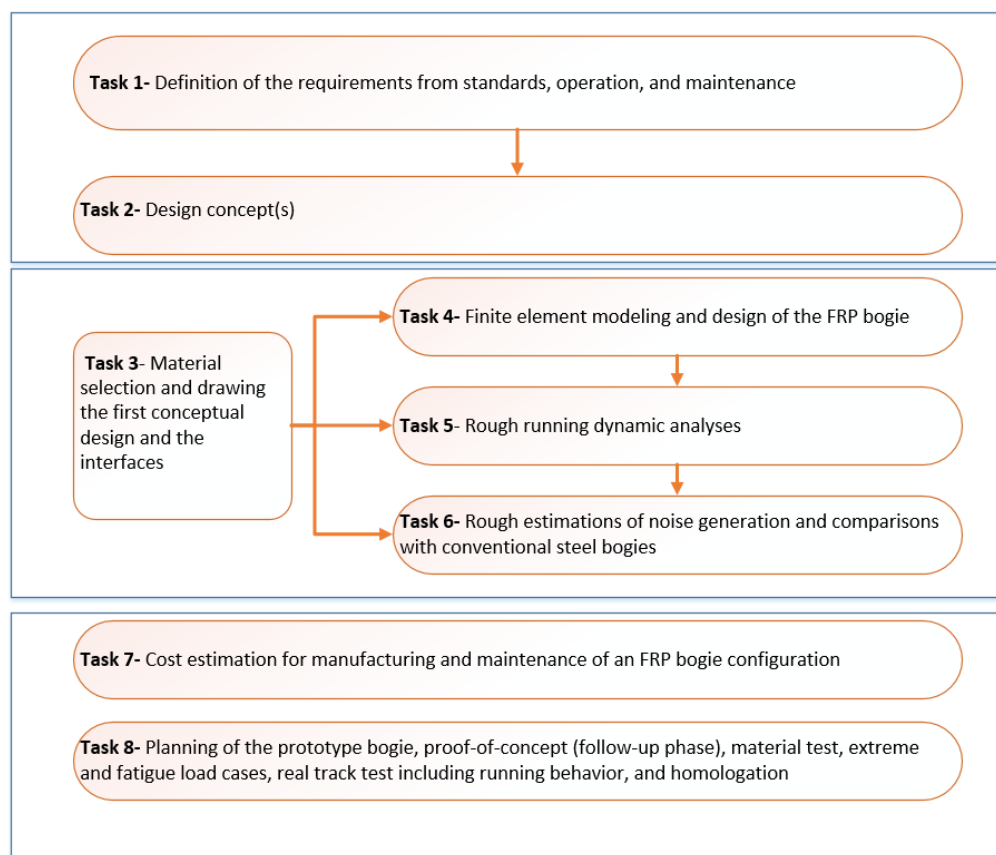


Figure 2- The defined tasks for the feasibility phase of the FRP bogie project

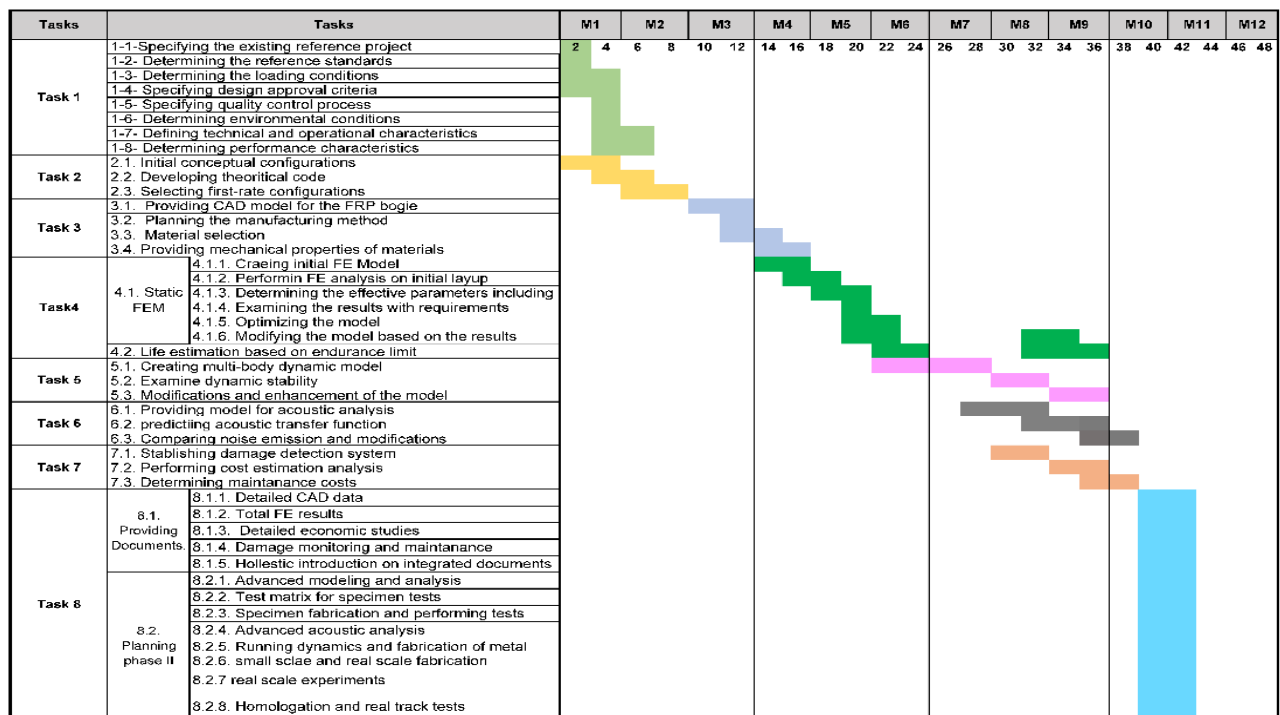


Figure 3- The time plan for the feasibility phase of the FRP bogie project (with some margins for possible delays)

3- Design specifications

General specifications should be determined to design and analyze a new concept for bogies. At first, the reference standards and norms regarding the bogie analysis are considered to extract the required design parameters, including geometries, load cases, verifications, and experiments. A list of related standards that were utilized for determining the design specifications is as follows:

TSI-Wagon: COMMISSION REGULATION (EU) No 321/2013 of 13 March 2013 concerning the technical specification for interoperability relating to the subsystem 'rolling stock — freight wagons' of the rail system in the European Union and repealing Decision 2006/861/EC

EN 13749: Railway applications - Wheelsets and bogies - Method of specifying the **structural** requirements of bogie frames.

EN 15827: Railway applications - Requirements for bogies and running gears (**Loading cases**)

EN 14363: Railway applications - Testing and **simulation** for the acceptance of running characteristics of railway vehicles - Running behavior and stationary tests

EN 16235: Railway application - **Testing** for the acceptance of running characteristics of railway vehicles - Freight wagons - Conditions for dispensation of freight wagons with defined characteristics from on-track tests according to EN 14363

EN 15663: Railway applications - Vehicle reference **masses**;

General requirements, including bogie type, design load cases, vehicle conditions, and interfaces, and particular requirements, including materials, manufacturing, and assembly, are the main specifications that should be determined before designing the new bogie.

As previously mentioned in the project overview, the reference bogie type for the current project is the Y25 bogie. This bogie type can be considered the most widely used freight bogie and is currently being rebuilt by various manufacturing companies. The frame of the standard Y25 bogie has only primary suspension with duplex coil springs. The springs provide a non-smooth characteristic. The axle box does not provide allowance and frictional damper. Flex-coil effect is used for lateral suspension [11]. The interface for connecting the car body is a hemispherical bogie pivot with a 190 mm radius. The properties and specifications of the Y25 traditional bogie are presented in Table 2. A sample of the Y25 bogie with the components is shown in Figure 4.

Table 2- Characteristics of standard Y25 bogie

Parameter	description
Axel Load	22.5 T
Maximum running speed	120 km/h
Bogie components	wheelset, axle box, suspension device, bogie frame, basic brake rigging, load proportional device
Suspension	Two level stiffness spring suspension- 16 coil spring
Brake system	Two-side brake system
Tare weight	≤ 4.7 Ton
Dimensions	3250 mm length, 2200 mm width
Diameter of wheels	920 mm
Center distance	1800 mm
Gauge	1435 mm

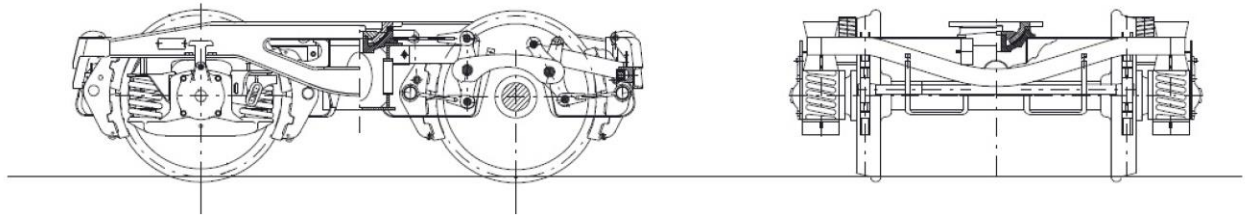


Figure 4- Schematic of the standard Y25 bogie and attached components [12]

Bogies are categorized into seven groups depending on their usage, suspension systems, and corresponding railway vehicles. Therefore, the load calculation for analysis of the bogie strongly depends on the bogie category. Figure 5 presents the defined categories for different types of bogies. As the present project is concentrated on the freight bogies to replace the Y25 traditional bogie, the target group is category B-V. The Y25 bogie has only the primary suspension systems and is categorized as single-stage suspension freight bogies. It is noteworthy to mention that in a two-stage suspension system, both primary and secondary suspensions are available, while in a single-stage suspension system, either primary or secondary suspension is provided in the bogie design. Primary and secondary suspension systems are schematically demonstrated in Figure 6.

- | | |
|-----------------------|---|
| category B-I | bogies for main line and inter-city passenger carrying rolling stock including high-speed and very high-speed vehicles, powered and un-powered; |
| category B-II | bogies for inner and outer suburban passenger carrying vehicles, powered and un-powered; |
| category B-III | bogies for metro and rapid transit rolling stock, powered and un-powered; |
| category B-IV | bogies for light rail vehicles and trams; |
| category B-V | bogies for freight rolling stock with single-stage suspensions; |
| category B-VI | bogies for freight rolling stock with two-stage suspensions; |
| category B-VII | bogies for locomotives. |

Figure 5- Bogie type categories according to EN13749 [13]

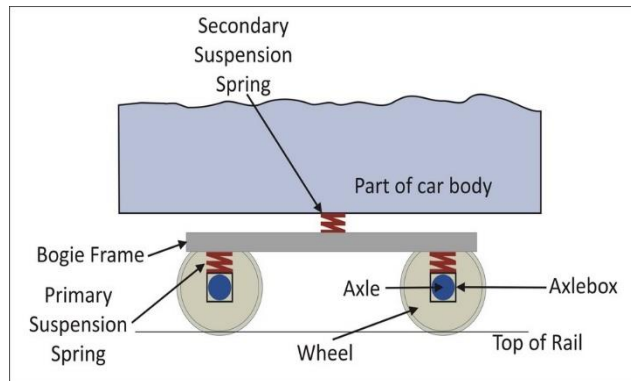


Figure 6- Schematic of primary and secondary suspension systems in bogies [14]

4- Load calculations

Load calculations were performed according to EN13749. Two types of loads should be examined in the analysis step, namely exceptional loads and fatigue loads. The exceptional loads represent the extreme conditions that rarely occur during the service life of the bogie. The bogie structure should withstand exceptional loads without damage or out-of-limit deformation. On the other hand, fatigue load cases represent the conditions that repeatedly occur during the service life of the bogie.

In another view, the applied loads can be divided into external and internal loads. External loads can be resulted from running on the track, starts and stops, loading and unloading cycles in the bogie service life, and also loads resulting from lifting and jacking. The internal loads are generated by the bogie-mounted components such as brakes, dampers, and motors. In the feasibility phase of the FRP bogie design, only external load cases are considered. The effect of internal loads on the structural integrity and dynamic behaviors of the bogie structure will be examined in the detailed design step, using experimental and numerical tools.

Definition of the directions of the applied external loads, displacements, and rotations are shown in Figure 7, and Table 3. According to the standards, longitudinal, transverse, and vertical directions are indicated by x, y, and z, respectively.

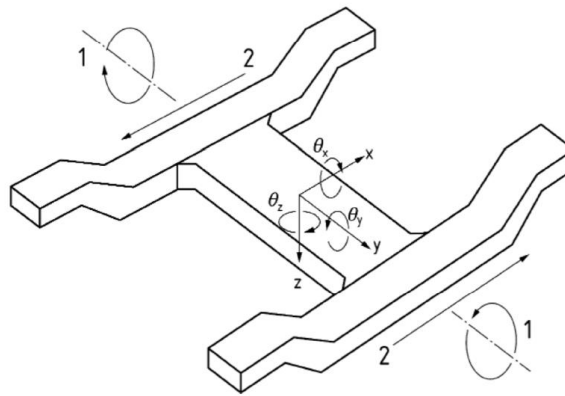


Figure 7- Schematic of the force and deflection directions in the bogie [13]

Table 3- Definition of force and displacement directions for bogie analysis [13]

Direction	Symbol	Description
Longitudinal	x	Linear in the direction of travel
Transverse	y	Linear parallel to the plane of the track, perpendicular to the direction of travel
Vertical	z	Linear perpendicular to the plane of the track
Roll	θ_x	Rotation about the longitudinal axis
Pitch	θ_y	Rotation about the transverse axis
Yaw	θ_z	Rotation about the vertical axis
Twist	—	Out-of-plane (x-y) movement resulting in relative rotation of the sideframes
Lozenging	—	Shear due to relative longitudinal movement of sideframes

The external loads due to the running behavior of the vehicle depend on the applied weights in fully loaded and unloaded conditions. Definitions of the required masses for load calculations are presented in Table 4.

Table 4- Definition of mass parameters for bogie analysis [13]

Mass (kg)	Symbol
Vehicle in working order	M_v
Vehicle body	m_1
Bogie mass without any secondary spring masses (if present)	m^+
Bogie primary sprung mass	m_2
Design mass under exceptional payload	P_1
Design mass under normal service payload	P_2

An Excel tool was prepared to calculate the applied loads on the bogie. The assumptions and load cases were checked and modified by PROSE. The mass properties, geometrical properties and accelerations are the required input parameters for load calculations, as shown in Figure 8.

Input Parameters							
Initial specifications	Bogie Class (Table A6)	5		Accelerations for bogie and vehicle body	Vertical (m/s ²) a _{zc} & a _{zb}	Vehicle body	Bogie (primary sprung)
	Vehicle category (Table 3)	3			Transverse (Dynamic)(m/s ²) a _{yc} & a _{yb}		
					Centrifugal (quasi-static)(m/s ²) a _{ycc} & a _{ycb}		
Masses properties	Vehicle in Working order (kg)	90000	Mv	Accelerations for bogie and vehicle body	Longitudinal (m/s ²) a _{xc} & a _{xb}		
	Vehicle body (kg)	16000	m1				
	Bogie mass without secondary springs (kg)	5000	m+		Gravity(m/s ²) g	9.8066	
	Bogie primary sprung mass (kg)	1100	m2		Acceleration at collision (m/s ²) a _{col}	49.033	
	Design mass under exceptional payload (kg)		P1				
	Design mass under normal service payload (kg)		P2				
Geometrical/ Mechanical properties				Acceleration for attached equipments	Vertical	Exceptional	Fatigue
					Lateral	20g	6g
					Longitudinal	10g	5g
						5g	2.5g
	Spacing between side bearres (m)	1.7	2b _g	Attachment forces	Reference force of damper		
	Bounce coefficient	0.3	β		Break Force		
	Adhesion or friction coefficient		μ		Traction force		
number of axels per bogie	2	n _a					

Figure 8- Input parameters for load calculations

The exceptional and fatigue loads are calculated in the Excel tool, using the prepared input parameters and the standard formulation. Figure 9 shows the calculated loads due to bogie running. The internal loads due to attached components can also be calculated once the mechanical properties of the components are determined.

Loads due to bogie running							
Exceptional loads (N)				Normal loads (N)			
Roll coefficient for exceptional loads		0.3	α	Roll coefficient for normal service		0.2	α
Vertical	F_z Total vertical load supported by bogie	392,264.00		Vertical	F_{zp} (Applied only to pivot)	392,264.00	Case 1
	F_{zpmax} (applied only to pivot)	784,528.00	Case 1		F_{zp}	313,811.20	Case 2
	F_{zpmax} applied to pivot	411,877.20	Case 2		F_{z1} or F_{z2}	78,452.80	
	F_{z1max} or F_{z2max} applied to sidebearer	176,518.80					
Transverse	F_{ymax} (Applied to each axle)	167,099.00		Transverse	F_y (Applied to each axle)	88,259.40	
	F_{y1max}	83,549.50			F_{y1}	44,129.70	
	F_{y2max}	83,549.50			F_{y2}	44,129.70	
Longitudinal	F_{x1max} (Applied to each wheel)	44,129.70	Lozenging	Longitudinal	F_{x1} (Applied to each wheelset)	22,064.85	
	From test or (bogie mass*acceleration at collision)	245,165.00	Shunt				
Twisting	Exceptional case: with exceptional vertical and transverse frame should withstand the loads resulting from 1% twisting		Case 1	Twisting	The loads resulting from 0.5% twisting		
	Empty case (vertical load only): complete unloading of one wheel with the vertical displacement of the wheel being limited by rail height		Case 2				
Loads due to attached components							
Exceptional loads (N)				Normal loads (N)			
Equipment attached to frame	Table D.1			Equipment attached to frame	Table D.1		
Equipment attached to axle box	Table D.2			Equipment attached to axle box	Table D.2		
Viscos dampers	twice the reference load of dmaper	0		Viscos dampers	Reference force of damper	0	
Braking		0		Braking		0	
Traction Motors		0		Traction Motors		0	
Anti-Roll system	corresponds to maximom bogdie inclination			Anti-Roll system	based on bogdie-bogie inclination		

Figure 9- Calculated exceptional and normal service loads for bogie analysis

The calculated loads are finally employed to define the loading cases. Twelve exceptional and 15 normal service loading cases are considered to be examined in the analysis step. The defined exceptional and normal service loading cases are shown in Figure 10 and Figure 11, respectively.

Load combinations Exceptional loads (N)						
Case Number	Load combinations	Fz (on pivot)	or Fz2 (on side frame)	Fy	Fx	Twist (e.g. delta Z)
1	Vertical (Case1)	784528	0	0	0	0
2	Vertical (Case2)	411877.2	176518.8	0	0	0
3	Vertical (Case1)+ Transverse	784528	0	83549.5	0	1% twist
4	Vertical (Case2)+ Transverse	411877.2	176518.8	83549.5	0	1% twist
5	Vertical (case 1) +longitudinal (Lozenging)	784528	0	0	44129.7	0
6	Vertical (case 2) +longitudinal (Lozenging)	411877.2	176518.8	0	44129.7	0
7	Vertical (Case 1)+ Transverse+Twist (Case 1)	784528	0	83549.5	0	1% twist
8	Vertical (Case 2) + Transverse+Twist (Case 1)	411877.2	176518.8	83549.5	0	1% twist
9	Vertical (Case 1)+ twist case 2(unloading of a wheel)	TARE Weight	0	0	0	32mm at wheel contact point
10	Vertical (Case 2) + twist case 2(unloading of a wheel)	411877.2	176518.8	83549.5	0	32mm at wheel contact point
11	Vertical (case 1)+ Shunt	784528	0	0	245165	0
12	Vertical (Case 2)+ Shunt	411877.2	176518.8	0	245165	0

Figure 10- Load combinations for exceptional forces

Normal service loads (N)							
Case Number	Load combinations	Fz (on pivot)	Fz1 (on side frame1)	Fz2 (on side frame2)	Fy	Fx	Twist (e.g. delta Z)
1	Vertical (Case1)	392264	0	0	0	0	0
2	Vertical (Case2)	509943.2		0	0	0	0
3	Vertical (Case3)	274584.8		0	0	0	0
4	Vertical - Transverse	407954.56	0	101988.64	-88259.4	0	0.50%
5	Vertical - Transverse	407954.56	101988.64	0	88259.4	0	0.50%
6	Vertical - Transverse	219667.84	0	54916.96	-88259.4	0	0.50%
7	Vertical - Transverse	219667.84	54916.96	0	88259.4	0	0.50%
8	Vertical - Transverse- twist	407954.56	0	101988.64	-88259.4	0	-0.50%
9	Vertical - Transverse- twist	407954.56	101988.64	0	88259.4	0	-0.50%
10	Vertical - Transverse- twist	219667.84	0	54916.96	-88259.4	0	-0.50%
11	Vertical - Transverse- twist	219667.84	54916.96	0	88259.4	0	-0.50%
12	Vertical+ Longitudinal	392264	0	0	0	0	0
13	Vertical+ Longitudinal	392264	0	0	0	22064.85	0
14	Vertical+ Longitudinal	392264	0	0	0	-22064.85	0
15	Vertical+ Longitudinal braking						

Figure 11- Load combinations for normal service forces

The calculated load cases will be used in Task 4 of the project, in finite element analysis of the new FRP bogie.

5- Evaluation parameters

For evaluating the effective parameters for the design of the new FRP bogie and collecting ideas regarding the FRP concepts, a workshop meeting was held on 4. March 2022 with the partners. The evaluation parameters with possible options and discussions on their advantages and limitations were

prepared and sent to the partners before the workshop meeting. The parameters and forms were modified during the workshop and new ideas were collected and added to the evaluation documents. 7 major parameters regarding the basic layout of the bogie and 4 main design concepts for the FRP frame were discussed and evaluated in the workshop. The evaluating parameters are presented in Figure 12.

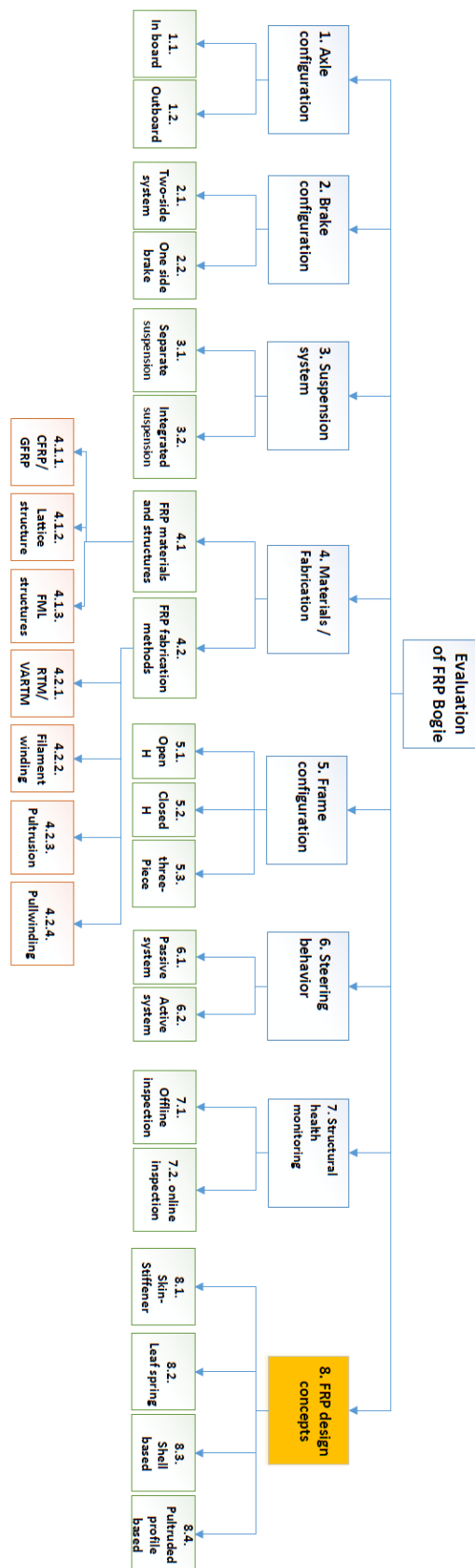


Figure 12- The evaluation parameters for basic layout and FRP design concepts

For evaluation of the parameters related to the basic layout and FRP frame concepts, two evaluation forms were prepared to be modified and filled in the workshop meeting. The evaluation form for the basic layout is presented in Table 5.

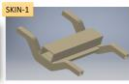

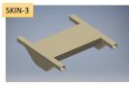








Table 5- Evaluation form for the basic layout of the new FRP bogie

Subject	Suggested concepts	Scores (1-10)			
		Technical	Economic	Manufacturing	Maintenance
1. Axle configuration	1.1. Inboard axle				
	1.2. Outboard axle				
2. Brake configuration	2.1. Two-side				
	2.2. One side (Push brake)				
3. Suspension systems	3.1. Separate suspensions				
	3.2. Integrated primary or secondary suspension				
	3.3. Integrated both suspensions				
4. Materials and fabrication	4.1.1. GFRP/CFRP				
	4.1.2. Lattice structure				
	4.1.3. FML structure				
	4.2.1 RTM/VARTM				
	4.2.2. Filament winding				
	4.2.3. Pultrusion				
	4.2.4. Pullwinding				
5. Frame basic configuration	5.1. Open-H				
	5.2. Closed-H				
	5.3. 3-Piece				
6. Steering behavior	6.1. Self-Steering				
	6.2. Connected wheels				

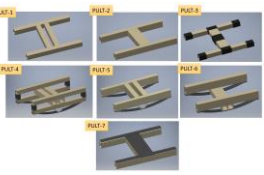
	6.3.	Active steering				
7. Structural health Monitoring	7.1.	Regular NDT				
	7.2.	Fiber Bragg sensors				
	7.3.	Piezoelectric sensors				

Another evaluation form was also prepared for the FRP design concepts. Effective parameters with different weight ratios are examined. For each parameter, participants give their scores to the presented concepts. Averaging the final scores determines the best design concept with the highest priority. The Evaluation form for the design concepts is presented in Table 6.

Table 6- Evaluation form for FRP frame concept for the new FRP bogie

Subject	Evaluating parameters	Weight ratio	Scores (1-10)					Schematic
			SKIN	LEAF	SHEL	PULT	other	
8. FRP design concepts	Weight reduction	5						SKIN: Skin-Stiffener structures    
	Estimated manufacturing costs	4						
	Cost of raw materials	4						
	Expected structural integrity	3						
	Compatibility with Y25 component	3						LEAF: Leaf spring based structures     
	Ease of assembling	2						
	Maintenance ability	3						
	Expected noise emission	2						
	Steering behavior	2						SHEL: Shell based structures  
	Stiffness controlling	1						
	Dynamic stability	3						PULT: Pultruded profile structures



Possible damping behavior	1							
Ease of maintenance	1							
Compatibility with monitoring system	2							
Innovative design	2							

After introducing the evaluation process and the related forms, in the following, the basic layout parameters and the selected plan for each parameter after discussions in the workshop are presented.

- Axle configuration

The first parameter regarding the basic layout of the new bogie type was the axle configuration. As shown in Figure 13, internal and external axle bearings can be employed to design the bogie. Although internal bearing results in a smaller bogie frame, it requires stronger bearings and possibly a larger diameter for the wheel axel. Therefore, the external configuration was selected as the first priority in the workshop, as presented in Table 7.

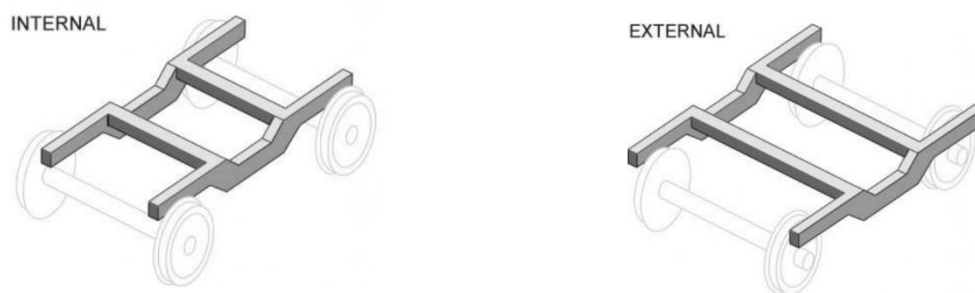


Figure 13- Schematic of inboard and outboard axle configuration [15]

Table 7- Evaluation results for axle configuration

Subject	Suggested concepts	Priority
1. Axle configuration	1.1. Inboard axle	2
	1.2. Outboard axle	1

- Brake configuration

The standard Y25 bogie has a two-sided brake system that requires additional metallic links to support the brake components. As another alternative, the one-side brake system makes it possible to remove the additional links and reduce the weight of the bogie. However, there are speed limitations for using the one-sided brake system. The third option for the brake system is employing the disc brakes, which leads to significant noise reduction for the bogie and is compatible with the standards. After discussion, as presented in Table 8, the disc brake system was recognized as the first priority for the new bogie design.

Table 8- Evaluation results for brake configuration

Subject	Suggested concepts	Priority
2. Brake configuration	2.1. Two-side	P2
	2.2. One side (Push brake)	P3
	2.3. Disc brake	P1

- Suspension system

For the suspension systems, there are three available options. The first one is to consider a separate suspension system with the FRP frame. This concept is easier to design and analysis, but it can be considered only as a material replacement and the main benefits of composite structures will not be fully employed. Therefore, the first priority was selected to be an integrated suspension system and as most freight bogies have single-stage suspensions, the integrated primary suspension system with the FRP frame was selected as the best possibility (Table 9).

Table 9- Evaluation results for suspension systems

Subject	Suggested concepts	Priority
3. Suspension	3.1. Separate suspensions	P3
	3.2. Integrated primary suspension	P1
	3.3. Integrated both suspensions	P2

- Materials & Fabrication

Several material systems and structures can be examined for the new FRP bogie system. This includes using glass fiber reinforced polymers (GFRP), carbon fiber reinforced polymers (CFRP), fiber-metal laminates (FML), lattice structures, and also combinations of the mentioned materials and structures. Considering the mechanical and economic aspects of the material selection, the priorities for the materials are determined. The first priority was employing GFRPS and after that, the hybrid multi-material system has the highest priority (Table 10).

Table 10- Evaluation results for materials and structures

Subject	Suggested concepts	Priority
4. Materials and fabrication	4.1.1. GFRP	P1
	4.1.2. CFRP	P4
	4.1.3. Hybrid multimaterial	P2
	4.1.4. Recycled CFRP	P4
	4.1.5. Hybrid GFRP/CFRP	P3
	4.2.1 RTM/VARTM	
	4.2.2. Filament winding	
	4.2.3. Pultrusion	
	4.2.4. Pullwinding	

The fabrication methods were also discussed in terms of the total costs, mechanical properties of the final product, and the ability to fabricate composite elements with required geometries and fiber directions. As presented in Table 11, Pull-winding and RTM methods were selected as the first and second priorities.

Table 11- Evaluation results for fabrication methods

Subject	Suggested concepts	Priority
4. Materials and fabrication	4.2.1 RTM/VARTM	P2
	4.2.2. Filament winding	
	4.2.3. Pultrusion	
	4.2.4. Pullwinding	P1

- Frame basic configuration

The basic configuration of the frame can be selected among open-H, closed-H, and 3-piece bogie frame configurations. The most frequently used design for bogies is the open H-frame because of its lightweight. This frame shape is commonly combined with a swing arm with helical springs as the elastic element.

The alternative design is the closed H-frame. In this design, a bolster connects the extremes of the H frame. Torsional resistance is enhanced in closed H bogie types but on the other hand. The bogie weight is also increased [16].

The third type of bogie frame is called a three-piece frame. This type of frame consists of two side frames linked to the central bolster by the secondary suspension. The connection from the bolster to the car body is by a central pivot and side bearers with sliding surfaces. There is no primary suspension between the wheels and the side frames in most of these bogies [16].

According to Table 12, the open-H frame was selected as the first priority due to its lighter weight. However, the 3-piece configuration makes it possible to employ a multi-material system and also to integrate the suspension systems with the FRP frame. Therefore, the second priority is dedicated to the 3-piece bogies.

Table 12- Evaluation results for basic frame configurations

Subject	Suggested concepts	Priority
5. Frame basic configuration	5.1. Open-H	P1
	5.2. Closed-H	P3
	5.3. 3-Piece	P2

- Steering behavior

The steering mechanism controls the bogie behavior when running in the curves. The steering behavior can be defined as the bogies' capacity on the wheelset to adopt a radial position in curves.

The lack of a proper steering system will result in the following challenges:

- Large lateral force on rails,
- High-frequency noises,
- Severe wear of wheel,
- Significant wheel load change at transition curves

The steering system can be active (by employing sensors and actuators) or passive. Passive systems can be implemented by self-steering design or employing connected wheels. The self-steering mechanism gets the yaw of the wheelset through the interaction between the rail and the wheel. In the connected steering systems, the yaw angles of the wheelsets are determined by the angle of the bogie relative to the vehicle body, the wheelsets are forced to get a radial position due to the linkages between the wheelset and the vehicle body [17]. Different types of the steering system are presented in Figure 14.

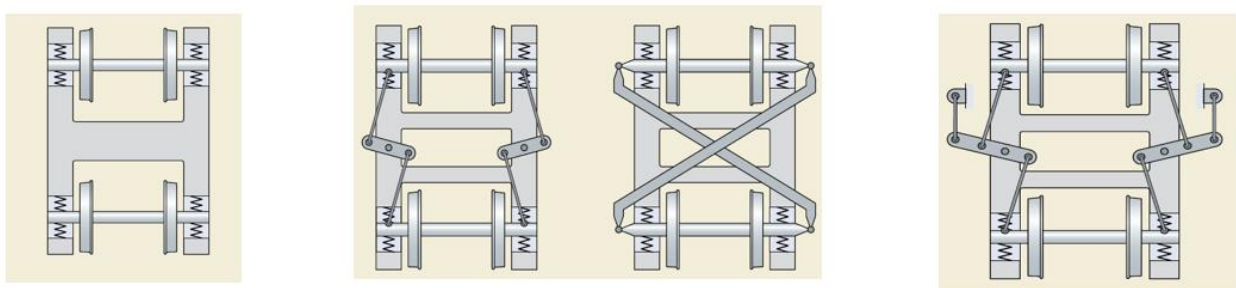


Figure 14- Schematic of steering configuration. Self-steering, connected wheels, connecting to the car body [18]

The first priority in the steering behavior is dedicated to the self-steering system that uses flexible properties of composites to locate the wheels in the proper positions (Table 13). The second priority

is self-steering behavior using the contact force between the wheelsets and rail. The connecting links can also be added to the bogie to enhance the steering and stability properties if needed.

Table 13- Evaluation results for steering behavior

Subject	Suggested concepts	Priority
6. Steering behavior	6.1. Self-Steering (using wheel rail contact)	P2
	6.2. Self-Steering (using composite flexibility)	P1
	6.3. Connected wheels	P3
	6.3. Active steering	P4

- Structural health monitoring-

Structural health monitoring was the last parameter discussed in the workshop meeting. It is possible to embed fiber bragg sensors within the composite laminate or employ piezoelectric sensors; however, utilizing a regular NDT system has the highest priority regarding the simplicity and economic aspect of the feasibility study phase, as presented in Table 14.

Table 14- Evaluation results for structural health monitoring

Subject	Suggested concepts	Priority
7. Structural health Monitoring	7.1. Regular NDT	P1
	7.2. Fiber Bragg sensors	
	7.3. Piezoelectric sensors	

6- Developing a theoretical tool for weight estimation

A theoretical tool was also developed for a rough estimation of the required dimensions (and weights) for the FRP elements. Flexural strength, shear strength, and local buckling of the FRP parts are considered. The inputs needed for the analysis are:

- Strength of FRP parts in longitudinal and transverse directions
- Elastic moduli in longitudinal and transverse directions
- Shear modulus and Poisson's ratio of the laminate
- Geometrical parameters, including the cross-section of the profile and thicknesses

The required geometrical parameters such as moments of area and location of the neutral axis are calculated and will be used for stress analysis. Figure 15 shows the abovementioned input parameters for the theoretical tool.

Strengths of the profile			
F _{If}	Characteristic longitudinal strength of the flange	3.0000E+02	MPa
F _{Iw}	Characteristic longitudinal strength of the web	3.0000E+02	MPa
F _I	Characteristic longitudinal strength (in tension or compression) of the member	3.0000E+02	MPa
F _{It}	Characteristic in-plane shear strength	3.1000E+01	MPa
Material constants			
E _{If}	Characteristic longitudinal modulus of the flange	1.7200E+04	MPa
E _{Iw}	Characteristic longitudinal modulus of the web	1.7200E+04	MPa
E _{tf}	Characteristic transverse modulus of the flange	5.5000E+03	MPa
E _{tw}	Characteristic transverse modulus of the web	5.5000E+03	MPa
G _{It}	Characteristic in-plane shear modulus	2.9000E+03	MPa
nu _{It}	Characteristic longitudinal Poisson's ratio	3.0000E-01	
Rho	Density of the profile	1.2500E+03	kg/m ³
Geometrical parameters			
b _f	Full width of the flange	2.4000E+02	mm
h	Full height of the member	2.8000E+02	mm
t _f	Thickness of the flange	1.8000E+01	mm
t _w	Thickness of the web	1.8000E+01	mm
I _f	Moment of inertia of the flange(s) about the axis of bending	1.4850E+08	mm ⁴
I _w	Moment of inertia of the web(s) about the axis of bending	4.3580E+07	mm ⁴
I	Moment of inertia of the member about the axis of bending	2.1684E+08	mm ⁴
As	Shear Area	8.6400E+03	mm ²
y _f	Distance from the neutral axis to the extreme fiber of the flange,	1.4000E+02	mm
y _w	Distance from the neutral axis to the extreme fiber of the web	1.2200E+02	mm
y	Distance from the neutral axis to the extreme fiber of the member	1.4000E+02	mm

Figure 15- Material and geometrical input parameters for the theoretical tool

Using theoretical formulation for FRP profiles [19], the stress analysis is performed on the composite components. Material rupture and instability in bending and shear cases are considered for the analysis. As demonstrated in Figure 16, the flexural and shear strength of the FRP parts are calculated based on the provided input properties.

Bending			
Material Rupture			
Mn _f	The nominal flexural strength of flange	4.1161E+08	N-mm
Mn _w	The nominal flexural strength of web	4.7234E+08	N-mm
Mn	The nominal flexural strength for rupture	4.1161E+08	N-mm
Phi _R	Resistance factor for material rupture	1.0000E+00	
Landa _r	Time effect factor	1.0000E+00	
Mu	Required flexural strength	4.1161E+08	N-mm
Local Instability			
Landa _b		1.0000E+00	
Phi _b		1.0000E+00	
kr	Rotational spring constant	2.9982E+04	kN/rad
Kesi	Coefficient of restraint	2.1900E-01	
F _{cr_f}	Compression flange local buckling	7.6756E+02	
F _{cr_w}	Web local buckling	1.4796E+03	
Mn _f	Compression flange local buckling	1.0531E+09	
Mn _w	Web local buckling	2.0300E+09	
Mn	Nominal flexural buckling strength	1.0531E+09	
Mu	The nominal flexural strength for Buckling	1.0531E+09	N-mm
Shear			
Shear Rupture			
Vn	Nominal shear strength of members due to rupture	2.6784E+05	N
Phi _{R_she}	Resistance factor for material rupture in shear	1.0000E+00	
Landa _{r_sh}	Time effect factor for shear	1.0000E+00	
Vu	Required shear strength	2.6784E+05	N

Figure 16- Calculated bending and shear strength for the FRP component

Finally, considering the 3-piece bogie, the safety factors for cross and side beams are calculated (Figure 17). The total weight of the FRP frame can now be estimated based on the calculated dimensions and the density of the FRP structure. Such rapid and rough estimations make it possible to easily compare different bogie configurations before using finite element analysis on the selected concepts.

		Safety factor for cross beam			
Sr	Safety factor against rupture	1.242			
Sb	Safety factor against local buckling	3.177			
Ss	Safety Factor againts Shear	0.687			
		Safety factor for side beam			
Sr	Safety factor against rupture	1.141			
Sb	Safety factor against local buckling	2.919			
Ss	Safety Factor againts Shear	1.374			
W	Total weight of the frame	320.688	kg		

Figure 17- Calculated safety factors for the FRP components

7- FRP frame concepts

Several FRP concepts can be used for designing the new FRP bogie. Some of the possible concepts are as follow:

- Leaf spring concept for eliminating suspension elements
- Employing skin-stiffener or sandwich panel components for maximizing weight reduction
- Inducing variable stiffness properties in the structure using multi-part frame
- Controlling lateral stiffness or using extra FRP elements for inducing self-steering behavior
- Using pre-fabricated pultruded profiles
- Possible replacements for other components such as FRP bolster

Several configurations for the FRP bogie frame were prepared using the abovementioned concepts and in a brainstorming procedure. The configurations can be categorized into four general groups. In the following, each group will be introduced with some discussions on the benefits and the limitations of each concept.

7-1- Skin-Stiffener-based structures

Skin stiffener structures are the most frequently used composite components in the transportation industry; some previously presented FRP bogies are made with skin-stiffener FRP composites, such as KRRI [4], CaFiBo [9], and CG rail [10]. Therefore, some suggested configurations for designing FRP bogie with the skin-stiffener concept were prepared as shown in Figure 18 to Figure 21.

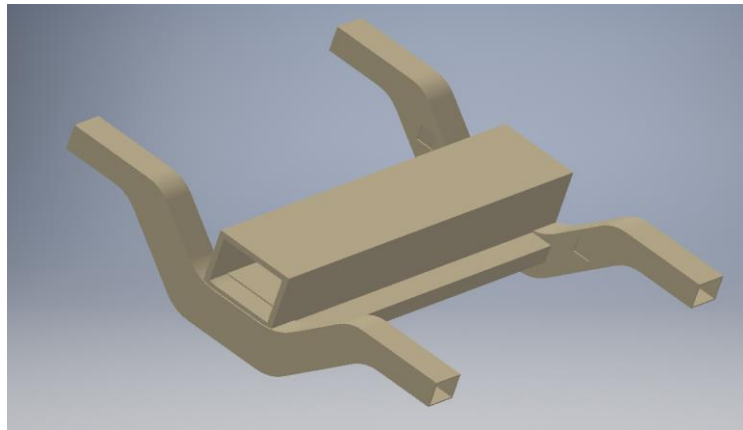


Figure 18- Example 1 of using skin-stiffener concept for bogie frame

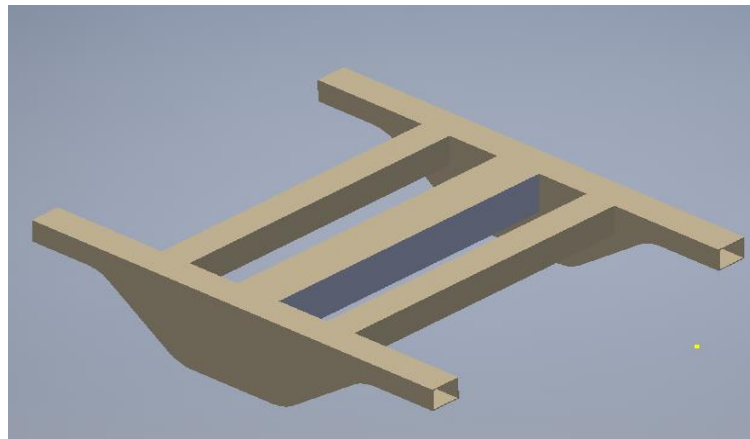


Figure 19- Example 2 of using skin-stiffener concept for bogie frame

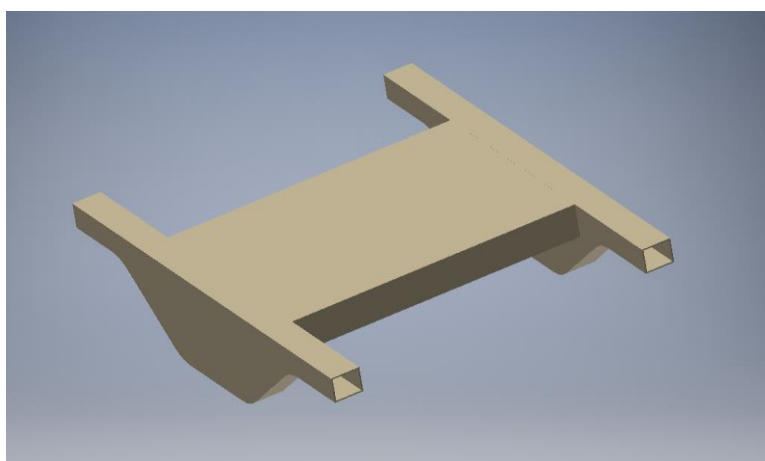


Figure 20- Example 3 of using skin-stiffener concept for bogie frame

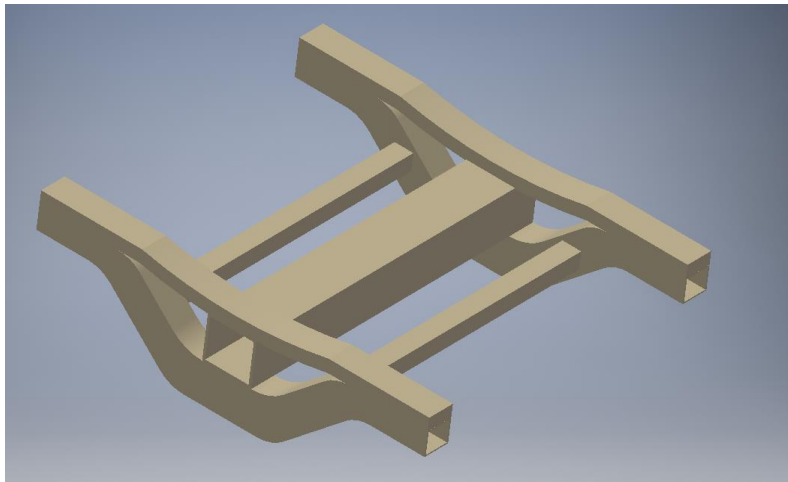


Figure 21- Example 4 of using skin-stiffener concept for bogie frame

The skin-stiffener concept for the bogie has the following advantages:

- It enables defining optimum stacking sequence and fiber orientation
- It enables embedding monitoring system
- It enables the possible use of hybrid material design
- It is compatible with both adhesively bonded and mechanically bolted joints

The main limitations of using this concept for the FRP bogie are as follow:

- High cost of manufacturing
- Difficulty in the design of joints and connections
- Difficulty in flexibility and stiffness control (hard to implement integrated suspension system)

7-2- Leaf spring-based structures

Employing leaf spring-based structures makes it possible to integrate the suspension system with the FRP frame. The CFRP leaf-springs can be used together with skin-stiffener structures or pultruded profiles to fabricate a multi-material system. Efwing bogie is an example of using CFRP leaf spring in bogie frames [7, 8]. Some suggested FRP bogie frames based on skin-stiffener structures are presented in Figure 22 to Figure 26.

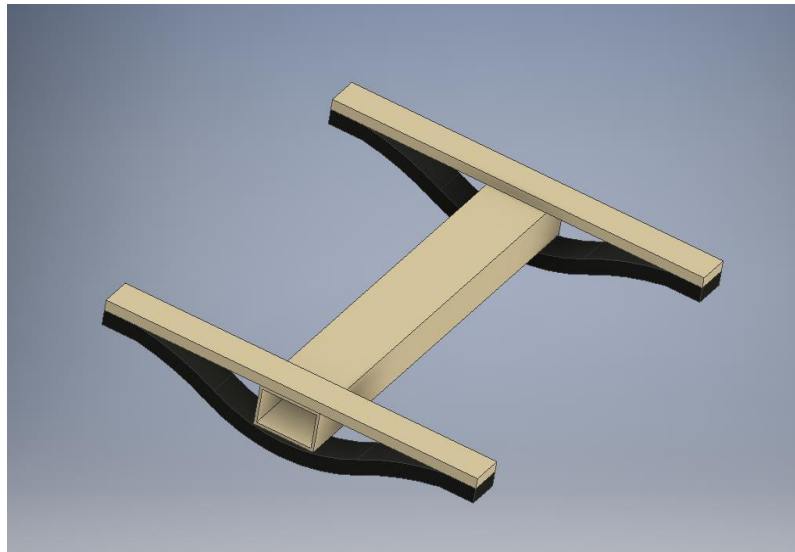


Figure 22- Example 1 of using leaf-spring concept for bogie frame

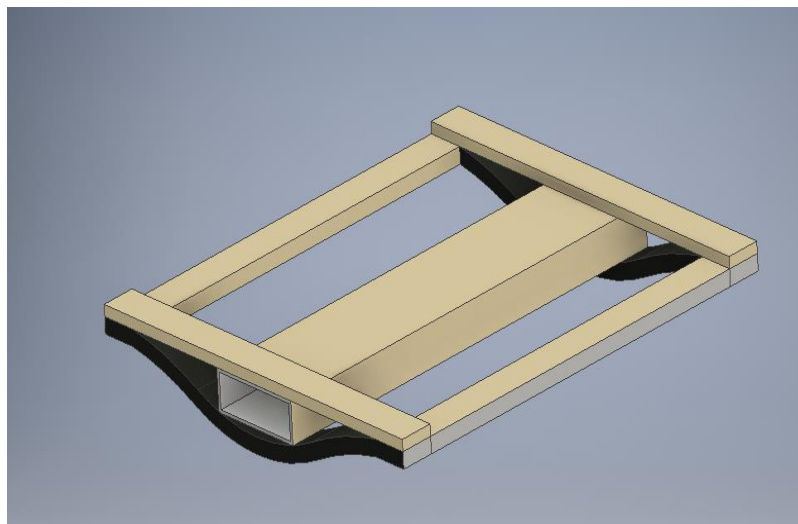


Figure 23- Example 2 of using leaf-spring concept for bogie frame

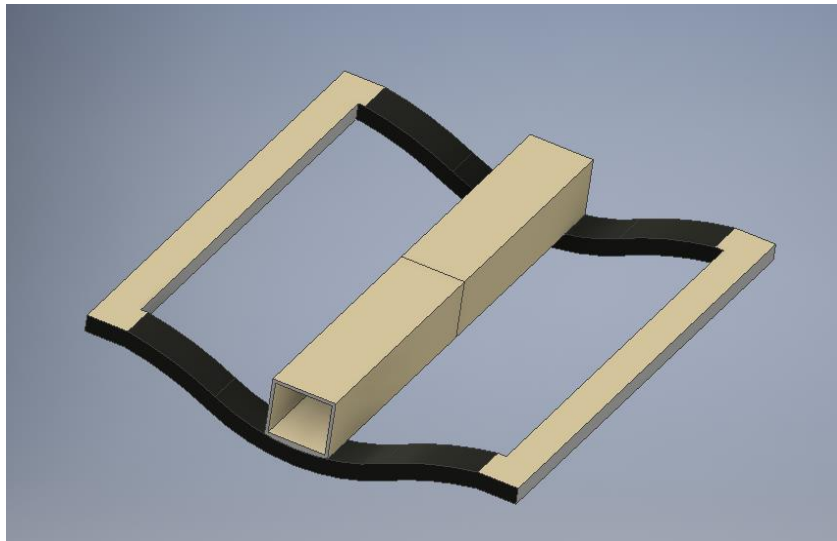


Figure 24- Example 3 of using leaf-spring concept for bogie frame

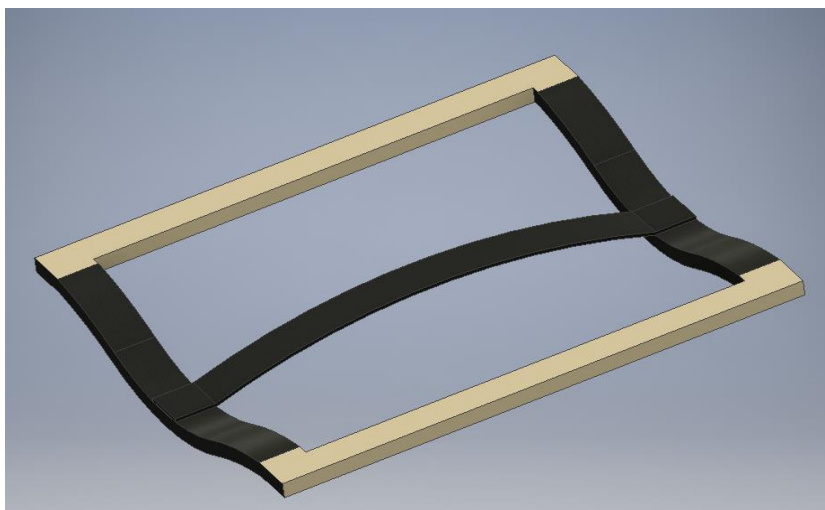


Figure 25- Example 4 of using leaf-spring concept for bogie frame

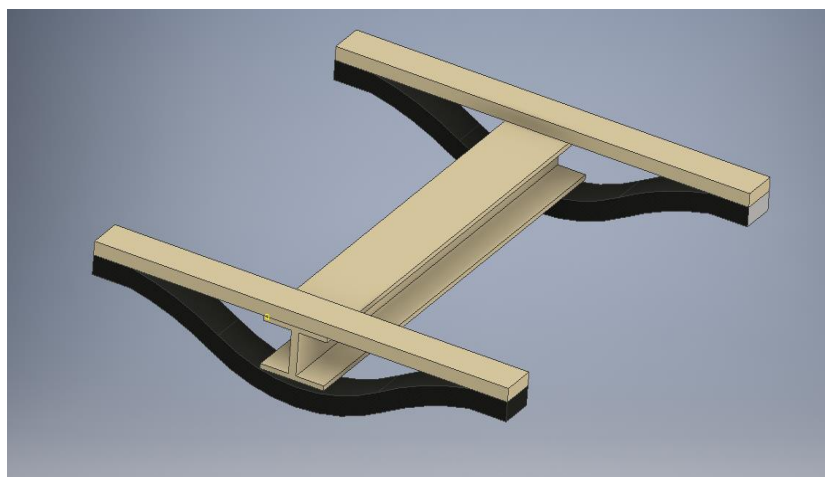


Figure 26- Example 5 of using leaf-spring concept for bogie frame

The main advantages of the leaf spring concept are as follow:

- Primary (and/or) secondary suspension systems can be removed
- Stiffness and strength of the structure can be optimized
- It enables the possible use of hybrid material design

And the main limitations are:

- High cost of materials (in case of using CFRP leaf springs)
- Relatively high cost of manufacturing (required RTM fabrication method)
- Difficulties in the design of joints and connections
- Repair and maintenance

7-3- Shell –based structures

Shell-based structures are ideal candidates for the fabrication of low-price bogie frames (due to the use of GFRPs) and integration of the suspension system. A well-known example of the shell-based structures for the bogie frame is Ecobogie [6]. As illustrated in Figure 27 and Figure 28, Ecobogie concept can be modified by adding steering elements, or GFRP leaf springs in the side elements. However, according to a previously performed analysis on the stability of the mentioned bogie, it is hard to obtain both stability and steering properties using the shell-based concept.

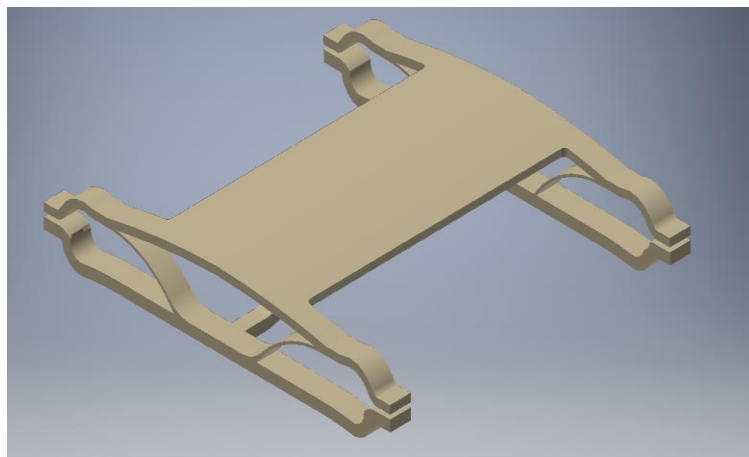


Figure 27- Example 1 of using shell-based concept for bogie frame

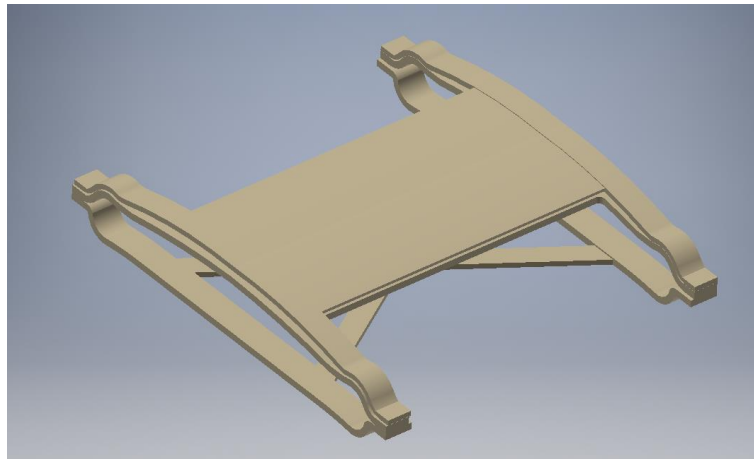


Figure 28-Example 2 of using shell-based concept for bogie frame

Following are the expected advantages of shell-based structures for FRP bogie frames:

- Primary (and/or) secondary suspension systems can be removed
- Variable stiffness behavior can be used to improve dynamic behavior
- Low material costs

There are also some limitations for using such shell-based structures as the bogie frame:

- Compatibility with current metallic components
- High cost of manufacturing
- Possibly generates higher noise due to increased contacts

7-4- Pultruded/pull-winding profile based structures

Low fabrication cost for pre-fabricated pultruded or pull-wounded profiles has attracted attention for employing them in structural applications. Various shapes of pre-fabricated profiles can be combined and assembled to form the FRP bogie frame. However, reinforcing the profiles should be performed to enhance the mechanical properties of the elements in the matrix direction. The suggested configurations based on pultruded profiles are shown in Figure 29 to Figure 35. Local filament winding or using carbon sheets are some suggested reinforcement methods for pultruded profiles. Adding carbon strips can also enhance the mechanical properties of the structure, but it requires designing of special supports for holding and pre-stressing the strips.

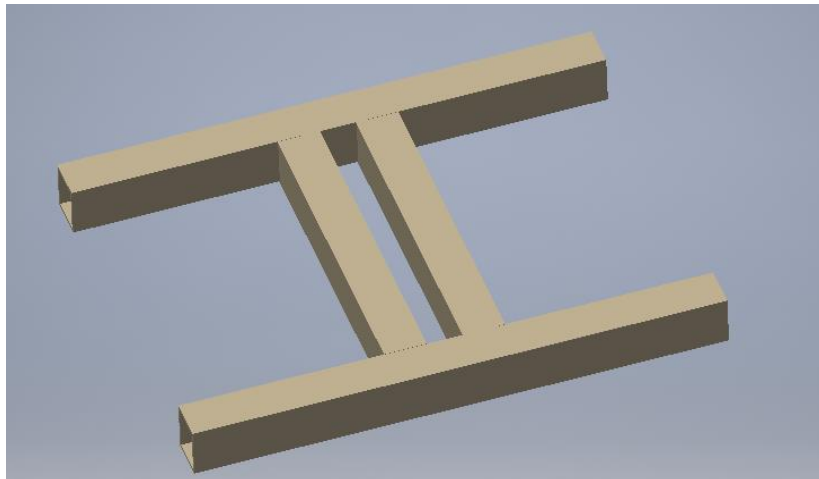


Figure 29- Example 1 of using pre-fabricated profiles for bogie frame

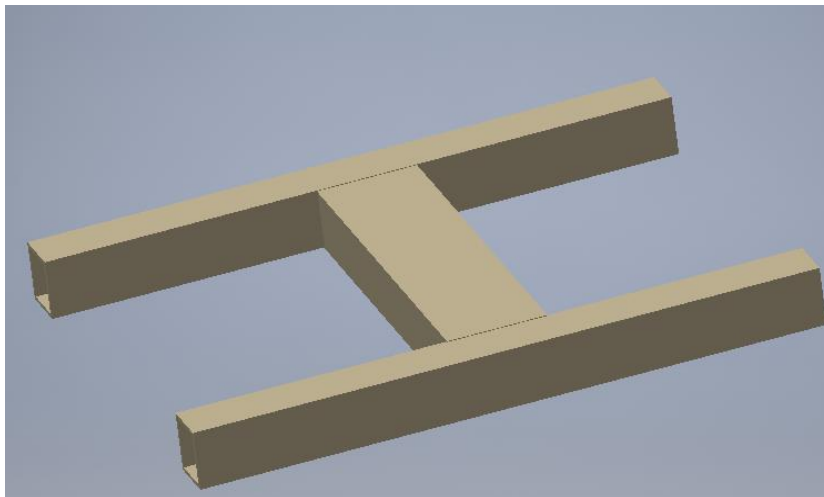


Figure 30-Example 2 of using pre-fabricated profiles for bogie frame

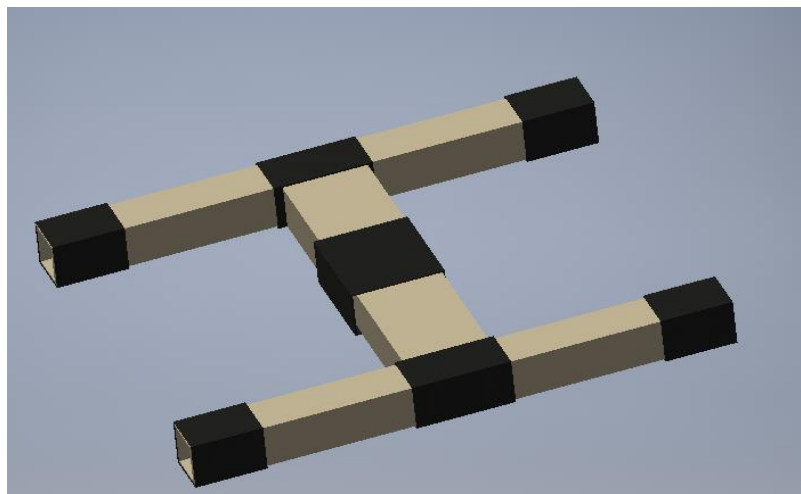


Figure 31- Example 3 of using pre-fabricated profiles for bogie frame

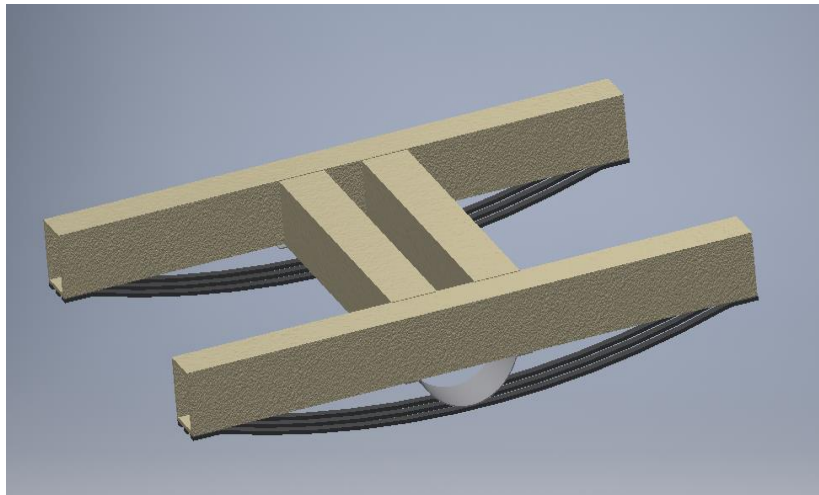


Figure 32- Example 4 of using pre-fabricated profiles for bogie frame

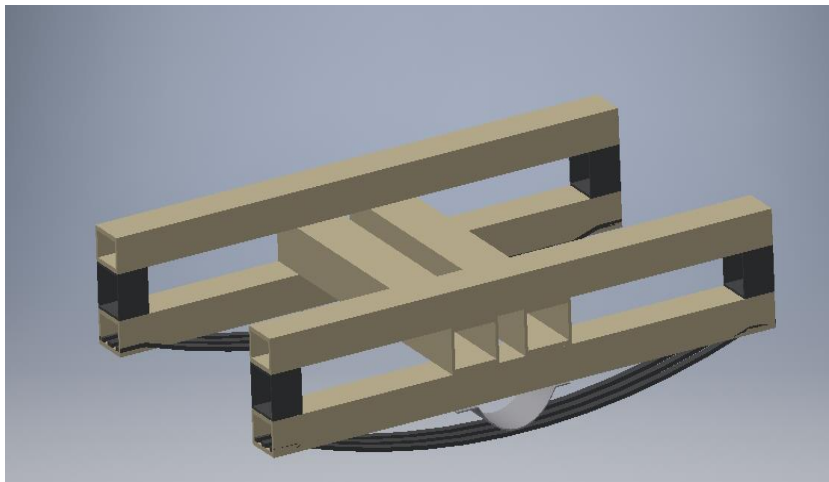


Figure 33- Example 5 of using pre-fabricated profiles for bogie frame

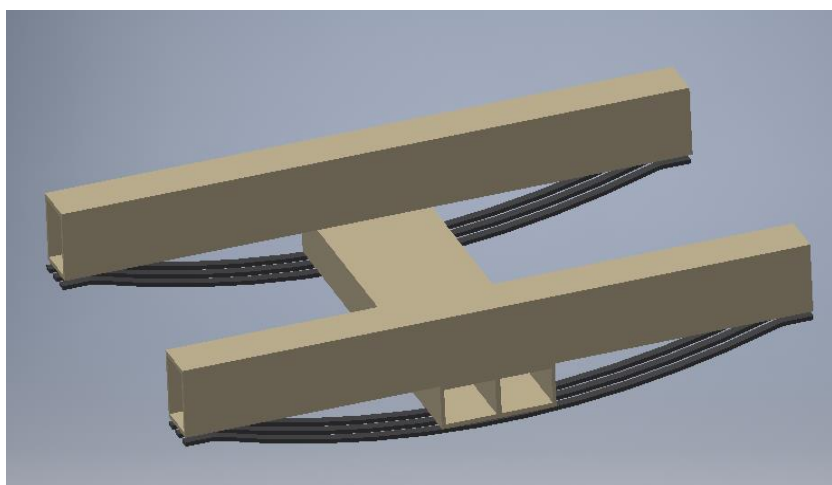


Figure 34- Example 6 of using pre-fabricated profiles for bogie frame

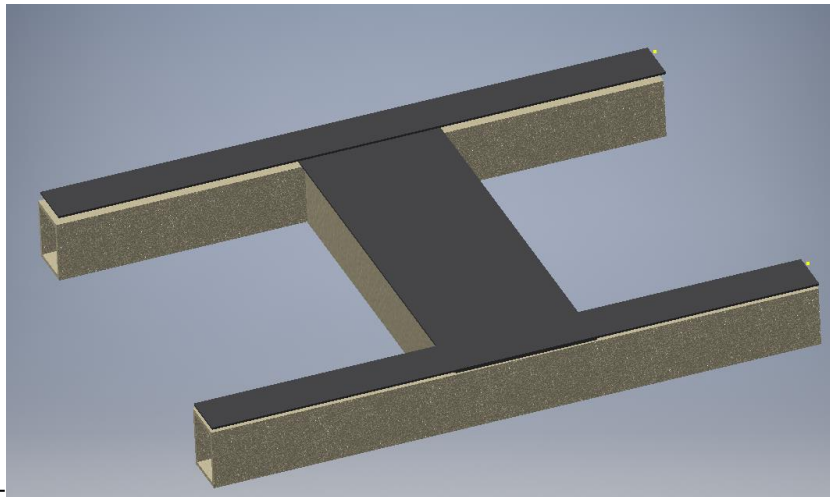


Figure 35- Example 7 of using pre-fabricated profiles for bogie frame

The main advantages of pultruded based structures are as follow:

- Low manufacturing costs
- Low material costs
- Easy maintenance and replacement
- Enables the possible use of hybrid material design
- Available fire resistance specifications for the pultruded products

There are also some major limitations for using such structures in the bogie frame:

- Low mechanical properties in the transverse direction
- Drilling limitations (due to low transverse strength)
- Limitation for the design of the overall shape of the bogie frame

8- Workshop scores for concepts

During the workshop meeting, each design concept (and some prepared sub-concepts) were discussed by considering static integrity, running dynamic, fabrication, and cost aspects. Finally, the concepts were ranked based on their scores. The evaluation form was modified during the meeting and some parameters that could not be evaluated without analysis or parameters that were similar to all the presented concepts were eliminated for averaging the result. Moreover, as a new suggestion, modification of shell-based concept and developing 3-piece bogie design were presented. More detailed discussions on the suggested bogies were performed in the second workshop on 7 April. The results of the concept evaluation are presented in Figure 36. The modified 3-piece bogie and modified shell-based structures have the highest scores and will be discussed and evaluated in the second workshop.

Subject	Evaluating parameters	Weight ratio	Scores (1-10)				
			SKIN	LEAF	SHEL	PULT	Modified
FRP design concepts	Weight reduction	5	5	5	9	8	8
	Estimated manufacturing costs	5	4	3	4	8	7
	Assembling costs	5	6	5	6	3	6
	Compatibility with Y25 component	3	6	3	6	6	6
	Stiffness controlling	1	5	2	5	2	8
		Average	5.2	3.7	6.4	5.6	7.0

Figure 36- Evaluation results for FRP frame concept for the new bogie

9- New ideas in the 2nd workshop

Based on the selected priorities in the first workshop, new suggestions were provided to be discussed in the second workshop on 7. April 2022. The main focus was on the 3-piece bogie frames with the ability to integrate the suspension system with the FRP frame. Three different concepts were suggested to be discussed in the workshop meeting. The first model is a simple 3-piece concept with CFRP leaf springs as the side beams and a square profile as the bolster (Figure 37). As discussed in the second workshop by the partners, it is necessary to use special supports at the axlebox to employ this concept. Therefore, the suspension system cannot be entirely integrated into the frame. The two other models are prepared to address this problem.

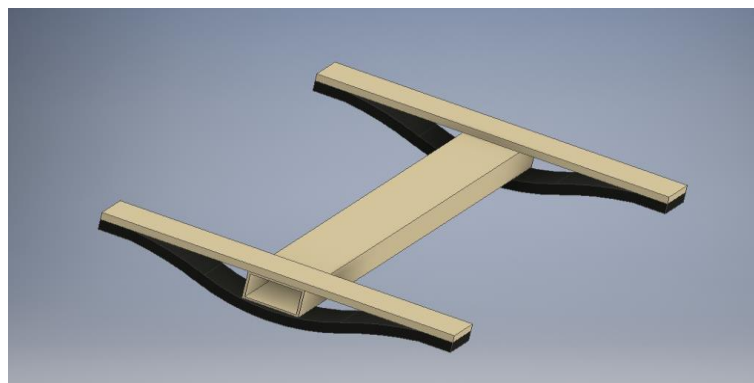


Figure 37- First presented three-piece model in the second workshop

In the second model (Figure 38), a suggested concept for de-coupling vertical and longitudinal stiffness using geometry modifications, is presented. In this case, the effect of vertical displacement of the side-beam on the horizontal separation of the axle box can be minimized. By proper design of stacking sequence of composite laminate and thicknesses, vertical and longitudinal stiffness can be adjusted. The L-shape links may also be employed to enhance longitudinal stiffness.

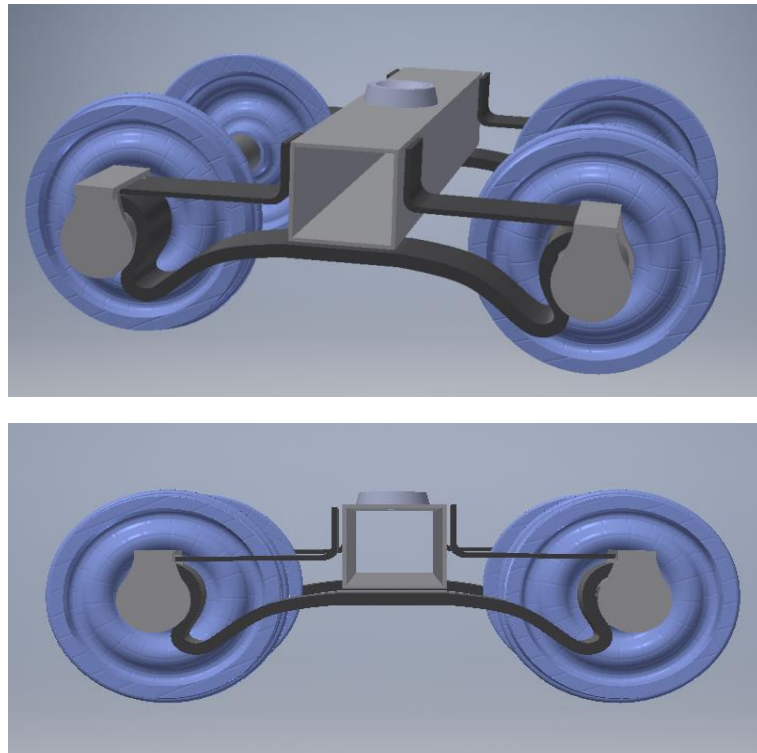


Figure 38- Second presented three-piece model in the second workshop

The third model contains two FRB curved beams with opposite curvatures as the side beam (Figure 39). Similar to the second concept, this concept was also proposed to reduce the effect of vertical load on the horizontal deflection of the frame. By proper design of axlebox, the horizontal deflection of the frame can be converted to a rotation around the axlebox.

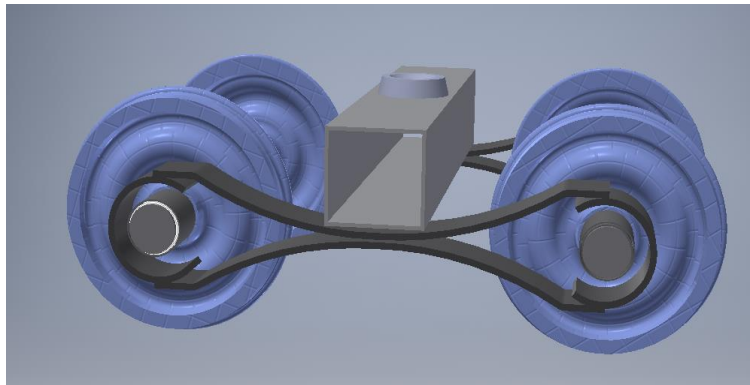


Figure 39- Second presented three-piece model in the second workshop

According to the discussions on the presented concepts in the second workshop, four main challenges should be considered in FE analysis to be addressed in the final concept. The main challenges are:

- Primary suspension: The frame should be designed in a way that the force-deflection behavior of the primary suspension is close enough to that of the standard bogie frames. Prose provided a force-deflection curve for their FORMICA bogie project.
- Damping behavior: The damping properties of the suggested concept should be examined and if required, be enhanced by additional damping elements.
- Stability: Low longitudinal stiffness can lead to instability of the bogie in running dynamic characterization. As a suggested solution, adding a cross-link element (Figure 40) can enhance the stability of the bogie. Therefore, it can be added to the presented bogie concepts.
- Steering behavior: Similar to stability, adding cross-link element improves the steering behavior of the bogie. It will be examined in the running dynamic simulation step.

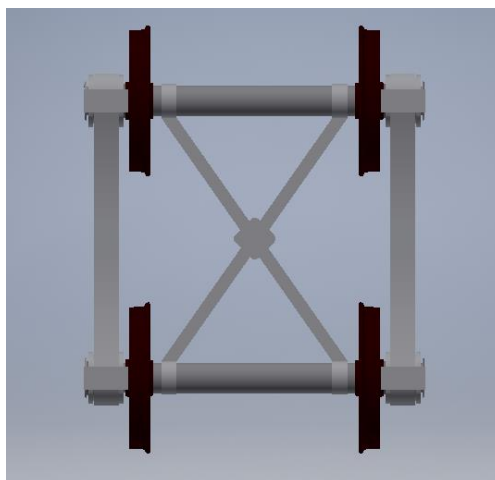


Figure 40-Cross link components for enhancement of steering and stability

By considering the discussed parameters and challenges regarding the design and analysis of the new FRP bogie, finite element analysis will be performed on the selected concept (Figure 41) to examine the mechanical properties and functionality of the concept. The concept can be finalized after initial FE analysis and running dynamic simulations.

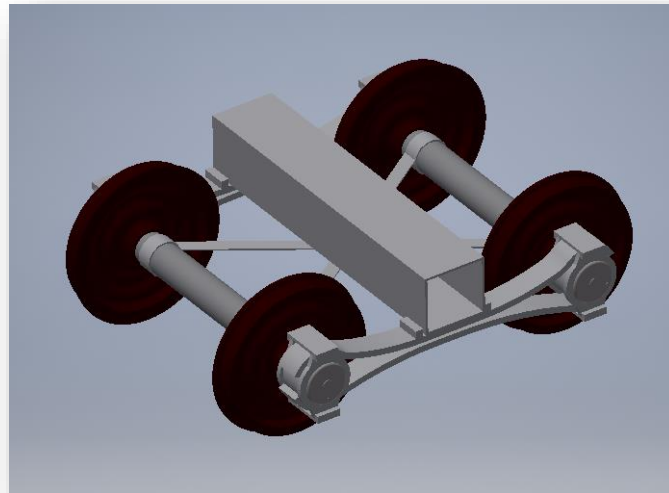


Figure 41- Initial model for performing finite element analysis

10- Conclusions

In the first interim report, a summary of the progress of the project in the first three-month is presented. The main discussion and the results of the workshop meeting are also presented. After determining the required specifications, including standards, load calculations, and validation procedures in Task 1, the presented design concepts were examined in Task 2 of the project. During the first workshop with PROSE, Stinger, Empa noise, SBB cargo, and Wascosa, the basic layout parameters were evaluated, and the configurations with the highest priorities were determined. The FRP concepts for the bogie frame are also evaluated considering technical, economic, and fabrication aspects. A second workshop was also held to be concentrated on the modified three-piece bogie plans to obtain the best possible design concept. Three suggested concepts were presented in the second workshop and the main challenges and possible solutions were discussed. The detailed CAD file will be prepared for FE analysis after finalizing the design concept.

11- References

- [1]. Geuenich, W., C. Gunther, and R. Leo, The Dynamics of Fiber Composite Bogies with Creep-controlled wheelsets. *Vehicle System Dynamics*, 1983. 12(1-3): p. 134-140.
- [2]. Geuenich, W., C. Guenther, and R. Leo. DYNAMICS OF FIBER COMPOSITE BOGIES WITH CREEP-CONTROLLED WHEELSETS. in *Dynamics of Vehicles on Roads and on Tracks, Proceedings of IAVSD Symposium (International Associa.* 1984.
- [3]. Maurin, L., et al. FBG-based smart composite bogies for railway applications. in *2002 15th Optical Fiber Sensors Conference Technical Digest, OFS 2002.* 2002.
- [4]. Kim, J.S., H.J. Yoon, and K.B. Shin, Design of a composite side beam for the railway bogie frame, in *Materials Science Forum.* 2010. p. 2676-2679.
- [5]. Kim, J.S., W.G. Lee, and I.K. Kim, Manufacturing and testing of a GFRP composite bogie frame with straight side beam members. *Journal of Mechanical Science and Technology*, 2013. 27(9): p. 2761-2767.
- [6]. Hou, J. and G. Jeronimidis, A novel bogie design made of glass fibre reinforced plastic. *Materials and Design*, 2012. 37: p. 1-7.
- [7]. Nishimura, T., efWING® ' --new-generation railway bogie. *Japanese Railway Engineering*, 2016.
- [8]. Gorbunov, M., et al., EXPERIMENTÁLNÍ A VÝPOČTOVÉ METODY V INŽENÝRSTVÍ 2017.
- [9]. Developing a carbon fibre railway bogie for passenger trains. 2020, Available from: <https://www.globalrailwayreview.com/article/102360/carbon-fibre-bogie-passenger-trains-irr/>.
- [10]. ERCI Innovation Award 2020 for bogie frames by CG Rail, ERCI Innovation Award 2020 für Drehgestellrahmen von CG Rail - Leichtbauwelt, [Accessed 05. 2022].
- [11]. Lack, T., & Gerlici, J. (2018). Y25 freight car bogie models properties analysis by means of computer simulations. In *MATEC Web of Conferences (Vol. 157, p. 03014).* EDP Sciences.
- [12]. Solčanský, S., & Knap, S. (2021, November). Simulation of running a vehicle with a Y25 bogie on a theoretical track. In *IOP Conference Series: Materials Science and Engineering (Vol. 1199, No. 1, p. 012079).* IOP Publishing.
- [13]. EN13749, Railway applications - Wheelsets and bogies - Method of specifying the structural requirements of bogie frames.
- [14]. Railway technical, <http://www.railway-technical.com/trains/rolling-stock-index-1/bogies.html>, [Accessed 05. 2022].
- [15]. C. WRIGHT, "The Contact Patch," 27 November 2014. [Online]. Available: <http://the-contact-patch.com/book/rail/r1114-railway-suspension>, [Accessed 05. 2022].
- [16]. Fandos, M. M. (2018). Investigation and Classification of Bogie Designs and their Potential to Adopt Lightweight Structures by Means of a Database. Bachelor Thesis Institute of Vehicle System Technology Rail System Technology–2018.–81p.
- [17]. Iwnicki, S. (2006). *Handbook of railway vehicle dynamics.* CRC press.
- [18]. SKF Railways, *Railway technical handbook, volume 1, Bogie designs.*

[19]. American Society of Civil Engineers. (2010). Pre-Standard for Load & Resistance Factor Design (LRFD) of Pultruded Fiber Reinforced Polymer (FRP) Structures.

Differences from the time plan according to the application

All expected tasks in the proposal have been carried out. A second workshop was also planned to obtain the best design concept for FRP bogie frame.

Outlook to the next working steps

1. In the next step, the CAD file of the selected configuration will be prepared for finite element analysis.
2. A detail static analysis followed by running dynamic simulation and noise emission will be carried out in Tasks 4, 5 and 6, respectively.

Diverse

There is no diverse compare to the plan.